12-2017

DETERMINATION OF CRITICAL EXPERIMENT CORRELATIONS VIA THE MONTE CARLO SAMPLING TECHNIQUE

William Jay Marshall
University of Tennessee, Knoxville, wmarshal@vols.utk.edu

To the Graduate Council:

I am submitting herewith a dissertation written by William Jay Marshall entitled "DETERMINATION OF CRITICAL EXPERIMENT CORRELATIONS VIA THE MONTE CARLO SAMPLING TECHNIQUE." I have examined the final electronic copy of this dissertation for form and content and recommend that it be accepted in partial fulfillment of the requirements for the degree of Doctor of Philosophy, with a major in Nuclear Engineering.

Ronald E. Pevey, Major Professor

We have read this dissertation and recommend its acceptance:

Steven E. Skutnik, Howard L. Hall, Vasilios Alexiades

Accepted for the Council:

Dixie L. Thompson

Vice Provost and Dean of the Graduate School

(Original signatures are on file with official student records.)

DETERMINATION OF CRITICAL EXPERIMENT CORRELATIONS VIA THE MONTE CARLO SAMPLING TECHNIQUE

A Dissertation Presented for the
Doctor of Philosophy
Degree
The University of Tennessee, Knoxville

William Jay Marshall
December 2017

To my wife, Robyn Joy Marshall, without whom none of this would have been possible.

To my son, Ian Jay Marshall, who has tolerated a tremendous loss of play time so this thing can be brought to a successful completion.

And finally, to the 2016 Chicago Cubs, the ultimate low probability, high weight event.

ACKNOWLEDGMENTS

There are so many people to thank in the execution of a project and a document like this. I will endeavor to thank all the important ones, but I will inevitably forget some and for this I am truly sorry.

First, thanks to Dr. Pevey. He willingly took me on as a part time doctoral student while I was (and still am) working full time at Oak Ridge National Laboratory, despite working with me more than 10 years prior when I was at UTK working on my Master of Science degree. He also allowed me the freedom to take classes and make progress on my research around my full time day (and night and weekend) job at the lab. Also, crucially, he reconsidered allowing me to use this project as my dissertation after initially rejecting it.

Second, thanks also the other official members of my committee: Dr. Steven Skutnik, Dr. Howard Hall, and Dr. Vasilios Alexiades. They each dedicated time and effort to my work here despite having other things to do. I'm sure reviewing a dissertation isn't high on anyone's list of desired activities. Thanks to each of the committee members for their time, insights, and careful review.

Third, thanks to the courtesy member of my committee Dr. Bradley Rearden. His support of my efforts in this area began in Stockholm, Sweden, in March, 2013, and have continued over the past 4 years. He saw the potential of this project as a doctoral dissertation despite my early protests, and supported me with discussion, some funding at the lab, and plenty of encouragement. He also supported my trips to Europe to discuss my ideas within the OECD/NEA Working Party on Nuclear Criticality Safety Expert Group on Uncertainty Analysis for Criticality Safety Assessment (WPNCS/UACSA). All of this has been invaluable to the pursuit and final conclusion of this effort.

Fourth, thanks to Dr. Mike Dunn, Mr. Steve Bowman, and Dr. Doug Bowen at Oak Ridge National Laboratory for supporting my pursuit of a PhD while working for them full time at the lab. All three have provided support and encouragement despite this effort taking away from time I would have had to work on projects for them. I also need to thank the laboratory itself for paying the lion's share of my tuition over the last 5 years as I have toiled along in this endeavor.

Fifth, thanks to Elizabeth Jones, Emily Fenske, Jon Gill, and Dr. Adam Stratz for befriending an old guy like me. Having a few friends among the other graduate students has certainly made this easier and a whole lot more enjoyable.

Sixth, thanks to the members of WPNCS/UACSA for generating a benchmark on this topic at a convenient time for me. Thanks also for thoughtful discussions during meetings, especially in Paris in 2015 and 2016 and in Garching in 2016. A special thank you to Dr. Maik Stuke, Dr. Fabian Sommer, and Dr. Elisabeth Peters at the Gesellschaft für Analgen- und Reaktorseicherheit (GRS), who have also spent a considerable amount of time struggling with critical experiment correlations.

Seventh, thanks to Rob Lefebrve, Will Wieselquist, and Brandon Langley. Each of them implemented some sort of improvements somewhere in the tool chain of Sampler based on my experiences. All of the changes, except the "plus_x" thing, were improvements. Many of them, like speeding Sampler by about a factor of 50, were tremendously helpful in completing all the work presented here.

Eighth, thanks to my parents for providing a loan to make sure I could take enough coins to the ivory tower when required. Their financial and moral support for all my educational and extracurricular activities is greatly appreciated, and I'll pay that loan back soon. Promise.

Ninth, finally, and most importantly, I owe an incredible debt of gratitude to my wife Robyn and my son Ian. They both put up with the lost time of me going to class, working on research, and writing this dissertation. Ian's been as tolerant of my ignoring him at times as any 7 – 12 year old can be. Robyn has provided the right mix of support, encouragement, nagging, sympathy, and patience somehow at all the right times. She has also cooked, cleaned, raised a child, run a household, taught preschool, and earned a master's degree and teaching certification in the meantime. There's no way that my degree or this document could have been completed without her.

ABSTRACT

Critical benchmark experiments are the foundation of validation of the computational codes used in criticality safety analyses because they provide a basis for comparison between the calculated results and the physical world. These experiments are often performed in series varying a limited number of parameters to isolate the effect of the independent parameter. The use of common materials, geometries, machines, procedures, detectors, or other shared features can create correlations among the resulting experiments. Most validation techniques used in criticality safety practice do not treat these correlations explicitly, and the effect of this is unclear as the correlations themselves are not well known. Generalized linear least squares methods used for advanced validation or in data adjustment studies also rely on correlation coefficients to constrain the adjustments allowed in critical experiment results. The purpose of this dissertation is to develop a methodology for the calculation of critical experiment correlations using a Monte Carlo sampling technique. The use of this technique allows for the determination of the uncertainty in each individual experiment, and identical perturbations applied to shared parameters provide estimates of the covariance between the experiments. The correlation coefficient is then calculated by dividing the covariance between any pair of experiments by the product of the individual experiment standard deviations. This technique is applied to high-enriched uranium solution experiments and low-enriched uranium pin lattice experiments to determine correlation coefficients for these types of systems. The important parameters governing the correlation coefficients are determined, and the results are compared with correlation coefficients in the literature determined using other methods at other institutions. The general method for the determination of the correlation coefficients is presented along with other conclusions and recommendations for further study in this area.

TABLE OF CONTENTS

LIST OF TABLES

LIST OF FIGURES

CHAPTER I: INTRODUCTION

Criticality safety is the branch of nuclear engineering concerned primarily with preventing an unintended nuclear chain reaction from occurring during the handling or storage of fissionable material [1]. One of the primary metrics used to analyze systems containing fissionable material is the neutron multiplication factor, or k_{eff}. The k_{eff} is calculated as the ratio of the neutron production rate to the neutron loss rate [1]. Thus a system that has a k_{eff} of 1, referred to as "critical," has a constant neutron population; production is exactly balanced by losses to absorption in the system and leakage from the system. A system with a decreasing neutron population over time has a k_{eff} less than 1, and is called "subcritical". A "supercritical" system has a k_{eff} greater than 1 and an increasing neutron population.

The community of criticality safety practitioners is made up of nuclear engineers who specialize in analyzing processes and systems to ensure all operations stay safely subcritical. The community is further divided into several subdisciplines. The most evident division within the criticality safety community is into the types of analyses performed. The three main types of analyses that are performed are process criticality safety analysis, transportation criticality safety analysis, and burnup credit criticality safety analysis. Each of these areas will be discussed in more detail below. It is also important to recognize that in the United States (US) multiple regulatory bodies exist. Some facilities are regulated by the Department of Energy (DOE) or the National Nuclear Security Administration (NNSA) and others are regulated by the Nuclear Regulatory Commission (NRC). The DOE/NNSA sites tend to be related to military applications of nuclear technology, while the NRC regulated sites are generally related to civilian nuclear power. The DOE/NNSA sites are generally required to follow consensus ANSI/ANS standards and applicable DOE orders. The NRC regulated sites are required to follow the various applicable chapters of Title 10 of the Code of Federal Regulations (10CFR). Both communities also support transportation operations, which are generally similar in most cases because Department of Transportation (DOT) regulations are also involved.

Process criticality safety analyses include assessments for operations involving the handling, storage, and/or processing of fissionable material. These analyses require consideration of both normal conditions of operation and credible upsets. The criticality safety analyst is part of multidisciplinary team while performing these analyses so that appropriate, relevant aspects of operations are considered. These aspects often include considerations of chemistry, operations, human factors, and process engineering and frequently extend to broader topics including structural engineering and fire protection. A wealth of information is needed to construct the appropriate set of credible upset conditions. In DOE/NNSA facilities, the criterion to be satisfied is called the "process analysis" (PA) requirement. The ANSI/ANS-8.1 standard [2] defines the PA requirement, "Before a new operation with fissionable material is begun, or before an existing operation is changed, it shall be determined that the entire process will be subcritical under both normal and credible abnormal conditions." Note that in the standard, the use of the word "shall" indicates a requirement. Generally, NRC-regulated sites are required to use the "double contingency principle" (DCP). As defined in ANSI/ANS-8.1, the DCP requires that "[p]rocess designs

should incorporate sufficient factors of safety to require at least two unlikely, independent, and concurrent changes in process conditions before a criticality accident is possible." Aside from the difference in the fundamental requirement, process analyses are largely similar and consider the same range of parameters which affect neutron multiplication in fissionable material systems. In process criticality analyses it is important to acknowledge that criticality safety is just one branch of the overall safety analysis for a facility. Unnecessary controls to prevent criticality accidents may reduce overall safety by, for example, increasing worker dose or adding heavy lifts. It is also important to generate an appropriate set of controls on the operation so that the operation can be performed efficiently and economically. The subcriticality requirements can be demonstrated through multiple different approaches. The preferred method is by comparison to an experiment confirming the safe limits for the process being analyzed. This is nearly never possible, so other alternatives include use of reference sources (handbooks or standards) containing data and limits, performing hand calculations, or executing computer codes. The overall analysis ranges from simple to very complex depending on the process under consideration.

Transportation criticality safety analyses are similar to process criticality safety analyses in many regards, but only consider fissionable material during transport. The highest level requirements for safe transport of fissionable material are set forth by the International Atomic Energy Agency (IAEA) in Specific Safety Requirements No. 6 (SSR-6) [3]. These requirements are codified in the US in 10 CFR Part 71 [4], and for NRC-regulated transportation further details are included in the Standard Review Plan (SRP) for Transportation Packages for Radioactive Material (NUREG-1609) [5]. DOT regulations are also applicable, and can be found in 49 CFR parts 107 [6], 171-180 [7], and 390-397 [8]. Analyses are required for both normal conditions of transport (NCT) and hypothesized accident conditions (HAC). Testing of packages to meet these requirements is required for certification, and the specific test procedure for both NCT and HAC is specified in SSR-6. The results of explicit tests and structural analyses can be combined to allow the criticality safety analyst to demonstrate that subcriticality can be demonstrated in the required conditions. As with the process criticality safety analyses, these analyses require the coordination of a large amount of information from a range of different disciplines. Generally, the final demonstration of subcriticality is made by performing computer calculations.

Burnup credit (BUC) criticality safety analyses are primarily used in the storage, transportation, and disposal of commercial spent nuclear fuel (SNF). BUC is crediting the reduction in fuel assembly reactivity due to the depletion of fissionable materials and the buildup of neutron absorbing fission products. SNF storage immediately after discharge from the reactor is performed in the spent fuel pool (SFP), where fuel assemblies are placed in stainless steel racks. These racks frequently contain fixed neutron absorber panels for criticality control. Pressurized-water reactor (PWR) SFPs also contain boric acid dissolved in the water to provide additional reactivity control. Storage in the SFP is regulated under 10 CFR 50.68 [9]. After several years of cooling in the SFP, fuel assemblies can be transferred into a storage canister for dry storage at the plant site. The analysis of dry storage installations is governed by 10 CFR Part 72 [10]. Additional details are included in the SRP for Spent Fuel Dry Storage facilities (NUREG-1567 [11]). In many cases, the canisters may

also be analyzed for transportation of SNF. As discussed above, transportation regulations are contained in 10 CFR Part 71. The SRP for Transportation Packages for Spent Nuclear Fuel is NUREG-1617 [12]. BUC analyses consider a more limited range of upset conditions because the fuel assemblies are the only fuel form considered. Instead, a broad knowledge of reactor physics and the impacts of various reactor operating parameters on discharged fuel assembly reactivity is required. These parameters are discussed in NUREG/CR-6665 [13], and in many cases in subsequent NUREG/CR documents examining specific parameters in more detail. The demonstration of acceptable fuel assembly loading conditions is always performed via computer calculations because of the complexities involved in the fuel depletion calculations. The depletion calculations are performed in a computer code or set of codes designed for reactor depletion analysis and the depleted isotopic number densities are subsequently input to a criticality analysis code package.

One of the few things that all three types of criticality safety analysis have in common is the need for computer code calculations. These codes are used to calculate k_{eff} for models of the nominal and credible upset scenarios for a system of interest. In this context, the system of interest can be a step within a process or procedure, or it could be a storage configuration. Unintended criticalities create significant radiation fields which can injure or kill nearby workers or cause damage to nearby equipment. It is therefore necessary to demonstrate that each state is reliably subcritical, not merely subcritical on a best estimate basis. The maximum k_{eff} calculated by a computer code that can be asserted to be subcritical is called the upper subcritical limit (USL). In many cases, the calculated k_{eff} is increased by twice the stochastic uncertainty of the calculation before comparison with the USL if a Monte Carlo transport code is used. The USL is determined by reducing the physical k_{eff} value of 1 by the bias of the computational method being used, the uncertainty in the bias, and an additional margin of subcriticality (MOS). The MOS, also sometimes called a minimum subcritical margin, is selected for each analysis based on characteristics of the system, frequency of the operation, accessibility of the components, and other considerations. The bias and bias uncertainty are determined by validating the computational method.

The validation process is performed by comparing the results of critical experiments with the calculated results from models of the experiments using the computational method [2, 14]. Critical experiments are controlled systems that achieve a k_{eff} of 1 to investigate the parameters at which such a critical condition is achieved [1]. Thousands of critical experiments have been conducted, evaluated, and reported in the literature for validation. Currently, the most complete source of evaluated critical experiment descriptions is the International Handbook of Evaluated Criticality Safety Benchmark Experiments, referred to as the ICSBEP Handbook [15]. A key part of the validation process is the selection of experiments that are representative of the system or systems to be analyzed. The bias of the computational method is dependent on the materials in the model and the neutron energy spectrum in the system, so the selection of inappropriate experiments can lead to significant errors in the apparent bias for the system of interest. The experiment selection process is therefore carefully documented and reviewed during the validation process. All the critical experiment models are also developed, documented, and reviewed, to ensure the bias is not impacted by modeling errors.

For each experiment used in the validation, the difference between the calculated and measured k_{eff} results is determined. The experiments used in the validation are selected based on similarity to the application model being analyzed. It is important to determine the bias for the system of interest, and it is expected to be the same for similar systems. Thus the estimate of the bias of the computational method used in modeling the experiments, also referred to as the computational bias, is determined as the mean of these differences. The bias can alternatively be determined as a function of a system parameter using a trending technique, most frequently linear regression. The system parameter used is typically a property of the fissionable material, such as the enrichment if uranium is used in the experiment, or a property of the system, such as the neutron energy spectrum in the system. Often several different parameters are used in the trending analysis to determine which parameter gives the best prediction of the bias. This approach may improve the accuracy of the bias estimate by determining it for the exact value of this independent parameter in the application case model.

There is uncertainty in the bias estimate for a number of reasons. First, there are uncertainties associated with each experiment. These can be measurement uncertainties, dimensional uncertainties, the result of incompletely characterized materials, or come from other unknown or uncertain characteristics in the experimental materials or configuration. Secondly, there is also uncertainty in the bias estimate because it is the result of sampling a fixed set of experiments; the sample is used to estimate the true bias which is not known. There is also a computational uncertainty associated with calculating k_{eff} for the experiment models. Criticality safety calculations most frequently use Monte Carlo neutron transport, which is a stochastic technique and therefore yields a k_{eff} value with some calculation uncertainty. This calculation uncertainty is generally significantly lower than the experimental uncertainties. Deterministic methods have uncertainties associated with discretization of the problem geometry to conform to the required spatial mesh. Deterministic methods and some Monte Carlo implementations use multigroup representation of the energy variable which may also contribute to the bias or its uncertainty. The uncertainty in the bias is also increased to provide greater statistical confidence that the estimated bias and uncertainty bound the actual bias. The population variance, which is a measure of the variability of the differences from each experiment, is used in the overall determination of the bias uncertainty. The statistical margins often lead to the bias uncertainty being several times the magnitude of the bias itself, so proper quantification of the uncertainty is essential.

An entirely different, and relatively new, method of bias determination is called data adjustment or data assimilation, and uses critical experiments quite differently than the methods described thus far. These techniques have been used historically in applications other than criticality safety validation. Perhaps the most common application historically has been in the design and analysis of fast reactors. Data adjustment applications within criticality safety, such as those included in the TSURFER tool in the SCALE code system [16], perform a generalized linear least squares (GLLS) adjustment to determine a set of cross section adjustments that minimize inconsistencies among calculated k_{eff} values. The same cross section adjustments must be used in all models which use the cross section. These data adjustment methods use a larger number of critical experiment models so that a large amount of data is available to yield accurate adjustments. The cross section adjustments

are constrained by the uncertainties in the cross sections; models that cannot be brought into agreement with other cases are rejected. The experimental k_{eff} values can also be adjusted within their uncertainty bands; experiments that are correlated are further constrained by these critical experiment correlations. The correlations between each pair of experiments must therefore be determined and supplied as an input to the data adjustment process. The measured k_{eff} values for the experiments can be adjusted, but must be adjusted consistently among correlated experiments.

Verification is distinct from validation, and is the process of confirming the algorithms used in the code are coded correctly and functioning properly. This can be accomplished with a range of tests including simplified problems with known, often analytical, solutions, processing known inputs to ensure the expected outputs are generated, running inputs that are designed to fail, and other tests. Generally the verification testing done at installation is performed by executing a suite of test problems provided by the code developer and comparing the results to those provided. Both verification and validation must be performed and documented before results from the computer code can be used in any safety assessment.

A series of critical experiments is often performed with a limited number of parameters varied systematically to cover a range in some parameter space. This approach serves multiple purposes. Primarily, performing experiment series allows for the determination of system sensitivity to specific parameters, for example lattice pitch or reflector thickness. Unlike some types of experiments, critical experiments cannot vary only a single, independent parameter. Any change to a critical system makes it either subcritical or supercritical, so an offsetting additional change must be made to restore criticality. Some experiments are controlled with the mass of fuel present, while others are controlled with material separation, amount of moderating material present, or concentration of neutron absorber in the system. Generally, the system response to one parameter change, for example material separation, is well understood and is therefore used to offset changes in a different parameter. This allows for an estimation of the sensitivity of the system to changes in the second parameter, though the sensitivity is not necessarily known with the same accuracy as is possible in experiments with single variable controls. An additional benefit to performing experiments in series is that several related experiments can be done at lower cost per experiment and in less time than if each experiment had been performed in isolation.

The use of experiment series in traditional, non-data adjustment validation techniques creates additional complexities because of the correlations among the individual experiments within the series. The correlation between a pair of experiments is a result of shared experimental components which include, but are not limited to, fissile, reflector, or absorbing materials, detector systems, and procedures. Many of these shared characteristics should have very little effect on the results of the experiments or the independence of the data measured or derived from the experiments. The use of common materials and fixtures, however, can create correlations among the experiments that demonstrably reduce the independence of each experiment in a series. This can impact the determination of the computational bias, but is far more likely to affect the uncertainty in the bias. The

uncertainty is increased because several measurements of the same system do not provide as much unique information as the same number of measurements of different systems. Thus the correlation among experiments in a series acts to reduce the effective number of experiments in a validation set. The smaller number of effective experiments would lead to a larger uncertainty, so neglecting the correlations is nonconservative because it results in a lower bias uncertainty. As discussed previously, the existence of correlations is not problematic in data adjustment techniques, but the correlations must be provided so that the adjustment process is properly constrained.

In some critical experiments, a high degree of correlation is a desired characteristic. The maximum amount of information can be extracted from substitution experiments only when other parameters are constant or nearly so. For these experiments, a lack of correlation would cause the impact of the substitution to be difficult to determine. The value of these experiments, especially when incorporated into data adjustment, is greatly increased by a high degree of correlation.

A current challenge facing criticality safety practitioners and regulators is to establish a reliable method of determining the correlations among the critical experiments, and ultimately to determine methods to incorporate them into usable validation techniques. The correlations can be quantified as correlation coefficients (both terms are used interchangeably in this work) which are calculated by dividing the covariance between two experiments by the product of the standard deviations of the two experiments. More detail regarding the calculation of correlation coefficients is provided in the last section of the next chapter.

A range of methods to determine and implement critical experiment correlation coefficients have been introduced since 2003 [17], including both deterministic and Monte Carlo techniques [18]. The next chapter reviews existing literature regarding the determination of correlation coefficients for critical experiments. After a discussion of codes, methods, and models in Chapters III, a description of the new work performed in this dissertation is presented in Chapter IV. Chapters V through VII document research intended to establish a framework for determining correlation coefficients in low-enriched uranium (LEU) pin lattice systems and high-enriched uranium (HEU) solution systems. The recommended process for the calculation of critical experiment correlation coefficients is provided in Chapter VIII along with other conclusions in Chapter IX. The procedure outlined in Chapter VIII can be used to determine correlations among critical experiments, but many challenges related to the documentation of the critical experiments themselves remain. Potential future work is discussed in Chapter X.

CHAPTER II: LITERATURE REVIEW

An extensive body of literature exists relating to validation of computational methods in criticality safety. Attempts to quantify and account for correlations among related critical benchmark experiments are a fairly recent innovation and first appear in the literature in 2003 [17]. The potential for validation errors due to drawing all experiments from a single series has been recognized for significantly longer, and practitioners are advised to avoid this practice in the current consensus standard on validation [14].

Literature relevant to the determination of critical experiment correlations can be grouped into five areas: statistical techniques needed to develop and compare correlation coefficients, current validation guidance documents, a description of the problems introduced in validation by correlated experiments, methods for determining correlation coefficients, and applications of critical experiment correlation coefficients. Although this research is primarily concerned with the 4th category, each of these areas will be discussed in greater detail in the following subsections.

Review of Statistics

The work performed in this dissertation relies extensively on statistics, indeed the correlation coefficient is a statistical quantity. The Monte Carlo method, used both to generate perturbed models and perform neutron transport calculations, is also a statistical method. No discussion is provided here of the Monte Carlo method or its application to neutron transport. A complete discussion is provided in [18] and [19]. A brief discussion is provided reviewing the definition and calculation of the correlation coefficient since it is the central theme of this work. Finally, the Fisher z transformation is reviewed as it can be used to determine confidence intervals on determined correlation coefficients.

Correlation Coefficient

The correlation coefficient used in this work is the Pearson correlation coefficient (ϱ), which is a measure of the linear relationship between two variables [20]. It is calculated as shown in Equation 1 [20]:

$$\rho_{xy} = \frac{\mathrm{cov}(x,y)}{\sigma_x \sigma_y} \qquad \text{Eqn (1)}$$

Where: ϱ_{xy} is the correlation coefficient between variables X and Y
cov(x,y) is the covariance between the variables X and Y
σ_X is the standard deviation of variable X
σ_Y is the standard deviation of variable Y

The covariance between the two variables is estimated as shown in Equation 2 [20]:

$$\mathrm{cov}(x,y) = \frac{\sum_{i=1}^{n}(x_i - \hat{x})(y_i - \hat{y})}{n-1} \qquad \text{Eqn (2)}$$

Where: cov(x,y) is the covariance between two variables, X and Y

x_i is a single sample of the variable x

$\hat{x}$ is the average value of the variable x

y_i is a single sample of the variable y

$\hat{y}$ is the average value of the variable y

n is the total number of samples

It should be noted that the subscripts of x and y are the same because they are compared for each sample. Also, in this work, x and y are k_{eff} values resulting from calculations of two different, potentially correlated, critical experiment models. Each specific sample, *i*, represents a set of perturbations of physical properties within their uncertainty ranges. The same perturbations are applied to both systems, x and y, when the physical properties are shared between the two systems. It should also be noted that $\hat{x}$ and $\hat{y}$ are the average k_{eff} values of the *n* realizations of each system and not the nominal results.

The correlation coefficient is essentially a normalized covariance such that all values are between -1 and 1. A value of 1 means that a perfect positive linear relationship exists, -1 indicates a perfect inverse linear relationship exists, and a value of 0 indicates no linear relationship between the two variables. Low values should be treated with care because it is possible that a strong non-linear relationship exists between the two variables. A purely quadratic relationship will result in a correlation coefficient of 0, even though a strong relationship exists between the two variables.

It should also be noted that the sample correlation coefficient, r_{xy}, is used to estimate the population correlation coefficient, ϱ_{xy}. The population correlation coefficient is a property of a bivariate normal distribution, which typically results when both variables are themselves normally distributed. The method for determining a confidence interval for a correlation coefficient is strongly reliant on the assumption of a bivariate normal distribution of the two variables [20]. If the bivariate normality assumption if violated, the methods discussed will not yield accurate results. The primary method of confirming the normality assumption is to perform normality testing on each variable separately. Accurate assessment of bivariate normality is beyond the scope of this work.

Assessment of Non-zero Correlation Coefficient

It is of significant interest to determine whether a calculated correlation coefficient is statistically significantly different from zero. If it is not, then the null hypothesis that the correlation coefficient is zero, and that the variables are independent, is accepted. Within the context of criticality safety validation, this would allow the use of typical methods which assume uncorrelated experiments. The test statistic for this test is shown in Equation 3 [21]:

$$t^* = \frac{r_{xy}\sqrt{n-2}}{\sqrt{1-r_{xy}^2}} \quad \text{Eqn (3)}$$

Where: t^* is the test statistic
r_{xy} is the sampled correlation coefficient between the variables X and Y
n is the number of samples

The null hypothesis is that the correlation coefficient is zero. If this hypothesis is correct, t^*, calculated from the sampled correlation coefficient, follows a t distribution with n-2 degrees of freedom. Therefore, if the absolute value of t^* is less than or equal to $t(1-\alpha/2; n-2)$, the null hypothesis is accepted and the correlation coefficient is accepted as statistically indistinguishable from zero. If the test statistic t^* is larger than the t value, then the null hypothesis is rejected and the correlation coefficient is concluded to be nonzero [21]. In the above comparison, $t(1-\alpha/2; n-2)$ is the value of Student's t-distribution with a significance level of $1-\alpha/2$ and n-2 degrees of freedom. The significance level, α, is the probability of rejecting the hull hypothesis when it is true [20].

Confidence Interval Estimation for Correlation Coefficients

The confidence interval for a correlation coefficient can be constructed based on the Fisher z transformation [21]. The transformation is shown in Equation 4 [21]:

$$z' = \frac{1}{2}\ln\left(\frac{1+r_{xy}}{1-r_{xy}}\right) \quad \text{Eqn (4)}$$

Where: z' is the Fisher z value
r_{xy} is the estimated correlation coefficient between X and Y

For large sample sizes (i.e. more than 25 samples [21]), z' is distributed normally with an expected value and variance of:

$$E\{z'\} = \frac{1}{2} ln\left(\frac{1+\rho_{xy}}{1-\rho_{xy}}\right) \quad \text{Eqn (5)}$$

$$\sigma^2\{z'\} = \frac{1}{n-3} \quad \text{Eqn (6)}$$

Equation 5 uses the population statistic, ϱ_{xy}, as the estimator, r_{xy}, is assumed to be unbiased. In the unbiased case, r_{xy} is equal to ϱ_{xy}.

Because z' is distributed normally, the confidence interval on the expected value of z' can be determined as shown in Equation 7 [21]:

$$z' \pm z\left(1-\frac{\alpha}{2}\right)\sigma\{z'\} \qquad \text{Eqn (7)}$$

Where: z' is the Fisher z value
$z(1-\alpha/2)$ is the $(1-\alpha/2)100$ percentile of the standard normal distribution

Finally, the confidence interval on the correlation coefficient itself can be determined by transforming the confidence limit on z' back into correlation coefficients using Equation 8.

$$\rho_{CI} = \frac{e^{2z'}-1}{e^{2z'}+1} \qquad \text{Eqn (8)}$$

Where: ρ_{CI} is the correlation coefficient confidence interval bound
z' is the confidence interval bound as the Fisher z value

The confidence interval about the sampled correlation coefficient, r_{xy}, is therefore $r_{xy} \pm \rho_{CI}$.

Current Validation Guidance Documents

A range of validation guidance documents exist currently for use by criticality safety practitioners. One of the most important is the consensus standard on validation of computational methods in criticality safety validation: ANSI/ANS-8.24 [14]. Other documents include ANSI/ANS-8.1 [1], NUREG/CR-6698 [23], NUREG/CR-6361 [24], and NUREG/CR-5661 [25]. Only two of these documents, ANSI/ANS-8.24 and NUREG/CR-5661, have any statements that address correlation of critical experiments or could be interpreted to do so. This speaks to the relative inexperience in the community with the quantification and application of these correlation coefficients.

One statement in NUREG/CR-5661 [25] could be interpreted as, in part, warning of correlations among critical experiments. The statement comes from Section 5.1, which is titled "Selection of Critical Experiments," and states that a practitioner "should model a sufficient variety of critical experiments to demonstrate the capability of the calculational method in predicting k_{eff} for each individual experiment that has characteristics that are also judged to be important to the k_{eff} of the package." This statement is most likely intended to ensure that all important processes within the package model are properly validated, but the specific wording of "a sufficient variety of critical experiments" could be interpreted as a recommendation to select experiments from a range of different experiments. Regardless, this discussion is followed in NUREG/CR-5661 with a recommendation to consult NUREG/CR-6361 [24] for additional guidance on selecting critical experiments. Unfortunately, there is no mention of the correlations among experiments in NUREG/CR-6361.

NUREG/CR-6698 [23] provides thorough guidance for validating computational tools for use in criticality safety. This guidance includes a discussion of the purpose of validation,

definition of the range of parameters to be validated, selection and modeling of critical experiments, analysis of the results, definition of the area of applicability, and documentation of the entire validation process. The recommended method for performing the statistical analysis of the results, included in Section 2.4.1, uses uncertainty weighting to determine the population variance and bias. No treatment is included for correlations, so the data are treated as completely uncorrelated. This approach most likely understates the total uncertainty in the bias in many cases, though the magnitude of the difference is unquantifiable without correlation coefficients and a validation method that incorporates them.

The best discussion of critical experiment correlations is in ANSI/ANS-8.24, although no guidance is provided on how to treat the correlations. In Section 5 of the standard, titled "Selection and Modeling of Benchmarks," paragraph 5.6 states "To minimize systematic error, benchmarks should be drawn from multiple, independent experimental series and sources." The expressed intent of this statement is to eliminate the possibility that a validation will be in error because a single set of experiments contains a large, shared bias. This is closely related to some of the effects of correlations, but focuses on the potential for an undetected error in the bias and not on the potential to underestimate the uncertainty in the bias. An additional, more explicit statement appears in Section 8, "Documentation and technical review," in paragraph 8.1.4 which states that "Limitations of the validation (e.g., gaps in the data, correlated data points, missing or limited data) shall be described." No further discussion is provided as to how to identify, treat, or mitigate the "correlated data points."

One additional resource should be discussed in this section. Although it is not a guidance document for validation, the International Handbook of Evaluated Criticality Safety Benchmark Experiments (ICSBEP handbook) [15] is a repository of critical benchmark experiment descriptions used in a wide range of criticality safety validations. The associated DICE (Database for the ICSBEP) tool contains some information about correlations among critical experiments. Primarily, the interface shows the user sets of experiments that are likely to have correlations. Some of the correlation coefficients determined in [17] are included and compared to results generated in Chapter VII.

The Problems Introduced in Traditional Criticality Safety Validation by Correlated Critical Experiments

As discussed in the previous section, current validation guidance documents do not consider the treatment of correlations among experiments. The methods that are included in these documents, such as [23], include statistical methods assuming all data points are uncorrelated. One recent publication concerning the effects of correlations includes the warning that "validation of calculation methods is another area where the weaknesses [in correlation treatments] really show up" [26]. Quantitatively, another study that determined and applied correlation coefficients in validation saw the uncertainty in the bias increase by a factor of 1.7 [17]. The uncertainty assessment included for each experiment in the ICSBEP Handbook [15] also does not treat these correlations, leading to the observation that "a

complication in specifying the experimental uncertainty is how to treat the correlations among different experiments" [27]. The complication is a result of the correlations acting to reduce the amount of independent information contributed to the validation by each experiment, thus lowering the effective number of experiments included in the validation suite. Reference 17 observed that the uncertainty resulting from the 77 experiments, considering correlations, could have been achieved with only 25 experiments had they been independent. Clearly, the potential increase in the uncertainty of the bias is of primary concern in traditional trending and non-trending validation approaches when correlations are present among the critical experiments used.

Proper quantification of correlations is also important where they exist. Some evaluations in [15] make qualitative statements regarding correlation. One example is taken from Section 3.5 of the MIX-SOL-THERM-007 evaluation:

> The experiments within this series are highly correlated. All use essentially the same fissile solution, the same experimental vessel and reflector tank, and the same measurement systems. The only difference is the amount of gadolinium that is present in each experiment and this parameter was measured and mixed in the same manner for each experiment.

This is a correct assessment of the correlation among the parameters, but without more analysis it is difficult to know to what extent the results are correlated and how much information is truly shared among the cases. In this particular case, the change in gadolinium concentration will also drive a change in neutron spectrum which could significantly reduce the correlations. Regardless, there is no current guidance on how to incorporate such observations as provided above into the validation of computation methods for criticality safety.

The appropriate treatment of the correlations can also change the bias itself. This result appears less common and, when present, less extreme than the impacts of the correlations on the uncertainty of the bias. Reference 17 presents a validation study using a general linear least-squares (GLLS) method including 77 experiments, including results for 5 separate subgroups of these experiments. For all 6 scenarios, the average deviation and its uncertainty is presented both with and without treatment of the correlations among the 77 experiments. The bias changes in all 6 cases, but there is no clear pattern to the changes in the bias values. This indicates that the impact of incorporating the correlations will vary among different applications. The change in the bias varies from +0.08% Δk to -0.06% Δk; these changes are clearly small and are typically less than half of the uncertainty in the bias.

In many criticality safety applications, the bias and bias uncertainty are combined and added to the calculated k_{eff} value, potentially in combination with other reactivity allowances, to determine the design k_{eff} value. This design value is then compared to the regulatory limits to demonstrate compliance, indicating one more area where an accurate assessment of the uncertainty in the bias is important. It is possible that the design k_{eff} value will result from a case that is not the most reactive calculated configuration if larger uncertainties apply to a

different case. This possibility is discussed in [28] and is a scenario which can result from an incomplete treatment of uncertainties.

This section has focused on the shortcomings of traditional validation techniques in the face of critical experiment correlations. Ultimately, the impact of these correlations will be determined in new methods which incorporate the correlation coefficient matrices. Some of these methods are discussed in a subsequent section of this proposal. Regardless of the magnitude of these effects, it is important to remember that the correlations are also needed for data adjustment techniques and must be determined.

Correlation Coefficient Determination

A range of methods has been proposed for the determination of critical experiment correlations. As is often the case, these methods can be broken down into deterministic methods and Monte Carlo methods. Each of the methods will be discussed in more detail in this section, but some general observations can be made here to compare and contrast the two approaches.

There are several key similarities between the deterministic and Monte Carlo methods for determining critical experiment correlations. The first similarity is that both require a detailed knowledge of the experiments' design and components. Such details include not just obvious parameters, like the materials used in the experiment, but also more subtle details related to the uncertainties in the compositions and dimensions of these components. Obviously it is also important to know which components and parameters are shared and which are not since these are the sources of the correlations. In many cases, information that is needed for accurate correlation calculations is not captured in the ICSBEP evaluation or primary source documents. These details relate to aspects that often seem irrelevant to modeling a single experiment. One example is whether the same rod is always placed in the same location in a lattice critical experiment, and another is whether or not reflecting walls are disassembled between experiments. Both of these examples can impact whether or not uncertainties relating to the fuel rods or reflector dimensions and position are shared among all the experiments in a series or are unique to each case. These types of details can have significant influence on the correlation coefficients and are needed in all methods.

The deterministic and Monte Carlo approaches to correlation determination also have noticeable differences. The deterministic methods tend to calculate sensitivities of k_{eff} to each uncertain parameter and combine these sensitivities with the parameter uncertainties to determine the overall uncertainty in each case. In this section, the reactivity uncertainty determined by multiplying the parameter uncertainty and the k_{eff} sensitivity is denoted δk_x. The x subscript is generic in this case, but specific subscripts are used to identify each term with a specific uncertain parameter. The shared uncertainties are then combined to determine the covariance and thus the correlation coefficient. This approach can lead to either a detailed subdivision of uncertainties until each component is clearly shared or unique or expert judgment of the correlation of the uncertainty that is partially shared and partially unique. The Monte Carlo methods sample dimensions and compositions within the expected

ranges, but this leads to potential difficulties in determining appropriate distributions from which to sample in many cases. These methods are also prone to questions of sufficiency of sampling and convergence. Also, the uncertain components must either use the same sampled values, for shared components, or different sampled values, for unique components; the methods do not include any methods for partially correlated samples. The Monte Carlo methods tend to require more computational time and resources, but are capable of handling very complicated problems. One complex model discussed in this section is a benchmark on correlation coefficients generated for the Nuclear Energy Agency (NEA) Working Party on Nuclear Criticality Safety (WPNCS) Expert Group on Uncertainty Analysis for Criticality Safety Assessment (UACSA) considering LEU pin array experiments. The Monte Carlo methods are capable of sampling the location of each pin uniquely in each case. It would be impossible to determine the sensitivity of k_{eff} to the position of each rod while each neighboring rod was also perturbed. On the other hand, the deterministic approaches are well suited for other examples such as some simple fast metal benchmarks. This example is also discussed in more detail later in this section. As would be expected, both deterministic and Monte Carlo approaches to calculating correlation coefficients have strengths and weaknesses and are best suited for different types of applications.

Deterministic Methods for Calculating Critical Experiment Correlation Coefficients

A variety of deterministic methods have been proposed for calculating critical experiment correlations. All of them involve using k_{eff} sensitivities and uncertainties (δk_x), combined with correlation coefficients among the correlated uncertainty contributors to calculate covariances and overall uncertainties. The covariances and δk_x values are used in turn to determine the correlation coefficients. Generally, the differences among these methods are related to how the k_{eff} sensitivities are calculated and how much decomposition of uncertain parameters is performed.

The first method proposed to quantify critical experiment correlations was proposed by Ivanova et al. in 2003 [17]. The uncertainties in the fundamental parameters (e.g., nitric acid concentration, impurity concentrations, etc.) are used to determine k_{eff} uncertainties derived from each uncertain parameter. These reactivity uncertainties are represented as a series of δk_x terms in [17], with a unique subscript applied for each parameter. The determination of these reactivity uncertainties is not described in the reference; the values are simply provided in Table I of [17]. In all cases, the reactivity uncertainties are provided in $\%k_{eff}$. These reactivity uncertainties are then combined using the square root of the sum of squares of the individual uncertainty components to calculate the uncertainty in the system k_{eff}. The covariance is determined using the formula shown in Equation 9, taken from [17]. The reactivity uncertainties related to uncertainty in enrichment (δk_ε), uranium concentration in solution (δk_U), nitric acid concentration (δk_{acid}), and impurities (δk_{imp}) are all assumed to be fully correlated. The reactivity uncertainty due to uncertainty in the solution density (δk_{sol}), the solution height (δk_h), the tank radius (δk_R) and the tank wall thickness (δk_t) are assumed to have variable degrees of correlation. The tank radius and wall thickness uncertainties, and associated reactivity uncertainties, are assumed to be fully correlated in the case of shared tanks and completely uncorrelated in experiments performed in different tanks. The

correlation for the uncertainty in the density determination, and the associated reactivity uncertainty, was assumed after discussions with the experimentalists regarding the uncertainty in the measurement and an estimate of the systematic and random components. Experiments carried out in the 1980s are assumed to be 50% correlated based on the assumption that the random and systematic components of the 1 mm solution height uncertainty are equal. The resulting reactivity uncertainty due to the solution height uncertainty is also therefore assumed to be 50% correlated. The solution height uncertainties for experiments carried out in the 1960s are assumed to be fully correlated since the tank was filled from the same dispenser. The assumed correlation coefficients for each of these individual components is represented as a $\gamma_x^{i,j}$ term in Equation 9. There is no evidence presented to defend either the partitioning of the uncertainties in the later experiments or the lack of any random uncertainty in the early experiments. This last point is indicative of the greatest weakness in this method: correlations of uncertain components are assumed in the process of calculating the covariances, which are used to calculate the overall experiment correlation coefficient. The resulting coefficients are therefore sensitive to underlying assumed correlation coefficients. In different ways all the methods for calculating correlation coefficients have shortcomings in areas where this sort of detailed information is lacking, and there is no evidence in [17] that the authors undertook a sensitivity study of their assumptions. The resulting correlations are therefore at least somewhat open to question, but have been included in [15] without such rigorous examination.

$$\delta k_i \delta k_j \rho_{i,j} = \delta k_{\varepsilon,i}\delta k_{\varepsilon,j} + \delta k_{U,i}\delta k_{U,j} + \delta k_{sol,i}\delta k_{sol,j}(0.64 + 0.36\gamma_{sol}^{i,j}) + \delta k_{acid,i}\delta k_{acid,j} + \delta k_{imp,i}\delta k_{imp,j} + \delta k_{h,i}\delta k_{h,j}(0.5 + 0.5\gamma_h^{i,j}) + (\delta k_{R,i}\delta k_{R,j} + \delta k_{t,i}\delta k_{t,j})\gamma_R^{i,j} \quad \text{Eqn (9)}$$

Where: δk_i is the total uncertainty in case i

Δk_j is the total uncertainty in case j

$\varrho_{i,j}$ is the correlation coefficient between cases i and j

$\gamma_{sol}^{i,j} = 0$ for two experiments performed with the solutions having different concentrations

$\gamma_{sol}^{i,j} = 1$ for experiments with the solutions of the same concentration

$\gamma_h^{i,j} = 1$ for experiments carried out in the 1960s

$\gamma_h^{i,j} = 0$ for experiments carried out in the 1980s

$\gamma_R^{i,j} = 0$ for experiments performed in different tanks

$\gamma_R^{i,j} = 1$ for experiments performed in the same tanks

Another deterministic method was proposed by Ivanova et al. in 2009 [29]. This newer method calculates partial correlation coefficients for each uncertainty component and then combines the partial correlation coefficients once each set of partial correlation coefficients is known. The equation for each partial correlation coefficient ($\varrho^n_{i,j}$) is shown in Equation 10 [29] and for the overall correlation coefficient ($\varrho_{i,j}$)in Equation 11 [29]. In both equations, δ^n_i and δ^n_j are the *n*th component of uncertainty for experiments *i* and *j*, respectively. Additional superscripts appear in Equation 10 to denote the random (r) or systematic (s) portions of the

components. Systematic portions are shared and random portions are unique to each experiment. It is evident from the equations that ultimately this formulation leads to the standard statistical formula for the correlation coefficient: covariance divided by the product of individual case uncertainties. In other words, Equation 11 is equivalent to Equation 9, used in the previous method, and both are detailed implementations of Equation 1.

$$\rho_{i,j}^{n} = \frac{\delta k_i^{n(s)} \delta k_j^{n(s)}}{\delta k_i^{n} \delta k_j^{n}}, \left[\delta k_i^{n}\right]^2 = \left[\delta k_i^{n(s)}\right]^2 + \left[\delta k_i^{n(r)}\right]^2, \left[\delta k_i\right]^2 = \sum_n \left[\delta k_i^{n}\right]^2 \qquad \text{Eqn (10)}$$

$$\rho_{i,j} = \frac{1}{\delta k_i \delta k_j} \sum_n \delta k_i^{n} \delta k_j^{n} \rho_{i,j}^{n} \qquad \text{Eqn (11)}$$

The method generated in [29] is used as the basis for the determination of critical experiment correlation coefficients used in data adjustment by the Working Party on International Nuclear Data Evaluation Co-operation (WPEC) subgroup 33 [30], and two related journal articles [31, 32]. In this implementation, there are three defined stages in the evaluation of the correlation coefficients. The first is to explicitly separate uncertainty components until each component is either wholly shared (systematic) or entirely independent (random). This approach eliminates the requirement in the 2003 Ivanova deterministic method [17] to estimate correlation coefficients for partially correlated uncertainty components. It is not always possible to make definitive assessments that components are either shared or unique, and it is not clear that sensitivity studies were attempted to investigate the impact of these determinations. The second stage is the summation of the common and independent uncertainties to calculate the total uncertainty in each experiment. The total uncertainty values are shown as the diagonal term in the covariance matrix, and would be unity in a correlation matrix. In this case, the uncertainties are presented in %; in a covariance matrix the diagonal term is typically the variance of the experiment. In this case, the standard deviation was shown because the experimental uncertainty is typically reported and not the variance. The final stage of the correlation coefficient calculation is to determine the correlation coefficients for all the off diagonal terms using the standard correlation coefficient formula. In some cases considered in [30], there was insufficient information available to determine correlation coefficients so values were copied from a different experiment. Once again, no sensitivity studies are provided to investigate the impact of this assumption. The experimental covariance matrix generated in [30] is shown in Figure 1. The diagonal of the matrix presents the total experimental uncertainty for each case and the off-diagonal terms are the correlation coefficients between cases. The method proposed in [30] generally works well as applied in part because only 20 total experiments are considered and the experiments are drawn from different series at different laboratories. Most criticality safety validations consider a larger number of experiments, and frequently many cases from each of several series. In such cases with a great number of common uncertainty components, the method proposed in [30] may present intractable problems. The separation of components until they are entirely shared or unique, Stage 1, is the most likely source of such difficulties.

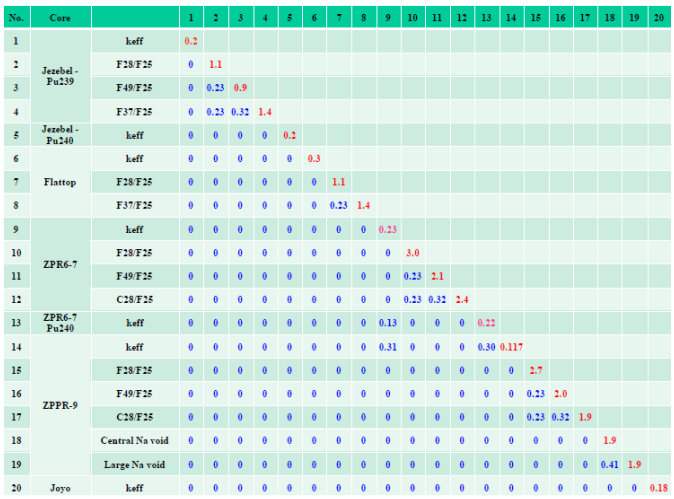

No.	Core		1	2	3	4	5	6	7	8	9	10	11	12	13	14	15	16	17	18	19	20
1	Jezebel - Pu239	keff	0.2																			
2		F28/F25	0	1.1																		
3		F49/F25	0	0.23	0.9																	
4		F37/F25	0	0.23	0.32	1.4																
5	Jezebel - Pu240	keff	0	0	0	0	0.2															
6	Flattop	keff	0	0	0	0	0	0.3														
7		F28/F25	0	0	0	0	0	0	1.1													
8		F37/F25	0	0	0	0	0	0	0.23	1.4												
9	ZPR6-7	keff	0	0	0	0	0	0	0	0	0.23											
10		F28/F25	0	0	0	0	0	0	0	0	0	3.0										
11		F49/F25	0	0	0	0	0	0	0	0	0	0.23	2.1									
12		C28/F25	0	0	0	0	0	0	0	0	0	0.23	0.32	2.4								
13	ZPR6-7 Pu240	keff	0	0	0	0	0	0	0	0	0.13	0	0	0	0.22							
14	ZPPR-9	keff	0	0	0	0	0	0	0	0	0.31	0	0	0	0.30	0.117						
15		F28/F25	0	0	0	0	0	0	0	0	0	0	0	0	0	0	2.7					
16		F49/F25	0	0	0	0	0	0	0	0	0	0	0	0	0	0	0.23	2.0				
17		C28/F25	0	0	0	0	0	0	0	0	0	0	0	0	0	0	0.23	0.32	1.9			
18		Central Na void	0	0	0	0	0	0	0	0	0	0	0	0	0	0	0	0	0	1.9		
19		Large Na void	0	0	0	0	0	0	0	0	0	0	0	0	0	0	0	0	0	0.41	1.9	
20	Joyo	keff	0	0	0	0	0	0	0	0	0	0	0	0	0	0	0	0	0	0	0	0.18

Figure 1. Experimental uncertainty matrix generated in [30].

The third deterministic approach in the literature was proposed by Ivanova, Ivanov, and Bianchi in 2014 [27]. This approach includes different methods depending on the physics of the system being studied. Fast spectrum systems use a method essentially equivalent to that proposed in [29], with sensitivities determined in homogenized models and perturbation theory algorithms in a neutron diffusion theory code. Reference [27] is also the only deterministic method to present an approach for calculating correlation coefficients for LEU pin array benchmarks. The experiments considered are LEU-COMP-THERM-007 and LEU-COMP-THERM-039 from [15]; these experiments are the primary experiments considered in the UACSA benchmark on critical experiment correlations [33]. The underlying method for determining the correlation coefficients is the same as for fast systems, proposed in [29], but the reactivity sensitivities (δk_x) are determined using three-dimensional (3D) Monte Carlo calculations. The pin arrays in some cases considered from LEU-COMP-THERM-039 [15] include two regions: one with a full lattice of fuel rods and the other with every other rod removed. Sensitivity coefficients are determined for each region of the model after it has been artificially partitioned in this way. Some sensitivities are quite well behaved, as shown in Figure 2 (Fig. 5 of [27]). Unfortunately, some of the resulting sensitivities are not well behaved. An example of this behavior is shown in Figure 3, which is Fig. 7 of [27]. The overall correlations coefficients for the cases within LEU-COMP-THERM-039 are quite high, between 0.989 and 0.999, which is in good agreement with results from a Monte Carlo approach to be discussed in the next section [34]. These coefficients result if the spacing among all pairs of pins is assumed to be constant. The approach used in [27] cannot be used if the position of each fuel rod is assumed to be independent because the number of independent sensitivity calculations that are required becomes too large.

The final deterministic method is proposed in [35]. This method uses uncertainties taken from the ICSBEP evaluation [15] and identifies the largest contributors to total uncertainty. These controlling uncertainties are then classified as shared or unshared, and decision trees are used to assign the fraction of shared uncertainty. Unfortunately, the shared uncertainty

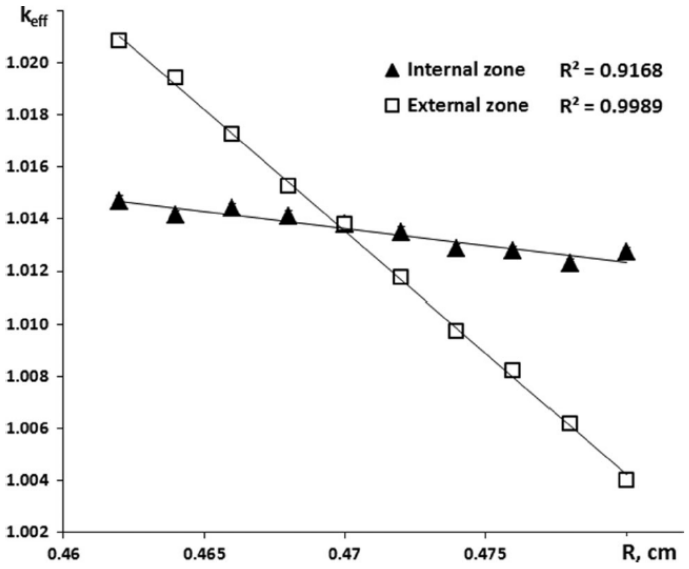

Figure 2. Well behaved sensitivity calculation presented in [27].

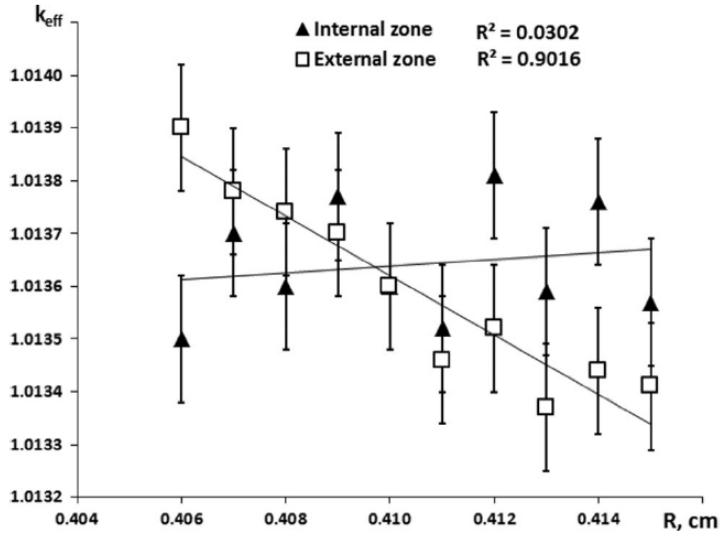

Figure 3. Poor sensitivity calculation presented in [27].

fractions are completely subjective and selected without any documented evidence for the values chosen. Such values can never be rigorously defended to a regulator, and essentially reduce the determination of correlation coefficients to arbitrary choices. The method touts its reproducibility and transparency; the method is transparent to the extent that it can be documented in a spreadsheet and reproducible if the shared uncertainty fractions can be universally identified. No method is proposed in the reference for establishing such universal uncertainty sharing rules. The proposed method is rigorous in identifying the controlling uncertainties, but does not significantly alter the difficulties in determining the shared or unique uncertainty components. There is also no attempt at providing a justification for the values chosen to generate a large number of correlation coefficients.

Monte Carlo Methods for Calculating Critical Experiment Correlation Coefficients

One basic Monte Carlo approach to the determination of critical experiment correlations has been proposed [22], and the method has been implemented in at least two code packages. One is the Sampler sequence in SCALE 6.2 from Oak Ridge National Laboratory (ORNL) [16, 36] and the other is the Sensitivities and Uncertainties in Criticality Inventory and Source Term Tool (SUnCISTT) developed at the Gesellschaft für Anlagen- und Reaktorsicherheit (GRS) [37]. This section first presents the general Monte Carlo method for determination of critical experiment correlations and then reviews several studies using the method in the implementations mentioned above.

The primary reference for the development of critical experiment correlations via Monte Carlo sampling is [22], which expands on general Monte Carlo applications to criticality safety presented in [38]. Conceptually, the Monte Carlo approach is straightforward. A series of realizations of the critical experiment model are created with the inputs sampled from random distributions describing the underlying distribution believed to represent the parameters. Shared quantities, such as the dimension of common parts or the number densities of shared materials, use the same sampled values for these common parameters in each realization. Unique parameters are sampled independently. After a sufficient number of realizations has been generated and used, the calculated k_{eff} values are used to determine covariance for all pairs of experiments and uncertainty values for each individual experiment. These quantities are then used to determine the correlation coefficient. The difficulties in this technique primarily arise in the implementation. A large number of realizations is required to assure convergence of the correlation coefficient, and distributions must be determined that represent the uncertain parameters appropriately. Another difficulty, which is shared with the deterministic methods, is the determination of shared and unique parameters. As with the deterministic methods, partially correlated uncertainties, those coming from a combination of systematic and random contributions, present additional challenges. The primary advantage of the Monte Carlo method is that it can be used to calculate uncertainties and covariances without separately determining sensitivities for individual uncertainty components. As mentioned previously, the correlation coefficient is calculated directly from the system k_{eff} values resulting from the perturbed models. The difficulty of determining a reactivity sensitivity for each independent system parameter is exacerbated for LEU pin array systems in which each pin is positioned independently.

The fundamental approach to the Monte Carlo sampling sequence Sampler within SCALE 6.2 is outlined in [36], and more details are provided in the SCALE manual [16]. The first use of Sampler to determine correlations for critical experiments is documented in [36], and includes all ten cases in HEU-SOL-THERM-001 [15]. The results presented are essentially a proof of principle implementation, and not all uncertain parameters were considered.

The next published use of Sampler for the determination of critical experiment correlations is presented in [39]. In this case, the seven cases of LEU-COMP-THERM-042 [15] were considered. The calculated total uncertainty in k_{eff} for each case is not presented, but it is noted that the assumptions made regarding fuel pin pitch sampling are the largest influence in the calculated correlation coefficients. It is reasonable to assume that this parameter also has a significant impact on the resulting uncertainties for each case. A figure is presented in [39] showing the dependence of the correlation coefficients on the range of pin pitches sampled; this figure is reproduced here in Figure 4.

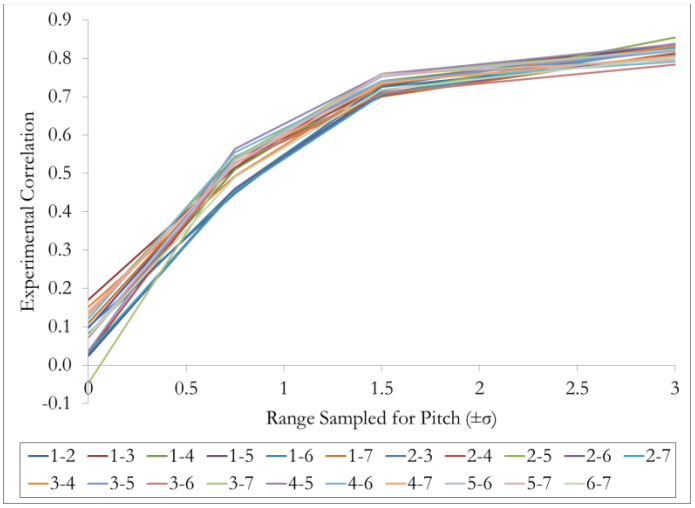

Figure 4. Critical experiment correlations for LEU-COMP-THERM-042 vs. range of pitch sampling [39].

Additional studies using Sampler to investigate critical experiment correlations are presented in [40] for both LEU-COMP-THERM-042 [15] and the LEU-COMP-THERM-007 and LEU-COMP-THERM-039 [15] experiments used in [33]. Similar information is presented regarding LEU-COMP-THERM-042, but in this paper the overall case uncertainties are reported. In most cases, the reported uncertainty from the Sampler calculations is on the order of 1.5 times that reported in the evaluation if the pitch is sampled uniformly over the range of $\pm 3\sigma$. This may indicate that the uncertainties are not being sampled within the appropriate ranges or with the appropriate distributions. Based on the individual case uncertainties presented in Table III of [40], the individual case uncertainties are in good agreement with the evaluation when the pitch is sampled over the range of $\pm 0.75\sigma$. It seems unlikely that the pin pitches are all within 0.75σ of the nominal value, so this likely is an indication that the assumption that all pin pitches are identical is not adequate to capture the overall uncertainties correctly.

Several different papers have presented preliminary results for the UACSA benchmark proposed in [33] and its earlier revisions. As mentioned in the previous section, [34] presents results from a draft in which all pin pitches are assumed to be identical. This scenario was considered in [27] using a deterministic method, and is also included in [40]. The case uncertainties resulting from the uniform pitch assumption are typically on the order of three times as large as the evaluated uncertainty, according to Table VII of [40]. This uncertainty is most likely the result of the pitch assumption, and is thus shared among all cases. The pitch uncertainty causes the large k_{eff} uncertainties. It is evident in Figure 4 of [40] that the uncertainty is significantly lower for cases with different pitch assumptions. A range of different assumptions is investigated in [41], including a fully random pin position treatment. This scenario lowers the correlation coefficients to something on the order of 0.6, but still considers significant shared uncertainty based on the fuel content in each rod. Different assumptions lead to other correlation coefficients, ranging from near 0 [42] to approximately 0.3 [43]. The results are sensitive to assumptions made about fuel composition in various cases and among the fuel rods, to the Monte Carlo uncertainty of each k_{eff} calculation, and, to some degree, to the number of realizations. It is evident that the treatment of pin pitch uncertainties drives the overall correlation coefficients. Meanwhile, significant work remains to understand the dependence of calculated correlation coefficients on other input assumptions and it is clear that detailed knowledge of the experiments being modeled is required to generate reliable correlations.

Application of Correlation Coefficients

As discussed in earlier sections, critical experiment correlation coefficients have application to multiple types of analyses. Much of the focus of this literature review has been related to criticality safety validation, but an equally important implementation of correlation coefficients is in data adjustment techniques. There have also been proposals to use data adjustment as part of the criticality safety computational method validation process [44, 45].

Many of the earliest documented investigations of critical experiment correlations included validation results demonstrating the impact of the correlations [17, 29]. As discussed previously, the primary impact demonstrated in these early references is an increase in the bias uncertainty that can be as large as a factor of almost 2 [17]. Other research has investigated generic application of correlation coefficients to trending analyses as typically performed in validation. One example in the literature uses a CERN statistical package, ROOT [46], with an add-on from the Karlsruhe Institute of Technology called RooFiLab [47] to perform trending of critical experiments with the independent variable the energy of the average lethargy of neutrons causing fission (EALF) [48]. It is clear that something is wrong with the implementation in this case, as it claims a positive bias (overprediction of k_{eff}) despite all benchmarks being calculated with lower than expected k_{eff} values. It is possible that further development in this area has resolved the issue, but no publications can be found providing updated results.

Different approaches have been developed for integrating the effect of critical experiment correlations on the results of criticality safety validations using Bayesian updating techniques

[49, 43]. The Bayesian updating approach is very different from the frequentist approaches used in the guidance documents referenced above [23, 24, 25], but has been favored in recent years particularly in Germany [38]. The results presented in [49] consider a toy model and the experiments included in the UACSA benchmark [33]. The toy model is defined in Appendix I of [33], and is intended to simplify comparisons among different mathematical approaches for calculating and applying correlation coefficients without the complications associated with modeling real systems. For the toy model, lower correlations lead to a lower post-adjustment k_{eff} and higher confidence than do higher correlations for the prior distribution. The post-adjustment k_{eff} is lowered by the Bayesian adjustment process. A figure showing the prior and post adjustment distributions for the toy model is included here in Figure 5. The results from the UACSA benchmark are not quite as well behaved in that the mean of the post adjustment distributions of k_{eff} values are closer to the mean of the prior distribution than is the post adjustment distribution without accounting for correlations, as shown in Figure 6. These results do share the narrowing of the distribution post adjustment with the toy model; lower correlation coefficients result in significantly narrower distributions of post adjustment k_{eff} values. This is consistent with other results indicating that the primary effect of critical experiment correlations is to increase the uncertainty. This increased uncertainty manifests in Bayesian updating schemes as a wider post adjustment distribution. The effect on the bias itself varies among different validations because of different benchmarks and application systems.

Another approach has been proposed [50, 51] to integrate correlation coefficients into the frequentist validation approaches suggested in the guidance documents discussed earlier [23, 24, 25]. This method incorporates the covariance matrix into the trending process, but potentially suffers from some shortcomings. First, it is assumed that the dependent variable, that is k_{eff}, has a linear dependence on the independent variable. In this case, the independent variable could be any of the typical parameters used in validation trending such as EALF, enrichment, fuel pin pitch, or others. Also, the method assumes that the computational bias has a multivariate normal distribution with zero mean. It is unclear how this multivariate normality assumption would be checked or confirmed. The computational bias is also not zero, though the impact of this is not discussed in the literature. Furthermore, it is assumed that the distribution of critical experiments is also normal. This assumption is frequently violated when multiple series of experiments are considered; the data are often clumped because of correlations within the experiment and thus are not distributed normally. The method does have positive characteristics as well, including the potential to be expanded to multivariate trending. Typically, a series of separate trends is generated and the most conservative bias or bias and uncertainty is used. An example validation is presented in both papers [50, 51] for a plutonium system and 30 experiments. The results are shown in Figure 7, taken from [51]. A comparison is possible for the proposed method and other standard methodologies. The USL1 and USL2 values generated by the USLSTATS trending program [Appendix C of Reference 24] are shown along with the single-sided simultaneous tolerance band recommended in [23]. If all experiments are assumed to be uncorrelated, shown in Figure 7 as the red triangles with 0% correlation, the proposed methodology replicates the simultaneous tolerance band perfectly. Larger assumed correlations lower the USL because the uncertainty in the trend is increasing. The USL is

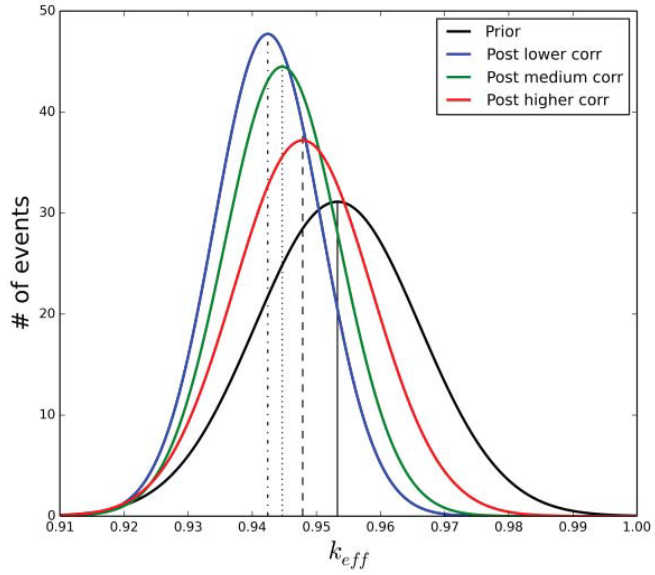

Figure 5. Prior and post update distributions for the Toy Model, from [49].

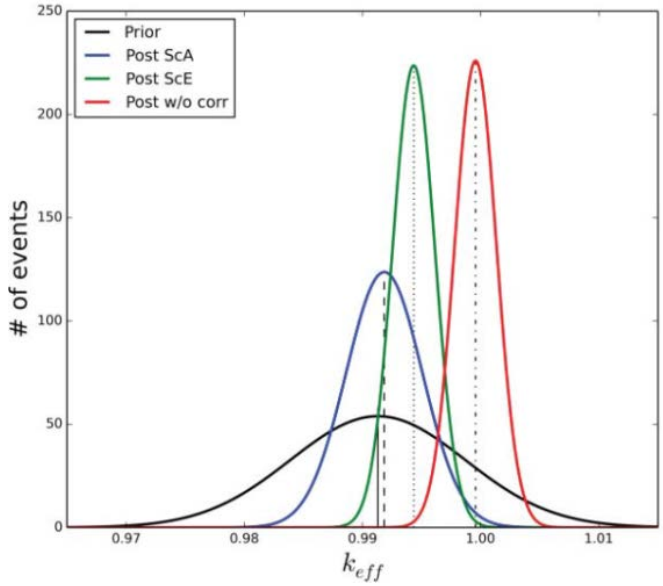

Figure 6. Prior and post update distributions for LEU-COMP-THERM-079, from [49].

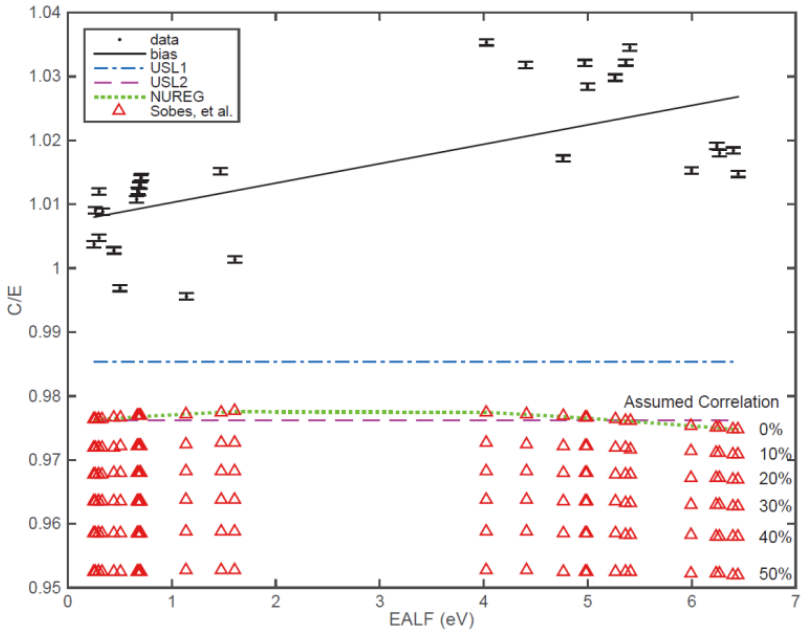

Figure 7. Comparison of proposed validation technique including critical experiment correlations with currently recommended techniques [51].

lowered by ~2.5% Δk if all the experiments have correlation coefficients of 0.5. This is in good agreement with other results discussed previously that accounting for the correlations present among benchmark experiments can significantly increase the uncertainty of the computational bias in a criticality safety validation.

A new area that should include the application of critical experiment correlations is the MCNP Whisper methodology for validation [45, 52]. The Whisper methodology incorporates many different aspects of sensitivity/uncertainty analysis to select and weight experiments for trending in validation. The method utilizes extreme value theory (EVT) [53] to generate a conservative USL. EVT has some similarities to the non-parametric methods suggested in [23] for use when the benchmark experiments are not normally distributed. Whisper also uses a data adjustment process based on the GLLS method, but unlike TSURFER [27] the Whisper GLLS implementation does not consider correlations among the experiments. Furthermore, there is no treatment of critical experiment correlations anywhere else in the methodology. Currently, because "assigning meaningful correlation values to the set of benchmarks would require extensive studies taking years of effort, these benchmarks are currently assumed to be uncorrelated" [52]. Instead, a 99% confidence interval is used because it "should provide enough conservatism to account for this approximation" [52]. No quantitative estimates of the conservatism introduced by shifting from the 95% confidence interval to the 99% confidence interval is provided, nor is any estimate of the impact of accounting for correlations provided. It is therefore impossible to draw any conclusion regarding the veracity of the lack of explicit treatment of correlations among the benchmark experiments.

Another area in which data adjustment techniques, and thus critical experiment correlations, have been applied within the literature is in the examination of nuclear data for use in fast reactor systems [30, 31, 32]. Recent work in this area has also proposed using these techniques within criticality safety validation [44, 45, 52, 54, 55]. The correlations among experiments are needed to constrain the data adjustment process. Nonphysical adjustments could be determined through the data adjustment process if the proper correlations are not supplied to force similar adjustments to be made to correlated systems. The proposals to use data adjustment techniques in criticality safety validation are based on using the final data adjustments to calculate a bias in the application system [44, 54]. This is accomplished by propagating the adjustments with the system sensitivities. The lack of viable critical experiment correlations has been a significant impediment to the implementation of these methods. No statement is made in Ref. [55] regarding the correlation coefficients assumed in the results presented in Appendix C. Ref. [54], however, includes a sensitivity study to various assumed correlations, and concludes that statistically significant differences are introduced in the data adjustments. This is a strong argument that reliable, high-fidelity correlation matrices are needed.

CHAPTER III: DESCRIPTIONS OF COMPUTER CODES, EXPERIMENTS, AND MODELS

The primary purpose of determining critical experiment correlations is to enable a more accurate accounting for them in criticality safety validation and data adjustment studies. Two computer codes are used for the majority of the calculations presented here determining an appropriate methodology for the determination of experimental correlations via the Monte Carlo sampling method first proposed in [22]. The neutron multiplication factor, k_{eff}, for each realization of each critical experiment model is generated using the KENO V.a Monte Carlo transport code embedded in the CSAS5 sequence in SCALE 6.2 [16]. The Sampler sequence from SCALE 6.2 [16] is responsible for the generation of the perturbed models used to determine the variances and covariances, and hence the correlation coefficients, of the various critical experiments. Each of these sequences is described here in some detail. First, a description is provided of the SCALE TemplateEngine, which is used extensively to facilitate the creation of repetitive sections of the large KENO and Sampler inputs required in several portions of this work. After discussion of KENO and Sampler, this section concludes with a brief description of a FORTRAN program written to calculate correlation coefficients for the LEU-COMP-THERM-042 and HEU-SOL-THERM-001 experiments.

The SCALE TemplateEngine

The SCALE TemplateEngine was introduced with the release of SCALE 6.2. It allows for variables to be embedded in input and evaluated at the time of execution and expanded or replaced with values that support SCALE execution. Templates can also be evaluated off-line, via command line execution of the TemplateEngine. This tool is particularly useful in this research as simple input patterns are repeated hundreds of times in some inputs. This use is described in detail, including examples, in this section.

As discussed below, the geometric description of space in the KENO V.a Monte Carlo code involves repeated structures, called *arrays*, that may include multiple instances of the same unit cell. Each of these basic, self-contained portions of the problem geometry is called a *unit*. In the LEU lattice systems modeled in this work, a single fuel rod (also referred to as a pin) and the surrounding water and support plate make up a unit. The array of rods can thus be modeled as a repeating array of this unit; however, unique units are needed for each rod if the rods are to be positioned independently from each other within their units. An example of the input describing the geometry of a typical fuel rod unit is provided below in Figure 8. The geometry and materials for each of the hundreds of fuel rods modeled in the problem are identical, but each fuel rod must be created in its own unit to allow the modification of its position by Sampler to be performed uniquely. An example of the TemplateEngine input used to facilitate this is shown in Figure 9, along with a portion of the input created by the TemplateEngine in Figure 10. Note that the *for* construct on the first line of Figure 9 allows the same unit to be created 1170 times. Also, the expression enclosed in braces is evaluated such that the unit number generated, as shown in Figure 10, is 20001. The 1170 "fueled section" units generated are numbered 20001 to 21170 in the full input.

```
104 unit 2
105 ' fueled section
106  cylinder 1 1  0.5588 91.44 0
107  cylinder 6 1  0.6350 91.44 0
108  cuboid   9 1  0.842 -0.842  0.842 -0.842  91.44 0
```

Figure 8. Example input to KENO for a fuel rod unit.

```
1 #for(i=1; i<=1170; i=i+1){
2 '
3  unit #{20000+i}
4 ' fueled section
5  cylinder 1 1  0.5588 91.44 0  origin 0 0
6  cylinder 6 1  0.6350 91.44 0  origin 0 0
7  cuboid   9 1  0.842 -0.842  0.842 -0.842  91.44 0
```

Figure 9. Example TemplateEngine input for the example fuel rod unit provided in Figure 8.

```
111 unit 20001
112 ' fueled section
113  cylinder 1 1  0.5588 91.44 0  origin 0 0
114  cylinder 6 1  0.635  91.44 0  origin 0 0
115  cuboid   9 1  0.842 -0.842  0.842 -0.842  91.44 0
```

Figure 10. Portion of the KENO input generated by the TemplateEngine input shown in Figure 9.

The TemplateEngine is also used to create the Sampler input to modify each of the thousands of units created as described above. The looping functionality provided by the *for* construct is used in the same way as described above to loop over all 1170 instances of the fuel rod unit cells. Examples of the TemplateEngine input for Sampler are not provided here because they are significantly longer than the KENO input.

CSAS/KENO

The CSAS5 sequence within SCALE [Section 2.1 of 16] provides automated cross-section resonance processing and three-dimensional (3D) neutron transport via the Monte Carlo technique. The multigroup (MG) processing is provided by XSProc [Section 7.1 of 16], incorporating the functions provided in earlier SCALE releases by BONAMI, CENTRM, PMC, and WORKER. The working library generated by XSProc is then passed to KENO V.a for the calculation of the effective neutron multiplication factor, k_{eff}. A flowchart of the entire sequence is provided in Figure 11.

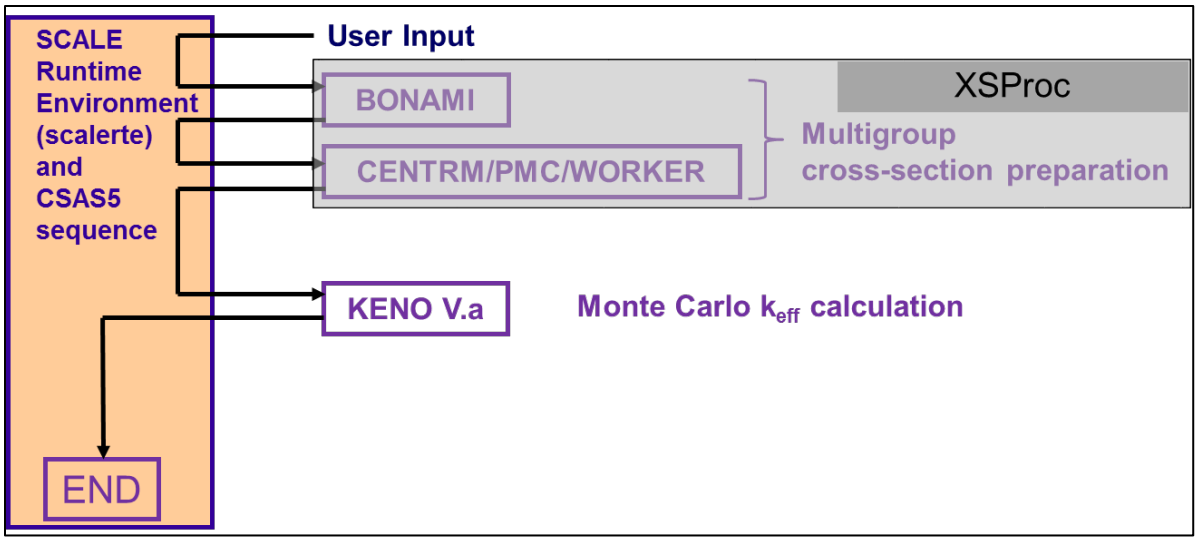

Figure 11. Flowchart of the CSAS5 sequence for multigroup k_{eff} calculations.

KENO V.a [Section 8.1 of 16] is a 3D Monte Carlo transport program used within SCALE primarily to calculate k_{eff} values. The geometry capabilities are somewhat restricted, but these limitations allow for significantly faster execution times compared to generalized geometry alternatives. KENO V.a supports all the geometric descriptions needed in this work, including primarily cylinders and rectangular parallelepipeds (called *cuboids* in KENO). Complete descriptions of the geometry capabilities, physics treatments, and numerical methods used in KENO V.a can be found in [Section 8.1 of 16] and [56].

The repeated geometry structure capabilities in KENO are especially useful when modeling systems such as LEU pin arrays. The repeated structure is referred to as an *array*, and is composed of several *unit*s. Each unit is a self-contained geometry region with a cuboid as its outer boundary. These requirements are well suited for fuel pin arrays with a square pitch, or

configuration. As discussed in the previous section, a single pin can be defined and used as many times as necessary to describe the desired model. Each pin must be modeled in its own unit for Sampler to modify unique pin positions. A simple input which contains a single unit cell might consist of fewer than 75 lines of input to fully describe a problem containing an array of over 1100 rods. The same input, with unique fuel rod units, expands to over 35,000 lines. This huge volume of input necessitates the use of the TemplateEngine, as discussed in the previous section.

Most of the calculations performed in this effort use the 252-group neutron cross section library based on ENDF/B-VII.1 [57]. As mentioned above, the MG cross section processing is provided by XSProc. The unit cells used for this processing are either the SQUAREPITCH LATTICECELL or the infinite, homogeneous medium (INFHOMMEDIUM) cell. The fuel rod unit cells are processed as LATTICECELLs, and other mixtures are processed as infinite homogeneous medium cells. Some calculations are performed with KENO in continuous energy mode to confirm that the MG results are accurate.

Sampler

The Sampler sequence is the most important computer code used in this research. Sampler [Section 6.7 of 16] is referred to as a "super-sequence" within SCALE because it wraps around other sequences, such as CSAS, and perturbs inputs via Monte Carlo sampling. This section will provide a detailed description of several aspects of Sampler that are used for the determination of critical experiment correlations in this work. It should be noted that none of the nuclear data sampling capabilities are used at all; these capabilities are described in [Section 6.7 of 16]. The composition and dimension sampling used here is activated with the *perturb_geometry* option.

Methodology and Terminology

As mentioned above, Sampler performs perturbations of input parameters as directed by user input to quantify uncertainties in and correlations among various models and model parameters. Sampler uses the term *case* to identify a unique input model; for example, the seven experiments within the LEU-COMP-THERM-042 evaluation [15] are seven different cases. Each complete perturbed model written by the sequence is referred to as a *sample*, though the term *realization* will also be used in this work. Each sample or realization is a complete input with sampled values used for all specified inputs. The number of individual variables sampled, which ranges from a few to over 10,000 depending on the scenario, does not change the number of samples reported even though vastly differing numbers of random numbers are used.

Sampler generates a nominal model, designated perturbation 0, using nominal values for all sampled variables. This case provides an input to confirm that all nominal values are correctly specified and that all expressions are evaluated correctly.

In the work described here, KENO models for each case are created prior to Sampler input generation. The inputs are imported in *case blocks* in the Sampler input; each case gets a unique case identifier in the input. LEU-COMP-THERM-042-001, for example, is designated as "Case1" in Sampler input. Because the inputs are imported in the case block, and not specified with placeholders, the SCALE Input Retrieval Engine (SIREN) is used to create the perturbed inputs. A description of SIREN and its use is provided below.

Sampler has the capability to run the perturbed cases, but this capability is not used in this work. Instead, the perturbed inputs are generated and subsequently run on the *Romulus* cluster at Oak Ridge National Laboratory. Romulus is a homogenous cluster consisting of over 1200 cores, allowing for the execution of a large number of SCALE calculations at the same time. The homogeneity of the cluster hardware and software ensures that only differences in the Monte Carlo transport simulations will be a result of input perturbations, not different random numbers or round-off errors. This guarantees repeatability for identical calculations, but also allows calculations to be run on different nodes without introducing differences in calculated results. Such differences introduced by different random numbers would act to artificially decrease correlation among experiments. The load leveling of the Sampler and subsequent KENO calculations, as well as any other work on the cluster, is performed by a scheduler on the cluster. This is usually more convenient than the job management capabilities available in Sampler with the SCALE 6.2 release.

The KENO models are developed first, as discussed in a subsequent section of this report. The Sampler input can then be developed to perturb the desired values in the KENO input. Perturbations are applied to most number densities, temperatures, and dimensions used in the models. The details of the distributions available in Sampler and input specifications are provided in a subsequent subsection of this section.

Each variable in Sampler is applied to a user specified case or set of cases. This allows for the correlation of random variables that is the crux of this research. Inputs that are sampled uniquely are applied to just the relevant case, whereas shared values are applied to multiple cases. For example, all cases with the same fissile material would use the same sampled value of the ^{235}U number density in each sample. This is the situation for LEU lattice experiments that use the same fuel rods in all cases within the evaluation. Different values would be sampled for cases with differing fissile materials, such as multiple different solutions used in solution experiments. The same initial random number seed is used in all Sampler executions, so it is possible to replicate the same stream of random numbers in different inputs. In some cases, this behavior is advantageous but in others it is problematic. Further details will be provided later in this report, as necessary, in discussing the details of modeling for each experiment.

Sampler post-processing capabilities are not used in this work. Instead, a series of scripts have been written to collect the k_{eff} values resulting from the KENO outputs of the perturbed cases. Some correlation coefficients have been calculated in spreadsheets, and others have been calculated using a FORTRAN utility written for calculating correlation coefficients and their confidence intervals. The FORTRAN utility is described later in this section.

Variable Blocks

The majority of the Sampler input is in the form of *variable blocks*. Following parameter inputs and case blocks, the entirety of the input is the definition of variables and desired responses. In this work, no responses are collected so no input is provided in the *response block*. Four types of variables are supported in Sampler: uniform distributions, normal distributions, beta distributions, and expressions.

The uniform distribution, also called a constant distribution in Sampler, is specified with the keywords *distribution=uniform*. The inputs are a nominal value and the maximum and minimum values. The nominal value is used in the nominal case. The value of the variable is sampled uniformly between the minimum and maximum values specified for all perturbed cases. An example of a uniform variable input block is shown in Figure 12.

```
55 read variable[u235_mass_per_rod]
56   distribution=uniform
57   minimum = 17.0513 value = 17.08 maximum = 17.1087
58   cases = Case1  end
```

Figure 12. Example variable input block demonstrating the uniform distribution.

The normal distribution is specified with the keywords *distribution=normal*, and samples from a user-specified normal (Gaussian) distribution. Sampler supports sampling from either an infinite or a truncated normal distribution. In both cases, the nominal value and the standard deviation are provided. For the truncated distribution, maximum and/or minimum values are also specified. Sampled values beyond the truncation limits are discarded, and the value of the variable is resampled until an acceptable value is generated. It should be noted that there is no capability to sample directly from an offset normal distribution, that is one that is normally distributed about a value other than the nominal value for the variable. Such a distribution could be generated by sampling from a normal distribution, and subsequently shifting the sampled value appropriately using an expression to account for the difference between the average and nominal values. An example of a truncated normal variable input block is shown in Figure 13.

```
85 read variable[wo_u235]
86   distribution = normal
87   value = 2.35
88   stddev = 0.00333
89   minimum = 2.34
90   maximum = 2.36
91   cases = Case1  end
92 end variable
```

Figure 13. Example variable input block demonstrating the normal distribution.

The third distribution that can be used within Sampler is the Beta distribution. This option is specified with the keywords *distribution=beta*. The beta distribution is a family of distributions defined by two parameters, α and β, allowing a range of different symmetric or skewed distributions to be created. The Beta function is defined as shown in Equation 12 [16]:

$$f(x;\alpha,\beta) = \frac{\Gamma(\alpha+\beta)}{\Gamma(\alpha)\Gamma(\beta)} x^{\alpha-1}(1-x)^{\beta-1} \quad \text{Eqn (12)}$$

Where: f(x; α, β) is the Beta distribution
Γ(α+β) is the gamma function of α+β
Γ(α) is the gamma function of α
Γ(β) is the gamma function of β
Γ(n) = (n-1)! [58]

The Beta distribution is defined on the interval from 0 to 1, so the minimum and maximum values are input to Sampler so that the distribution can be scaled to the appropriate range desired by the user. The α and β parameters are also provided, as is a nominal value. The beta distribution is used vary sparingly in this work, as there are essentially no instances in which the distribution of a parameter is known or expected to be skewed. An example of a beta distribution variable input block is shown in Figure 14.

```
1037 read variable[plex_t5]
1038   distribution = beta
1039   beta_a = 4
1040   beta_b = 2
1041   minimum = 0 value = 0.296 maximum = 0.394667
1042   cases = Case5 end
1043 end variable
```

Figure 14. Example variable input block demonstrating the beta distribution.

The final option for the *distribution* keyword is *expression*. This option allows the value of the variable to be set as a constant, user-specified value or calculated using other variables defined throughout the input. The complete list of supported operations is provided in Section 6.7B of [16] and is sufficient for all applications in this work. An example of the use of the expression option to calculate a value is inputting atomic weights for the calculation of number densities when other parameters, such as density or enrichment, have been sampled. Expressions to calculate the value of a variable are used in many instances, including calculating the balance of a set of isotopic abundances to ensure that the abundances sum to 100%. Expressions are also used in many geometry variables in which an outer boundary may be calculated from a sampled inner boundary and a sampled thickness. The distribution option is the most common type of variable block used in this work. An example of a distribution variable input block is shown in Figure 15.

```
47 read variable[fuel_rad_comps]
48   distribution = expression
49   expression = "fuel_diam_comps / 2"
50   cases = Case5  end
51 end variable
```

Figure 15. Example variable input block demonstrating an expression.

SIREN

SIREN is used within Sampler to change values within a SCALE input. A complete description of SIREN is provided in Appendix 6.7A of [16], and a summary is provided here. The discussion here will focus on SIREN input and use, and not on the details of the software implementation.

The key concept enabling SIREN use is the creation of a document object model, or DOM, from the SCALE input. This allows each individual piece of input, or token, to be identified uniquely and specified using an XPath designation. These XPath designations are akin to a dendritic file structure. The DOM can be created and viewed using the *InputViewer* executable provided with SCALE.

The highest level of the DOM is the sequence being executed, which for all the calculations performed in this work is CSAS5. The next level is the SCALE input block, for example *comps* for composition block or *geom* for the geometry block. The names used in the DOM for each input block are fixed, regardless of the specific declaration used in the CSAS input. This can be very useful when modifying several cases at once because the underlying CSAS inputs may have been developed with different terse block names. The lower levels of the XPath depend on the block, but ultimately each numerical input is a leaf in the DOM. Each of these leaves can be selected and changed via SIREN statements. Figure 16 shows an example variable block including a SIREN statement for changing an isotopic number density. Figure 17 shows a similar variable block with a SIREN statement for changing the diameter of the fuel in the celldata block. As shown in both figures, the sequence level of the DOM can be omitted in these cases since both instances occur in the only sequence in this input file: CSAS5. The slash is still required to maintain the appropriate hierarchy level, hence the consecutive forward slashes at the beginning of the SIREN statements.

```
read variable[atom_density_u235]
  distribution = expression
  expression = "(u235_g_density * avogadro)/atomic_mass_u235"
  siren = "//comps/stdcomp[name='u-235']/aden"
  cases = Case5  end
end variable
```

Figure 16. Example variable block with a SIREN statement modifying ^{235}U number density.

```
read variable[fuel_diam_geom]
  distribution=uniform
  minimum = 1.1049 maximum = 1.1303 value = 1.1176
  siren="//cells/lattice/fueld/dimension"
  cases = Case1 Case2 Case3 Case4 Case5 Case6 Case7 end
end variable
```

Figure 17. Example variable block with a SIREN statement modifying the fuel diameter in the celldata block.

SIREN supports a range of options for resolving potential conflicts within the DOM. This disambiguation can be performed with names, for example, when changing standard compositions. An example of this is shown in Figure 16, using "stdcomp[name='u-235']". This can be interpreted as "select the standard composition whose name is u-235." Mixture

numbers can also be used to select one or more instances to be modified, as shown in Figure 18. In this instance, the chromium number density will be modified in mixtures 4, 5, and 6.

```
read variable[aden_Cr_6061]
  distribution = expression
  expression = "6.2310e-5 * rel_mult_Cr_6061"
  siren="//comps/stdcomp[name='cr'][mixture='4',mixture='5',mixture='6']/aden"
  cases = Case1 Case2 Case3 Case4 Case5 Case6 Case7 end
end variable
```

Figure 18. Example variable block with a SIREN statement selecting multiple compositions.

More complicated cases arise in geometry modification. The origin of multiple cylinders must all be changed to the same sampled value so that the fuel material and its cladding move to the same location. The top or bottom surface of a number of geometry elements must be modified consistently as the length of that section changes. In some of these cases, it can be convenient to pool all the dimensions used in a unit and then subsequently select specific elements from this list. SIREN also supports selection of ranges, such as selecting units 1 through 4. It is also possible to define ranges with nonconsecutive elements. For example, the range can be defined as 1 to 5 by 2. This allows for the selection of the 1st, 3rd, and 5th entry, which can represent the positive X, Y, and Z faces of a cuboid in CSAS5 geometry. Finally, the range can also be created as a comma delimited list of elements. An example of this approach is shown in Figure 19, which selects the positive X and Y faces of the cuboid setting the fuel rod pitch in the first four units of the LEU-COMP-THERM-042 models.

```
read variable[pitch_p]
  distribution = normal
    value = 0.842
    stddev = 0.0038
    minimum = 0.8306
    maximum = 0.8534
    siren="//geometry/unit[1:4]/cuboid/dimensions/*[1,3,7,9,13,15,19,21]"
    cases = Case1 Case2 Case3 Case4 Case5 Case6 Case7 end
end variable
```

Figure 19. Example variable block with a complex SIREN statement.

It is important to check SIREN statements generated while developing Sampler input, especially complex statements such as those shown in Figure 19. This can be done with the *InputSelector* utility included in with SCALE. The arguments for command line execution include the file name and the SIREN statement. InputSelector then returns the values of the leaf or leaves selected from the DOM by the specified SIREN statement.

correlations_single

The simple FORTRAN program developed to calculate the correlation coefficients for some of the experiments examined in this work is named correlations_single. It is an outgrowth of an earlier program for calculating correlation coefficients for the LEU-COMP-THERM-007 and LEU-COMP-THERM-039 experiments as part of the WPNCS/UACSA benchmark [33]. This earlier code is not documented here as it is a reduced version of the final

FORTRAN program. As mentioned previously, correlations_single is used here only for the correlations among cases with the LEU-COMP-THERM-042 and HEU-SOL-THERM-001 experiments. The source code, correlations_single.f90, is provided in Appendix A. The four inputs provided to correlations_single in each execution are described below, followed be a discussion of the program flow and outputs.

Inputs

The first input is a list of data files containing the k_{eff} values for all realizations for the cases to be considered. Each of these files must contain the unlabeled k_{eff} values in the first 8 columns of each line; additional information can be provided in columns further to the right on each line as this information is not read or processed by the program. An example of the first few lines of such a data file is provided in Figure 20.

```
0.997125 0.000099
0.994019 0.000099
1.002991 0.000098
0.994180 0.000097
0.999256 0.000098
0.988753 0.000099
1.001893 0.000099
0.997060 0.000094
1.000978 0.000100
0.997527 0.000098
```

Figure 20. First 10 lines of a data file containing k_{eff} values for use in correlations_single.

The second input is a file containing the case names for the experiments in the series under consideration. These case names are used for labeling in output files, and are expected to be character strings of 10 or fewer characters. Each label must be on a separate line. Ten characters is viewed to be sufficient because the prefix identifying the experiment, HST for HEU-SOL-THERM for example, is not included since correlations among different types of systems are not investigated here. The evaluation number and case number have been used, though this shorthand only requires 7 characters. The case names used for the HEU-SOL-THERM-001 evaluation are shown in Figure 21.

```
001-001
001-002
001-003
001-004
001-005
001-006
001-007
001-008
001-009
001-010
```

Figure 21. File listing case names for the HEU-SOL-THERM-001 evaluation.

The final two inputs are the number of cases in the matrix and the number of realizations for each case. Both of these values could be determined during execution, but soliciting input from the user simplifies the program.

Program Flow

The code for correlations_single is organized into several sections. First is various header comment information and variable declarations, followed by collecting the four inputs discussed in the previous section from the user. A small section provides some statistical values, followed by processing data out of the user-supplied files. The average k_{eff} value and the standard deviation of the realizations are then calculated for each case. The next steps are the calculation of the correlation coefficients, significance testing, and confidence interval generation. The last section of the code provides the format statements for generating legible output. Further details for relevant portions of the code are provided in this section.

The first portion of the program declares array variables, solicits input from the user, and dimensions the array variables based on the input number of cases and realizations. The Student's t value and z values are hardcoded in this section as well. Both are set for 95% confidence, and the Student t also includes 297 degrees of freedom, which is appropriate for 300 samples. All correlation coefficients calculated using this program used 300 realizations per case, so this approach is acceptable. General implementation would require access to statistical distribution libraries for the t and z scores. The confidence interval half-width for the correlations in Fisher z space is also calculated here. The confidence interval width is ultimately only a function of the z score and the number of samples, as shown in Equation 6.

The next section processes the user-supplied data files. Primarily, this simply requires reading data into the appropriate arrays. The number of realizations in the first half of the sample is also calculated here and stored in the variable *nfirsthalf*. The first realization of the second half of the sample is called *nsecondhalf*, and is simply *nfirsthalf* plus one. This represents a slightly inconsistent nomenclature, but the last realization of the second half of the sample is also the last realization and already assigned to the variable *numreal*. The determination of this split between the first half and second half is used later to determine separate correlation coefficients for the first half and second half of the realizations separately as an indication of convergence.

The average of all the perturbed realizations is calculated for each case along with the standard deviation of these k_{eff} estimates. The average k_{eff} value can be compared to the nominal result to ensure that the sampling has not generated any unexpectedly skewed results. The standard deviation of the k_{eff} values gives an estimate of the uncertainty in the experiment if all the variable quantities are sampled correctly. The standard deviation from the samples is compared to the estimate of the benchmark uncertainty from Section 2 of the evaluation [15]. It is not clear at this writing that these values should be in agreement because of differences between the recommended approach to evaluating some uncertainties for the ICSBEP Handbook [15] and the sampling approach used here. Some studies have indicated

that the sampling approach results in more accurate estimates of the experimental uncertainty [59]. The averages of the perturbed cases in the first and second half of the sample are also determined separately, along with their associated standard deviations, for use in determining the correlations coefficients later in the program. The average and standard deviation of all realizations are written to an output file for review by the user.

The correlation coefficients are then calculated for each pair of cases using all the realizations. Once each coefficient is calculated, it is transformed to a Fisher z, see Equation 4, and the confidence interval is determined. The confidence interval half-width had already been determined in the first section of the program, as discussed previously. The confidence interval boundaries are then translated back into correlation coefficients using Equation 8. The *t*-test on significance is also executed, see Equation 3, at this point for each correlation coefficient. The correlation coefficients are written to an output file, the confidence intervals are written to a second, and the results of the *t*-test are written to a third.

Finally, the correlation coefficients for the first half and second half of the realizations are calculated and written to two additional output files. As mentioned previously, the purpose of this step is provide an indication that the correlation coefficients have converged. More detailed studies were performed, as described below, to investigate the number of realizations needed to achieve convergence of the correlation coefficient. These studies require a significant amount of additional post-processing of the k_{eff} results, and are therefore not repeated frequently. A more robust correlation coefficient calculation program could include this additional check as an optional step when desired by the user.

Outputs

The outputs generated by correlations_single are touched on in the description of the program flow in the previous section. This section provides a description of the six output files generated by the execution of the program. These files are named: *mean_stdev.dat*, *significant.dat*, *correlations.dat*, *confidence_intervals.dat*, *correlations_firsthalf.dat*, and *correlations_secondhalf.dat*.

The file *mean_stdev.dat* contains the mean and standard deviation for each of the cases. As discussed previously, the mean is calculated over all 300 perturbed realizations. The standard deviation is similarly calculated over all realizations. These values can be compared with the nominal case k_{eff} and the evaluated benchmark uncertainty; again, the uses of these values has been discussed previously. Each line in the output file contains a case label, the average k_{eff}, and the standard deviation of sampled k_{eff} values. A portion of this file is shown in Figure 22.

The results of the t-test on statistical significance are printed in *significant.dat*. These results indicate whether there is at least 95% confidence that the correlations coefficient is non-zero. The test statistic, t*, is calculated using Equation 3. The correlation coefficient is accepted as significant if the absolute value of the test statistic is greater than the Student's *t* value for 95% confidence and n-2 degrees of freedom. A pair of case identifiers is printed to

```
001-001    0.997481 0.006302
001-002    0.995558 0.006297
001-003    1.001227 0.001992
001-004    0.998200 0.001955
001-005    0.997830 0.002439
```

Figure 22. A portion of the *mean_stdev.dat* output from correlations_single.

each line of the output file along with either the word "nonzero" or "insignificant". The correlation coefficients are not printed in this file. The test on significance is informative, but is probably not as useful as the confidence intervals determined via the Fisher z transformation. The first few lines of an example output file for the t-test are shown in Figure 23.

```
001-001    001-002         nonzero
001-001    001-003   insignificant
001-001    001-004   insignificant
001-001    001-005   insignificant
001-001    001-006   insignificant
```

Figure 23. First several lines of the *significant.dat* output file from correlations_single.

The aforementioned confidence intervals are printed in *confidence_intervals.dat*. The calculation of these confidence intervals is discussed in the previous section on the program flow. The confidence intervals are printed in a matrix; each element in the matrix contains the 95% confidence interval for the correlation coefficient between the two cases. The confidence intervals are derived only from the variability of the sampled results, and do not include any uncertainty derived from the assessments of correlated uncertainties, distributions of variable parameters, or any related inputs. In other words, the confidence interval determination assumes perfect knowledge and description of the benchmark experiments and the correlated and independent uncertainty components of the experiments. Part of a representative output file is shown in Figure 24.

```
          001-001         001-002         001-003         001-004
001-001             ( 0.995, 0.997) (-0.127, 0.100) (-0.129, 0.098)
001-002                             (-0.127, 0.099) (-0.130, 0.096)
001-003                                             ( 0.990, 0.994)
```

Figure 24. First few lines of the *confidence_intervals.dat* output file from correlations_single.

The correlation coefficients themselves are printed in *correlations.dat* for all realizations, and for the first and second half of the realizations in *correlations_firsthalf.dat* and *correlations_secondhalf.dat*, respectively. The correlations are printed in a matrix format, akin to *confidence_intervals.dat*, except that only a single number is printed to each matrix element. The format of all three files is identical, so a portion of only one of them is provided here in Figure 25.

	001-001	001-002	001-003	001-004	001-005
001-001		0.996	-0.014	-0.016	0.048
001-002			-0.014	-0.017	0.049
001-003				0.992	-0.020
001-004					-0.019

Figure 25. Beginning section of a correlation coefficient output file from correlations_single.

Description of Experiments and Models

A number of KENO models are needed for this work. A total of four ICSBEP handbook [15] evaluations are used here: LEU-COMP-THERM-007, LEU-COMP-THERM-039, LEU-COMP-THERM-042, and HEU-SOL-THERM-001. The following subsections provide additional details of the KENO models used here and their sources.

LEU-COMP-THERM-007 and LEU-COMP-THERM-039

LEU-COMP-THERM-007 (LCT-007) and LEU-COMP-THERM-039 (LCT-039) are used in the WPNCS/UACSA benchmark on critical experiment correlations [33]. These evaluations are the subject of the benchmark because both series of experiments used the same fuel rods and were performed at Valduc, France, on "Apparatus B" [15]. Only the first four, square-pitched cases of LCT-007 are included, as are all 17 cases of LCT-039. These cases were initially expected to have significant correlation because of the shared fuel material, though the range of pitches and loading patterns used in the two series provides an opportunity to investigate the effect of other parameters on the correlation coefficients.

The first case of LCT-007 and all cases in LCT-039 use a 1.26 cm center-to-center fuel rod spacing. The other three cases considered from LCT-007 have fuel rod spacing of 1.6 cm, 2.1 cm, and 2.52 cm. The 4 cases from LCT-007 use uniform arrays of rods, but the 17 cases in LCT-039 each have different patterns of fuel rods and empty lattice locations [15]. The simple lattices used in LCT-007 are shown in Figure 26, and some example configurations from LCT-039 are shown in Figure 27. In all cases from both evaluations, water height is the controlled parameter to approach criticality.

The models for these experiments were built for use in the benchmark. The details of the fuel rods, including end plugs, fissile material, and plenum space, coupled with the grid plates necessitate 9 axial units for each rod. Radial arrays are constructed for each of the 9 axial levels, and these 9 radial arrays are used in an axial array to build the complete model of the fueled portion of the model. The number of fuel rods in each model ranges from 225 to 484. In cases with individual rod positioning, thousands of units must be created and perturbed. Also, the 9 axial units must be uniformly perturbed; much of this input is created using the TemplateEngine, as discussed previously. The details of the benchmark models are provided in Section 3 of the ICSBEP evaluations for these experiments [15]. The dimensions, isotopic or elemental number densities, and mixture temperatures are all provided. In all cases, the dimensions provided in the evaluation are nominal. The nominal input for Case 1 of LCT-007 is included in Appendix B. No example input is provided for the cases supporting

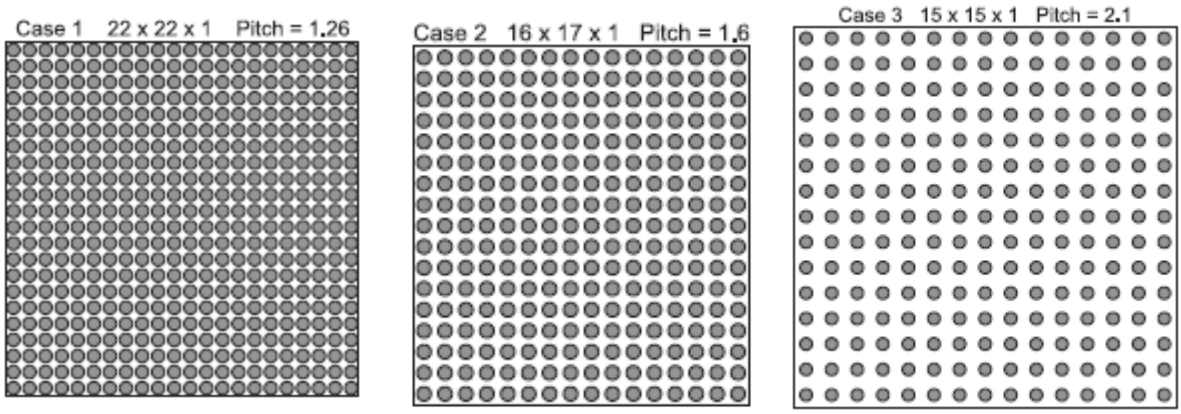

Figure 26. Fuel rod arrays for Cases 1-3 of LCT-007 [15].

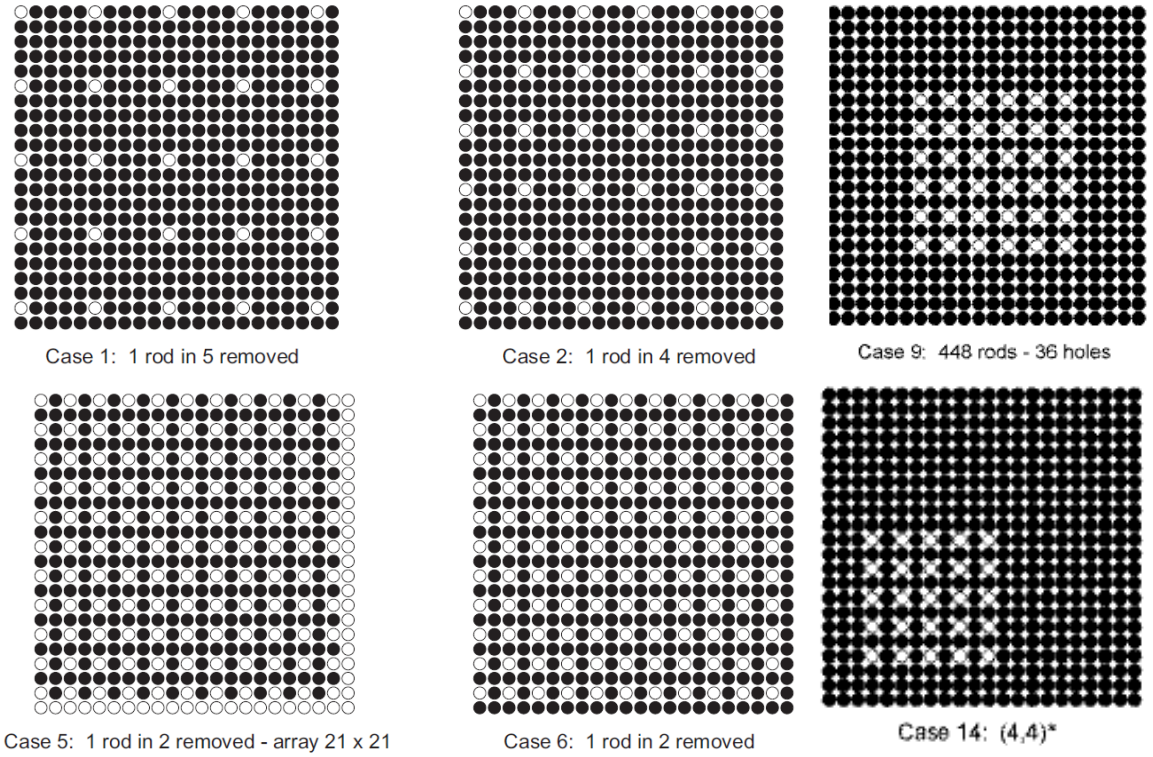

Figure 27. Fuel rod arrays for Cases 1, 2, 5, 6, 9, and 14 of LCT-039 [15].

individual fuel rod placement because of the length of these models.

The variable parameter distributions and associated distribution parameters are all taken from the WPNCS/UACSA Benchmark specification [33]. No attempt has been made here to independently confirm the accuracy or appropriateness of these choices. The parameters and their distributions will be discussed later. Also, a range of scenarios is defined in the benchmark correlating different uncertain parameters to examine the impact of these variations on the correlation coefficients. This work only considers Scenarios A and E. Scenario A corresponds to fully correlated fuel rod spacing and Scenario E represents each fuel rod positioned independently within randomly positioned holes in the grid plates.

LEU-COMP-THERM-042

LEU-COMP-THERM-042 (LCT-042) is used in this work as another LEU pin array experiment. The experiments were performed at the Critical Mass Laboratory of the Pacific Northwest Laboratories in 1979 and 1980. This evaluation is used in this work because all 7 cases share the same fuel rods and same pitch, but different neutron absorber panels are included in each case. Experiments like LCT-042 are frequently used in the validation of fuel storage and transportation systems, so it is also useful to investigate because of this common implementation. Finally, with only 7 cases, as compared to the 21 in the original WPNCS/UACSA benchmark, LCT-042 represents a more manageable challenge in terms of the computer time needed to determine correlation coefficients.

All 7 cases have a fuel rod pitch of 1.684 cm. The rods are placed in three fuel rod clusters, and separation between the central cluster and the side clusters is the controlled parameter to achieve criticality. The central cluster is a 25 x 18 array and the side clusters are both 20 x 18 arrays. Stainless steel walls are included as neutron reflectors approximately 1.3 cm from the long faces of the fuel rod clusters. The general layout of the experiments is shown in Figure 28. A different neutron absorbing material is included in each experiment on the short outer faces of the central cluster. The panel locations are indicated in Figure 28. The neutron absorber materials are: 304L stainless steel, 1.1 wt% borated stainless steel, Boral, Boraflex, cadmium, copper, and a copper-cadmium mixture with approximately 1 wt% cadmium. The arrays are fully flooded with water, and a minimum of 30 cm of reflection is present on all four sides of the fuel arrays. Nearly 10 cm of water reflection exists above the top of the fuel rods and more than 15 cm of water reflection is below the rods. The rods contain 5 cm top end plugs and 1.27 cm bottom end plugs, so the distance from the ends of the fuel material to the end of the water reflector are greater than the dimensions provided from the ends of the fuel rods.

The models for these experiments are taken from the Verified, Archived Library of Inputs and data (VALID library), maintained by the Reactor and Nuclear Systems Division at Oak Ridge National Laboratory [60]. The VALID procedure requires models to be built in accordance with an acceptable reference, which in this case was the LCT-042 evaluation from the ICSBEP Handbook [15]. The models and associated outputs are reviewed by an independent, qualified individual to provide higher confidence that the models are correct.

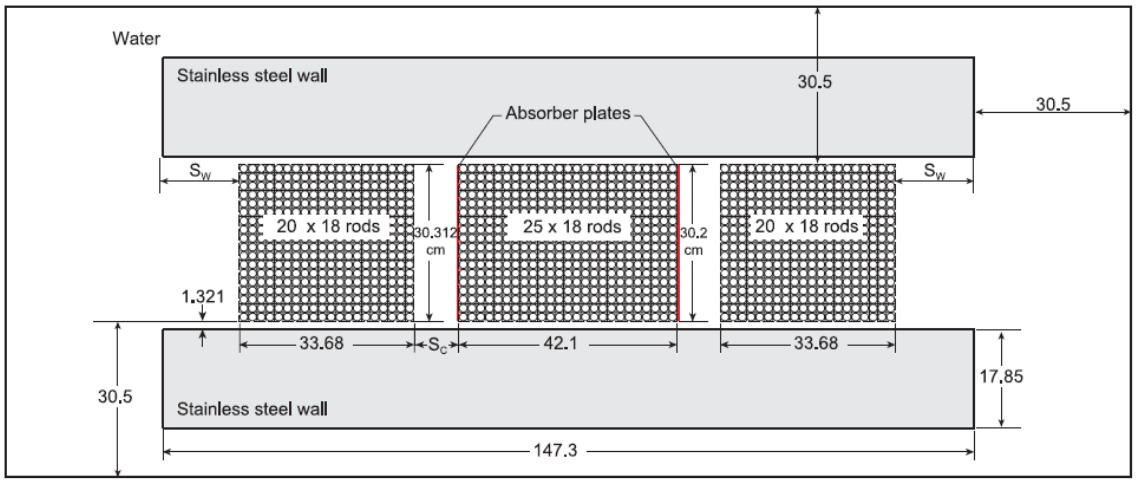

Figure 28. Plan view of the LCT-042 experiments [15].

These models are therefore expected to be of high quality and are judged to be reliable for inclusion in this work. The nominal input for Case 1 of LCT-042 is included in Appendix C.

Modifications were made to the models taken from VALID to allow independent fuel rod positioning via Sampler. The addition of units is automated, so it is highly reliable. There are fewer axial units needed for modeling LCT-042, so fewer total units are needed even though a total of 1170 fuel rods are present in the experiments.

The variable parameter distributions and associated distribution parameters are developed based on the uncertainty analysis performed in Section 2 of the ICSBEP Handbook evaluation [15]. The vast majority of the input parameters are modified. The uncertainty treatment for LCT-042 is more complete than the simplified list of parameters modified in LCT-007 and LCT-039 as part of the WPNCS benchmark. In this respect, the LCT-042 correlations are a more exhaustive examination of the potential correlations among critical experiments. The details of these parameters, distributions, and distribution parameters will be discussed in detail in a later section. As with the LCT-007 and LCT-039 cases, a range of parameters is investigated to examine the sensitivity of the correlation coefficients to these parameters.

HEU-SOL-THERM-001

HEU-SOL-THERM-001 (HST-001) is used in this work as a representative solution experiment. It is selected as it was in the earliest study to provide quantitative estimates of critical experiment correlations [17]. The experiments were performed at the Rocky Flats Plant in the mid-1970s, and consist of an individual tank containing the solution inside a concrete room [15]. The concrete room is not included in the benchmark model, leaving an extremely simple model containing just the solution and tank. The simplicity of this model makes it attractive to study the contribution of several different uncertain parameters to the correlation coefficient.

A total of 10 cases are included in the HST-001 evaluation. Four different tanks are used, including one stainless steel tank and three different aluminum tanks. Eight different solutions are used in the ten cases; there are two solutions that are used twice each.

The models for this evaluation are taken from the VALID library. No modifications to the models are required for this work as there is only the single tank in the model. The nominal input for Case 1 of HST-001 is included in Appendix D. A radial slice of the model for Case 1 is shown in Figure 29.

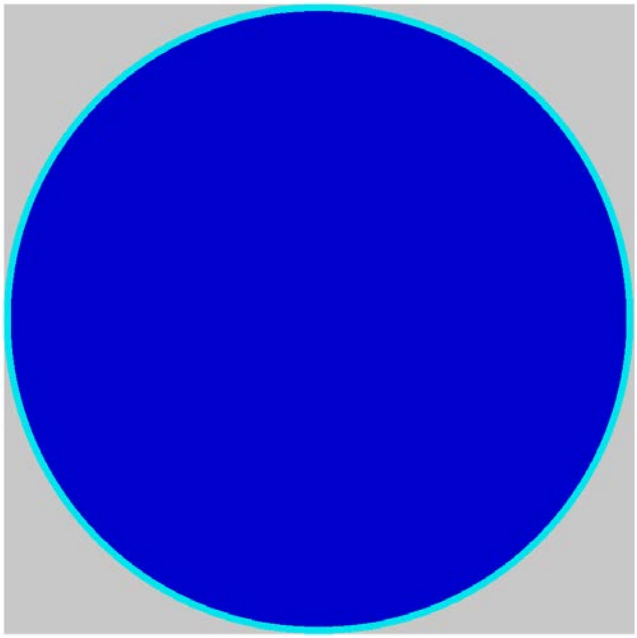

Figure 29. Radial slice of HST-001 Case 1, with a tank inner diameter of 27.92 cm.

The variable parameter distributions and associated distribution parameters are developed based on the uncertainty evaluation performed in Section 2 of the ICSBEP Handbook evaluation dated September 30, 2004 [15]. As with LCT-042, most of the parameters are perturbed in HST-001. Given the significantly smaller number of parameters, correlation coefficients are determined including different groups of uncertain parameters, including the geometry, the tank composition, the uranium enrichment, and the solution composition. The details of these studies are provided below, and the purpose of this phased approach is to examine which parameters have the largest impact on the correlation coefficients. Some of the parameters are also varied assuming each set of uncertain parameters are shared and unique to examine these impacts on the correlation coefficients. These studies are feasible for this simple model in a way they are not for the complex geometrical arrangements used in the LEU pin array cases.

CHAPTER IV: DESCRIPTION OF NEW WORK

This work extends the state of the art of nuclear criticality safety validation methods by developing a method for practitioners to use in the determination of reliable critical experiment correlations. The determination of critical experiment correlations via the Monte Carlo sampling method as implemented in Sampler began with the capability demonstration in 2013 discussed in Chapter II [36]. This capability demonstration was not performed by the author, but all other results presented from Sampler are the result of the author's work. Initial results for experiments included here were published in 2014 [39], and led to further involvement with the international community efforts in this area. This involvement included being a contributing author on the WPNCS/UACSA benchmark on critical experiment correlations [33] and presenting results for the benchmark and other results in the open literature [40] and at meetings related to the benchmark [42, 43]. Results presented in the relevant references [39, 40, 42, 43] form the basis for further results expanding those investigations and the development of a recommended procedure for the determination of critical experiment correlations via the Monte Carlo technique. The purpose of this dissertation is to develop this recommended approach for critical experiment correlation determination. The approach is detailed in Chapter VIII, and is developed through a series of investigations on three different sets of potentially correlated critical experiments.

Chapter V contains the results for the LCT-007 and LCT-039 experiments used in the WPNCS/UACSA benchmark [33]. Some of the results in this chapter have been published previously [40, 42, 43], including most of the work on pin positioning, some investigation of the effect of the stochastic uncertainty of the KENO calculations, initial investigations of correlation coefficient convergence, and some of the work on the reproducibility of the calculated correlation coefficients. Many of the previously presented results have been updated, and the summary and observations are derived from all the most recent and complete results.

Chapter VI contains the results for the LCT-042 experiments. Initial results for these correlations were presented in [39, 40], and are discussed in Chapter II. Most of the results presented in Chapter VI are extensions of those preliminary results, and are generally intended to confirm results generated as part of the work on LCT-007 and LCT-039. It is important to ensure that the observed impacts of pin position modeling, the stochastic uncertainty, and the convergence of correlation coefficients are applicable to different LEU pin array experiments. Unlike LCT-007 and LCT-039, each case in LCT-042 contains a unique absorber panel, ensuring at least a modest source of unique uncertainty in each experiment. Another unique aspect of the work on LCT-042 is the derivation of the sampling inputs for the uncertain parameters in the benchmark description provided in [15]. The vast majority of the results presented in Chapter VI have not been published elsewhere.

Chapter VII presents results for the HST-001 experiments. This particular experiment was selected to allow comparisons with other published results [17]; the methodology used to generate the reference results is presented in Chapter II. All of the results presented in

Chapter VII are new, and are primarily concerned with the impact of different uncertainties and their treatments on the resulting correlation coefficients.

Taken together, a significant amount of new work is presented in this dissertation. It is also worth noting, however, that the results that have been published previously are also part of the methodology development documented here for the determination of critical experiment correlations. The work that has been performed as a part of the international community and has established the reputation of the author within that community as an expert in this area.

CHAPTER V: ANALYSIS OF CORRELATIONS AMONG CASES FROM LEU-COMP-THERM-007 AND LEU-COMP-THERM-039

The WPNCS/UACSA benchmark for critical experiment correlations originally used Case 1-4 of LCT-007 and all 17 Cases of LCT-039. The final, published benchmark uses a reduced set of these cases [33]. The results presented here include the initial 20 cases considered. Later results include 21 cases since the 4th case of LCT-007 was added. The benchmark includes a range of scenarios with different degrees of correlation among the variable parameters. This work includes only Scenario A and Scenario E: Scenario A, as discussed below, models fully correlated fuel rod spacing. Scenario E is the opposite, with completely independent positioning of fuel rods.

This section presents several aspects of the LCT-007 and LCT-039 work. First, the variable parameters are discussed, including the distributions and distribution parameters chosen for the benchmark effort. This section will include a more detailed discussion of the two scenarios examined for these experiments. The next subsection will provide the base case results for both scenarios included in this work. A variety of studies performed with these cases is also presented. These studies include examining the number of realizations needed to achieve convergence of the correlation coefficients, the effect of the uncertainty in the KENO calculations for each realization, the repeatability of the correlation coefficient determination, and the use of continuous-energy (CE) KENO in place of MG calculations. Finally, a summary of the results and studies performed with these experiments will be presented.

Variable Parameters

The parameters chosen to vary and the assignment of these variations as shared or unique are defined in the benchmark for these cases [33]. The variable parameters and their assigned distributions are discussed first, followed by a discussion of the two scenarios included in this work.

Parameters and Their Distributions

The majority of the inputs in the LCT-007 and LCT-039 models are sampled from variable distributions defined in the benchmark specification [33]. The sampled inputs include fuel rod dimensions, fuel rod positions, the uranium isotopic distribution, and critical water heights, among others. Most of the variable inputs are assumed to be normally distributed, using the standard deviation provided in Section 2 of the ICSBEP Handbook reports [15]. The fuel rod cladding inner diameter, fuel rod cladding thickness, and the angular position of fuel rods within the support grid holes (in Scenario E) are distributed uniformly. The complete list of variable parameters, their distributions, and distribution parameters are provided in Table 1.

Scenario Descriptions

The WPNCS/UACSA benchmark includes a series of scenarios examining the effect of different parameters on the resulting critical experiment correlations. The set of cases varies

Table 1. Variable Parameters, Distributions, and Distribution Parameters for LCT-007 and LCT-039 [33]

Input Parameter	Distribution	Distribution Parameters
Fuel rod cladding inner diameter	Uniform	[0.81, 0.83] (cm)
Fuel rod cladding thickness	Uniform	[0.055, 0.065] (cm)
Fuel pellet diameter	Normal	μ=0.7892, σ=0.0017 (cm)
x-displacement of hole relative to nominal	Normal	μ=0, σ=0.000742 (cm)
y-displacement of hole relative to nominal	Normal	μ=0, σ=0.000742 (cm)
Angle of rod center within its grid hole	Uniform	[0, 2π] (radians)
Hole diameter	Normal	μ=1.0105, σ=0.0085 (cm)
Height of fissile column	Normal	μ=89.7, σ=0.3 (cm)
Fuel density	Normal	μ=10.38, σ=0.0133 (g/cm^3)
Fuel impurity (modeled as ^{10}B)	Normal	μ=6.9037 x 10-8, σ=8 x 10^{-9} (a/b-cm)
^{234}U content in U	Normal	μ=0.0307, σ=0.0005 (at%)
^{235}U content in U	Normal	μ=4.79525, σ=0.002 (at%)
^{236}U content in U	Normal	μ=0.1373, σ=0.0005 (at%)
^{238}U content in U	Normal	μ=95.03675, σ=0.01 (at%)
Critical water height LCT-007-001	Normal	μ=90.69, σ=0.1 (cm)
Critical water height LCT-007-002	Normal	μ=73.53, σ=0.1 (cm)
Critical water height LCT-007-003	Normal	μ=77.98, σ=0.06 (cm)
Critical water height LCT-007-004	Normal	μ=79.85, σ=0.1 (cm)
Critical water height LCT-039-001	Normal	μ=81.36, σ=0.07 (cm)
Critical water height LCT-039-002	Normal	μ=77.69, σ=0.06 (cm)
Critical water height LCT-039-003	Normal	μ=73.05, σ=0.06 (cm)
Critical water height LCT-039-004	Normal	μ=89.07, σ=0.06 (cm)
Critical water height LCT-039-005	Normal	μ=84.37, σ=0.06 (cm)
Critical water height LCT-039-006	Normal	μ=58.77, σ=0.06 (cm)
Critical water height LCT-039-007	Normal	μ=69.71, σ=0.06 (cm)
Critical water height LCT-039-008	Normal	μ=66.79, σ=0.06 (cm)
Critical water height LCT-039-009	Normal	μ=64.47, σ=0.07 (cm)
Critical water height LCT-039-010	Normal	μ=58.37, σ=0.07 (cm)
Critical water height LCT-039-011	Normal	μ=81.34, σ=0.06 (cm)
Critical water height LCT-039-012	Normal	μ=75.38, σ=0.07 (cm)
Critical water height LCT-039-013	Normal	μ=72.52, σ=0.06 (cm)
Critical water height LCT-039-014	Normal	μ=71.14, σ=0.06 (cm)
Critical water height LCT-039-015	Normal	μ=69.88, σ=0.06 (cm)
Critical water height LCT-039-016	Normal	μ=69.4, σ=0.06 (cm)
Critical water height LCT-039-017	Normal	μ=68.75, σ=0.06 (cm)

from correlated uncertainties for fuel rod positions and dimensions to fully uncorrelated parameters. Scenario A includes fully correlated dimensions and rod positions. This scenario also models the fuel rods as centered in the holes in the grid plates; this is a common nominal assumption in critical experiment modeling despite being physically impossible. Scenario B randomly positions the grid holes, but maintains correlations for the rod dimensions and positions. Progressing through the remaining scenarios to Scenario E switches various parameters from correlated to uncorrelated to isolate the effect each one has on the critical experiment correlations. The complete matrix of scenarios is provided in Table 2. Given the extensive computational effort needed for each scenario and the fact that Scenarios B, C, and D are optional in the final benchmark specification, only Scenarios A and E are examined here.

Table 2. Correlation of Uncertain Parameters in WPNCS/UACSA Benchmark [33]

Scenario	Displacement of grid hole position	Radial displacement of rod center from hole center	Grid hole diameters	Fuel rod cladding inner diameters	Fuel rod cladding thicknesses
A	None	R=0	Correlated	Correlated	Correlated
B	Uncorrelated	$R = r_h - r_{gap} - t_{clad}$	Correlated	Correlated	Correlated
C	Uncorrelated	$R = r_h - r_{gap} - t_{clad}$	Uncorrelated	Correlated	Correlated
D	Uncorrelated	$R = r_h - r_{gap} - t_{clad}$	Uncorrelated	Uncorrelated	Correlated
E	Uncorrelated	$R = r_h - r_{gap} - t_{clad}$	Uncorrelated	Uncorrelated	Uncorrelated

Note: r_h is hole radius, r_{gap} is gap radius, and t_{clad} is cladding thickness

Some evidence is available indicating that Scenario E is the more plausible of the scenarios for representing the actual experiments. Measurements of the grid plates used in LCT-007 and LCT-039 are not available, but measurements are available for a similar series of experiments also performed at the critical experiment facility at Valduc, France. The Haut Taux de Combustion (HTC) experiments [61-64] were performed a few years after LCT-007 and LCT-039, and the grid plates used in those experiments were measured at the request of ORNL. The results of these measurements [65] (included in Appendix E) indicate that there is no accumulating error in the placement of the holes in the grid plates. The grid plates contain 2500 holes in a 50 x 50 array, creating 49 pitches in the x and y directions. Multiple measurements are made across each plate in both directions as well as along the diagonals. For the 1.3 cm pitch grid plate, the largest deviation from nominal in these measurements is 0.053 mm. The average pitch indicated by the 12 measurements of these two grid plates is a maximum of 0.001 mm, or 1 μm, off from nominal. Individual hole separation distances are not reported, so it is not possible to evaluate the uncertainty in each hole placement, but the results provide a very strong indication that the fuel rod locations are not systematically biased.

Initial Results

This section presents initial results for the WPNCS/UACSA benchmark for LCT-007 and LCT-039. These results were used as the baseline for the studies discussed in the next section.

Scenario A

Scenario A, as described above, assumes that all fuel rods are centered in the holes in the grid plates. It is further assumed that the spacing between all pairs of rods is identical. This uniform pitch assumption leads to large reactivity variations between realizations since the spacing between all fuel rods expands or contracts simultaneously. This relatively large reactivity effect is also shared among all cases, thus increasing the correlation coefficients. It should be noted that LCT-007 Case 4 was never included in the Scenario A results; this has no bearing on the usefulness of the other results.

The nominal k_{eff} for each case along with the average k_{eff} over all samples and its standard deviation are provided in Table 3. The expected k_{eff} value and its uncertainty from the ICSBEP Handbook evaluation [15] are also included in Table 3. The critical experiment correlations were generated with 150 realizations per experiment. The Monte Carlo uncertainty of the individual KENO calculations for these calculations ranged between approximately 0.00050 Δk and 0.00080 Δk. Each individual calculation was finished in under 15 minutes, leading to a total run time on the order of 550 CPU-hours. The correlation coefficient results are shown in Figure 30.

The nominal k_{eff} value for each of the 20 cases considered here is slightly below the expected value from the evaluation of 1.0 [15]. This is expected as there has been a slight negative bias for LEU array systems in KENO for some time [66]. The first important result from Table 3 is that the average of the 150 realizations is within one standard deviation of the nominal value for all 20 cases. While the average over the realizations is in good agreement, it should be noted that the average k_{eff} value is higher than the nominal value for all 20 cases. Second, the standard deviation of the realizations is significantly larger than the benchmark uncertainty provided in the evaluation for all 20 cases. The ratio of sampling uncertainty to evaluation uncertainty ranges from approximately 1.9 for LCT-007 Case 3 to about 3.4 for LCT-039 Case 7. It is worth noting that the ratio is 1.9 for LCT-007 Case 3, 2.8 for LCT-007 Case 2, and generally around 3 or slightly higher for the remainder of the cases. This result suggests that the overprediction of the uncertainty is more pronounced for the smaller pitch cases, with correspondingly higher sensitivity to fuel rod pitch. This may indicate that the fully correlated pitch modeling is driving this higher estimation of the uncertainty.

The correlation coefficient results show extremely high correlations for most experiment pairs. It is evident that LCT-007 Case 3 has much lower correlation coefficients with the other experiments than the rest of the sample examined. This is caused by the fuel rod pitchof LCT-007 Case 3 being significantly higher (2.1 cm) than that for the other cases. It is in fact overmoderated, so the response of the system to changes in pitch is significantly different than for the other cases. LCT-007 Case 1 and all cases in LCT-039 have a 1.26 cm pitch; LCT-007 Case 2 has a pitch of 1.60 cm. This latter case is slightly undermoderated,

Table 3. k_{eff} Results for Scenario A Calculations

Case	Expected k_{eff}	Evaluation Uncertainty	Nominal k_{eff}	Nominal k_{eff} Uncert.	Average of Realizations	Standard Deviation
7-1	1.00000	0.00140	0.99392	0.00010	0.99594	0.00461
7-2	1.00000	0.00080	0.99614	0.00010	0.99768	0.00226
7-3	1.00000	0.00070	0.99654	0.00010	0.99736	0.00130
39-1	1.00000	0.00140	0.99539	0.00010	0.99742	0.00426
39-2	1.00000	0.00140	0.99460	0.00010	0.99676	0.00409
39-3	1.00000	0.00140	0.99627	0.00010	0.99838	0.00383
39-4	1.00000	0.00140	0.99348	0.00010	0.99558	0.00376
39-5	1.00000	0.00090	0.99552	0.00010	0.99737	0.00293
39-6	1.00000	0.00090	0.99484	0.00010	0.99697	0.00296
39-7	1.00000	0.00120	0.99377	0.00010	0.99588	0.00404
39-8	1.00000	0.00120	0.99383	0.00010	0.99613	0.00389
39-9	1.00000	0.00120	0.99365	0.00010	0.99599	0.00389
39-10	1.00000	0.00120	0.99466	0.00010	0.99703	0.00336
39-11	1.00000	0.00130	0.99266	0.00010	0.99465	0.00426
39-12	1.00000	0.00130	0.99287	0.00010	0.99502	0.00424
39-13	1.00000	0.00130	0.99284	0.00010	0.99517	0.00416
39-14	1.00000	0.00130	0.99346	0.00010	0.99559	0.00408
39-15	1.00000	0.00130	0.99384	0.00010	0.99619	0.00398
39-16	1.00000	0.00130	0.99687	0.00010	0.99901	0.00394
39-17	1.00000	0.00130	0.99353	0.00010	0.99577	0.00400

but near optimum moderation. A careful examination of the results in Figure 30 shows that the correlations coefficients with the LCT-039 cases are also lower for LCT-007 Case 2 than for the LCT-007 Case 1. The correlations for Case 2 with the LCT-039 cases is around 0.93; while still a high correlation this is a noticeably lower value than the 0.96 to 0.98 correlation coefficients generated among the experiments with the same fuel rod pitch.

All the correlations shown in Figure 30 are statistically significantly different from 0 at the 95% level. In fact, for 150 samples, any correlation coefficient exceeding 0.161 is statistically significant. The highest correlation coefficient between LCT-007 Case 2 and any other case is 0.940, with LCT-039 Case 10. The 95% confidence interval on this correlation coefficient is from 0.918 to 0.956. This indicates that the correlation coefficients for all cases, except LCT-007 Case 3, are statistically equivalent. One of the lower correlation coefficients among other cases is 0.956, between LCT-007 Case 1 and LCT-039 Case 5. The 95% confidence interval on this coefficient ranges from 0.940 to 0.968. This confirms that these two confidence intervals just overlap. It is also worth noting that most other correlation coefficients are higher than 0.97 for LCT-007 Case 1. The correlation coefficients between LCT-039 Cases 5 and 6 all appear to be lower than many other correlation coefficients. These cases stand out as different as they are the only cases with every other rod removed from the lattice. The energy of the average lethargy causing fission (EALF) for these two cases is much lower, around 0.14 eV, than for the other LCT-039 cases. The other LCT-039 cases have EALF values of approximately 0.18 to 0.23 eV, with most of the values over 0.20 eV. The correlation coefficients for all cases are therefore consistent with the underlying physics similarities and differences exhibited by each system.

These results indicate that statistically significant correlation coefficients may be able to be determined with a relatively modest computational burden. Certainly more than 500 CPU-hours is not a trivial amount of calculation, but for even some large desktop computers this represents little more than a weekend of time. On some computing clusters, this amount of computing time could be dedicated within just one or two hours.

The results presented in Figure 30 also indicate that shared fissile material is not necessarily the only consideration to driving large correlation coefficients. LCT-007 Case 3 uses the same fuel rods as all the other cases, yet correlation coefficients of only approximately 0.4 result. At this point it is evident that LEU fuel rod array experiments must have the same fissile material and a similar fuel rod pitch for very high correlation to exist. In this context, "similar" means at least being on the same side of optimum moderation. This conclusion is logical given the different moderation regimes that these differing cases could occupy.

Scenario E

Scenario E presents a significantly greater challenge than Scenario A. The individual placement of each fuel rod requires models of much greater length and complexity. The complexity drives the use of the TemplateEngine, as discussed in Chapter III, to create up to 484 copies of the individual fuel rod used in nominal models such as those shown in Appendix B. Random pin locations should also result in lower reactivity effects that are also

	7-1	7-2	7-3	39-1	39-2	39-3	39-4	39-5	39-6	39-7	39-8	39-9	39-10	39-11	39-12	39-13	39-14	39-15	39-16	39-17
7-1	1.000	0.933	0.391	0.978	0.975	0.974	0.974	0.956	0.957	0.974	0.971	0.978	0.969	0.977	0.972	0.980	0.979	0.973	0.977	0.978
7-2	0.933	1.000	0.557	0.923	0.920	0.925	0.930	0.925	0.929	0.933	0.920	0.936	0.940	0.925	0.924	0.928	0.933	0.928	0.937	0.931
7-3	0.391	0.557	1.000	0.405	0.390	0.409	0.417	0.459	0.463	0.415	0.389	0.434	0.451	0.384	0.406	0.405	0.382	0.399	0.418	0.420
39-1	0.978	0.923	0.405	1.000	0.978	0.970	0.973	0.957	0.958	0.976	0.972	0.970	0.973	0.979	0.976	0.976	0.981	0.977	0.972	0.977
39-2	0.975	0.920	0.390	0.978	1.000	0.972	0.970	0.953	0.954	0.975	0.967	0.968	0.963	0.974	0.974	0.976	0.977	0.970	0.972	0.977
39-3	0.974	0.925	0.409	0.970	0.972	1.000	0.967	0.945	0.954	0.971	0.963	0.971	0.966	0.974	0.969	0.974	0.971	0.967	0.972	0.970
39-4	0.974	0.930	0.417	0.973	0.970	0.967	1.000	0.956	0.954	0.971	0.965	0.968	0.965	0.972	0.971	0.973	0.974	0.968	0.973	0.978
39-5	0.956	0.925	0.459	0.957	0.953	0.945	0.956	1.000	0.946	0.958	0.944	0.955	0.955	0.953	0.949	0.952	0.952	0.954	0.951	0.958
39-6	0.957	0.929	0.463	0.958	0.954	0.954	0.954	0.946	1.000	0.956	0.953	0.960	0.961	0.955	0.954	0.963	0.955	0.957	0.958	0.960
39-7	0.974	0.933	0.415	0.976	0.975	0.971	0.971	0.958	0.956	1.000	0.973	0.974	0.970	0.979	0.978	0.974	0.979	0.974	0.979	0.978
39-8	0.971	0.920	0.389	0.972	0.967	0.963	0.965	0.944	0.953	0.973	1.000	0.964	0.970	0.973	0.966	0.970	0.973	0.964	0.964	0.966
39-9	0.978	0.936	0.434	0.970	0.968	0.971	0.968	0.955	0.960	0.974	0.964	1.000	0.967	0.976	0.968	0.976	0.976	0.969	0.975	0.974
39-10	0.969	0.940	0.451	0.973	0.963	0.966	0.965	0.955	0.961	0.970	0.970	0.967	1.000	0.964	0.968	0.969	0.966	0.964	0.968	0.970
39-11	0.977	0.925	0.384	0.979	0.974	0.974	0.972	0.953	0.955	0.979	0.973	0.976	0.964	1.000	0.973	0.980	0.979	0.977	0.977	0.977
39-12	0.972	0.924	0.406	0.976	0.974	0.969	0.971	0.949	0.954	0.978	0.966	0.968	0.968	0.973	1.000	0.978	0.976	0.968	0.972	0.976
39-13	0.980	0.928	0.405	0.976	0.976	0.974	0.973	0.952	0.963	0.974	0.970	0.976	0.969	0.980	0.978	1.000	0.977	0.979	0.976	0.976
39-14	0.979	0.933	0.382	0.981	0.977	0.971	0.974	0.952	0.955	0.979	0.973	0.976	0.966	0.979	0.976	0.977	1.000	0.976	0.977	0.979
39-15	0.973	0.928	0.399	0.977	0.970	0.967	0.968	0.954	0.957	0.974	0.964	0.969	0.964	0.977	0.968	0.979	0.976	1.000	0.970	0.973
39-16	0.977	0.937	0.418	0.972	0.972	0.972	0.973	0.951	0.958	0.979	0.964	0.975	0.968	0.977	0.972	0.976	0.977	0.970	1.000	0.976
39-17	0.978	0.931	0.420	0.977	0.977	0.970	0.978	0.958	0.960	0.978	0.966	0.974	0.970	0.977	0.976	0.976	0.979	0.973	0.976	1.000

Figure 30. Initial Critical experiment correlations for WPNCS/UACSA benchmark for LCT-007 and LCT-039, Scenario A.

less correlated. The reactivity effects are lower because the overall moderation ratio within the lattice of fuel rods is largely unchanged by the random perturbations. The effects are uncorrelated because the perturbations of fuel rod locations are unique to each case.

The assumption of random pin placement is predicated on the belief that the fuel rods must move to some degree between experiments. This belief can be difficult to impossible to confirm given the level of information currently contained in ICSBEP Handbook evaluations. These evaluations are mostly concerned with the nominal description of the experiment. An uncertainty evaluation is also included to examine the confidence that can be placed in the specific configuration, but many aspects of this uncertainty assessment are not captured in the primary experiment reports used in the generation of the evaluations.

Many factors influence the degree of randomness of fuel rod locations and the variability of those locations between experiments. The two primary considerations are the preparation of the grid plates used in the experiment and the handling of fuel rods between experiments. Each of these factors merits some discussion here.

The first consideration is the method for laying out and drilling the holes in the support plates used in the experiments. Most fuel rod array experiments use support plates of some type to keep the fuel rods aligned. Some are various forms of plastic and others are metal, but the requirement for holes is obvious and independent of material. The locations of these holes may be determined independently from a single reference point, or each hole may be positioned relative to the previous hole. It is also conceivable that lines are measured for the rows and columns of holes, again either from a single reference point or from the previous rank or file. Each of these options leads to a different degree of correlation among the hole locations. Holes that are each located relative to a single reference point are likely to have fairly low correlations among themselves; the correlation is likely higher for holes positioned relative to the previous hole. This correlation can be exacerbated if a gauge is used to control the spacing instead of independent measurements. Finally, it is possible to create correlations within rows or columns of holes if they are laid out along lines that are placed on the plates. The WPNCS/UACSA benchmark scenarios include either fully correlated or uncorrelated hole locations; no scenario examines partial correlations such as those resulting from lines of holes. Other factors can also influence the correlation, such as the order in which the holes are drilled and the frequency with which drill bits are replaced. A significant amount of information must be obtained about the fabrication of the plates and retained in documentation to allow these factors to be understood and addressed in attempts to understand the correlations that exist among critical experiments using these plates. Reference measurements of the spacing among various pairs of holes would be quite helpful in quantifying the uncertainty and correlation among grid plate holes. Measurements of the overall envelope of the holes, such as those reported in [65], can also be helpful. A combination of both would be nearly ideal documentation. Newer experiments may also be able to provide descriptions of the computerized machining performed to create the grid plates.

The handling and use of individual fuel rods in each experiment within a series can also have profound impacts on the correlations between the individual experiments. Some of these

aspects impact the degree of correlation of the fuel rod positions, while others are related to the composition and dimensions of the rods themselves. These latter factors are more obvious. A higher degree of correlation will be created between experiments if the same rods are used in all cases, and even more so if the same rods are used in the same locations. While Scenario A assumed that all fuel rods were identical, Scenario E samples the physical dimensions of each rod separately. There is no consideration of the possibility that the same rod may be used in the same location in each experiment. This possibility has been examined to some degree in the literature [41], and bears further study. The placement of the fuel rods within the assembly also has a bearing on the correlation of the experiments. It is possible that some aspect of the loading of the rods, manipulation of the hardware, or tilt in the experimental facility could lead all rods to shift in the same direction within the support plate holes. This will create stronger correlations of rod positions within an experiment and also strong correlations between experiments. No scenario within the WPNCS/UACSA benchmark considers this type of correlation. The operational aspects involved in this include questions about the unloading and reloading of fuel rods between experiments. In LCT-039, many locations have a fuel rod in different experiments; it is not known if the fuel rods were offloaded and reloaded into Apparatus B for each experiment. The stand holding the rods (see Figure 2 of the ICSBEP Handbook evaluation of LCT-039 [15]) was removed from the tank between experiments so that the new fuel rod patterns could be created. The handling of this stand with a crane is likely to have randomized the locations of the rods within the holes, but also presents an opportunity for all the rods to shift the same direction depending on crane movement. Again, the collection and retention of a large amount of extremely detailed information is needed to make informed assessments of the degree of correlation of fuel rod positions within and between experiments. Unfortunately, much of this information was never collected and is lost to history.

Table 4 provides the k_{eff} results for Scenario E. The expected k_{eff} values, their uncertainties, the nominal k_{eff} values, and their uncertainties are all the same as those shown in Table 3. The values are repeated to simplify comparisons. The results were again generated using 150 realizations, with each KENO calculation converged to an uncertainty of 0.00050 Δk to 0.00080 Δk. The total computational burden was once again approximately 550 CPU-hours. The initial results for Scenario E correlation coefficients are shown in Figure 31.

The average over the 150 realizations for Scenario E is not, in most cases, within two standard deviations of the average value. This is apparent because the uncertainties are so much lower for each case in Scenario E than for Scenario A. In general, the differences between the average k_{eff} value and the nominal values are very similar between Scenario A and Scenario E. No reason has been identified that causes the average of the realizations to be more reactive than the nominal case, but it cannot be related to the fuel rod position modeling given that the differences from nominal are in good agreement for both scenarios.

The k_{eff} values for the individual realizations are shown in Figure 32 for LCT-007 Case 1 and Figure 33 LCT-007 Case 3. These cases are selected as LCT-007 Case 1 has the same pitch as the LCT-039 cases and has the highest standard deviation of realizations, while LCT-007 Case 3 has the lowest standard deviation. The low variability of realizations for the latter case

Table 4. k_{eff} Results for Scenario E Calculations

Case	Expected k_{eff}	Evaluation Uncertainty	Nominal k_{eff}	Nominal k_{eff} Uncert.	Average of Realizations	Standard Deviation
7-1	1.00000	0.00140	0.99392	0.00010	0.99605	0.00102
7-2	1.00000	0.00080	0.99614	0.00010	0.99911	0.00060
7-3	1.00000	0.00070	0.99654	0.00010	0.99796	0.00063
39-1	1.00000	0.00140	0.99539	0.00010	0.99592	0.00074
39-2	1.00000	0.00140	0.99460	0.00010	0.99680	0.00071
39-3	1.00000	0.00140	0.99627	0.00010	0.99624	0.00069
39-4	1.00000	0.00140	0.99348	0.00010	0.99556	0.00063
39-5	1.00000	0.00090	0.99552	0.00010	0.99733	0.00068
39-6	1.00000	0.00090	0.99484	0.00010	0.99690	0.00084
39-7	1.00000	0.00120	0.99377	0.00010	0.99590	0.00075
39-8	1.00000	0.00120	0.99383	0.00010	0.99609	0.00066
39-9	1.00000	0.00120	0.99365	0.00010	0.99610	0.00064
39-10	1.00000	0.00120	0.99466	0.00010	0.99689	0.00071
39-11	1.00000	0.00130	0.99266	0.00010	0.99475	0.00072
39-12	1.00000	0.00130	0.99287	0.00010	0.99499	0.00075
39-13	1.00000	0.00130	0.99284	0.00010	0.99498	0.00072
39-14	1.00000	0.00130	0.99346	0.00010	0.99555	0.00071
39-15	1.00000	0.00130	0.99384	0.00010	0.99570	0.00069
39-16	1.00000	0.00130	0.99687	0.00010	0.99609	0.00075
39-17	1.00000	0.00130	0.99353	0.00010	0.99580	0.00071

	7-1	7-2	7-3	39-1	39-2	39-3	39-4	39-5	39-6	39-7	39-8	39-9	39-10	39-11	39-12	39-13	39-14	39-15	39-16	39-17
7-1	1.000	0.016	-0.017	0.038	-0.031	-0.033	0.063	-0.032	0.082	0.000	0.082	0.098	0.128	0.061	0.099	0.152	0.135	0.212	0.042	0.058
7-2	0.016	1.000	0.066	-0.116	-0.088	0.127	0.224	0.118	0.037	0.150	-0.045	0.016	0.076	-0.037	0.028	0.101	-0.056	-0.054	0.057	-0.024
7-3	-0.017	0.066	1.000	0.044	0.048	0.073	0.064	0.135	0.133	0.031	0.042	0.128	0.141	0.048	0.036	0.041	-0.078	0.081	0.094	0.057
39-1	0.038	-0.116	0.044	1.000	0.125	0.063	0.133	0.175	0.192	0.110	0.165	0.096	0.205	0.103	0.071	-0.020	0.173	0.073	0.115	0.158
39-2	-0.031	-0.088	0.048	0.125	1.000	0.016	0.155	-0.006	0.207	0.088	0.053	0.139	0.106	-0.009	0.054	0.217	-0.043	0.136	0.007	0.092
39-3	-0.033	0.127	0.073	0.063	0.016	1.000	0.081	0.092	0.036	0.087	-0.030	0.030	0.197	0.007	0.092	0.254	-0.002	0.023	0.145	0.114
39-4	0.063	0.224	0.064	0.133	0.155	0.081	1.000	0.130	0.158	0.080	-0.007	0.052	0.065	-0.024	0.031	0.152	0.073	0.033	0.099	0.021
39-5	-0.032	0.118	0.135	0.175	-0.006	0.092	0.130	1.000	0.185	0.090	0.090	0.211	0.186	0.114	0.054	0.164	0.250	0.039	0.265	0.067
39-6	0.082	0.037	0.133	0.192	0.207	0.036	0.158	0.185	1.000	0.124	0.029	0.094	0.146	0.096	0.083	0.080	0.010	0.155	0.226	0.154
39-7	0.000	0.150	0.031	0.110	0.088	0.087	0.080	0.090	0.124	1.000	0.168	0.070	0.113	0.086	0.050	0.129	0.116	0.100	0.158	0.023
39-8	0.082	-0.045	0.042	0.165	0.053	-0.030	-0.007	0.090	0.029	0.168	1.000	-0.043	0.113	-0.046	0.018	0.036	0.049	0.064	0.033	0.048
39-9	0.098	0.016	0.128	0.096	0.139	0.030	0.052	0.211	0.094	0.070	-0.043	1.000	0.089	0.023	0.166	-0.032	0.134	-0.082	-0.003	0.118
39-10	0.128	0.076	0.141	0.205	0.106	0.197	0.065	0.186	0.146	0.113	0.113	0.089	1.000	0.072	0.169	0.069	0.112	0.100	0.052	0.036
39-11	0.061	-0.037	0.048	0.103	-0.009	0.007	-0.024	0.114	0.096	0.086	-0.046	0.023	0.072	1.000	0.038	0.127	-0.071	0.013	0.130	-0.036
39-12	0.099	0.028	0.036	0.071	0.054	0.092	0.031	0.054	0.083	0.050	0.018	0.166	0.169	0.038	1.000	0.199	0.215	0.046	0.058	0.035
39-13	0.152	0.101	0.041	-0.020	0.217	0.254	0.152	0.164	0.080	0.129	0.036	-0.032	0.069	0.127	0.199	1.000	0.238	0.230	0.287	0.177
39-14	0.135	-0.056	-0.078	0.173	-0.043	-0.002	0.073	0.250	0.010	0.116	0.049	0.134	0.112	-0.071	0.215	0.238	1.000	0.188	0.105	0.133
39-15	0.212	-0.054	0.081	0.073	0.136	0.023	0.033	0.039	0.155	0.100	0.064	-0.082	0.100	0.013	0.046	0.230	0.188	1.000	0.105	-0.011
39-16	0.042	0.057	0.094	0.115	0.007	0.145	0.099	0.265	0.226	0.158	0.033	-0.003	0.052	0.130	0.058	0.287	0.105	0.105	1.000	-0.037
39-17	0.058	-0.024	0.057	0.158	0.092	0.114	0.021	0.067	0.154	0.023	0.048	0.118	0.036	-0.036	0.035	0.177	0.133	-0.011	-0.037	1.000

Figure 31. Initial Critical experiment correlations for WPNCS/UACSA benchmark of LCT-007 and LCT-039, Scenario E.

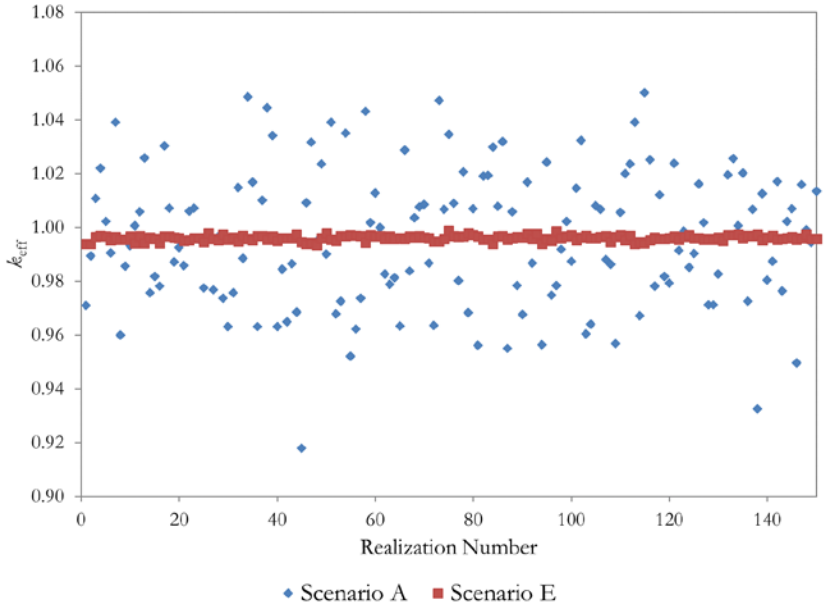

Figure 32. Individual realization k_{eff} values for LCT-007 Case 1.

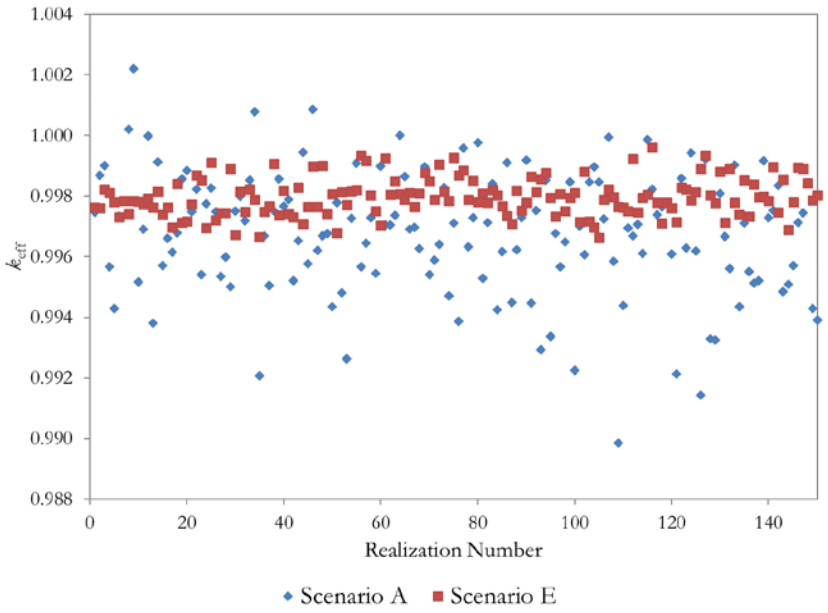

Figure 33. Individual realization k_{eff} values for LCT-007 Case 3.

is due to the near-optimum pitch used in the array. The figures illustrate the dramatically reduced variation in system reactivity associated with Scenario E and random pin placement as opposed to Scenario A and systematic pin pitch changes. It is also clear that the uncertainty is lower in both scenarios in LCT-007 Case 3 with the larger nominal pitch. The standard deviation of the realizations is on the order of 50% of the uncertainty from the ICSBEP evaluation [15]. As mentioned in Chapter III, other studies [59] have indicated that the current uncertainty guide in the ICSBEP Handbook [15] overestimates the uncertainty of LEU pin array experiments. These results could be further support for this observation or could indicate that the random, independent fuel rod placement model underestimates uncertainty.

The correlation coefficients shown in Figure 31 are quite low. There is no apparent pattern to the results. There are a few cases that appear to have higher correlation coefficients, such as LCT-039 Case 16 with Cases 5, 6, and 13. LCT-039 Cases 5 and 6 have fuel rods loaded in every other location, as shown in Figure 27. LCT-039 Case 16 has a similar loading configuration to LCT-039 Case 14 (see Figure 27), except that the lower left corner of the 2x2 loading region is in location (6,6) instead of (4,4). It is entirely possible that high correlations exist between Cases 5 and 6 with Cases 11 through 17, which also have a region with removed fuel rods. Such a scenario should include higher correlations for all these cases, but this is not evident in the results. Also, it seems logical that the correlation between Cases 5 and 6 would be at least as high. This is also not evident in Figure 31.

Further investigation shows that the 95% confidence interval on the correlation coefficient between LCT-039 Case 13 and LCT-039 Case 16 is from 0.133 to 0.428. This indicates that correlations coefficients for LCT-039 Case 16 with Cases 5 and 6 are all statistically equivalent. The remaining 16 cases in the matrix have lower correlation coefficients that are statistically significantly different. There is no clear explanation for this result. This apparent anomaly is one of the reasons additional studies were performed on the cases considered in the WPNCS/UACSA benchmark.

An examination of the correlations among LCT-039 Cases 11 through 17 is also warranted given the qualitative similarities evident in the loading configurations noted above. LCT-039 Case 11 does not appear to be correlated at all with Cases 12 through 17. Case 12 appears to be moderately correlated with Cases 13 and 14, but not Cases 15 through 17. Case 13 appears to have correlations with Cases 14 through 17, and potentially more strongly with Cases 14 through 16 than with Case 17. Case 14 appears to be correlated with Case 15, but not with Cases 16 or 17. Case 15 does not appear to be correlated with Case 16 or 17, and Case 16 also appears to be uncorrelated to Case 17. These results are puzzling, and also contribute to the desire for additional studies to explain the apparently anomalous results.

Ignoring the apparent anomalies for the moment, only 28 of the 190 correlation coefficients are statistically significantly nonzero. No correlation coefficient is as high as 0.3, which is a dramatic departure from the Scenario A results. These results make it clear that the treatment of fuel rod pitch has a significant impact on calculated correlation coefficients. This conclusion is physically intuitive, especially given the obvious impact of the pitch

modeling shown in Figure 32 and Figure 33. Further investigation, presented in the next section, is clearly necessary to confirm these results and the associated conclusion.

Additional Studies

The results presented in the previous section are the result of an initial attempt at calculating critical experiment correlations for these experiments. There are some anomalous results, especially in Scenario E, and further investigation of these results is warranted given the general lack of experience with the Monte Carlo sampling method for calculating critical experiment correlations. The two primary studies both regard convergence. The first looks at the convergence of the correlation coefficients to determine if enough realizations have been created and run to achieve converged correlation coefficient estimates. The second study investigates the impact of the final Monte Carlo uncertainty in each realization on the correlation coefficients. Lower numbers of realizations and higher stochastic uncertainties are both advantageous for practitioners to minimize the run-time investment in the determination of the correlations. The final study documented in this section compares KENO calculations performed in CE mode to the correlation resulting from MG calculations. Again, MG calculations are faster and therefore desirable in comparison to CE calculations. Essentially all of these studies are attempts to establish the minimum run-time investment to generate useful, reliable, and plausible correlation coefficients.

Correlation Coefficient Convergence

This study examines the number of realizations that are necessary to generate converged correlation coefficient estimates from the Monte Carlo sampling technique. All Monte Carlo sampling problems require this type of study, as the random sampling generates a string of estimates of the quantity of interest. After enough samples are generated, the average estimate of the quantity, in this case the correlation coefficient, stops changing. In most cases, this final result is used as the best estimate of the quantity of interest. The sampling approach to generate correlation coefficients does not suffer from the correlated sampling effects that are endemic to Monte Carlo calculations of k_{eff} because each sample is uncorrelated from the others. In this instance, sequential realizations of particular experiments are uncorrelated. Each realization of potentially correlated experiments will share identical sampled values for shared uncertain parameters.

The method for examining convergence of the correlation coefficient is simple. The correlation coefficient is calculated with increasing number of realizations until the estimated correlation coefficient stabilizes on a value. This convergence will be judged graphically, though in principle more advanced statistical methods could be used to determine convergence. It is also worth noting that there is no requirement to discard initial estimates because there is no initial guess at the correlation coefficient. In this regard, the Monte Carlo sampling technique for determining correlation coefficients is analogous to fixed source Monte Carlo transport calculations and not eigenvalue calculations.

Two example convergence checks are provided in Figure 34 for Scenario A. Both correlation coefficients examined involve LCT-007 Case 1. The correlation to LCT-007 Case 3 is

included as an example of a moderate correlation coefficient, and the correlation with LCT-039 Case 1 is included to represent high correlation cases. As shown in the figure, the high correlation coefficient case convergences more quickly, as expected, and probably needs only approximately 75 realizations to achieve convergence. The lower convergence case is probably converged by about 95 realizations. It appears that 150 is a sufficient number of realizations for both situations in Scenario A.

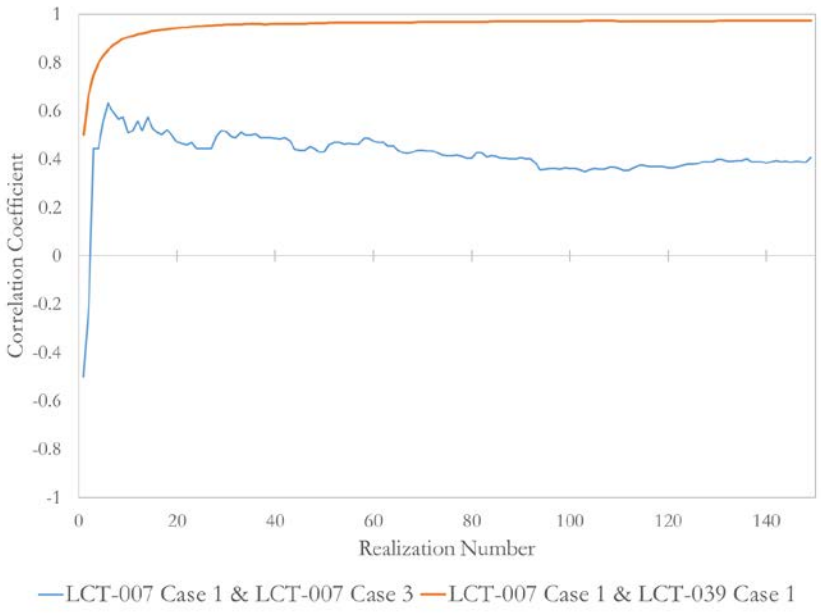

Figure 34. Convergence summary for two correlation coefficients, Scenario A.

Similar convergence checks are performed for Scenario E, as shown in Figure 35. The correlation between the same two pairs of cases is used for consistency. The correlation coefficient between LCT-039 Cases 13 and 16 is also included because that is the largest correlation coefficient in the Scenario E results, as shown in Figure 31. The correlation between LCT-039 Cases 1 and 14 is also added as it is an intermediate value for the range of coefficients observed in Scenario E. The results shown in Figure 35 generally look acceptable. The LCT-007 Case 1 coefficients both look well converged, as does the correlation between LCT-039 Cases 13 and 16. There may be a slight indication of nonconvergence for LCT-039 Cases 1 and 14, especially at approximately realization 125. Based on these results, a study expanding to 300 realizations was conducted to ensure convergence had been achieved, specifically in Scenario E.

The k_{eff} values and their standard deviations from all 300 realizations are provided in Table 5. These values are in good agreement with the average values shown in Table 4, indicating that the average k_{eff} estimates converge more quickly than the correlation coefficients. A plot of the convergence of k_{eff} as a function of realizations is shown in Figure 36. The convergence of the average k_{eff} value for LCT-007 Cases 1 and 3 and LCT-039 Case 1 are presented. The k_{eff} values are converged in all cases by realization 100, and in LCT-007 Case 3 and LCT-039 Case 1 by approximately realization 40. Clearly, the convergence of the k_{eff}

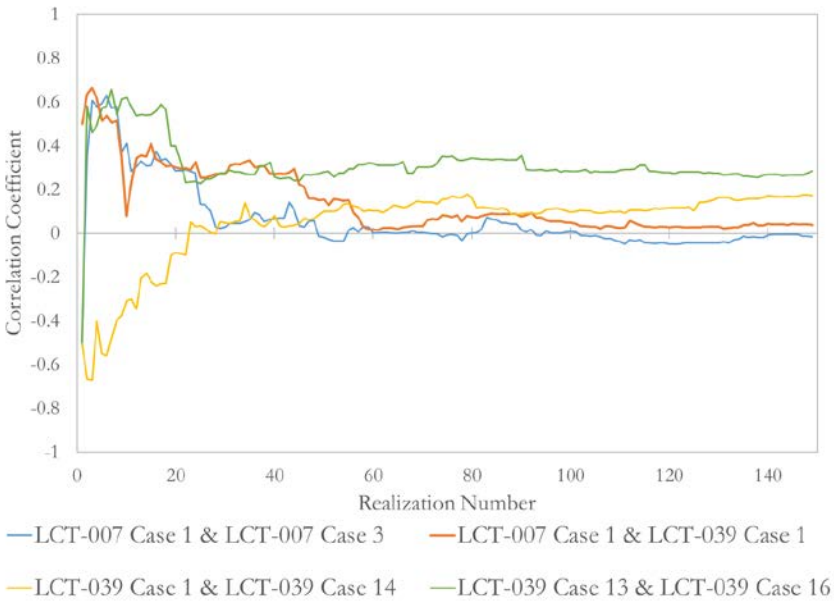

Figure 35. Convergence summary for four correlation coefficients, Scenario E, 150 realizations.

Table 5. k_{eff} Results for Scenario E Calculations with 300 Realizations

Case	Expected k_{eff}	Evaluation Uncertainty	Nominal k_{eff}	Nominal k_{eff} Uncert.	Average of Realizations	Standard Deviation
7-1	1.00000	0.00140	0.99392	0.00010	0.99609	0.00095
7-2	1.00000	0.00080	0.99614	0.00010	0.99910	0.00066
7-3	1.00000	0.00070	0.99654	0.00010	0.99797	0.00067
39-1	1.00000	0.00140	0.99539	0.00010	0.99582	0.00073
39-2	1.00000	0.00140	0.99460	0.00010	0.99675	0.00071
39-3	1.00000	0.00140	0.99627	0.00010	0.99625	0.00072
39-4	1.00000	0.00140	0.99348	0.00010	0.99555	0.00064
39-5	1.00000	0.00090	0.99552	0.00010	0.99734	0.00067
39-6	1.00000	0.00090	0.99484	0.00010	0.99688	0.00077
39-7	1.00000	0.00120	0.99377	0.00010	0.99586	0.00073
39-8	1.00000	0.00120	0.99383	0.00010	0.99609	0.00071
39-9	1.00000	0.00120	0.99365	0.00010	0.99608	0.00064
39-10	1.00000	0.00120	0.99466	0.00010	0.99691	0.00071
39-11	1.00000	0.00130	0.99266	0.00010	0.99474	0.00072
39-12	1.00000	0.00130	0.99287	0.00010	0.99501	0.00073
39-13	1.00000	0.00130	0.99284	0.00010	0.99501	0.00070
39-14	1.00000	0.00130	0.99346	0.00010	0.99558	0.00068
39-15	1.00000	0.00130	0.99384	0.00010	0.99573	0.00065
39-16	1.00000	0.00130	0.99687	0.00010	0.99607	0.00070
39-17	1.00000	0.00130	0.99353	0.00010	0.99580	0.00068

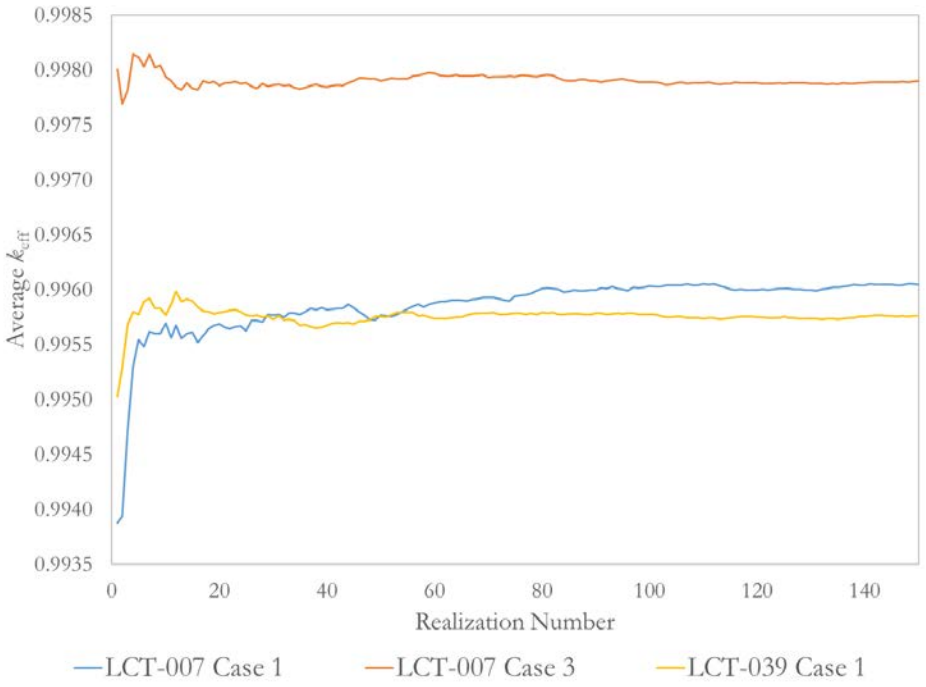

Figure 36. Convergence summary for k_{eff}, Scenario E, 150 realizations.

values cannot be used to confirm convergence of the correlation coefficients. As indicated in Table 5, the standard deviation of the k_{eff} estimates is reduced slightly with 300 realizations compared to the results from 150 realizations provided in Table 4. Doubling the number of realizations appears to lower the standard deviation of the k_{eff} estimates by approximately 10%.

The convergence of the same four cases used in Figure 35 is examined after 300 realizations in Figure 37. The convergence of the average k_{eff} values is provided in Figure 38. The entire set of correlation coefficients generated with 300 realizations is shown in Figure 39. The convergence results again look generally good, though there is still a question as to whether or not the correlation coefficient between LCT-039 Cases 1 and 14 has converged. The average k_{eff} values are clearly converged by 150 realizations, reinforcing the conclusion that convergence of the average k_{eff} values is not an indicator of convergence of the correlation coefficient. Given that a sampling of only 4 of the 190 correlation coefficients has been examined, it is difficult to assert that 300 realizations are always sufficient. The results shown in Figure 39 show the same general pattern as those shown in Figure 31. A careful examination shows that a smaller number of correlations are still significantly different from zero. After 300 realizations, only 9 of 190, or about 4.7%, are statistically significant. This also provides some evidence that 150 realizations may not be sufficient. Many, but not all, of the anomalous correlations have resolved themselves by reducing to a level of insignificance. It seems that 300 realizations are probably sufficient for most cases. The results of the study on the effect of the KENO uncertainty presented in the next section further bolster this observation.

Stochastic Uncertainty in KENO Calculations

The Monte Carlo (stochastic) uncertainty associated with the k_{eff} calculation in KENO may impact the correlation coefficients determined via the Monte Carlo sampling method. The estimate of the correlation coefficient is calculated deterministically, as shown in Equation 1, assuming a string of k_{eff} estimates with no uncertainty. In truth, uncertainty of the k_{eff} determination is unavoidable using Monte Carlo transport. This study is intended to examine the potential impact of this calculational uncertainty in the k_{eff} estimates. The correlation coefficients in Scenario E are particularly susceptible to this effect given the lower uncertainties in this approach to locating fuel rods.

The initial results, presented in the previous section, were performed with a Monte Carlo uncertainty of approximately 0.00060 – 0.00080 Δk. This is on the same order as the overall uncertainty in the k_{eff} value averaged over all realizations. The k_{eff} values for LCT-007 Case 3 Scenario E, also shown in Figure 33, are shown in Figure 40 including the uncertainty reported by KENO. The magnitude of the uncertainty is evident in the figure.

The study performed here aims to reduce the uncertainty in the individual k_{eff} calculations to 0.00010 Δk. This is accomplished by setting the *SIG*= parameter in KENO to 0.00010. The number of generations to be run (*GEN*= parameter) is set to a sufficiently large number to allow the calculation to reach the requested uncertainty. A total of 300 realizations is used for this study, based on the results presented in the previous section. Each individual KENO

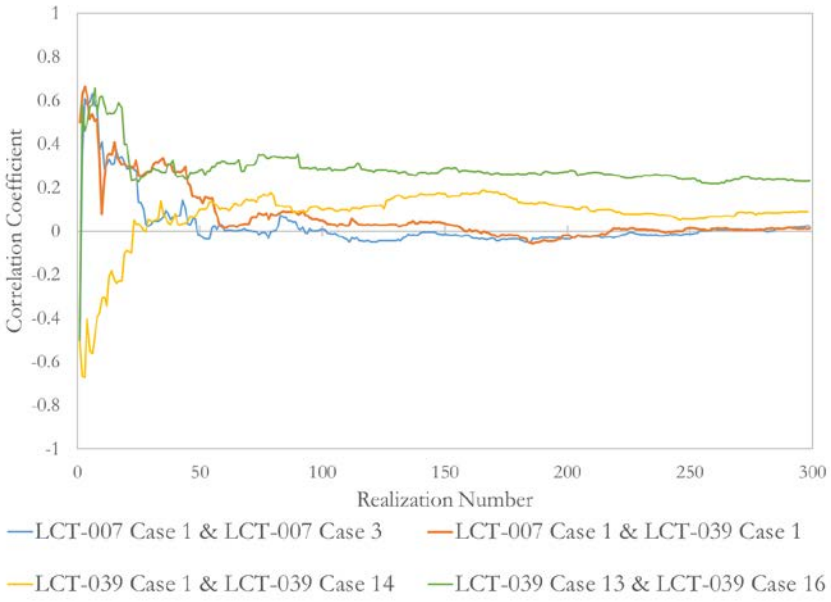

Figure 37. Convergence summary for four correlation coefficients, Scenario E, 300 realizations.

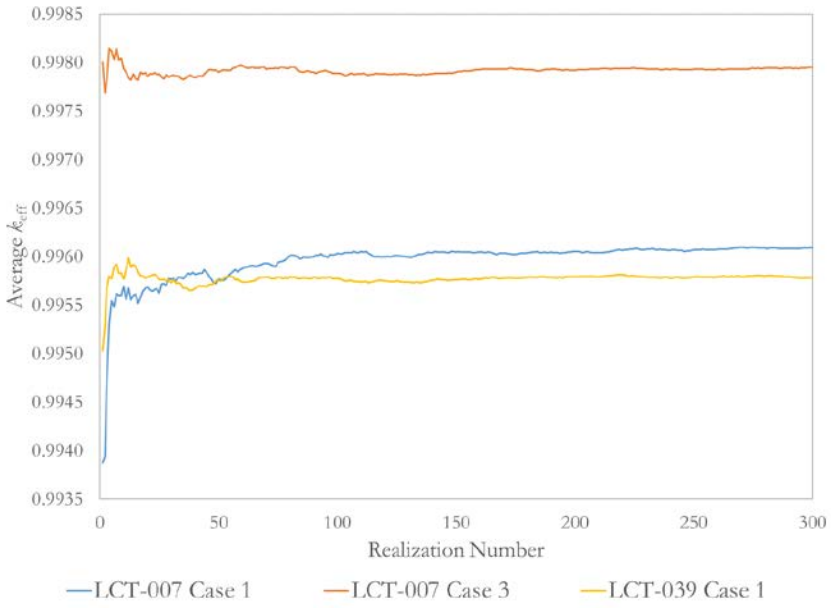

Figure 38. Convergence summary for k_{eff}, Scenario E, 300 realizations.

	7-1	7-2	7-3	39-1	39-2	39-3	39-4	39-5	39-6	39-7	39-8	39-9	39-10	39-11	39-12	39-13	39-14	39-15	39-16	39-17
7-1	1.000	0.034	0.023	0.012	0.005	-0.040	0.069	-0.009	0.071	0.067	0.082	0.088	0.049	0.044	0.042	0.063	0.088	0.139	-0.021	0.082
7-2	0.034	1.000	0.074	-0.045	0.020	0.040	0.181	0.086	0.065	0.041	-0.028	-0.034	0.009	-0.030	0.018	0.047	-0.041	0.023	0.061	-0.028
7-3	0.023	0.074	1.000	0.118	0.063	0.094	0.061	0.086	0.201	0.079	0.100	0.134	0.047	0.091	0.012	0.125	0.050	0.117	0.172	0.055
39-1	0.012	-0.045	0.118	1.000	0.121	0.138	0.076	0.071	0.124	0.034	0.100	0.085	0.135	0.023	0.037	0.037	0.087	0.083	0.115	0.149
39-2	0.005	0.020	0.063	0.121	1.000	0.034	0.075	0.037	0.130	0.041	0.055	0.049	0.009	0.025	0.095	0.100	-0.050	0.124	-0.003	0.115
39-3	-0.040	0.040	0.094	0.138	0.034	1.000	0.079	0.077	0.044	0.007	0.048	-0.064	0.145	0.076	0.061	0.090	0.067	0.059	0.088	0.116
39-4	0.069	0.181	0.061	0.076	0.075	0.079	1.000	-0.051	0.090	-0.012	-0.017	0.036	0.026	-0.021	0.034	0.088	0.042	-0.004	0.025	-0.018
39-5	-0.009	0.086	0.086	0.071	0.037	0.077	-0.051	1.000	0.138	0.081	0.043	0.140	0.112	0.059	0.085	0.131	0.184	0.001	0.161	0.093
39-6	0.071	0.065	0.201	0.124	0.130	0.044	0.090	0.138	1.000	0.103	-0.014	0.035	0.149	0.051	0.062	0.116	0.013	0.074	0.153	0.127
39-7	0.067	0.041	0.079	0.034	0.041	0.007	-0.012	0.081	0.103	1.000	0.131	0.007	0.004	0.024	-0.003	0.111	0.053	0.081	0.173	0.035
39-8	0.082	-0.028	0.100	0.100	0.055	0.048	-0.017	0.043	-0.014	0.131	1.000	-0.067	0.047	-0.016	0.063	0.004	0.030	0.013	0.050	0.070
39-9	0.088	-0.034	0.134	0.085	0.049	-0.064	0.036	0.140	0.035	0.007	-0.067	1.000	0.082	0.041	0.070	0.000	0.046	-0.081	-0.009	0.077
39-10	0.049	0.009	0.047	0.135	0.009	0.145	0.026	0.112	0.149	0.004	0.047	0.082	1.000	0.080	0.069	-0.004	0.041	0.115	0.119	0.047
39-11	0.044	-0.030	0.091	0.023	0.025	0.076	-0.021	0.059	0.051	0.024	-0.016	0.041	0.080	1.000	0.115	0.022	-0.087	-0.048	0.112	0.046
39-12	0.042	0.018	0.012	0.037	0.095	0.061	0.034	0.085	0.062	-0.003	0.063	0.070	0.069	0.115	1.000	0.132	0.112	0.006	0.065	0.069
39-13	0.063	0.047	0.125	0.037	0.100	0.090	0.088	0.131	0.116	0.111	0.004	0.000	-0.004	0.022	0.132	1.000	0.184	0.206	0.232	0.138
39-14	0.088	-0.041	0.050	0.087	-0.050	0.067	0.042	0.184	0.013	0.053	0.030	0.046	0.041	-0.087	0.112	0.184	1.000	0.148	0.051	0.204
39-15	0.139	0.023	0.117	0.083	0.124	0.059	-0.004	0.001	0.074	0.081	0.013	-0.081	0.115	-0.048	0.006	0.206	0.148	1.000	0.090	0.037
39-16	-0.021	0.061	0.172	0.115	-0.003	0.088	0.025	0.161	0.153	0.173	0.050	-0.009	0.119	0.112	0.065	0.232	0.051	0.090	1.000	-0.023
39-17	0.082	-0.028	0.055	0.149	0.115	0.116	-0.018	0.093	0.127	0.035	0.070	0.077	0.047	0.046	0.069	0.138	0.204	0.037	-0.023	1.000

Figure 39. Critical experiment correlations for WPNCS/UACSA benchmark of LCT-007 and LCT-039, Scenario E, 300 realizations.

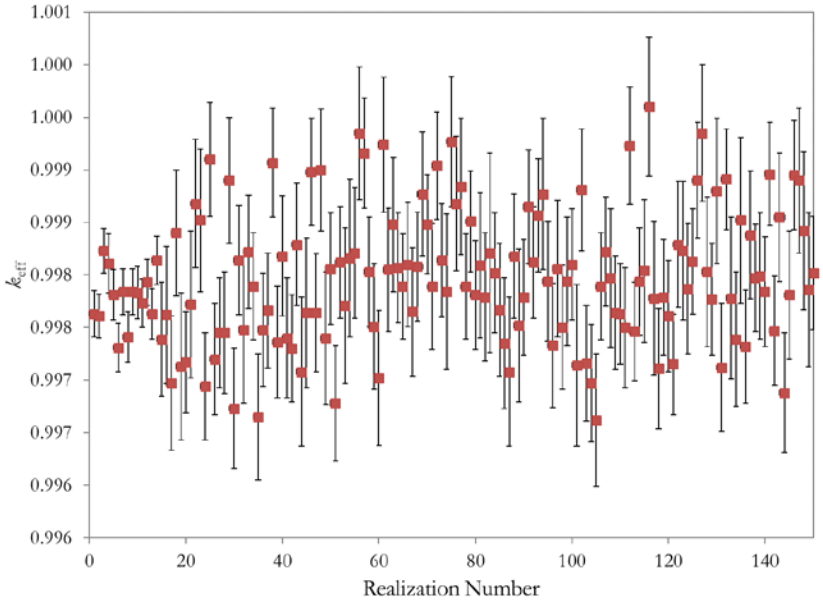

Figure 40. Initial 150 k_{eff} results, Scenario E, showing stochastic uncertainty of each realization.

case completes in about 4 hours. This run-time increases the requirement for completing the WPNCS/UACSA benchmark matrix from approximately 550 CPU-hours to something on the order of 24,000 CPU-hours. The increase is a combination of both doubling the number of realizations and reducing the stochastic uncertainty of each realization.

The remaining case, LCT-007 Case 4, has been added in this set of calculations. This case has 306 fuel rods in an 18x17 fuel rod array with a 2.52 cm pitch. The fuel rod spacing is established using the same grid plate as LCT-007 Case 1, but with three out of every 4 holes empty to double the separation between rods. In reality, this would likely create a shared uncertainty component with Case 1, but this effect is not specified in the benchmark. It is therefore also omitted from this analysis.

The average of the 300 realizations with lower KENO uncertainties are provided in Table 6. These average values are in good agreement with those shown in Table 4 and Table 5, again indicating that the average k_{eff} value is converged prior to the correlation coefficient. The standard deviation of the 300 realizations, however, is much smaller than those shown in Table 4 or Table 5. The uncertainty is reduced by a factor of about 3 for most cases compared to the initial estimates provided in Table 4. This means a significant portion of the uncertainty is a result of the stochastic uncertainty of the individual KENO calculations. This component should be random, and thus not shared among the cases. Reducing the Monte Carlo uncertainty in the individual KENO calculations should therefore increase the correlation coefficient for all cases. This is an intuitive conclusion that does not need to be proven; determining the magnitude of the effect on the correlation coefficients is the goal of this study.

Table 6. k_{eff} Results for Scenario E Calculations with 300 Realizations Converged to 0.00010 Δk

Case	Expected k_{eff}	Evaluation Uncertainty	Nominal k_{eff}	Nominal k_{eff} Uncert.	Average of Realizations	Standard Deviation
7-1	1.00000	0.00140	0.99392	0.00010	0.99609	0.00029
7-2	1.00000	0.00080	0.99614	0.00010	0.99908	0.00027
7-3	1.00000	0.00070	0.99654	0.00010	0.99785	0.00032
7-4	1.00000	0.00080	0.99837	0.00010	0.99861	0.00041
39-1	1.00000	0.00140	0.99539	0.00010	0.99574	0.00033
39-2	1.00000	0.00140	0.99460	0.00010	0.99672	0.00029
39-3	1.00000	0.00140	0.99627	0.00010	0.99625	0.00030
39-4	1.00000	0.00140	0.99348	0.00010	0.99549	0.00029
39-5	1.00000	0.00090	0.99552	0.00010	0.99728	0.00030
39-6	1.00000	0.00090	0.99484	0.00010	0.99686	0.00029
39-7	1.00000	0.00120	0.99377	0.00010	0.99581	0.00029
39-8	1.00000	0.00120	0.99383	0.00010	0.99604	0.00030
39-9	1.00000	0.00120	0.99365	0.00010	0.99601	0.00022
39-10	1.00000	0.00120	0.99466	0.00010	0.99687	0.00031
39-11	1.00000	0.00130	0.99266	0.00010	0.99473	0.00029
39-12	1.00000	0.00130	0.99287	0.00010	0.99501	0.00030
39-13	1.00000	0.00130	0.99284	0.00010	0.99504	0.00029
39-14	1.00000	0.00130	0.99346	0.00010	0.99560	0.00030
39-15	1.00000	0.00130	0.99384	0.00010	0.99565	0.00031
39-16	1.00000	0.00130	0.99687	0.00010	0.99609	0.00031
39-17	1.00000	0.00130	0.99353	0.00010	0.99581	0.00029

The correlation coefficients presented in Figure 41 are clearly different than the initial results for Scenario E (see Figure 31) or the results with 300 realizations and higher KENO uncertainties (see Figure 39). Interestingly, it appears that LCT-007 Cases 3 and 4 are more correlated with the LCT-039 cases than LCT-007 Case 1 despite the latter experiment having the same pitch. This is likely a result of the fact that LCT-007 Case 3 is near optimum moderation and Case 4 is slightly overmoderated, so the fuel rod location uncertainty contributes less to the uncertainty in these cases. The elimination of the fuel rod position uncertainty leaves the fuel composition as a dominant, and shared, uncertainty component. The results also indicate that LCT-039 Case 9 has the highest correlation coefficient with most of the other cases. In many cases, the 95% confidence interval for the coefficients with LCT-039 Case 9 overlap the confidence intervals for adjacent experiments in the matrix, but this does not offer an explanation for the observed behavior. While this behavior is anomalous, the majority of the anomalies identified in the initial results have been resolved. The correlation coefficients are in much better agreement for similar experiments, which is the expected behavior. It is therefore concluded that the individual realization stochastic uncertainty must be reduced to about 0.00010 Δk to determine accurate correlation coefficients. This effect is also studied with the LCT-042 correlations presented later. The LCT-042 experiment has only seven cases, so it provides a less costly computational test bed for driving the Monte Carlo uncertainty of each realization to lower values.

The convergence of the correlation coefficient with the number of realizations is also potentially impacted by lower uncertainty values for the individual realization k_{eff} calculations. The same four correlation coefficients examined in Figure 35 and Figure 37 are examined, as is the correlation of LCT-007 Cases 3 and 4. This last correlation is added because it has the highest correlation coefficient for any pair of experiments in Scenario E. The results, shown in Figure 42, indicate much faster convergence for the cases with more rigorous KENO calculations. It appears that the correlation coefficients are converged within 150-200 realizations. This result bolsters the confidence that 300 realizations is sufficient, as concluded in the prior section.

Repeatability of Correlation Coefficient Determination

The goal of this study is to determine if the correlation coefficient determination process is repeatable and generates a unique solution. There are two aspects of this question: the first is with respect to the random sampling of input parameters by Sampler and the second is related to the KENO calculations for each realization. The effect of input generation in Sampler is not examined here as there is currently no simple way to change random number seeds and thus change the sampled parameters. This study therefore focuses on the effects of changing KENO random number seeds.

The study consists of running 9 additional sets of KENO calculations for all 300 realizations. The only correlation coefficient examined in this study is the correlation of LCT-039 Cases 6 and 7, due to the large run-time associated with these calculations. The average k_{eff} values for all 300 realizations of each case for each trial are shown, with their standard deviations, in Table 7. The 10 correlation coefficients are also shown in Table 7.

	7-1	7-2	7-3	7-4	39-1	39-2	39-3	39-4	39-5	39-6	39-7	39-8	39-9	39-10	39-11	39-12	39-13	39-14	39-15	39-16	39-17
7-1	1.000	0.362	0.457	0.359	0.453	0.196	0.203	0.315	0.328	0.367	0.249	0.241	0.358	0.236	0.227	0.179	0.235	0.221	0.222	0.232	0.226
7-2	0.362	1.000	0.642	0.641	0.288	0.300	0.315	0.328	0.425	0.404	0.322	0.298	0.547	0.345	0.294	0.302	0.326	0.327	0.318	0.325	0.321
7-3	0.457	0.642	1.000	0.853	0.417	0.451	0.452	0.440	0.589	0.550	0.474	0.431	0.710	0.472	0.403	0.437	0.441	0.477	0.449	0.473	0.463
7-4	0.359	0.641	0.853	1.000	0.437	0.447	0.486	0.450	0.613	0.521	0.470	0.446	0.697	0.486	0.424	0.432	0.448	0.488	0.450	0.473	0.477
39-1	0.453	0.288	0.417	0.437	1.000	0.234	0.241	0.229	0.299	0.380	0.260	0.270	0.358	0.269	0.210	0.232	0.278	0.265	0.283	0.273	0.263
39-2	0.196	0.300	0.451	0.447	0.234	1.000	0.244	0.244	0.298	0.375	0.277	0.267	0.412	0.290	0.245	0.225	0.254	0.263	0.272	0.265	0.241
39-3	0.203	0.315	0.452	0.486	0.241	0.244	1.000	0.235	0.278	0.337	0.230	0.238	0.420	0.252	0.210	0.224	0.251	0.267	0.264	0.276	0.240
39-4	0.315	0.328	0.440	0.450	0.229	0.244	0.235	1.000	0.270	0.333	0.200	0.245	0.394	0.255	0.184	0.222	0.248	0.243	0.243	0.259	0.245
39-5	0.328	0.425	0.589	0.613	0.299	0.298	0.278	0.270	1.000	0.334	0.278	0.305	0.479	0.276	0.247	0.272	0.280	0.295	0.287	0.295	0.260
39-6	0.367	0.404	0.550	0.521	0.380	0.375	0.337	0.333	0.334	1.000	0.337	0.334	0.502	0.333	0.301	0.293	0.321	0.342	0.307	0.328	0.289
39-7	0.249	0.322	0.474	0.470	0.260	0.277	0.230	0.200	0.278	0.337	1.000	0.306	0.401	0.271	0.243	0.250	0.297	0.292	0.309	0.331	0.280
39-8	0.241	0.298	0.431	0.446	0.270	0.267	0.238	0.245	0.305	0.334	0.306	1.000	0.416	0.268	0.251	0.225	0.250	0.273	0.260	0.290	0.247
39-9	0.358	0.547	0.710	0.697	0.358	0.412	0.420	0.394	0.479	0.502	0.401	0.416	1.000	0.393	0.400	0.393	0.370	0.403	0.388	0.400	0.409
39-10	0.236	0.345	0.472	0.486	0.269	0.290	0.252	0.255	0.276	0.333	0.271	0.268	0.393	1.000	0.205	0.220	0.269	0.258	0.271	0.280	0.219
39-11	0.227	0.294	0.403	0.424	0.210	0.245	0.210	0.184	0.247	0.301	0.243	0.251	0.400	0.205	1.000	0.226	0.267	0.251	0.275	0.278	0.256
39-12	0.179	0.302	0.437	0.432	0.232	0.225	0.224	0.222	0.272	0.293	0.250	0.225	0.393	0.220	0.226	1.000	0.285	0.262	0.275	0.298	0.292
39-13	0.235	0.326	0.441	0.448	0.278	0.254	0.251	0.248	0.280	0.321	0.297	0.250	0.370	0.269	0.267	0.285	1.000	0.281	0.300	0.290	0.281
39-14	0.221	0.327	0.477	0.488	0.265	0.263	0.267	0.243	0.295	0.342	0.292	0.273	0.403	0.258	0.251	0.262	0.281	1.000	0.273	0.277	0.267
39-15	0.222	0.318	0.449	0.450	0.283	0.272	0.264	0.243	0.287	0.307	0.309	0.260	0.388	0.271	0.275	0.275	0.300	0.273	1.000	0.284	0.252
39-16	0.232	0.325	0.473	0.473	0.273	0.265	0.276	0.259	0.295	0.328	0.331	0.290	0.400	0.280	0.278	0.298	0.290	0.277	0.284	1.000	0.257
39-17	0.226	0.321	0.463	0.477	0.263	0.241	0.240	0.245	0.260	0.289	0.280	0.247	0.409	0.219	0.256	0.292	0.281	0.267	0.252	0.257	1.000

Figure 41. Critical experiment correlations for WPNCS/UACSA benchmark of LCT-007 and LCT-039, Scenario E, 300 realizations, individual realization calculations converged to 0.00010 Δk.

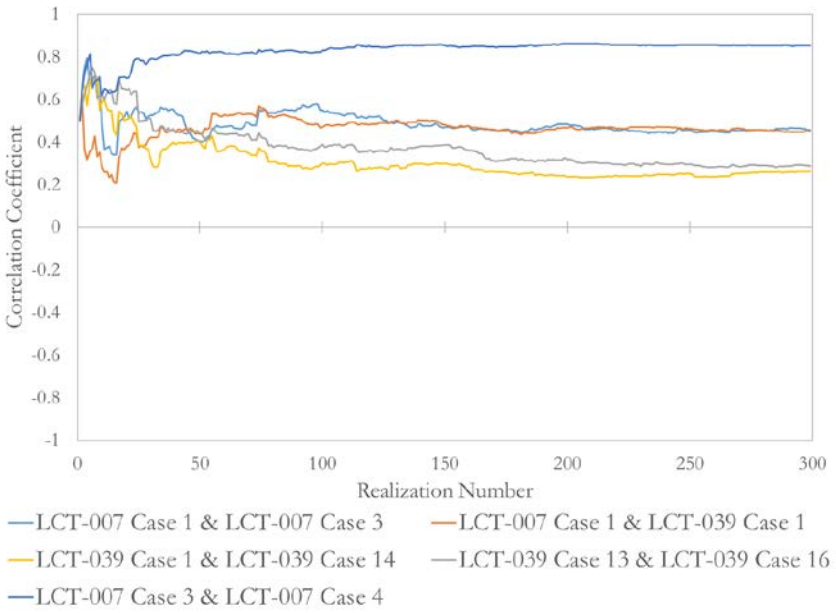

Figure 42. Convergence summary for five correlation coefficients, Scenario E, 300 realizations, individual calculations converged to 0.00010 Δk.

Table 7. Results for 10 Trials of Calculating the Correlation Coefficient Between LCT-039 Cases 6 and 7

Trial	LCT-039 Case 6		LCT-039 Case 7		Correlation Coefficient
	Average k_{eff}	Std. Dev.	Average k_{eff}	Std. Dev.	
0	0.99686	0.00029	0.99581	0.00029	0.337
1	0.99688	0.00029	0.99582	0.00028	0.281
2	0.99687	0.00029	0.99582	0.00029	0.310
3	0.99686	0.00028	0.99582	0.00029	0.301
4	0.99687	0.00029	0.99582	0.00028	0.302
5	0.99687	0.00028	0.99582	0.00028	0.283
6	0.99686	0.00027	0.99583	0.00028	0.298
7	0.99686	0.00028	0.99583	0.00028	0.316
8	0.99687	0.00030	0.99582	0.00029	0.250
9	0.99687	0.00028	0.99583	0.00030	0.289

Trial 0 is the default random number seed. All 600 KENO calculations have the same random number seed in each trial.

The average k_{eff} for both LCT-039 Cases 6 and 7 are very similar for all 10 trials. The difference between the maximum and minimum values for each case is 0.00002 Δk, which is much smaller than the standard deviation of the k_{eff} estimates. The variation in the standard deviations is also fairly small, though slightly larger than the variability in the average values themselves.

The average of the 10 estimates of the correlation coefficient is 0.297 and the standard deviation is 0.023. The Fisher transformation one-sigma uncertainty for a correlation coefficient of 0.297 is approximately 0.025. This is very good agreement, though more extensive studies would be needed to confirm any general agreement between these methods of estimating the uncertainty in the correlation coefficient.

Convergence of the correlation coefficients for Trials 0, 6, and 8 is examined in Figure 43. The trials are selected as they represent the maximum correlation coefficient (Trial 0), the minimum coefficient (Trial 8), and the coefficient closest to the average of all trials (Trial 6). All three trials shown here appear well converged, with convergence achieved by around realization 200. The general shape of the curves is similar because the same realizations are used, only the random number seed is changed. The variation in each calculated k_{eff} should be less than 0.00020 Δk in most cases because the one-sigma uncertainty for each calculation is set to 0.00010 Δk.

All 10 estimates are within two standard deviations of the average, though it should be noted that the original estimate is the maximum coefficient of the 10 trials. The 95% confidence interval on the original estimate of the correlation coefficient (0.337), based on the Fisher transformation, is from 0.233 to 0.434. All 10 trials result in correlations within this range. All 9 additional trials are more than one standard deviation away from the correlation calculated with the default random number seed in KENO. This is not a particularly comforting result, and may indicate that this single result is an outlier. Further investigation of the repeatability of the correlation coefficient determination may be warranted.

Continuous-energy KENO Calculations

The KENO calculations for all the individual realizations in all previous studies have used MG KENO. This decision is primarily based on the run-time savings for MG compared to CE calculations. As will be discussed shortly, the CE calculations take about 5 times as long as the MG calculations for these models. This factor would indicate a total of about 120,000 CPU-hours when applied to the entire suite of calculations needed to determine correlation coefficients for all the experiments in this benchmark. This represents almost 3 weeks of run-time with 256 cores continuously; this level of computational expense is prohibitive for the practical use of the Monte Carlo sampling method to determine critical experiment correlations.

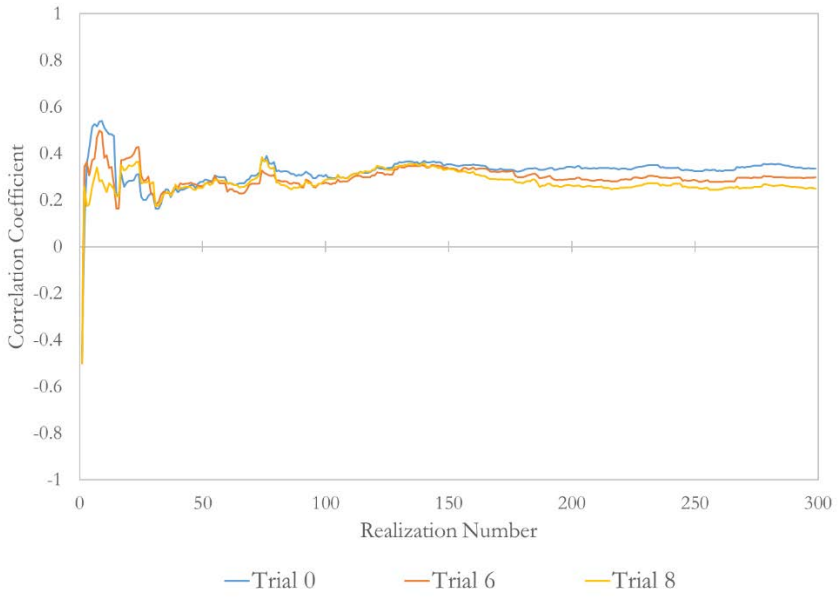

Figure 43. Convergence summary for three trials of LCT-039 Cases 6 and 7 correlation coefficient.

One concern with the MG calculations is that proper self-shielding of the cross section is not possible. The *latticecell* treatment used in SCALE assumes an infinite array of pins, but is a very good approximation when applied to large, uniform arrays. In Scenario E, the array is nonuniform in every direction as each rod is positioned independently. It is therefore possible that a bias is introduced in the KENO results using the MG approximation.

This possibility is investigated with a small and fairly simple study involving only the correlation coefficient between LCT-007 Cases 1 and 3. All 300 perturbed realizations for both cases are rerun with CE KENO, converging to a stochastic uncertainty of 0.00010 Δk. The perturbed inputs are identical between MG and CE, except for the single line declaring which cross section library should be used for the calculations. The CE library based on ENDF/B-VII.1 is used to ensure that the primary source of difference between the two sets of calculations is just the energy treatment.

The average k_{eff} values for both the MG and CE calculations, and their associated standard deviations, for both LCT-007 Cases 1 and 3 are provided in Table 8. A bias correction is applied to provide a direct, unbiased comparison. According to [67], the ENDF/B-VII.1 libraries in KENO V.a have a bias of -0.00085 Δk for MG calculations and -0.00030 Δk for CE calculations. Subtracting the appropriate bias from each average value provides the best estimate of the actual average k_{eff} value for each set of calculations. This step is not necessary for calculating correlation coefficients because the adjustment cancels exactly; the variation of the calculated k_{eff} values is measured to determine the correlation coefficients. The results shown in Table 8 indicate good agreement between the CE and MG results for these cases. In both cases, the difference between the average calculated k_{eff} value is less than the 2σ uncertainty in the difference.

Table 8. Average k_{eff} Results and Standard Deviations for MG and CE Calculations, LCT-007 Cases 1 and 3

LCT-007 Case	MG KENO		CE KENO		Bias Adjusted k_{eff} Values		Difference (MG – CE)	
	Avg k_{eff}	σ	Avg k_{eff}	σ	MG	CE	Δk	σ
1	0.99609	0.00029	0.99741	0.00030	0.99694	0.99771	-0.00078	0.00042
3	0.99785	0.00034	0.99827	0.00033	0.99870	0.99857	0.00013	0.00047

As indicated previously, the run-time differences are significant. For LCT-007 Case 1, the total CSAS execution time ratio range from 4.0 to 9.0. For Case 3, the ratios vary from 3.6 to 8.3. The average run-time ratios are 6.2 for Case 1 and 5.3 for Case 3. As shown in Figure 41, the correlation coefficient determined between LCT-007 Cases 1 and 3 with MG KENO calculations is 0.457. The correlation coefficient resulting from the CE calculations is 0.394. The 95% confidence interval for the correlation coefficient based on the MG KENO calculations is (0.363, 0.542), while for the CE KENO calculations it is (0.294, 0.486). The correlation coefficients are therefore statistically indistinguishable from each other. There is no evidence in this limited study that the MG KENO calculations are insufficient for determination of accurate correlation coefficients. A more extensive study would be needed to reach a definitive conclusion.

Summary of Correlations for LCT-007 and LCT-039

The WPNCS/UACSA benchmark [33] has been used as a vehicle to examine several aspects of critical experiment correlations. One of the primary points of investigation specific to modeling LEU pin array experiments is the treatment of the fuel rod pitch or location uncertainty. The other studies, regarding the number of realizations needed to establish correlation coefficients, the convergence of the individual KENO calculations, the reproducibility of the coefficients, and the agreement between CE and MG KENO, are all expected to be generically applicable to other systems. A brief synopsis of each of these studies is presented here, along with observations based on the results generated in these studies.

Fuel Rod Placement/Pitch

One of the primary areas to be investigated with the WPNCS/UACSA benchmark [33] is the impact of fuel rod placement on the correlation coefficient. This can also be interpreted as the effect of various treatments of the fuel rod pitch uncertainty. Scenario A assumes that the spacing between all pairs of rods is exactly the same, and that the uncertainty is therefore applied to all rods in the same way. This approach can introduce a large uncertainty in k_{eff} for cases that are far from optimum moderation, and the uncertainty is shared among all cases with the same pitch. The opposite extreme is embodied in Scenario E which assumes each rod is independently and randomly positioned. With this assumption, the uncertainty in k_{eff} is driven down because of the elimination of global moderation changes, and each experiment has a unique set of fuel rod locations.

The results for Scenario A are shown in Figure 30, and show a very high correlation among all cases with the same fuel rod pitch. The final results for Scenario E are provided in Figure 41, and show much lower correlations among the various cases. The different fuel rod pitch assumptions had the expected effects, and the magnitude of the difference is on the order of 0.6 in the correlation coefficients. The magnitude of the change in the correlation coefficients indicates that the treatment of the pin pitch uncertainty is extremely important in the determination of correlations among LEU pin array experiments. The pin pitch uncertainty has more impact on the correlation coefficient among these experiments than the shared fissile material.

Studies on Calculation of Correlation Coefficients

Several studies were performed with the cases in this benchmark to examine the calculation parameters necessary to determine accurate correlation coefficients. These studies examined the number of realizations needed to achieve convergence, the impact of lower stochastic uncertainties of the individual realization calculations, the repeatability of the correlation coefficient calculation, and the difference between CE and MG KENO calculations of the individual realizations.

The number of realizations necessary to converge the correlation coefficient appears to be somewhat variable with a dependence on the correlation coefficient itself. High correlations coefficients, such as those resulting from Scenario A, appear to reliably converge in fewer than 150 realizations. Lower correlation coefficients, such as those observed with Scenario E, require more realizations. A total of 200 to 250 realizations is sufficient in most cases, though 300 realizations were used in for the results presented in Figure 38 and Figure 41.

The impact of the stochastic uncertainty was examined specifically in Scenario E. As expected, a lower Monte Carlo uncertainty increases the correlation coefficients. This results because the stochastic uncertainty is unique to each case, so minimizing it reduces the unique uncertainty contribution. The correlation coefficients increase from 0.1 or less to values between 0.2 and 0.4. This difference appears small, but it is important because it increases the correlation coefficients sufficiently that all coefficients are statistically significant and nonzero.

A single correlation coefficient was calculated using the same set of 300 realizations with 10 different initial random number seeds in KENO. All ten estimates of the correlation coefficient are within two standard deviations of the average coefficient. It is not clear from the results of this study that a single set of realizations can be relied upon for accurate correlation coefficient determination, but since all results are with two standard deviations of the average value no definitive outliers exist. More study in this specific area may be warranted.

The last study presented relates to the reliability of MG KENO calculations to determine the k_{eff} value for each realization. The general disarray present in Scenario E may cause some inaccuracy in the MG cross section processing, so the calculations are also performed for

two cases with CE KENO to examine the accuracy of the MG calculations. The results for the single correlation examined indicate that the MG calculations are sufficiently accurate. A more extensive study is advisable to confirm this conclusion, but such a study was not undertaken as part of this work.

Observations

A variety of observations are noted here based on the results of the calculations and studies documented in this section.

- The computational resources necessary to perform the calculations to determine correlation coefficients among critical experiments are quite large. The generation of a matrix of correlation coefficients among 21 experiments consumed approximately 24,000 CPU-hours.
- The treatment of the pin pitch uncertainty in LEU pin array experiments can be the most important factor in the calculated correlation coefficients.
- The number of realizations needed for convergence of calculated correlation coefficients depends somewhat on the magnitude of the coefficient. High correlation coefficients appear to converge with 150 or fewer realizations, while lower correlation coefficients may require 200 to 250 realizations.
- The individual realization k_{eff} values need to be determined with the minimum feasible stochastic (Monte Carlo) uncertainty. Significant changes in the correlation coefficients are observed when the uncertainty is reduced from approximately 0.00050 Δk to 0.00010 Δk.
- MG KENO calculations appear to be provide sufficient accuracy for the determination of correlation coefficients. A more extensive study is needed to confirm this observation.
- It is not clear that a single set of realizations provides an accurate estimate of the correlation coefficient. This is potentially extremely problematic given the computational investment necessary to determine critical experiment correlations with the Monte Carlo sampling method.
- In-depth knowledge of the critical experiment materials, configurations, procedures, and setup are required for correct assessment of shared and unique uncertainty contributions. This level of information is typically not available in the ICSBEP Handbook [15], which is the primary reference at this time for critical experiment descriptions. Without this in-depth knowledge, it is difficult to make defensible determinations regarding the uncertainty sharing among different cases.

CHAPTER VI: ANALYSIS OF CORRELATION COEFFICIENTS AMONG THE CASES OF LEU-COMP-THERM-042

Critical experiment correlations among the seven cases in LCT-042 are examined here to provide another set of results for LEU pin array experiments. These experiments contain different neutron absorber panels, which contribute unique uncertainty components due to differing compositions, shapes, and array spacing. The correlation coefficients are likely to be quite different for these experiments, compared to the LCT-007 and LCT-039 cases, because of these unique uncertainty contributions. Also, the smaller number of cases reduces the computational burden to perform studies on the correlation coefficients. The LCT-042 experiments were performed at the Battelle Pacific Northwest Laboratory (PNL) in 1979 and 1980.

Three primary studies are performed on the LCT-042 correlation coefficients. The first two are related to the pin pitch uncertainty treatment and the third is related to the impact of the stochastic uncertainty in the individual realization calculations on the correlation coefficient estimates. The pin pitch studies examine the effect of the sampled variation with the assumption that the spacing between all pairs of rods is identical, and the second compares the uniform pitch assumption with correlation coefficients resulting from random pin placement. The first study is analogous to Scenario A in the WPNCS/UACSA benchmark [29], but investigates the effect of varying the uncertainty in pin pitch on the correlation coefficients. The second study is similar to the comparison of Scenario A and Scenario E from the benchmark. The final study is a more exhaustive examination of the effect of the stochastic uncertainty of the KENO calculations on the correlation coefficients. The results of the second and third studies can be directly compared with the results from the similar studies from the previous chapter.

The determination of critical experiment correlations for LCT-042 is performed with uncertainty information presented in Section 2 of the ICSBEP Evaluation [15]. The uncertain parameters, their distributions, and the distribution parameters are developed from the information provided in the evaluation. This is another key difference from the WPNCS/UACSA benchmark results presented in the last chapter. This approach is prototypic of how criticality safety practitioners will have to develop critical experiment correlations in the field, and highlights some of the challenges they are likely to face.

The discussion of the variable parameters and their development is presented in the next subsection. The following subsection provides preliminary results for the uniform pin pitch study. These initial results were determined prior to the WPNCS/UACSA benchmark discussed previously. A reexamination of the pin pitch study is subsequently presented, incorporating the lessons learned from the benchmark effort. The results of the stochastic uncertainty study are presented, followed by a summary of results and observations.

Variable Parameters

The variable parameters, the appropriate distributions, and the distribution parameters all must be developed for the LCT-042 correlations before any realizations can be created or calculated. As mentioned previously, this is a significant difference from the work described in the previous chapter on the WPNCS/UACSA benchmark. The uncertain parameters, their uncertainties, and the distributions to assume are all defined as part of the benchmark. For LCT-042, the uncertainty information provided in Section 2 of the evaluation in the ICSBEP Handbook [15] is used to develop the inputs to Sampler for all variable parameters.

The discussion of the variable parameter input is provided in the five subsections below. First, the general considerations and approaches are discussed. Then the treatment of the fuel composition is discussed, followed by details of the other compositions. A discussion of the fuel pin pitch uncertainty is provided before the rest of the dimension uncertainties are discussed in the last portion of this section.

General Considerations and Approaches

The most important part of the assessment of correlations among critical experiments is the determination of uncertain parameters, the distribution of these parameters, and the assignment of the uncertainties to individual or multiple experiments. All of these topics are extremely important; the correlation coefficient is the ratio of the shared uncertainty (covariance) to the total uncertainty in each experiment. Each the areas is discussed here in some detail.

The determination of the uncertain parameters is largely contained in Section 2 of the ICSBEP Handbook evaluation [15]. This can be problematic in general because the evaluations are not uniformly rigorous in the assessment of uncertainties. In the specific case of LCT-042, the uncertainty in most parameters is assessed. Some compositions do not have uncertainties for all constituents, and the pin pitch uncertainty is questionable. This last issue will be discussed fully below in the section regarding the uncertainty of the pin pitch. The overall quality of the uncertainty treatment is therefore judged to be adequate for this exercise, and it is envisioned that individual criticality safety practitioners would not be expected or able to perform their own assessments of the uncertainties beyond those available in the ICSBEP Handbook evaluations.

No information is available to form a basis for the distribution of the uncertainty in any of the parameters. This is a level of detail that has not been required or necessarily even envisioned in the evaluation process to date. The uncertainty in the parameter comes from a lack of precise knowledge of material constituents, geometric dimensions, or object positions. It is not necessarily correct to think about a range of enrichments being present within the fissile material, but the single average is unknown because a finite number of samples were analyzed to characterize the entire allotment. To some degree, this is also a question of homogeneity of material within an experiment, which is a discussion beyond the scope of this work. The distribution from which the parameter values are drawn should have a significantly lower effect on the correlation coefficient than the proper assignment of the

uncertainty as shared or unique. Most parameters are therefore assumed to be uniformly distributed, especially within tolerance bands if no further information is given. Variables with a standard deviation provided are assumed to be normally distributed. There is fundamentally no justification for these assumptions, but the effect of distributions was examined in [37] and found to have only small impact. No similar study on the impact of the assumed distributions of uncertain parameters has been performed as part of this work.

The ICSBEP evaluation does not contain sufficient detail regarding parameters that are shared by multiple cases or unique to a single case. In the specific case of LCT-042, it is not clear if the steel reflecting walls were assembled once, if they were rebuilt separately for each experiment, or if they remained assembled for some of the experiments but were reassembled later for others. This impacts the sampling of the position and size of the walls, in this instance, but there are several other similar aspects of the experiment descriptions for which sufficient detail is not supplied. A more subtle instance of this problem regards the fuel rods themselves. The variability of fuel rod loading is unknown, both in mass and in enrichment, and it is unknown if the same rods are used in the same locations in all experiments. This is more plausible for the LCT-042 experiments than for LCT-007 and LCT-039 because the same number of rods are used. Different rods could be used, or the locations could be changed if other experiments using other grid plates were performed between cases contained in the LCT-042 evaluation. Many additional details are needed to fully characterize the shared components among the cases included in this evaluation.

Fuel Composition Uncertainty Treatment

The uncertainty in the fuel composition is an important uncertainty, and because the same fuel material is used in all seven cases the uncertainty is treated as shared among all cases. It will therefore be an important contributor to the calculated correlation coefficients. The ICSBEP evaluation [15] provides number densities for each constituent. The uncertainties, however, are in other quantities, such as enrichment, density, and mass loading. This section discusses the uncertainties expressed in the evaluation and the process used to translate those uncertainties into perturbed isotopic number densities.

The mass of ^{235}U per rod and total mass of UO_2 are treated as fundamental parameters for the evaluation of isotopic number densities in the ICSBEP Evaluation [15]. The mass of ^{235}U is sampled early and is one of the primary variables sampled. No uncertainty in the mass of ^{235}U per rod is provided in the evaluation, despite this quantity being used as the fundamental known quantity related to the fissile material mass in the experiment. Instead, a range of different methods is used to determine the total uranium mass in Table 11 of the evaluation. This range (726g to 727.22g uranium) translates to a range of ^{235}U loadings of $\pm$0.0287g ($\pm$0.17%), which is applied in both directions about the nominal value of 17.08g ^{235}U per rod. The mass of ^{235}U per rod is thus sampled uniformly over the range from 17.0513 to 17.1087. This is twice the difference resulting from the total uranium mass range of 726g to 727.22g, but this is viewed as appropriate because it is indicative of the uncertainty in the mass per rod but not intended to be a bounding estimate.

The fuel diameter and fuel length are also sampled and subsequently used to calculate the volume of UO_2 in the fuel rod. The gram density of ^{235}U is then calculated based on the sampled gram loading and calculated volume. The resulting gram density is used to calculate the atom densities applied to all rods. This approach guarantees that the overall gram loading of ^{235}U stays within the desired range once isotopic number densities are generated and input to KENO. In other words, the volume and mass density are used consistently to ensure the desired range of mass loadings in the different realizations.

The enrichment of the fuel in LCT-042 is reportedly known quite accurately. The three-sigma uncertainty on the ^{235}U enrichment is reported as ±0.01 wt%, though this may also be the 95% confidence interval (two-sigma). Other reports cited in the ICBEP evaluation indicate the enrichment uncertainty to be ±0.05 wt%. Ultimately, the evaluation settles on the one-sigma uncertainty as ±0.003 wt%; this is in agreement with the reported three-sigma uncertainty and also a reported one-sigma uncertainty found in yet another reference. The uncertainty values in the other isotopes are not discussed as much, but are used as reported in Table 3 of the evaluation. The atomic masses of the uranium isotopes and oxygen, along with Avogadro's number, are taken from the 16th edition of the Chart of the Nuclides [68] and used to convert the sampled weight fractions to atom fractions.

The number density of ^{235}U is calculated based on the ^{235}U gram density calculated above, its atomic mass, and Avogadro's number. The isotopic number densities of ^{234}U, ^{236}U, and ^{238}U are next calculated based on the ratios of atomic fractions to ^{235}U and the ^{235}U isotopic number density. These four values are subsequently summed to determine the overall U number density. This uranium number density is multiplied by 2.012 to determine the oxygen number density; the stoichiometric value is taken from footnote (e) to Table 11 in the evaluation.

The uranium and oxygen isotopic number densities are assumed to be fully correlated among all 7 experiments. Each case therefore contains the same number densities for each specific realization. The number densities vary among the individual realizations based on newly sampled and recalculated values. The average ^{235}U number density over 300 realizations is 0.004% higher than the nominal value, and the standard deviation of the sampled number densities is 0.14% of the average.

Uncertainty Treatment for Other Compositions

The other compositions in the experiment include aluminum alloys, steel, poison panels, and water. Uncertainties are reported in different ways for each of the different materials, so a range of different treatments are implemented in the Sampler input. The uncertainties in the 7 poison panels are also reported in a variety of ways, so a range of different sampling techniques are used. A brief synopsis of each approach is provided in this section.

Three different aluminum alloys are used in the fuel rods used in the LCT-042 experiments. The cladding material is made from 6061 aluminum, the top end plug uses 1100 aluminum, and bottom end plug uses 5052 aluminum. The standard composition definitions of each of

these alloys is included in Table 4 of the evaluation. Most constituents have a specified maximum value, some have a nominal value and a range, and aluminum makes up the balance of the alloy. The nominal weight percent assumed for each constituent is provided in Table 24 of the evaluation. A relative multiplier is sampled uniformly over the range of the weight percents for each element in the alloy. For example, chromium in 6061 aluminum is present in a range of 0.04 to 0.35 weight percent. The nominal value assumed is 0.2 weight percent. The relative multiplier is therefore sampled uniformly between 0.2 and 1.75, so that the sampled weight percent ranges from 0.04 to 0.35. The relative multipliers are used directly to determine the perturbed number densities for the minor elemental constituents of the alloys so that perturbed mass densities need not be determined. The weight percent for each element in each of each alloy is determined in each realization by multiplying the relative multiplier by the nominal weight percent. The perturbed values are then each subtracted from 100 to determine the remainder that is aluminum. This perturbed aluminum weight percent is then divided by the nominal weight percent to determine the relative multiplier for the aluminum. The nominal number density is then multiplied by the relative multiplier. The perturbed mass densities for the alloys are unchanged in all realizations. A flow chart for this process is provided in Figure 44.

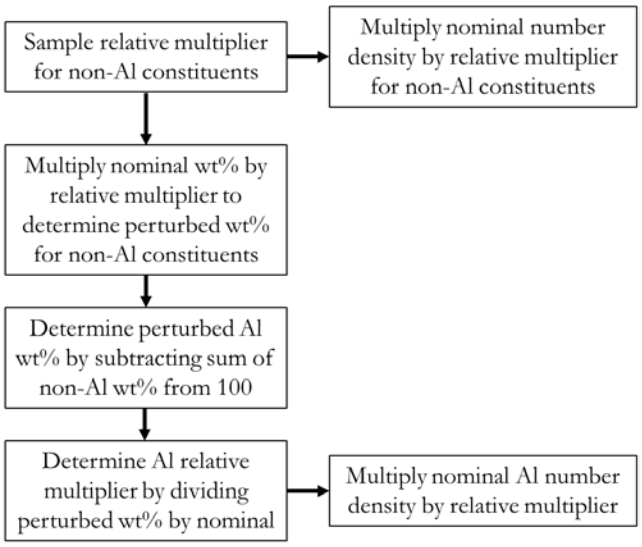

Figure 44. Flow chart of calculation of perturbed number densities in aluminum alloys.

The composition of the steel used in the reflecting wall is sampled using a different process. First, the uncertainty in the density of the steel is provided as ± 0.005 g/cm^3. This uncertainty is used in the evaluation because it is half of the last significant digit for the reported density of 7.84 g/cm^3. Uncertainties are also provided for 6 of the 10 elements in the steel in Table 5 of the evaluation. The weight percent values for these 6 elements (Fe, Mn, Ni, Mo, Cr, and Cu) are sampled uniformly over the range provided. The sum of the weight percents for these elements is normalized to the 99.58 wt% nominal sum. The normalization factor is used to adjust each individual weight fraction. The remaining 4 elements (C, P, S, and Si) have the same weight percent in all realizations. The perturbed number densities are then

calculated using the final weight percent values, molar masses and Avogadro's number [68], and the sampled mass density of the steel.

The ^{10}B content in boron is sampled for several of the poison panel materials. The same process, described here, is used for the borated stainless steel used in Case 2, the Boral used in Case 3, and the Boraflex used in Case 4. The ^{10}B atom percent is sampled uniformly between 19.1 and 20.8, with the remaining ^{11}B atom percent calculated. The atomic mass for the sampled boron composition is calculated prior to determining new boron number densities for each realization of each case.

Case 1 uses a stainless steel panel and Case 2 uses a borated stainless steel one. The general approach is the same as for the stainless steel reflecting wall. The weight percent of each element is sampled uniformly based on the uncertainties provided in Table 6 of the evaluation, the sum of the weight percents is normalized, and new number densities are calculated. No uncertainties are provided for the overall mass densities. Additionally, the boron composition is sampled as described above for the borated stainless steel panel in Case 2.

The poison panel in Case 3 is Boral with a nominal boron loading of 30.36 wt%. The total boron loading is sampled uniformly on a range of ±0.005 weight percent, based on the information provided in Table 18 of the evaluation, though no basis of this uncertainty is provided. The boron is present in Boral in the form of boron carbide (B_4C), so the increase in the carbon content is assumed to be proportional to the increase in total boron. The weight percent of aluminum is modified to maintain full density between the boron carbide and aluminum components. Lastly, the boron distribution is treated as discussed previously.

Case 4 contains Boraflex poison panels. Table 8 of the evaluation provides uncertainties for the weight percent of each of the 7 elements that are present in Boraflex. The sampling approach is essentially the same as that used in stainless steel, described earlier. The weight percent of each element is sampled, then the sampled weight percents are normalized and used to calculate perturbed number densities.

Case 5 uses a cadmium foil, with a trace of zinc the only other element in the poison material. The cadmium content is specified as 99.7 ± 0.3 weight percent in the evaluation, with zinc making up 0.3 weight percent. The cadmium content is sampled uniformly within the range, and the opposite change is made in zinc to maintain full density in the foil. No uncertainty is provided in the overall mass density, so once the weight percents are determined they are used to calculate the perturbed number densities.

The poison panels in Cases 6 and 7 are copper and copper with a nominal 1 wt% Cd, respectively. The composition of these panels, including some uncertainty data, is provided in Table 9 of the evaluation. The only element with reported uncertainty information for the copper panel is the copper itself, so the weight percent is sampled uniformly across the reported range. The perturbed number densities are calculated using the ratio of the sampled to the nominal weight percents. While this will result in a change in the material density, neither the other elements nor the overall mass density have reported uncertainties. The

cadmium and copper contents of the panel in Case 7 both have reported uncertainties, and are therefore sampled uniformly over the reported ranges. The uncertainties are different by about two orders of magnitude, so the sampling is performed independently. The perturbed number densities are determined based on sampled and nominal weight percent ratios. The trace of boron in the copper/cadmium panel is also treated for variable isotopic composition as described above.

Measurements of the uncertainty in the impurities in the water in the experiment tank are discussed in Sections 1.3.5 and 2.3 of the evaluation. The nominal benchmark model contains only hydrogen and oxygen, so no impurities are introduced or sampled for the water. The density is also not sampled or calculated to be consistent with the sampled temperature value for each experiment. Similarly, no uncertainty information is provided or assumed for the acrylic support plate on which the fuel rods rest.

Fuel Pin Pitch Uncertainty

The fuel pin pitch uncertainty is one of the key uncertainties for the determination of correlation coefficients among the 7 cases of LCT-042, and it is therefore of special interest. This section provides a discussion of the pin pitch uncertainty provided in the evaluation as well as the range of treatments used in the results presented later in this chapter regarding the correlations of and uncertainties in these cases.

The pin pitch uncertainty included in the evaluation is ±0.0076 cm, and the use of this value is explained in footnote (c) to Table 13 of the evaluation. The entire footnote is quoted here [15]:

> The largest standard deviation for sets of center-to-center spacing measurements for triangular-pitched lattice plates of Reference 8 [69] (Appendix E) was 0.003 inch (0.0076 cm). References 7 [70] (p. 2) and 8 [69] (p. 36 [sic]) give the uncertainty in pitch as ±0.005 cm. Reference 9 [71] (p 3.2) and Appendix D of Reference 10 [72] give the uncertainty in pitch as ±0.001 cm. Therefore, the calculated uncertainty for ±0.0076 cm is conservative.

There are several relevant facts that need to be discussed from this quote. First, the pitch uncertainty for the grid plates used in this experiment is unknown. No measurements of the plate are known to exist in any reference, so the uncertainty to be used is at best an estimate of the true uncertainty. This fact alone is enough to call into question any correlation coefficients calculated for these experiments.

LCT-042 is a series of square-pitched fuel array experiments. The use of a pitch uncertainty from a triangular-pitched lattice place is therefore difficult to justify. It is possible that similar fabrication techniques were used for both square- and triangular-pitched plates, but this assumption is not stated or justified in the evaluation. Page 3.6 of [69] does quote an uncertainty of ±0.005 cm, which is only about 2/3 of the value used in the evaluation. Furthermore, no pin pitch uncertainty of ±0.003 inch is found on review of the data

included in Appendix E of [69]. Also, none of the grid plates measured have the same pitch as was used in the LCT-042 experiments.

Similar problems also apply to the square-pitched experiments referenced in the evaluation. The fuel rods used in [70] have an outer diameter of 1.41 cm, which is considerably larger than the 1.27 cm outer diameter of the rods used in LCT-042. As with the cases discussed above, the pitch is different in both experiments included in [70] than in LCT-042. The experiments contained in [71] and [72] also use the larger fuel rods in the larger pitch.

The quote also makes evident that there are at least three different values with some pedigree that could have been used as the uncertainty value for the pin pitch. Ultimately, the evaluators chose to use the largest pitch uncertainty because its use was judged to be "conservative." Use of the largest pitch uncertainty is conservative in as much as it leads to the largest overall uncertainty, but this may not be conservative with regards to safety limits or other parameters of interest. In many validation studies the uncertainty of the experiment is used is a weighting factor so that uncertainties with lower experiments have more weight in the bias and bias uncertainty determinations [14, 23]. Mischaracterizing a shared uncertainty component will also impact the correlation coefficients developed from this evaluation. Overstating the magnitude of the shared uncertainty will increase the resulting correlation coefficients.

The uncertainty value selected in the evaluation is used here, despite being largely inappropriate for the experiment, because it is expected that individuals calculating critical experiment correlations will do so based on the information provided in the ICSBEP Handbook evaluations [15]. This task is already quite difficult and requires a significant, in-depth review of the evaluation. It is unreasonable to assume that the individual tasked with developing critical experiment correlations will also re-evaluate the experiments. This stretches the use of the uncertainty evaluations beyond their originally intending purpose, but other methods proposed for the determination of critical experiment correlations [35] depend exclusively on the use of these uncertainty values. In this regard, the expectation expressed here is no more radical than the prevailing opinion among other members of the community.

The implementation of the pin pitch uncertainty is examined using the same two assumptions that were used in the WPNCS/UACSA benchmark [33] discussed previously. A set of studies is performed assuming the pin pitch is the same between all pairs of rods, and subsequently random pin placement is examined as well. The pin pitch is sampled from a normal distribution, consistent with the general considerations discussed above.

The pin pitch distribution is truncated for the case in which all pin pitches are assumed to be the same; this approach is the same as Scenario A in the WPNCS/UACSA benchmark [33]. This assumption avoids unreasonable geometrical changes, and a series of different truncation ranges is examined to determine the sensitivity of the correlation coefficients to this parameter. The standard deviation for the normal distribution is assumed to be the ± 0.0076 cm uncertainty from the evaluation, and the sampling is truncated at $\pm 3\sigma$, $\pm 1.5\sigma$, and $\pm 0.75\sigma$. Correlations are also determined assuming the rods are fixed in their nominal

locations. This study provides an indication of the impact of the magnitude of the assumed pin pitch uncertainty. These results should provide useful insight on the general impact of the pin pitch uncertainty, but also in this specific case can be indicative of how sensitive the calculated correlation coefficients are to the questionable pin pitch uncertainty assumed in the evaluation. This study replicates the previous study documented in [39], but with lower stochastic uncertainties to yield more reliable correlation coefficients.

The random pin location study is akin to Scenario E from the WPNCS/UACSA benchmark. The displacement of each pin is sampled from a normal distribution with a standard deviation of ±0.0054 cm. This standard deviation is determined using the assumption that each pin is independently positioned. The uncertainty in each pin placement can then be combined with another using the square root of the sum of squares. Combining the standard deviation of 0.0054 cm for two pins with this technique yields the evaluation uncertainty of 0.0076 cm. Different assumptions could be made or investigated, but this is intended to give a direct comparison to the results of the uniform pin pitch models.

Uncertainty Treatment for Other Dimensions

Nearly every dimension in the model is perturbed based on the uncertainties provided in the evaluation. These uncertainties are related to poison panel dimension, reflecting wall placement and dimensions, and the array separations. Each of these is discussed in this section.

The uncertainties in poison panel dimensions are provided in Table 2 of the evaluation. The thicknesses of the poison panels are sampled uniformly over the range provided. The aluminum cladding of the Boral panels used in Case 3 has no specified thickness uncertainty, so it remains constant. The thickness of the plexiglass supports for the Boraflex used in Case 4 also has no specified uncertainty, so is left constant instead of using an assumed uncertainty with no basis.

The cadmium foil used in Case 5 presents a more complicated problem. No information was reported in the original references regarding the use of stiffeners with the foil, but the experimenter reported that plexiglass sheets were probably used [15]. The evaluation considered different thicknesses of plexiglass, and positioned the cadmium foil both closer to and farther away from the central fuel rod array. These conditions cannot be duplicated with Sampler, so a skewed distribution is used to determine the plexiglass thickness. The skewed distribution is a beta distribution with $\alpha=4$ and $\beta=2$. These constants are arbitrary since no information is available to guide the selection. The nominal value of the thickness is 0.296 cm, which is the thickness used in the evaluation, and the minimum thickness is 0 cm. The mode of a beta distribution can be calculated as shown in Equation 13 [73]:

$$\text{Mode} = \frac{\alpha - 1}{\alpha + \beta - 2} \qquad \text{Eqn (13)}$$

Where: Mode is the most likely value to be chosen

α is one of the distribution parameters
β is the other distribution parameter.

For the distribution chosen, the most frequently chosen thickness occurs 75% of the way through the range; it is desired that this thickness should be the nominal value of 0.296 cm. The maximum is thus set to 0.394667 cm so that the nominal value is the peak of the probability density function (PDF). A plot showing the resulting PDF is provided in Figure 45. Consistent with the assumption made in the evaluation, the plexiglass is assumed to be on the outboard side of the cadmium foil.

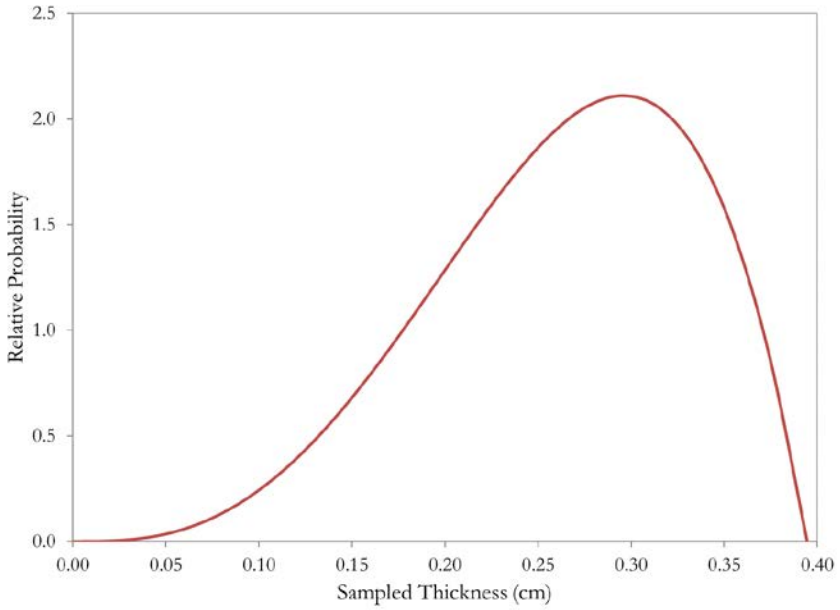

Figure 45. PDF for the plexiglass stiffener thickness in LCT-042 Case 5.

The thickness and width of the stainless steel reflecting walls are provided, along with uncertainties, in Figure 5 of the evaluation. The wall thickness uncertainty is stated to be ±0.4 mm and the width uncertainty is stated as ±0.32 cm. The wall thickness is therefore sampled uniformly between 17.81 cm and 17.89 cm. The plus and minus x coordinates of the ends of the wall are sampled independently, and the model is built with the origin at the center of the middle fuel pin array in the nominal model. Each end of the wall is sampled uniformly over a half-length range of 73.49 cm to 73.81 cm. Each end is sampled over the full range of uncertainties. A more accurate approach would have been to sample each end with a range of ±0.226 cm so that when the two uncertainties were combined using the square root of the sum of squares the total uncertainty would have been ±0.32 cm. The impact of this error is likely negligible as the ends of the reflecting walls are on the order of 20 cm beyond the ends of the fuel arrays. The same sampled values of the wall thickness and width are used in all 7 cases, based on the assumption that walls were built once and not changed within the series of experiments. Another simplifying assumption is that both walls are identical. While this is an unlikely assumption, the small differences between the wall dimensions are unlikely to have any impact on the resulting correlation coefficients.

The separation distance from the fuel rod arrays to the reflecting walls is also provided in Figure 5 of the evaluation, and is stated to be 1.321 ± 0.076 cm. The separation distance is sampled uniquely for each wall, so the walls are identical in dimension but are positioned independently in relation to the fuel arrays. The separation distance is sampled uniformly over the stated uncertainty range. The separation distances are also assumed to be the same among all 7 cases, consistent with the assumption that the walls were assembled and not changed during the experiment series.

The uncertainty in the fuel array separation distances is provided in Table 2 of the evaluation. The reported uncertainty is between fuel rod surfaces, so this dimension needs to be adjusted by the difference between the nominal fuel rod outer radius and the nominal half pitch for use in the KENO model. The uncertainty on the separation distance is applied entirely to this derived model dimension even though some of the uncertainty likely results from uncertainties in the fuel rod dimensions and positions. The separation distances are sampled uniformly over the range provided in the evaluation. The separations are also sampled independently since the separation distance is the control parameter for the experiment, and thus is a unique value for each case. Inherently this assumes that there is no correlated uncertainty in the measurement of the array separations. This assumption may not be entirely justified or defensible, but seems appropriate given that each measurement is unique and, at least to some degree, independent.

Initial Studies

Initial studies of the correlation coefficients among the 7 cases of the LCT-042 evaluation [15] are presented in Chapter II, the literature review. The results were published previously in [39] and [40], and the primary results will be summarized here. The analyses summarized here were performed in 2013 and 2014, prior to work on the WPNCS/UACSA benchmark [33].

Preliminary Results

The first set of correlation coefficients generated for LCT-042 are provided in [39, 40] and are shown in Figure 46. The initial studies only considered the uniform pitch assumption; these results assumed the pitch to be normally distributed over a range of ±3 standard deviations. A total of 275 realizations was used, and each realization was run until it achieved a Monte Carlo uncertainty of less than 0.00100 Δk. These correlations are those shown on the right-hand endpoint of the curves provided in Figure 4. The average k_{eff} values and the standard deviation of these estimates for each case is provided in Table 9, along with the uncertainty in the benchmark evaluation [15]. As mentioned previously, these correlations were developed prior to the studies on the effect of stochastic uncertainties on the correlation coefficients as a part of the WPNCS/UACSA benchmark [33]. Those studies are described in the Chapter V, and one outcome was that a similar study was performed with the LCT-042 experiments as well. The results of the study of the stochastic uncertainty of the individual realization calculations for LCT-042 are provided in the next section.

	42-1	42-2	42-3	42-4	42-5	42-6	42-7
42-1	1	0.83	0.83	0.83	0.84	0.80	0.81
42-2	0.83	1	0.83	0.83	0.85	0.81	0.83
42-3	0.83	0.83	1	0.83	0.82	0.78	0.82
42-4	0.83	0.83	0.83	1	0.84	0.79	0.81
42-5	0.84	0.85	0.82	0.84	1	0.82	0.80
42-6	0.80	0.81	0.78	0.79	0.82	1	0.80
42-7	0.81	0.83	0.82	0.81	0.80	0.80	1

Figure 46. Initial estimates of the correlation coefficients for LCT-042.

Table 9. Average k_{eff} Values and Their Standard Deviations, Initial Results for LCT-042

Case	Average k_{eff}	Standard Deviation	Evaluation Unc.
1	0.99642	0.00271	0.0016
2	0.99624	0.00285	0.0016
3	0.99763	0.00278	0.0016
4	0.99826	0.00288	0.0017
5	0.99801	0.00277	0.0033
6	0.99770	0.00266	0.0016
7	0.99594	0.00279	0.0018

The results provided in Table 9 indicate that the sampled uncertainty is generally 1.5 to 1.75 times higher than that provided in the evaluation. The exception is Case 5, which includes the Cd foil with its poorly characterized Plexiglas stiffener. The poor agreement of the uncertainty prediction for this case can be generally dismissed because it is impossible to evaluate the uncertainty in the stiffener over as wide a range as was done in the evaluation. The remaining cases provide evidence that the uniform pitch assumption, akin to Scenario A in the WPNCS/UACSA benchmark [33], introduces too much variability into the realizations.

The correlation coefficients are high and remarkably uniform. The large uncertainties are apparently mostly shared, indicating that they are related to compositions and/or the pin pitch. The desire to understand the contribution of each of these parameters led to the study varying the range over which the pitch is sampled. The results of this study are summarized in the next section.

Pitch Sampling Study

A study of the impact of the pin pitch impacts on the correlation coefficients is needed because of the lack of reliable information regarding the pin pitch and its uncertainty. When these initial results were generated in 2013, there was also considerable uncertainty on how to model pin placement. The uniform pitch approach was adopted because it was simple and straightforward to implement; results of a random pin positioning study are presented in the next section.

The 2013 study considered uniform pitch throughout the entire experiment, so the spacing between all pairs of rods in all three arrays of rods was assumed to be identical. This single parameter was sampled from a normal distribution as described above. The range over which the pitch was varied was selected at ±3 standard deviations in the initial results, presented in the previous section. Additional series of correlation coefficients were generated assuming different sampling ranges of ±1.5 standard deviations, and ±0.75 standard deviations. A final set of correlations was generated with the rod positions fixed. The results of this study should provide insight on the sensitivity of the correlations to the pin pitch uncertainty and the relative importance of the fuel material uncertainties and the pin positioning uncertainties.

The average k_{eff} for each case with each sampling range and their standard deviations are provided in Table 10. As shown in the table, the average value is unaffected by the different range but the standard deviations are reduced. These results are consistent with expectations given symmetric sampling and a shrinking uncertainty range. The fixed pin uncertainty provides an indication of the overall system k_{eff} uncertainty associated with material composition uncertainties, poison panel dimensional uncertainties, and fuel array spacing uncertainties.

The correlation coefficients are plotted as a function of sampling width in Figure 4, but the individual values are difficult to discern there. The actual coefficients are provided here for the scenario of ±1.5 standard deviations, Figure 47, ±0.75 standard deviations, Figure 48,

Table 10. Average k_{eff} Values and Their Standard Deviations, Initial Results of Pin Pitch Sampling Study for LCT-042

Case	±1.5σ Sampling Range		±0.75σ Sampling Range		Fixed Fuel Rods	
	Average k_{eff}	Std. Dev.	Average k_{eff}	Std. Dev.	Average k_{eff}	Std. Dev.
1	0.99649	0.00223	0.99635	0.00167	0.99666	0.00135
2	0.99681	0.00222	0.99641	0.00164	0.99660	0.00126
3	0.99783	0.00218	0.99761	0.00158	0.99778	0.00125
4	0.99853	0.00230	0.99837	0.00166	0.99842	0.00139
5	0.99837	0.00221	0.99814	0.00151	0.99820	0.00117
6	0.99790	0.00219	0.99783	0.00163	0.99800	0.00122
7	0.99619	0.00232	0.99593	0.00179	0.99628	0.00126

	42-1	42-2	42-3	42-4	42-5	42-6	42-7
42-1	1	0.72	0.76	0.74	0.73	0.73	0.70
42-2	0.72	1	0.73	0.70	0.71	0.71	0.71
42-3	0.76	0.73	1	0.73	0.74	0.71	0.76
42-4	0.74	0.70	0.73	1	0.76	0.74	0.74
42-5	0.73	0.71	0.74	0.76	1	0.75	0.76
42-6	0.73	0.71	0.71	0.74	0.75	1	0.72
42-7	0.70	0.71	0.76	0.74	0.76	0.72	1

Figure 47. Initial estimates of the correlation coefficients for LCT-042, sampling pitch ±1.5σ.

	42-1	42-2	42-3	42-4	42-5	42-6	42-7
42-1	1	0.46	0.51	0.51	0.53	0.46	0.53
42-2	0.46	1	0.45	0.54	0.54	0.46	0.45
42-3	0.51	0.45	1	0.49	0.54	0.52	0.54
42-4	0.51	0.54	0.49	1	0.56	0.56	0.53
42-5	0.53	0.54	0.54	0.56	1	0.54	0.52
42-6	0.46	0.46	0.52	0.56	0.54	1	0.49
42-7	0.53	0.45	0.54	0.53	0.52	0.49	1

Figure 48. Initial estimates of the correlation coefficients for LCT-042, sampling pitch ±0.75σ.

and fixed rod positions, Figure 49. The same trend is of course evident in an analysis of the detailed results as is available in the summary presentation in Figure 4: the correlations drop significantly as the range of pin pitch sampling drops. This is also consistent with the reduced uncertainty shown in Table 10. The change between ±3σ and ±1.5σ is modest, but larger changes are evident in the ±0.75σ scenario and the fixed rod case. This entire study was redone with lower stochastic uncertainties on the individual realizations after the impact of that parameter was shown to be significant during the investigation of the WPNCS/UACSA benchmark.

	42-1	42-2	42-3	42-4	42-5	42-6	42-7
42-1	1	0.02	0.17	0.07	0.10	0.08	0.11
42-2	0.02	1	0.10	0.03	0.14	0.03	0.04
42-3	0.17	0.10	1	0.15	0.08	0.07	-0.05
42-4	0.07	0.03	0.15	1	0.04	0.12	0.13
42-5	0.10	0.14	0.08	0.04	1	0.08	0.14
42-6	0.08	0.03	0.07	0.12	0.08	1	0.08
42-7	0.11	0.04	-0.05	0.13	0.14	0.08	1

Figure 49. Initial estimates of the correlation coefficients for LCT-042, fixed rod positions.

Additional Studies

Additional studies have been performed for the LCT-042 correlation coefficients after the completion of the work on the WPNCS/UACSA benchmark [33] presented in the Chapter V. The previous study of the impact of the range of pitch sampling on the correlation coefficients has been redone with the stochastic uncertainty on each of the realizations reduced to ±0.00010 Δk. The effect of the stochastic uncertainty on the LCT-042 correlations is examined in a study similar to the one performed for the WPNCS/UACSA benchmark, but with a greater range of stochastic uncertainties. Some work has also been done to examine the effect of random fuel rod positions on the correlation coefficients.

Pitch Sampling Study Revisited

Critical experiment correlation coefficients have been developed among the 7 cases of LCT-042 including the uniform pitch assumption. In all cases, the fuel rod is centered inside a unit cell and the size of the unit cell is varied to control the center-to-center pitch of the arrays. As with the study presented in the previous section, the pin pitch is sampled from a normal distribution truncated at ±3 standard deviations, ±1.5 standard deviations, and ±0.75 standard deviations as well as with fixed fuel pin locations. Each set of correlations is determined based on 300 realizations for each case, and the stochastic uncertainty of each realization is approximately 0.00010 Δk. Each set of correlations is presented here, along with a comparison of the results with each other and with the previous results.

The mean and standard deviation of the k_{eff} values for the 300 realizations assuming a pitch sampling range of ±3σ are provided in Table 11 for each of the 7 cases in LCT-042. The uncertainty in the benchmark evaluation is also provided for reference. The difference in the

absolute reactivity of the system compared to the initial results provided in Table 9 is most likely due to differences between the versions of KENO used in the previous study (SCALE 6.2 Beta 1) and this study (SCALE 6.2.1). The standard deviation of the k_{eff} values can be compared directly, and it is evident that the variability is somewhat lower with the new results. This is the expected outcome given the lower uncertainty in each calculation. The standard deviations are still noticeably larger than the evaluation, except for Case 5. Recall that Case 5 is the experiment with the Cd foil with a stiffener of indeterminant dimension. The stochastic uncertainty should not be shared among the different cases, so the overall effect is likely to be an increase in the correlation coefficients. The new correlation coefficients are provided in Figure 50, and bear out the prediction that the correlation coefficients are larger with lower stochastic uncertainties. The increase in correlation coefficients with reduced stochastic uncertainty in the individual realization calculations is consistent with the results observed for the WPNCS/UACSA benchmark. The 95% confidence intervals for these correlation coefficients are provided in Figure 51.

Table 11. Updated Average k_{eff} Values and Standard Deviations for LCT-042

Case	Average k_{eff}	Standard Deviation	Evaluation Unc.
1	0.99836	0.00238	0.0016
2	0.99800	0.00242	0.0016
3	0.99884	0.00253	0.0016
4	0.99955	0.00255	0.0017
5	0.99948	0.00246	0.0033
6	0.99960	0.00235	0.0016
7	0.99774	0.00250	0.0018

Table 12 provides the means and standard deviations for the 300 realizations of each case assuming a pin pitch sampling range of ±1.5σ. The average values are in good agreement with the values in Table 11, and the standard deviations are lower for all 7 cases. The uncertainties are still higher than those provided in the evaluation, except for Case 5. In this instance, the reduced uncertainty is expected to be dominated by the shared pin pitch uncertainty, so the correlation coefficients should drop relative to those shown in Figure 50. The correlation coefficients are provided in Figure 52, and are slightly lower than those in Figure 50. The 95% confidence intervals for the correlation coefficients sampling within ±1.5σ on pin pitch are provided in Figure 53, for comparison with those in Figure 51. While the correlation coefficients are modestly lower for the more restricted pin pitch sampling range, they are still significantly higher than the results considering higher stochastic uncertainties (Figure 47).

The updated means and standard deviations for the case sampling the pin pitch over the range ±0.75 standard deviations are provided in Table 13. The standard deviations have dropped more, and are lower than the evaluation estimates for all seven cases. The correlation coefficients, shown in Figure 54, are lower as expected. The difference from the initial, high uncertainty results provided in Figure 48, is dramatic. The coefficients are around 0.9 with the higher convergence of the individual realizations, as compared to values of

	42-1	42-2	42-3	42-4	42-5	42-6	42-7
42-1	1	0.97	0.99	0.97	0.99	0.99	0.98
42-2	0.97	1	0.97	0.96	0.97	0.98	0.96
42-3	0.99	0.97	1	0.97	0.99	0.99	0.97
42-4	0.97	0.96	0.97	1	0.98	0.98	0.96
42-5	0.99	0.97	0.99	0.98	1	0.99	0.98
42-6	0.99	0.98	0.99	0.98	0.99	1	0.98
42-7	0.98	0.96	0.97	0.96	0.98	0.98	1

Figure 50. Updated estimates of the correlation coefficients for LCT-042, pitch sampled ±3σ.

	042-002	042-003	042-004	042-005	042-006	042-007
042-001	(0.965, 0.978)	(0.981, 0.988)	(0.967, 0.979)	(0.989, 0.993)	(0.990, 0.994)	(0.970, 0.981)
042-002		(0.958, 0.973)	(0.949, 0.967)	(0.968, 0.979)	(0.971, 0.981)	(0.948, 0.967)
042-003			(0.962, 0.976)	(0.981, 0.988)	(0.983, 0.989)	(0.966, 0.978)
042-004				(0.968, 0.980)	(0.972, 0.982)	(0.947, 0.966)
042-005					(0.991, 0.995)	(0.970, 0.981)
042-006						(0.971, 0.981)

Figure 51. 95% confidence intervals for updated estimates of correlation coefficients for LCT-042.

Table 12. Updated Average k_{eff} Values and Standard Deviations for LCT-042, Pin Pitch Sampled ±1.5σ

Case	Average k_{eff}	Standard Deviation	Evaluation Unc.
1	0.99823	0.00177	0.0016
2	0.99788	0.00184	0.0016
3	0.99873	0.00188	0.0016
4	0.99942	0.00194	0.0017
5	0.99936	0.00184	0.0033
6	0.99948	0.00176	0.0016
7	0.99761	0.00185	0.0018

	42-1	42-2	42-3	42-4	42-5	42-6	42-7
42-1	1	0.95	0.97	0.95	0.98	0.99	0.96
42-2	0.95	1	0.94	0.93	0.96	0.96	0.93
42-3	0.97	0.94	1	0.94	0.97	0.98	0.95
42-4	0.95	0.93	0.94	1	0.95	0.96	0.93
42-5	0.98	0.96	0.97	0.95	1	0.99	0.96
42-6	0.99	0.96	0.98	0.96	0.99	1	0.96
42-7	0.96	0.93	0.95	0.93	0.96	0.96	1

Figure 52. Updated estimates of the correlation coefficients for LCT-042, sampling pitch ±1.5σ.

	042-002	042-003	042-004	042-005	042-006	042-007
042-001	(0.941, 0.962)	(0.966, 0.978)	(0.941, 0.962)	(0.980, 0.987)	(0.982, 0.989)	(0.946, 0.965)
042-002		(0.928, 0.954)	(0.914, 0.945)	(0.945, 0.965)	(0.953, 0.970)	(0.913, 0.944)
042-003			(0.930, 0.955)	(0.966, 0.978)	(0.968, 0.980)	(0.934, 0.958)
042-004				(0.943, 0.963)	(0.951, 0.968)	(0.909, 0.941)
042-005					(0.985, 0.990)	(0.947, 0.966)
042-006						(0.947, 0.966)

Figure 53. 95% confidence intervals for updated estimates of correlation coefficients for LCT-042; pin pitch sampled within ±1.5 σ.

Table 13. Updated Average k_{eff} Values and Standard Deviations for LCT-042, Pin Pitch Sampled ±0.75σ

Case	Average k_{eff}	Standard Deviation	Evaluation Unc.
1	0.99849	0.00128	0.0016
2	0.99814	0.00138	0.0016
3	0.99900	0.00136	0.0016
4	0.99969	0.00146	0.0017
5	0.99963	0.00133	0.0033
6	0.99974	0.00127	0.0016
7	0.99790	0.00137	0.0018

	42-1	42-2	42-3	42-4	42-5	42-6	42-7
42-1	1	0.92	0.95	0.91	0.97	0.97	0.91
42-2	0.92	1	0.90	0.87	0.92	0.93	0.87
42-3	0.95	0.90	1	0.89	0.95	0.95	0.89
42-4	0.91	0.87	0.89	1	0.92	0.93	0.87
42-5	0.97	0.92	0.95	0.92	1	0.98	0.92
42-6	0.97	0.93	0.95	0.93	0.98	1	0.92
42-7	0.91	0.87	0.89	0.87	0.92	0.92	1

Figure 54. Updated estimates of the correlation coefficients for LCT-042, sampling pitch ±0.75σ.

about 0.5. The standard deviation of the cases with the range of pin pitch reduced to ±0.75σ is on the order of 0.00130 Δk; the impact of the increased convergence requirement is more pronounced as the overall uncertainty is reduced. The stochastic uncertainty, 0.00010 Δk in the updated calculations, is no longer on the same order as the variability introduced by sampling the uncertain parameters. The reactivity variation from the pin pitch sampling is larger in the scenarios sampling the fuel rod pitch over larger ranges, thus reducing the impact of lowering the stochastic uncertainties. This effect is not surprising, but is also not exposed in the two scenarios examined in the WPNCS/UACSA benchmark. The convergence of the correlation coefficients between Case 2 and Case 4 and between Case 2 and Case 7 are checked graphically, as shown in Figure 55. As expected for correlation coefficients near 0.9, the convergence is excellent and is probably achieved within about 100 realizations.

Finally, the means and standard deviations for the fixed rod position scenario are provided below in Table 14. The standard deviations have dropped farther below the evaluation uncertainties with the removal of all uncertainty in fuel pin placement. The resulting correlation coefficients are shown in Figure 56. These correlations are obviously lower than any realistic correlation coefficients because the fuel rod locations cannot be known perfectly. The convergence of two of the lowest correlation coefficients is checked graphically, as shown in Figure 57. The correlation coefficient between Case 4 and Case 5 appears to be well converged by about 150 realizations. The coefficient between Case 4 and Case 7 may be converged, but may also still be drifting lower even by 300 realizations. Another indication of potential nonconvergence is a comparison of the correlation coefficients resulting from the first half and second of the realizations. These results are shown in Figure 58 for the first half of the realizations and Figure 59 for the second half.

The correlation coefficient between Cases 4 and 5 is in good agreement between the two halves and thus also for all realizations. The first half and second of the realizations are not in good agreement for Case 4 and Case 7. Low correlation coefficients resulting from cases with small uncertainties may require more than 300 realizations to converge reliably.

The standard deviations for each case and each pin pitch sampling range are plotted in Figure 60. The data are also shown in Table 11 through Table 14, but the plot shows the trends in the uncertainties. The uncertainty trend as a function of sampling range is generally the same among all 7 cases. The uncertainty increases significantly as the pin locations are first perturbed. The increase slows slightly at larger sampling ranges. Eventually, the uncertainty would cease increasing with larger pitch sampling ranges as the pin pitch reaches optimum moderation. Additional moderation near the peak has much less impact than additions in the significantly under-moderated nominal lattice. Pitch increases beyond peak moderation would lower reactivity, so the uncertainty would cease increasing at all despite a larger sampling range. Also, the same standard deviation is used in all cases, so increasing the sampling range beyond ±3 standard deviations does not add many realizations in the far tails of the distribution. The uncertainty as a function of pin pitch sampling will differ among different experiments with different gross moderation characteristics. For example, an evaluation containing a series of arrays with different pitches will not manifest the similarity of behavior apparent among the cases within the LCT-042 evaluation.

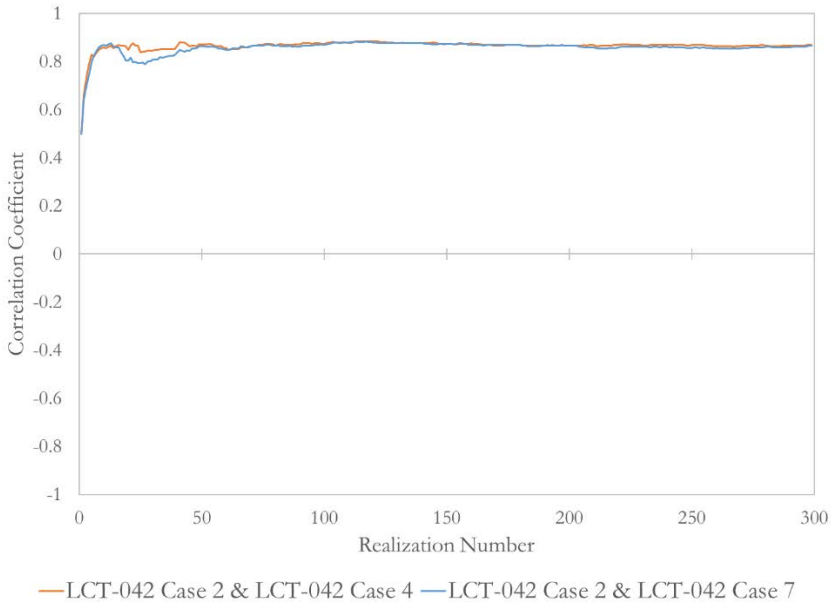

Figure 55. Convergence of two correlation coefficients, sampling pitch ±0.75σ.

Table 14. Updated Average k_{eff} Values and Standard Deviations for LCT-042, Fixed Pin Pitch Positions

Case	Average k_{eff}	Standard Deviation	Evaluation Unc.
1	0.99818	0.00046	0.0016
2	0.99781	0.00068	0.0016
3	0.99864	0.00052	0.0016
4	0.99933	0.00065	0.0017
5	0.99926	0.00044	0.0033
6	0.99941	0.00042	0.0016
7	0.99757	0.00066	0.0018

	42-1	42-2	42-3	42-4	42-5	42-6	42-7
42-1	1	0.60	0.64	0.46	0.75	0.79	0.48
42-2	0.60	1	0.49	0.37	0.58	0.62	0.49
42-3	0.64	0.49	1	0.41	0.64	0.66	0.53
42-4	0.46	0.37	0.41	1	0.46	0.53	0.30
42-5	0.75	0.58	0.64	0.46	1	0.79	0.49
42-6	0.79	0.62	0.66	0.53	0.79	1	0.57
42-7	0.48	0.49	0.53	0.30	0.49	0.57	1

Figure 56. Updated estimates of the correlation coefficients for LCT-042, fixed fuel rod positions.

Figure 57. Convergence of two correlation coefficients, fixed fuel rod positions.

	42-1	42-2	42-3	42-4	42-5	42-6	42-7
42-1	1	0.62	0.66	0.46	0.75	0.80	0.55
42-2	0.62	1	0.48	0.33	0.56	0.66	0.52
42-3	0.66	0.48	1	0.47	0.66	0.66	0.60
42-4	0.46	0.33	0.47	1	0.46	0.60	0.38
42-5	0.75	0.56	0.66	0.46	1	0.79	0.56
42-6	0.80	0.66	0.66	0.60	0.79	1	0.59
42-7	0.55	0.52	0.60	0.38	0.56	0.59	1

Figure 58. Estimates of correlation coefficients for LCT-042, fixed fuel rod positions, only first half of realizations.

	42-1	42-2	42-3	42-4	42-5	42-6	42-7
42-1	1	0.58	0.62	0.45	0.75	0.78	0.40
42-2	0.58	1	0.48	0.40	0.61	0.56	0.44
42-3	0.62	0.48	1	0.36	0.62	0.65	0.47
42-4	0.45	0.40	0.36	1	0.46	0.45	0.22
42-5	0.75	0.61	0.62	0.46	1	0.79	0.41
42-6	0.78	0.56	0.65	0.45	0.79	1	0.54
42-7	0.40	0.44	0.47	0.22	0.41	0.54	1

Figure 59. Estimates of correlation coefficients for LCT-042, fixed fuel rod positions, only second half of realizations.

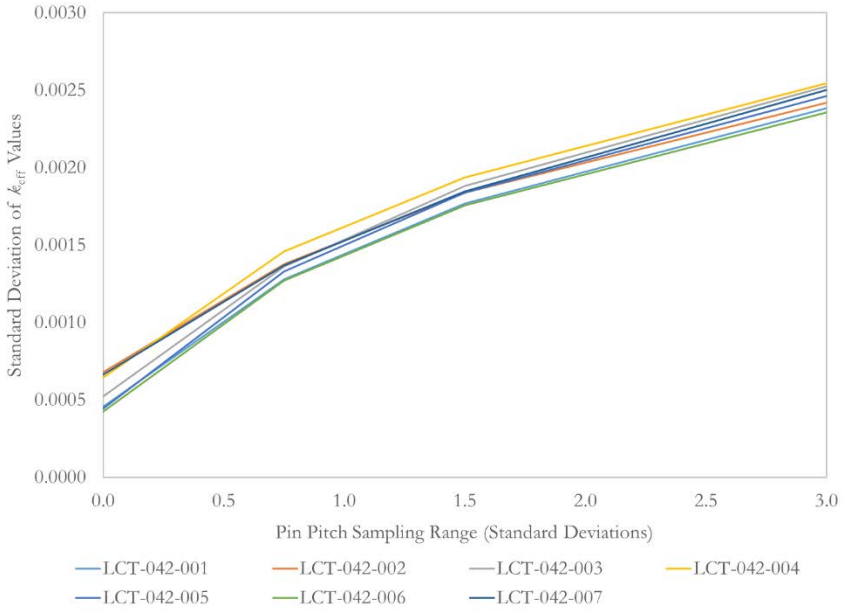

Figure 60. Standard deviation of k_{eff} values for 300 realizations converged to 0.00010 Δk.

The correlation coefficients between each pair of cases are shown as a function of pin pitch sampling range in Figure 61. The behavior of the correlation coefficients is more extreme than that of the uncertainties. With fixed pin locations, the coefficients range from 0.30 to 0.79 as shown in Figure 56. All the correlation coefficients increase dramatically with the introduction of shared uncertainty in pin locations. The coefficients are provided in Figure 54 when the pitch is sampled in the range of ±0.75 standard deviations, and range from 0.87 to 0.98. The variability among the coefficients is much lower, and is reduced as the pin pitch sampling range increases. These general trends are similar to those reported in the initial results, discussed in the previous section and in Chapter II. The correlation coefficients in this study are uniformly higher than the initial results shown in Figure 4, which is consistent with the studies performed as a part of the WPNCS/UACSA benchmark and presented earlier. The results presented in this section are likely a more realistic estimate of the magnitude of the correlations among the cases in LCT-042 under the uniform pin pitch assumption than the initial results presented previously. Results considering random pin placement are provided in a later section.

The results in Figure 61 summarize the correlation coefficients determined with the uniform pitch assumption for LCT-042. The next section presents results of a study examining the effect of stochastic uncertainty in each realization, analogous to the similar study performed for LCT-007 and LCT-039 in the WPNCS/UACSA benchmark. The subsequent section presents correlation coefficients for a random pin placement approach. It is worth pausing to reflect on the results shown here, and the implications for criticality safety validation and data adjustment techniques. It is unreasonable to believe that there is no uncertainty in pin locations or spacing. It seems likely that at least one standard deviation of variability must be considered in the analysis, and the correlation coefficients have already increased and converged with each other to a large degree by this point. The correlation coefficients likely

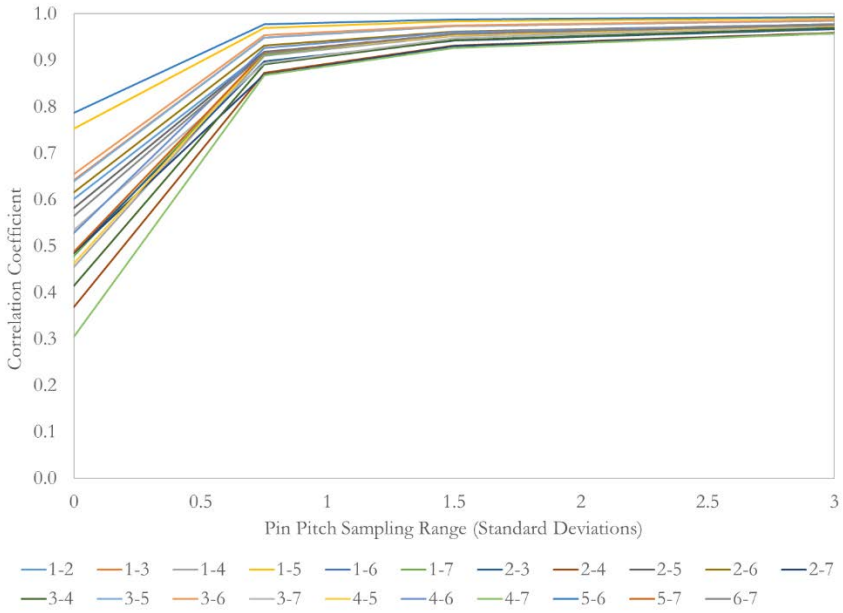

Figure 61. All 21 correlation coefficients for LCT-042 as a function of pin pitch sampling range.

vary between about 0.87 and 0.97 at this point; these correlations are quite high given the impacts seen in [50] and [51] considering correlations only as high as 0.5.

Effect of Stochastic Uncertainty in KENO Calculations

The effect of the stochastic uncertainty in each of the individual realizations is studied for LCT-042, as it was for LCT-007 and LCT-039 as part of the WPNCS/UACSA benchmark. A more complete study is possible for LCT-042 because of the reduced number of cases in the evaluation. A single set of 300 evaluations was generated, and subsequently run 5 different times with stochastic uncertainties of 0.00100 Δk, 0.00050 Δk, 0.00020 Δk, 0.00010 Δk, and 0.00005 Δk. The results of these calculations are presented in this section.

The average k_{eff} values for each case and each uncertainty level are provided in Table 15. The average values agree quite well for the cases with uncertainties of 0.00020 Δk, 0.00010 Δk, and 0.00005 Δk. All cases except Case 3 show small, but noticeable, deviation at 0.00050 Δk uncertainty. Larger differences are evident for all cases with uncertainties of 0.00100 Δk.

The standard deviation of the k_{eff} values from the realizations for each uncertainty level are shown in Table 16. The standard deviations are the same for all 7 cases between 0.00005 and 0.00010 Δk. Most cases show a very modest increase of about 0.00001 Δk between 0.00010 and 0.00020 Δk. Clearly as the uncertainty in the realizations increases it starts to influence the overall uncertainty. Uncertainties of 0.00020 Δk are still very small compared to the variability resulting from sampling the compositions, dimensions, and pin positions in the model. The stochastic uncertainty in each calculation becomes a more significant component of the uncertainty as it gets large, obviously, and this effect becomes apparent in the results at 0.00050 Δk an especially at 0.00100 Δk. The stochastic uncertainty will become a

Table 15. Average k_{eff} Values for Various Stochastic Uncertainties for Realizations

Case	0.00100 Δk	0.00050 Δk	0.00020 Δk	0.00010 Δk	0.00005 Δk
1	0.99766	0.99821	0.99835	0.99836	0.99836
2	0.99761	0.99791	0.99799	0.99800	0.99801
3	0.99862	0.99883	0.99883	0.99884	0.99885
4	0.99931	0.99947	0.99953	0.99955	0.99955
5	0.99919	0.99942	0.99946	0.99948	0.99948
6	0.99894	0.99948	0.99958	0.99960	0.99960
7	0.99748	0.99765	0.99773	0.99774	0.99774

Table 16. Standard Deviation of k_{eff} Values from Realizations with Differing Uncertainties

Case	0.00100 Δk	0.00050 Δk	0.00020 Δk	0.00010 Δk	0.00005 Δk
1	0.00264	0.00240	0.00239	0.00238	0.00238
2	0.00256	0.00245	0.00243	0.00242	0.00242
3	0.00276	0.00262	0.00255	0.00253	0.00253
4	0.00265	0.00258	0.00254	0.00255	0.00255
5	0.00261	0.00251	0.00247	0.00246	0.00245
6	0.00254	0.00241	0.00236	0.00235	0.00236
7	0.00278	0.00252	0.00251	0.00250	0.00250

significant contributor to overall uncertainty at lower stochastic uncertainties in other scenarios with smaller pin pitch sampling ranges.

The correlation coefficients resulting from the realizations with uncertainties of 0.00100 Δk are provide in Figure 62, 0.00050 Δk in Figure 63, 0.00020 Δk in Figure 64, and 0.00005 Δk in Figure 65. The coefficients with uncertainties of 0.00010 Δk are shown in Figure 50. As with the standard deviations, the correlation coefficients are largely unchanged from 0.00020 Δk to 0.00005 Δk. Slightly reduced correlations are apparent for uncertainties of 0.00050 Δk, and the coefficients drop to about 0.8 in the scenario with realization stochastic uncertainties of 0.00100 Δk. All 21 sets of correlation coefficients are plotted as a function of realization uncertainty in Figure 66 to ease the visual comparisons of the data.

The general trend of all 21 correlation coefficients is very similar as a function of stochastic uncertainty. The correlation coefficients increase, and the variability among the coefficients also reduces somewhat. The minimum and maximum correlation coefficients with 0.00100 Δk uncertainty are 0.76 and 0.84, respectively, for a total range of 0.08. With the uncertainty reduced to 0.00005 Δk, the range is reduced to 0.03 with a minimum correlation of 0.96 and a maximum of 0.99.

For LCT-042 and the shared pin pitch assumption, sampled over a range of $\pm 3\sigma$, it appears that the stochastic uncertainty of the individual realization KENO calculations should not exceed 0.00020 Δk. The required uncertainty will decrease as the sampling range of the pin pitch decreases. Smaller pin pitch sample ranges lead to smaller k_{eff} variability, as shown in

	42-1	42-2	42-3	42-4	42-5	42-6	42-7
42-1	1	0.80	0.81	0.79	0.80	0.78	0.81
42-2	0.80	1	0.81	0.78	0.77	0.76	0.80
42-3	0.81	0.81	1	0.80	0.82	0.80	0.84
42-4	0.79	0.78	0.80	1	0.80	0.79	0.79
42-5	0.80	0.77	0.82	0.80	1	0.80	0.81
42-6	0.78	0.76	0.80	0.79	0.80	1	0.81
42-7	0.81	0.80	0.84	0.79	0.81	0.81	1

Figure 62. Correlation coefficients resulting from realizations with uncertainties of 0.00100 Δ*k*.

	42-1	42-2	42-3	42-4	42-5	42-6	42-7
42-1	1	0.93	0.94	0.92	0.94	0.94	0.92
42-2	0.93	1	0.93	0.91	0.92	0.93	0.90
42-3	0.94	0.93	1	0.93	0.94	0.94	0.93
42-4	0.92	0.91	0.93	1	0.94	0.93	0.92
42-5	0.94	0.92	0.94	0.94	1	0.94	0.93
42-6	0.94	0.93	0.94	0.93	0.94	1	0.91
42-7	0.92	0.90	0.93	0.92	0.93	0.91	1

Figure 63. Correlation coefficients resulting from realizations with uncertainties of 0.00050 Δ*k*.

	42-1	42-2	42-3	42-4	42-5	42-6	42-7
42-1	1	0.97	0.98	0.97	0.99	0.99	0.97
42-2	0.97	1	0.96	0.96	0.97	0.97	0.95
42-3	0.98	0.96	1	0.97	0.98	0.98	0.97
42-4	0.97	0.96	0.97	1	0.97	0.97	0.95
42-5	0.99	0.97	0.98	0.97	1	0.99	0.97
42-6	0.99	0.97	0.98	0.97	0.99	1	0.97
42-7	0.97	0.95	0.97	0.95	0.97	0.97	1

Figure 64. Correlation coefficients resulting from realizations with uncertainties of 0.00020 Δ*k*.

	42-1	42-2	42-3	42-4	42-5	42-6	42-7
42-1	1	0.97	0.99	0.98	0.99	0.99	0.98
42-2	0.97	1	0.97	0.96	0.98	0.98	0.96
42-3	0.99	0.97	1	0.97	0.99	0.99	0.97
42-4	0.98	0.96	0.97	1	0.98	0.98	0.96
42-5	0.99	0.98	0.99	0.98	1	0.99	0.98
42-6	0.99	0.98	0.99	0.98	0.99	1	0.98
42-7	0.98	0.96	0.97	0.96	0.98	0.98	1

Figure 65. Correlation coefficients resulting from realizations with uncertainties of 0.00005 Δ*k*.

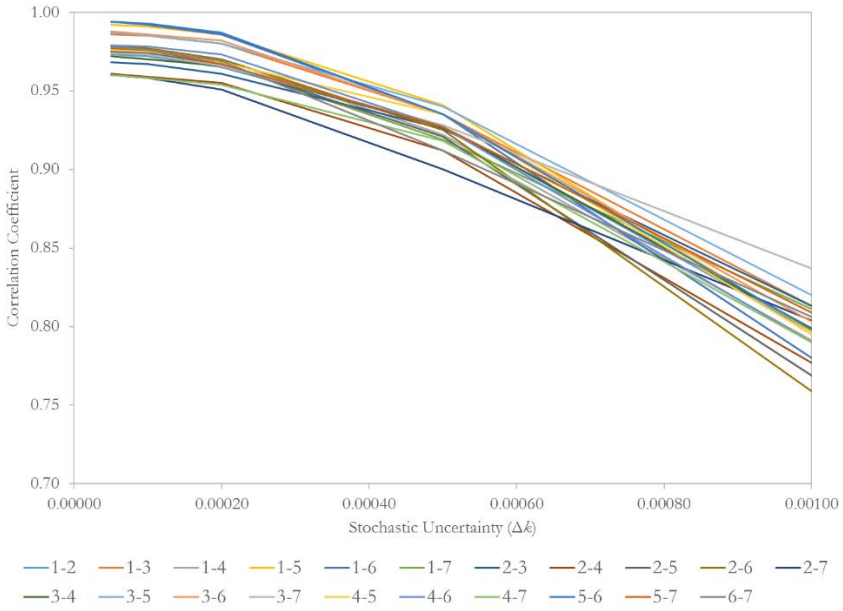

Figure 66. Correlation coefficients as a function of realization statistical uncertainty.

the previous section, and the stochastic uncertainty will make a significant contribution to the uncertainty at a correspondingly lower level.

Each of these LCT-042 KENO realizations with an uncertainty of 0.00020 Δk can be executed in about 1 hour on the *Romulus* cluster at ORNL, leading to a total run-time of approximately 2100 CPU-hours to determine a complete matrix of correlation coefficients. The ability to relax the uncertainty requirement reduces the required run-time by approximately a factor of 4, as expected for a doubled Monte Carlo uncertainty.

Random Fuel Pin Placement

Critical experiment correlations are also developed for the 7 cases of LCT-042 with random pin locations. This set of correlations is analogous to Scenario E from the WPNCS/UACSA benchmark [33] discussed in the previous chapter. The TemplateEngine is used to generate KENO models with each fuel rod in a unique unit and Sampler inputs to perturb the location of each rod. A total of 300 realizations is created for each case, and the location of each rod is sampled uniquely in each case. In other words, the position of each fuel rod is assumed to be independent in each of the 7 cases. As discussed in the section regarding Scenario E of the WPNCS/UACSA benchmark, there is some evidence [59, 65] that random pin location is a more accurate model of fuel pin array critical experiments than a uniform pitch uncertainty.

The average k_{eff} and its standard deviation from all 300 realizations for each case is provided in Table 17. The average k_{eff} values are in good agreement with the results from the uniform pitch scenarios, but the uncertainties are noticeably smaller. The individual fuel rods can move significantly, but since each one is positioned uniquely there are no overall changes in

moderation within the array. The elimination of moderation changes is the primary cause of reduced uncertainty in the random fuel rod position scenario. Also, the rod inner diameter and fuel length are sampled uniquely in each rod. The uniform pitch scenarios model a single fuel rod repeated for each array location, so fuel volume changes occur in all the fuel rods. The magnitude of the overall fuel volume changes is much lower while each rod is sampled independently. The reduced uncertainty in the random pin placement models is therefore also a result of smaller changes in fuel volume (and mass) and not entirely because of the rod positioning differences. The evaluation uncertainties are also provided in Table 17 for reference. The variability of the realizations in the random pin placement scenario is significantly less than those provided in the evaluation. Most cases have only a quarter to a third of the uncertainty in the evaluation. Approximately half of the uncertainty reported in the evaluation is related to the pin pitch uncertainty, so the logical outcome of random pin placement is the observed lowering of the overall uncertainty. It should be noted that the k_{eff} variability is still on the order of 3 to 6 times that of the individual realization k_{eff} uncertainty, so further reduction of the uncertainty is likely not needed for these cases. Lower KENO uncertainties would be advisable for experiments with k_{eff} variability on the same order as the stochastic uncertainty.

Table 17. Average k_{eff} Values and Standard Deviations for LCT-042, Random Pin Pitch Positions

Case	Average k_{eff}	Standard Deviation	Evaluation Unc.
1	0.99820	0.00036	0.0016
2	0.99773	0.00058	0.0016
3	0.99862	0.00046	0.0016
4	0.99932	0.00056	0.0017
5	0.99927	0.00034	0.0033
6	0.99941	0.00033	0.0016
7	0.99763	0.00061	0.0018

The correlation coefficients resulting from the random pin pitch modeling are provided in Figure 67. The coefficients are generally somewhat less than the fixed rod scenario results shown in Figure 56. This is a result of the differences discussed previously in the fuel rod dimension treatment, and the corresponding elimination of shared uncertainty related to fuel radius and length. The 95% confidence intervals for the random placement scenario correlation coefficients are provided in Figure 68. The confidence intervals demonstrate that while the best estimate coefficients are lower than the fixed rod coefficients, these differences are generally not statistically significant. Finally, the convergence of the correlation coefficients between Case 2 and Case 7 and between Case 6 and Case 7 is provided in Figure 69. As with the fixed pin location scenario, there is an indication that 300 realizations may not be sufficient for the convergence of low correlation coefficients resulting from pairs of low uncertainty systems.

An additional 600 realizations were created for Case 2 and Case 7 to examine the convergence behavior of the lowest correlation coefficient among the 7 cases of LCT-042 in

	42-1	42-2	42-3	42-4	42-5	42-6	42-7
42-1	1	0.33	0.52	0.42	0.52	0.63	0.43
42-2	0.33	1	0.32	0.48	0.42	0.37	0.19
42-3	0.52	0.32	1	0.29	0.59	0.61	0.48
42-4	0.42	0.48	0.29	1	0.46	0.31	0.26
42-5	0.52	0.42	0.59	0.46	1	0.67	0.49
42-6	0.63	0.37	0.61	0.31	0.67	1	0.46
42-7	0.43	0.19	0.48	0.26	0.49	0.46	1

Figure 67. Correlation coefficients for the random fuel rod placement scenario.

	042-002	042-003	042-004	042-005	042-006	042-007
042-001	(0.221, 0.424)	(0.430, 0.596)	(0.324, 0.510)	(0.437, 0.602)	(0.555, 0.693)	(0.331, 0.516)
042-002		(0.218, 0.421)	(0.384, 0.559)	(0.327, 0.513)	(0.265, 0.461)	(0.079, 0.297)
042-003			(0.186, 0.393)	(0.510, 0.658)	(0.536, 0.678)	(0.390, 0.565)
042-004				(0.363, 0.543)	(0.201, 0.407)	(0.146, 0.358)
042-005					(0.599, 0.725)	(0.403, 0.575)
042-006						(0.366, 0.545)

Figure 68. 95% confidence intervals for the random fuel rod placement scenario correlation coefficients.

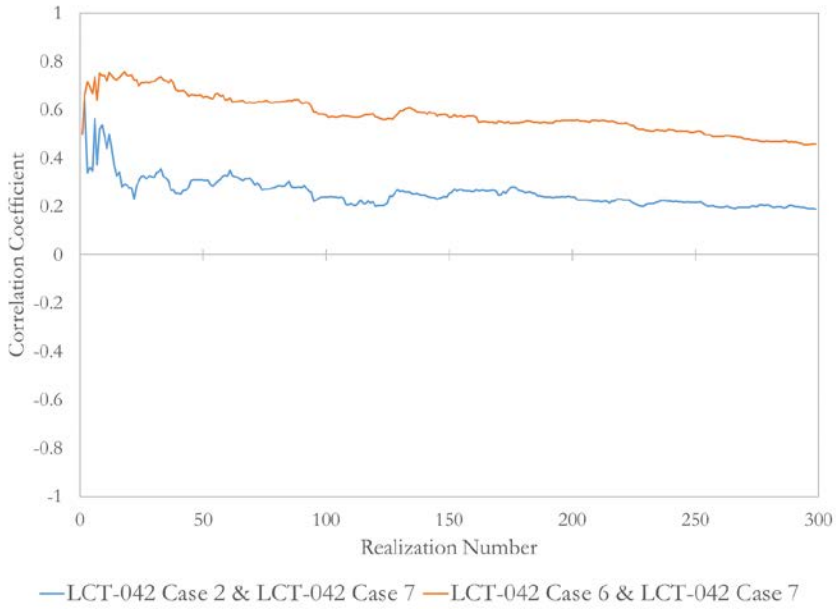

Figure 69. Convergence of two correlation coefficients, random fuel rod positions.

the random fuel rod placement scenario. The correlation coefficient considering all 900 realizations is 0.250 and the 95% confidence interval spans from 0.188 to 0.310. The estimate from 300 realizations, 0.190, is narrowly within this interval. The convergence behavior is shown in Figure 70, and indicates that convergence is likely achieved between 400 and 500 realizations. There appears to be a slight dip in the correlation coefficient estimate just before realization 300, but the estimate of the coefficient changes only slightly above about realization 200. It therefore is difficult to draw a generic conclusion regarding the number of realizations needed to assure convergence of the estimate of the correlation coefficient. High correlation coefficients converge quickly, in perhaps as few as 100 to 150 realizations. Moderate coefficients generally appear converged within about 300 realizations, but low correlation coefficients may take longer to converge. It is advisable to check convergence of correlation coefficients resulting from the Monte Carlo sampling technique; this same conclusion is well known in estimated k_{eff} using Monte Carlo transport.

Summary of Correlation Coefficients for LCT-042

The LCT-042 evaluation [15] has been used to examine several aspects of critical experiment correlations. The primary point of investigation specific to modeling LEU pin array experiments is the treatment of the fuel rod pitch or location uncertainty. Other studies, regarding the stochastic uncertainty of the individual realizations and the convergence of the correlation coefficients, are expected to be generically applicable to other systems. A brief synopsis of each of these studies is presented here, along with observations based on the results generated in these studies.

Fuel Rod Pitch/Position Uncertainty Effects

Two scenarios are examined for the fuel rod pitch uncertainty. The first is a uniform pitch assumption which is analogous to Scenario A in the WPNCS/UACSA benchmark described in the previous chapter. The second assumption for LCT-042 correlations is random pin placement, which results in a variety of pin pitches. This second assumption is similar to Scenario E from the WPNCS/UACSA benchmark.

Previous studies [39] examined correlation coefficients for the LCT-042 evaluation with the uniform pitch assumption, as shown in Figure 4. These studies were updated using the number of realizations and individual realization stochastic uncertainty constraints suggested by the results from the WPNCS/UACSA benchmark results. The updated results, as a function of pitch sampling range, are provided in Figure 61 and are much more reliable estimates of the correlation coefficients for the LCT-042 experiments given the uniform pitch assumption. The individual correlation coefficients are provided in Figure 50, Figure 52, Figure 54, and Figure 56. The results indicate that the correlations increase rapidly once the fuel rods are no longer fixed. Changes from a range of ± 0.75 up to ± 3 standard deviations show relatively modest increases in the correlation coefficients as the pin pitch uncertainty comes to dominate the overall case k_{eff} uncertainty. The conclusion of this study is that correlation coefficients will be high once a realistic pin pitch uncertainty range is

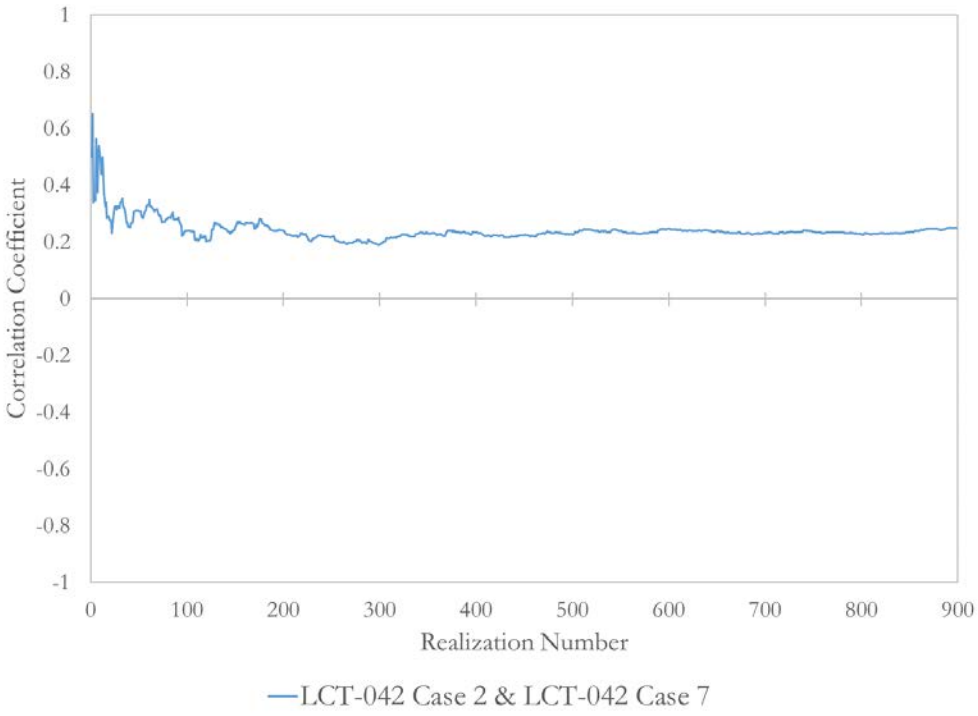

Figure 70. Convergence of LCT-042 Case 2 and Case 7 for 900 realizations.

sampled. In this case, it is assumed that a range of ±1 standard deviation or more represents a realistic uncertainty range.

The second assumption for treating the pin pitch uncertainty is to assume that each pin is located individually and that the uncertainty in pitch is a result of the variability of these locations. In the study presented here, the fuel rod dimensions are also varied individually. The resulting correlation coefficients are presented in Figure 67, and are much lower than those generated using the uniform pitch assumption. This conclusion is the same as that for the WPNCS/UACSA benchmark, and is an important conclusion of this work. The fuel rod modeling differences account for the change from the fixed pin location correlation coefficients presented in Figure 56. The individual rod positions are allowed to vary significantly more than ±3 standard deviations, but the random nature of the variability among the pins reduces the impact on k_{eff} and thus reduces its variability. The random rod locations are also assumed to be different in each case, eliminating a source of shared uncertainty. The overall uncertainty is very low compared to the evaluation, and more realizations may be required to achieve convergence of the correlation coefficients, as shown in Figure 69 and Figure 70.

Effect of Stochastic Uncertainty

The effect of the stochastic uncertainty on the correlation coefficients is examined for the uniform pitch scenario. Correlation coefficients are determined with realization stochastic uncertainties of approximately 0.00100 Δk, 0.00050 Δk, 0.00020 Δk, and 0.00005 Δk in addition to the base set of correlation coefficients which have a stochastic uncertainty of 0.00010 Δk. As shown in Figure 66, the correlation coefficients increase noticeably until the uncertainty is reduced to below about 0.00020 Δk, at which point the increase largely ends. A similar study is presented in the previous chapter for the WPNCS/UACSA benchmark, but that study did not extend below an uncertainty of 0.00010 Δk. It is likely, as mentioned in the discussion of the random rod placement scenario, that the required convergence of the stochastic uncertainty varies from evaluation to evaluation. Higher stochastic uncertainties will be acceptable for cases with higher total uncertainties; the stochastic uncertainty need only be small enough that it is not a significant contributor to the overall uncertainty.

Observations

A variety of observations are noted here based on the results of the calculations and studies documented in this chapter.

- The computational resources necessary to perform the calculations to determine correlation coefficients among critical experiments can be large. The generation of a matrix of correlation coefficients among 7 experiments consumed approximately 8,700 CPU-hours. With increased stochastic uncertainties in the individual realization calculations, this total may be reduced to approximately 2,100 CPU-hours. Further

increases in stochastic uncertainty, and associated decreases in run-time, are likely to result in less accurate correlation coefficient estimates.

- The treatment of the pin pitch uncertainty in LEU pin array experiments can be the most important factor in the calculated correlation coefficients. The uniform pitch assumption will likely lead to high correlation coefficients, while a random fuel rod placement approach will result in lower correlation coefficients.
- The evidence generated in this chapter indicates that for LCT-042 the correlations may be largely insensitive to the sampled pitch range given that a realistic range, that is at least ±1 standard deviation, is used. The resulting correlations are generally higher than 0.9 and represent a significant potential impact on validation and/or data adjustment.
- The number of realizations needed for convergence of calculated correlation coefficients depends on the magnitude of the coefficient. High correlation coefficients appear to converge with 150 or fewer realizations, while lower correlation coefficients may require 300 to 500 realizations.
- The individual realization k_{eff} values need to be determined with the minimum feasible stochastic (Monte Carlo) uncertainty. Significant changes in the correlation coefficients are observed when the uncertainty is reduced from approximately 0.00100 Δk to 0.00020 Δk. Further reductions in uncertainty have smaller effects for the LCT-042 experiments, but may be needed for other cases with lower uncertainties. Lower uncertainties may also be desired in the random fuel rod placement scenario.
- In-depth knowledge of the critical experiment materials, configurations, procedures, and setup are required for correct assessment of shared and unique uncertainty contributions. This level of information is typically not available in the ICSBEP Handbook [15], which is currently the primary reference for critical experiment descriptions. Without this in-depth knowledge, it is difficult to make defensible determinations regarding the uncertainty sharing among different cases.

CHAPTER VII: ANALYSIS OF CORRELATION COEFFICIENTS AMONG THE CASES OF HEU-SOL-THERM-001

The HST-001 evaluation contains 10 unreflected HEU solution experiments performed at the Rocky Flats Plant in the mid-1970s [15]. Four different tanks were used, including one stainless steel tank and three aluminum tanks with different radii. The ten experiments use 8 different solutions, and the solution height is the variable controlled to establish criticality.

The correlation coefficients determined in [17] are included in the ICSBEP Handbook [15], allowing a comparison of the results generated here with the previously published results. While it may seem logical to present the results from this evaluation first, given the simplicity of the models and the existence of other coefficients with which to compare results, these experiments are presented last as a demonstration that the approaches developed from the LEU fuel rod array cases can be reliably applied to other systems. The results presented in [17] are developed using a deterministic method, as discussed in Chapter II, and different assumptions are made about the uncertainty of parameters and the degree to which the uncertainty is shared among the cases. Agreement should therefore be expected in general trends in the correlation coefficients, though perhaps only to a limited extent in the absolute values presented for the correlation coefficients. The comparisons presented here, along with the results published by the OECD/NEA for the WPNCS/UACSA benchmark [33], should provide a basis for comparison for other methods of quantifying critical experiment correlations.

The previous two sets of critical experiment correlations have been determined for LEU fuel rod array experiments, and similarities and differences in the results and sensitivities have been discussed. The last set of experiments examined in detail is for the HST-001 evaluation. The parameters involved in this experiment are radically different than in the array cases. Primarily, the uncertainties pertain only to the geometry of the tank, the only significant geometry in the model, and the compositions of the tank and the solution itself. The simplicity of these experiments allows for careful examination of the effects of assumptions regarding independence of these variable parameters.

Variable Parameters

The uncertainties in the dimensions and compositions present in HST-001 are described in the evaluation. As with the LCT-042 experiments, the descriptions provided lead to varied approaches to modeling the uncertainties. For these experiments, most geometric uncertainties are sampled uniformly over the specified ranges and most composition uncertainties sample from untruncated normal distributions. As with previous series, these decisions are largely arbitrary.

Little information is provided in the evaluation to clarify the shared and unique uncertainty components. It is clear which cases shared the same tank and which cases shared the same solution, but no additional information is provided to clarify potential additional sources of

correlation. For example, the 8 solutions could have been separately diluted from a single stock of material. This would definitely introduce correlations in the uranium enrichment, and potentially in other solution parameters as well. It is also not discussed if the three aluminum tanks are made from the same material batch, which could also introduce additional correlation among the 8 cases in aluminum tanks. A series of studies is performed using these 10 experiments to investigate the sensitivity of the correlation coefficients to different assumptions about shared uncertainty parameters. Also, uncertain parameters are examined in groups to differentiate the importance of the different parameters to the apparent correlation. The geometry uncertainties are examined first, then tank compositions are introduced followed by treatment of the enrichment uncertainties. Finally, the remaining solution composition parameters are varied such that all known variable parameters are being sampled. For the tank composition and enrichment uncertainties, the new set of parameters is considered as both a shared and unique source of uncertainty. The previous uncertainty groups are all assumed to be fully correlated; this approach is taken to reduce the number of cases that must be considered compared to the full matrix. Each of the uncertainty groups is discussed in the remainder of this section.

Uncertainty Treatment for Dimensions

There are four different tanks used in the HST-001 experiments; one is fabricated from stainless steel and the other three from 6061 aluminum. The inner diameter and its uncertainty are provided for each tank in Table 1 of the evaluation. The provided uncertainties are taken as tolerances, and the inner diameters are sampled uniformly over the range. The same sampled diameters are used in each realization for cases that share a tank.

The thickness uncertainties of the sidewall and tank bottom are unknown. The evaluation states in a footnote that the original experimenter believed that "standard specification tolerances for metal plate are appropriate for estimating thickness and composition uncertainties" [15]. For each material, a range of thickness uncertainties is discussed in the evaluation. The uncertainties vary depending on the final heat and rolling treatment of the plate; the largest tolerances are assumed by the evaluator. The stainless steel tank therefore uses an uncertainty of ± 0.135 cm for the sidewall and ± 0.114 cm for the tank bottom. The aluminum tank is assumed to have uncertainties of ± 0.018 cm for the sidewall and ± 0.051 cm for the tank bottom. All tank dimensions are sampled uniformly across the specified range for each tank.

The uncertainty in the solution heights are provided in Table 3 of the evaluation. The solution height is sampled uniformly over the range, and all 10 solution heights are treated independently.

Uncertainties in Tank Compositions

The uncertainties in the tank compositions are provided in the text of Section 2.3.2 of the evaluation. The illegible dot characters are assumed to be less than symbols. For example, it is assumed that the carbon content of 304 stainless steel should be stated as $C < 0.08$. This

assumption seems to be consistent with the best estimate concentrations provided in Table 4 of the evaluation.

The stainless steel composition in the nominal benchmark model is provided in Table 17 of the evaluation, and includes C, Si, P, S, Cr, Mn, Fe, Ni, and Mo. Uncertainties are provided for each of these constituents except for Mo, so its trace concentration is treated as a constant. The other alloying elements, aside from iron, are sampled uniformly within the uncertainty ranges provided. The weight percent of iron is then determined by subtraction as it makes up the remainder of the material. Each of the sampled or calculated weight percents is then divided by the nominal weight percent to determine a correction factor to apply to that element. The correction factors are multiplied by the nominal number density to determine the perturbed number densities.

The aluminum tank compositions are modeled in the benchmark model as pure aluminum. The nominal number density is calculated from the nominal density of the alloy, 2.737 g/cm^3, and the 97.35 wt% nominal aluminum content. The weight percent of each minor constituent is sampled from the range provided in Section 2.3.2 of the evaluation, and the perturbed weight percent of aluminum is calculated as the difference between the sum of the minor and constituents and 100. The perturbed weight percent is divided by the nominal weight percent, and the correction factor is then applied to the nominal number density to determine the perturbed number density. None of the elements other than aluminum is included in the benchmark model, so they are also excluded from the perturbed models.

The tank compositions are treated differently in two sets of calculations. In the first case, each of the three aluminum tanks is assumed to be fabricated from different material and therefore the alloying constituents are sampled separately for each tank. Cases 3 and 4 share one tank, Cases 5 through 9 share a second tank, and Case 10 has a unique tank. The cases that share a tank also share compositions in all realizations. The second part of the study assumes that all tanks are fabricated from the same aluminum material. In this case, all 8 cases that use the aluminum tanks are assumed to have the same composition. No similar treatment is applied to Cases 1 and 2 because they share the only stainless steel tank in the series of experiments.

Enrichment Uncertainties

The enrichment of the uranium in the solutions is provided in Table 5, along with uncertainties in each weight percent. This presentation implies that a single stock solution with a single enrichment was used for all solutions, but this is neither stated nor refuted in the evaluation. Two sets of correlations are calculated including the effects of the enrichment uncertainties. Consistent with the treatment of the tank compositions in the previous section, the first assumes unique uncertainties for all experiments and the second assumes shared uncertainties across all 10 cases. The two pairs of cases which share the same solution are assumed to have shared enrichment uncertainties in both cases because of the shared solution. The enrichment uncertainty is the only uncertainty component considered for HST-001 that has the potential to create correlations among all 10 cases. The other

potentially shared sources of uncertainty have applicability only to some cases via a shared tank or solution.

New number densities are calculated for each sample. The atomic masses of the uranium isotopes and Avogadro's number were determined to reproduce the number densities provided in the evaluation to 4 decimal places. Equation 14 [15] is then used with sampled weight fractions for each isotope. The sampled weight fractions are not forced to sum to 1 since the atom densities are calculated and input.

$$N_i = \frac{W_{f,i} \cdot \rho_U \cdot N_A}{A_{w,i}}, \text{ for } i \in {}^{235}\text{U}, {}^{234}\text{U}, {}^{236}\text{U}, \text{ and } {}^{238}\text{U} \qquad \text{Eqn (14)}$$

Where: N_i is the number density of isotope i
$W_{f,i}$ is the weight fraction of isotope i
ρ_U is the density of uranium in the solution
N_A is Avogadro's number
$A_{w,i}$ is the atomic mass of isotope i

Solution Composition Uncertainties

The solution compositions vary along with the uranium concentration, excess nitric acid, and overall solution density. The values of each of these parameters, and their uncertainties, are provided for each case in Table 6 of the evaluation. The number density equations are provided for each solution component in Section 3.3.1 of the evaluation, but most of the symbols have not been rendered correctly and appear as dots. The correct equations, used in determining the perturbed number densities for all 10 cases, are provided in Equations 14 – 20. The uranium concentration in each solution, excess acid concentration, and solution densities are all sampled from normal distributions. The solution parameters are all assumed to be unique in each of the 8 solutions. Cases 1 and 8 share a solution, and Cases 4 and 9 share a different solution. These two pairs of cases therefore share perturbed number densities. The solutions are assumed to be independent as there is no known mechanism for diluting each solution with a common error or uncertainty, given the range of concentrations and densities present in the set of solutions.

$$\rho_{UO_2(NO_3)_2} = \frac{N_U \cdot M_{w,UO_2(NO_3)_2}}{N_A} \qquad \text{Eqn (15)}$$

Where: $\rho_{UO2(NO3)2}$ mass density of uranyl nitrate
N_U is the total uranium atom density
$M_{w,UO2(NO3)2}$ is the molecular weight of uranyl nitrate

$$\rho_{HNO_3} = \frac{N^{a}_{HNO_3} \cdot M_{w,HNO_3}}{1000} \qquad \text{Eqn (16)}$$

Where: ϱ_{HNO3} is the mass density of nitric acid
N^{a}_{HNO3} is the excess acid molarity
$M_{w, HNO3}$ is the molecular weight of nitric acid

$$\rho_{H_2O} = \rho_{solution} - \rho_{HNO_3} - \rho_{UO_2(NO_3)_2} \qquad \text{Eqn (17)}$$

Where: ϱ_{H2O} is the mass density of water
$\varrho_{solution}$ is the mass density of the solution

$$N_O = 8N_U + 3\left(\frac{\rho_{HNO_3} \cdot N_A}{M_{w,HNO_3}}\right) + \frac{\rho_{H_2O} \cdot N_A}{M_{w,H_2O}} \qquad \text{Eqn (18)}$$

Where: N_O is the total atom density of oxygen
$M_{w,H2O}$ is the molecular weight of water

$$N_N = 2N_U + \frac{\rho_{HNO_3} \cdot N_A}{M_{w,HNO_3}} \qquad \text{Eqn (19)}$$

Where: N_N is the total atom density of nitrogen

$$N_H = \frac{\rho_{HNO_3} \cdot N_A}{M_{w,HNO_3}} + \frac{2\rho_{H_2O} \cdot N_A}{M_{w,H_2O}} \qquad \text{Eqn (20)}$$

Where: N_H is the total atom density of hydrogen

Results

Several sets of critical experiment correlations are calculated for the HST-001 experiment series. Each of these results is presented in this section and compared with reference results included in [15] as originally determined in [17]. It is difficult, if not impossible, to determine which set of correlations is the best estimate of the real coefficients because of the information missing from the evaluation. The reference results are also not considered to be more or less accurate than any of the results determined as part of this effort. The relative importance of each set of uncertain parameters is also assessed. This information will provide potentially useful guidance to future evaluators related to how important each component of uncertainty is to the final correlation coefficients. The reference results from

the ICSBEP Handbook [15] are presented first, and compared with the results calculated here in each subsequent section.

ICSBEP Handbook Reference Results

The results included in the ICSBEP Handbook [15], originally generated in [17], are presented in Figure 74. In general, the correlation coefficients are between 0.4 and 0.5, and are fairly uniformly distributed. There are some pairs of cases that have noticeably higher correlations than the remainder of the cases. The highest correlation coefficient is between Cases 4 and 9, with a value of 0.77. The same solution is used in both cases, explaining the higher correlation for this pair. The experiments are performed in different tanks, but both tanks are aluminum. Cases 1 and 8 also share a solution, but Case 1 is in the stainless steel tank and Case 8 is in an aluminum tank. The correlation coefficient between Cases 1 and 8 is somewhat larger than others at 0.57.

There is no definitive reason that the correlations between Case 2 and Cases 4 and 9 should be higher than rest of the correlation coefficients. Cases 4 and 9 appear to be relatively strongly correlated, as noted previously, but they are not strongly correlated with Case 1. It appears that the reason for the higher correlation with Case 2 is a similar uranium concentration; the solution in Case 2 is 346.73 gU/cm^3 and for Cases 4 and 9 is 357.71 gU/cm^3. The other solution parameters are also very similar, so it is apparent that the solutions are similar. No detail is provided in [17] describing the details of the evaluation process for the HST-001 series, so no concrete conclusion can be drawn about why these cases are more strongly correlated than others.

In general, it appears that the primary driver of the correlation coefficients is the presumably shared enrichment and possible solution parameters among all 10 solutions. No detailed description of the development of these correlations is provided in [17], but the detailed description provided for a different set of experiments indicates that at least the solution densities are treated as correlated. Higher values, especially as noted for Cases 4 and 9, show pairs of cases that have greater shared uncertainty because of the shared solution. The increase in correlation caused by the shared solution does not appear to be as great for Cases 1 and 8, but Case 8 clearly has the highest correlated coefficient of any of the 9 other cases with Case 1. It is not clear why the correlation caused by the shared solution should create a higher correlation than the shared tank. The largest uncertainty contribution in the ICSBEP evaluation for the cases in the stainless steel tank is the inner diameter of the tank. This should lead to a strong correlation between Cases 1 and 2 which is not present in Figure 71. There is no cause reason for the higher correlations between Case 2 and Cases 4 and 9.

Results Considering Only Geometric Uncertainties

The results presented in this section are newly generated via Sampler, but include only the effects of sampling on geometry parameters. The geometry parameters include tank dimensions and solution height. The dimensions are assumed to be the same for each tank, but obviously differ between tanks. It is possible that the sidewalls and base plates of the

	1-1	1-2	1-3	1-4	1-5	1-6	1-7	1-8	1-9	1-10
1-1	1	0.47	0.46	0.44	0.42	0.42	0.46	0.57	0.44	0.44
1-2	0.47	1	0.42	0.58	0.42	0.42	0.41	0.44	0.58	0.46
1-3	0.46	0.42	1	0.46	0.43	0.43	0.46	0.46	0.42	0.43
1-4	0.44	0.58	0.46	1	0.42	0.42	0.42	0.44	0.77	0.46
1-5	0.42	0.42	0.43	0.42	1	0.54	0.48	0.47	0.46	0.48
1-6	0.42	0.42	0.43	0.42	0.54	1	0.48	0.47	0.46	0.48
1-7	0.46	0.41	0.46	0.42	0.48	0.48	1	0.51	0.45	0.43
1-8	0.57	0.44	0.46	0.44	0.47	0.47	0.51	1	0.48	0.44
1-9	0.44	0.58	0.42	0.77	0.46	0.46	0.45	0.48	1	0.46
1-10	0.44	0.46	0.43	0.46	0.48	0.48	0.43	0.44	0.46	1

Figure 71. Reference correlation coefficients as calculated in [17] and reported in [15].

aluminum tanks were made from the same lot of material and should have the same values assigned. This particular case was not examined.

A total of 300 realizations were created and run for each case, and each of the 3000 resulting KENO calculations were converged to a stochastic uncertainty of ±0.00010 Δk_{eff}. The mean of the 300 perturbed k_{eff} results and their standard deviation are shown in Table 18. The benchmark uncertainties, provided in Table 18 of the evaluation [15], are also provided in Table 18. The uncertainty in most cases is significantly lower than the evaluation uncertainty, as would be expected since most of the uncertain parameters are not perturbed. The uncertainty is Case 1, however, is larger than the uncertainty in the evaluation. A review of the uncertainty assessment in Section 2 of the evaluation [15] indicates that the largest contributors to uncertainty in Case 1 are the tank wall thickness and solution radius. Both of these parameters are included in this set of perturbed parameters. The other experiment in the stainless steel tank, Case 2, also has a large uncertainty compared to the 8 cases performed in the aluminum tanks.

The resulting correlation coefficients are shown in Figure 72. As expected, the cases which share a tank have very strong correlations and the other cases are largely uncorrelated. The 95% confidence interval for each correlation coefficient is provide in Figure 73. The results indicate that the correlations between cases in different tanks are statistically insignificant. Interestingly, 4 of the 5 cases in the 33 cm inner diameter aluminum tank are very highly correlated. Case 7 is significantly less correlated with the other four cases. The convergence of the correlations coefficients between Cases 1 and 10 and Cases 5 and 7 are shown in Figure 74. These results indicate that the correlation coefficients are well converged. The correlation coefficient between Cases 5 and 7 is particularly well converged, largely because of its high value. The correlation coefficient estimate for Cases 1 and 10 does not converge nearly as quickly.

The correlation coefficients calculated by perturbing only the geometric variables bear little resemblance to the reference results shown in Figure 71. This is the expected result since only some of the variables are considered. The effect of shared tanks is not clearly visible in the reference results, which is somewhat puzzling given that the main uncertainty components in at least some cases are geometric parameters.

Table 18. Average and standard deviation of 300 perturbed k_{eff} values sampling dimensions, HST-001

Case	Average k_{eff}	Standard Deviation	Benchmark Uncertainty
1	0.99557	0.00628	0.0060
2	0.99363	0.00627	0.0072
3	0.99947	0.00198	0.0035
4	0.99645	0.00194	0.0053
5	0.99596	0.00243	0.0049
6	0.99928	0.00248	0.0046
7	0.99551	0.00245	0.0040
8	0.99578	0.00222	0.0038
9	0.99228	0.00213	0.0054
10	0.98999	0.00413	0.0054

	1-1	1-2	1-3	1-4	1-5	1-6	1-7	1-8	1-9	1-10
1-1	1	1.00	-0.02	-0.02	0.04	0.02	0.01	0.05	0.04	-0.06
1-2	1.00	1	-0.02	-0.02	0.04	0.02	0.01	0.05	0.04	-0.06
1-3	-0.02	-0.02	1	0.99	-0.03	-0.03	-0.02	-0.02	-0.04	0.04
1-4	-0.02	-0.02	0.99	1	-0.02	-0.03	-0.02	-0.02	-0.04	0.04
1-5	0.04	0.04	-0.03	-0.02	1	0.96	0.87	0.98	0.96	0.04
1-6	0.02	0.02	-0.03	-0.03	0.96	1	0.85	0.96	0.94	0.04
1-7	0.01	0.01	-0.02	-0.02	0.87	0.85	1	0.88	0.87	0.02
1-8	0.05	0.05	-0.02	-0.02	0.98	0.96	0.88	1	0.97	0.05
1-9	0.04	0.04	-0.04	-0.04	0.96	0.94	0.87	0.97	1	0.04
1-10	-0.06	-0.06	0.04	0.04	0.04	0.04	0.02	0.05	0.04	1

Figure 72. Correlation coefficients among HST-001 cases perturbing only geometry variables.

	001-002	001-003	001-004	001-005	001-006	001-007	001-008	001-009	001-010
001-001	(0.995, 0.997)	(-0.129, 0.097)	(-0.130, 0.096)	(-0.074, 0.152)	(-0.090, 0.136)	(-0.102, 0.125)	(-0.063, 0.163)	(-0.071, 0.155)	(-0.173, 0.052)
001-002		(-0.129, 0.098)	(-0.131, 0.096)	(-0.076, 0.151)	(-0.090, 0.136)	(-0.102, 0.125)	(-0.065, 0.161)	(-0.072, 0.154)	(-0.173, 0.053)
001-003			(0.990, 0.994)	(-0.137, 0.089)	(-0.141, 0.086)	(-0.135, 0.092)	(-0.134, 0.092)	(-0.152, 0.075)	(-0.071, 0.155)
001-004				(-0.136, 0.090)	(-0.140, 0.086)	(-0.134, 0.092)	(-0.132, 0.094)	(-0.147, 0.079)	(-0.071, 0.155)
001-005					(0.949, 0.967)	(0.843, 0.898)	(0.975, 0.984)	(0.950, 0.968)	(-0.076, 0.150)
001-006						(0.818, 0.881)	(0.955, 0.971)	(0.931, 0.956)	(-0.070, 0.156)
001-007							(0.854, 0.905)	(0.842, 0.897)	(-0.092, 0.134)
001-008								(0.957, 0.972)	(-0.068, 0.158)
001-009		Significant		Not Significant					(-0.077, 0.149)

Figure 73. Confidence intervals for HST-001 correlation coefficients, only geometric perturbations.

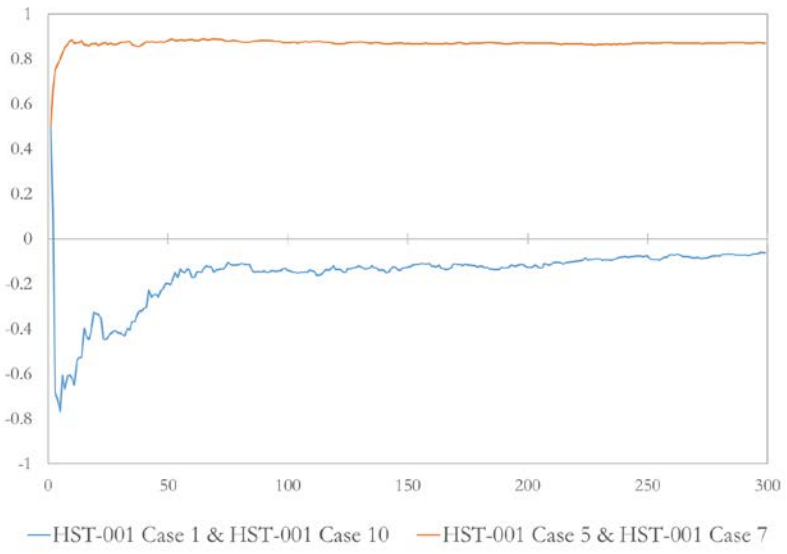

Figure 74. Convergence of two selected correlation coefficients, only geometric perturbations.

Results Considering Geometric and Tank Composition Uncertainties

The next set of parameters to be perturbed are the tank compositions. These variables are sampled in addition to the dimensions sampled in the previous section. As mentioned previously, there is no discussion in the evaluation to indicate whether the aluminum tanks were fabricated from the same lot of material. It is reasonable to conclude that this is likely true, but if the tanks were built at different times they would like have come from different lots with different impurities. These effects are somewhat mitigated for the aluminum tanks by the fact that only the aluminum itself is included in the benchmark model. The impurities in these tanks only impact reactivity by causing slight differences in the resulting effective density of the tank material. Regardless, correlation coefficients are calculated with the tank compositions sampled identically for all three aluminum tanks and also independently for each tank. The stainless steel tank used for Cases 1 and 2 is sampled uniquely in both scenarios since it is clearly a different material than the 6061 aluminum alloy used for the other tanks.

Correlation coefficients are calculated assuming independent tank compositions with 300 realizations for each of the 10 cases. As with the previous study, each of the KENO calculations is converged to ±0.00010 Δk. The average and standard deviation of the k_{eff} for each case is provided in Table 19. As before, the uncertainty from the evaluation is also included for reference. The uncertainties do not change appreciably for any case. Very small increases are noted for Cases 1 and 2. The variation is higher for these two cases because more constituents are included in the benchmark model for the steel tank than for the aluminum models. The tank compositions are clearly not a significant contributor to uncertainty.

The correlation coefficients are provided in Figure 75. The results are nearly identical to the correlations resulting from only dimension perturbations, shown in Figure 72. This is the

Table 19. Average and standard deviation of 300 perturbed k_{eff} values sampling dimensions and unique tank compositions, HST-001

Case	Average k_{eff}	Standard Deviation	Benchmark Uncertainty
1	0.99748	0.00630	0.0060
2	0.99556	0.00630	0.0072
3	1.00123	0.00198	0.0035
4	0.99819	0.00194	0.0053
5	0.99782	0.00243	0.0049
6	1.00114	0.00246	0.0046
7	0.99728	0.00246	0.0040
8	0.99756	0.00220	0.0038
9	0.99401	0.00214	0.0054
10	0.99182	0.00412	0.0054

	1-1	1-2	1-3	1-4	1-5	1-6	1-7	1-8	1-9	1-10
1-1	1	1.00	-0.02	-0.03	0.04	0.02	0.01	0.05	0.04	-0.06
1-2	1.00	1	-0.02	-0.03	0.04	0.02	0.01	0.05	0.04	-0.06
1-3	-0.02	-0.02	1	0.99	-0.02	-0.02	-0.02	-0.01	-0.03	0.05
1-4	-0.03	-0.03	0.99	1	-0.03	-0.02	-0.02	-0.02	-0.03	0.04
1-5	0.04	0.04	-0.02	-0.03	1	0.96	0.87	0.98	0.96	0.03
1-6	0.02	0.02	-0.02	-0.02	0.96	1	0.86	0.96	0.95	0.04
1-7	0.01	0.01	-0.02	-0.02	0.87	0.86	1	0.88	0.87	0.02
1-8	0.05	0.05	-0.01	-0.02	0.98	0.96	0.88	1	0.96	0.04
1-9	0.04	0.04	-0.03	-0.03	0.96	0.95	0.87	0.96	1	0.04
1-10	-0.06	-0.06	0.05	0.04	0.03	0.04	0.02	0.04	0.04	1

Figure 75. Correlation coefficients among HST-001 cases perturbing geometry and unique tank composition variables.

expected result given that there is virtually no difference in the uncertainties introduced with the sampling of tank compositions. Given the similarities, neither confidence intervals on the correlation coefficients nor a convergence plot are presented for these results.

The means and standard deviations for the scenario with all aluminum tank compositions identically sampled are provided in Table 20. The results are changed only very slightly from the previous scenario with unique compositions for each tank. This is as it should be as no new uncertainty is introduced, but how the uncertainty varies from one case to another is changed. There are correspondingly small changes in the correlation coefficients presented in Figure 76. Again, confidence intervals and correlations plots are not provided because of the small magnitude of the changes.

Sampling the tank compositions does not change the correlation coefficients appreciably whether the tanks are assumed to be fabricated from material drawn from the same lot or not. The correlation coefficients which result are provided in Figure 75 and Figure 76 and, as stated, are nearly identical to the results considering only dimensional uncertainties provided in Figure 72. The results still differ dramatically from the reference results provided in [15], as shown in Figure 71.

Results Considering Geometric, Tank Composition, and Enrichment Uncertainties

The enrichment uncertainty is added next, implemented as described earlier. The first set of calculations assumes that each unique solution is drawn from a different source and so has different enrichments. All 8 solutions are assumed to be described by the same uncertainties, as described above and described in Table 5 of the ICSBEP evaluation [15], but the exact enrichment for each solution is assumed to be unique. A more likely assumption, but one that cannot be confirmed with information included in the ICSBEP evaluation, is that all 8 solutions were diluted from a single original source. This scenario results in all 8 solutions having an identical enrichment, and therefore an additional source of shared uncertainty.

The average and standard deviation of the 300 realizations assuming unique solution enrichments are provided in Table 21, again with the evaluation uncertainty for reference. The results are not significantly different from those shown in the previous section. This indicates that the enrichment uncertainty does not have a significant impact on the uncertainty of the system k_{eff}. The correlation coefficients are provided in Figure 77, and also show essentially no difference from the previous correlations.

Table 22 provides the average and standard deviations of the 300 realizations for all 10 cases for the scenario assuming the enrichment is the same for all solutions. The results are nearly identical with the results assuming unique solution enrichments. This is expected because the same uncertainties are used in both scenarios, but in this scenario the sampled values are identical for all 8 solutions. The correlation coefficients are shown in Figure 78, and show no appreciable change from the first scenario. Convergence plots and confidence intervals are not provided because the coefficients are largely unchanged from those provided in previous sections.

Table 20. Average and standard deviation of 300 perturbed k_{eff} values sampling dimensions and shared tank compositions, HST-001

Case	Average k_{eff}	Standard Deviation	Benchmark Uncertainty
1	0.99748	0.00630	0.0060
2	0.99556	0.00630	0.0072
3	1.00123	0.00198	0.0035
4	0.99819	0.00194	0.0053
5	0.99783	0.00243	0.0049
6	1.00114	0.00247	0.0046
7	0.99730	0.00246	0.0040
8	0.99757	0.00221	0.0038
9	0.99401	0.00215	0.0054
10	0.99181	0.00414	0.0054

	1-1	1-2	1-3	1-4	1-5	1-6	1-7	1-8	1-9	1-10
1-1	1	1.00	-0.02	-0.03	0.04	0.02	0.01	0.05	0.04	-0.06
1-2	1.00	1	-0.02	-0.03	0.04	0.03	0.01	0.05	0.04	-0.06
1-3	-0.02	-0.02	1	0.99	-0.02	-0.01	-0.02	-0.01	-0.04	0.05
1-4	-0.03	-0.03	0.99	1	-0.02	-0.02	-0.03	-0.01	-0.04	0.05
1-5	0.04	0.04	-0.02	-0.02	1	0.96	0.87	0.98	0.96	0.03
1-6	0.02	0.03	-0.01	-0.02	0.96	1	0.85	0.97	0.94	0.04
1-7	0.01	0.01	-0.02	-0.03	0.87	0.85	1	0.88	0.87	0.02
1-8	0.05	0.05	-0.01	-0.01	0.98	0.97	0.88	1	0.97	0.04
1-9	0.04	0.04	-0.04	-0.04	0.96	0.94	0.87	0.97	1	0.04
1-10	-0.06	-0.06	0.05	0.05	0.03	0.04	0.02	0.04	0.04	1

Figure 76. Correlation coefficients among HST-001 cases perturbing geometry and shared tank composition variables.

Table 21. Average and standard deviation of 300 perturbed k_{eff} values sampling dimensions, shared tank compositions, and unique enrichment uncertainties, HST-001

Case	Average k_{eff}	Standard Deviation	Benchmark Uncertainty
1	0.99748	0.00630	0.0060
2	0.99556	0.00631	0.0072
3	1.00123	0.00198	0.0035
4	0.99820	0.00194	0.0053
5	0.99784	0.00244	0.0049
6	1.00117	0.00247	0.0046
7	0.99728	0.00247	0.0040
8	0.99757	0.00221	0.0038
9	0.99400	0.00215	0.0054
10	0.99180	0.00414	0.0054

	1-1	1-2	1-3	1-4	1-5	1-6	1-7	1-8	1-9	1-10
1-1	1	1.00	-0.02	-0.02	0.04	0.02	0.02	0.05	0.04	-0.07
1-2	1.00	1	-0.02	-0.02	0.04	0.03	0.02	0.05	0.04	-0.07
1-3	-0.02	-0.02	1	0.99	-0.03	-0.03	-0.03	-0.02	-0.05	0.04
1-4	-0.02	-0.02	0.99	1	-0.03	-0.03	-0.03	-0.02	-0.03	0.04
1-5	0.04	0.04	-0.03	-0.03	1	0.96	0.87	0.98	0.96	0.04
1-6	0.02	0.03	-0.03	-0.03	0.96	1	0.85	0.96	0.94	0.05
1-7	0.02	0.02	-0.03	-0.03	0.87	0.85	1	0.88	0.86	0.02
1-8	0.05	0.05	-0.02	-0.02	0.98	0.96	0.88	1	0.96	0.04
1-9	0.04	0.04	-0.05	-0.03	0.96	0.94	0.86	0.96	1	0.04
1-10	-0.07	-0.07	0.04	0.04	0.04	0.05	0.02	0.04	0.04	1

Figure 77. Correlation coefficients among HST-001 cases perturbing geometry, shared tank composition and unique enrichment variables.

Table 22. Average and standard deviation of 300 perturbed k_{eff} values sampling dimensions, shared tank compositions, and shared enrichment uncertainties, HST-001

Case	Average k_{eff}	Standard Deviation	Benchmark Uncertainty
1	0.99748	0.00630	0.0060
2	0.99556	0.00630	0.0072
3	1.00123	0.00199	0.0035
4	0.99820	0.00196	0.0053
5	0.99783	0.00244	0.0049
6	1.00115	0.00246	0.0046
7	0.99730	0.00246	0.0040
8	0.99757	0.00221	0.0038
9	0.99401	0.00213	0.0054
10	0.99181	0.00412	0.0054

	1-1	1-2	1-3	1-4	1-5	1-6	1-7	1-8	1-9	1-10
1-1	1	1.00	-0.01	-0.02	0.05	0.02	0.01	0.05	0.04	-0.06
1-2	1.00	1	-0.01	-0.02	0.05	0.03	0.01	0.05	0.04	-0.06
1-3	-0.01	-0.01	1	0.99	-0.02	-0.02	-0.02	-0.01	-0.02	0.04
1-4	-0.02	-0.02	0.99	1	-0.02	-0.02	-0.02	-0.01	-0.02	0.04
1-5	0.05	0.05	-0.02	-0.02	1	0.96	0.87	0.98	0.96	0.04
1-6	0.02	0.03	-0.02	-0.02	0.96	1	0.85	0.96	0.94	0.04
1-7	0.01	0.01	-0.02	-0.02	0.87	0.85	1	0.88	0.87	0.02
1-8	0.05	0.05	-0.01	-0.01	0.98	0.96	0.88	1	0.96	0.04
1-9	0.04	0.04	-0.02	-0.02	0.96	0.94	0.87	0.96	1	0.03
1-10	-0.06	-0.06	0.04	0.04	0.04	0.04	0.02	0.04	0.03	1

Figure 78. Correlation coefficients among HST-001 cases perturbing geometry, shared tank composition and shared enrichment variables.

The enrichment uncertainty, like the tank composition uncertainty, does not significantly impact the overall system k_{eff} uncertainty. It therefore also has no appreciable effect on the correlation coefficients of the 10 cases in the HST-001 evaluation. The correlation coefficients shown in Figure 77 and Figure 78 are statistically indistinguishable from those shown in Figure 72, Figure 75, and Figure 76. As noted in the previous sections, these results are significantly at odds with the reference results from the ICSBEP evaluation.

Results Considering All Uncertain Parameters

The last set of parameters to be included in the analysis of correlations among the 10 cases in the HST-001 evaluation relates to the composition of the solution. These parameters include the concentration of uranium in the solution, the excess acid, and the solution density. The implementation of these variables is described earlier, and involves Equations 14-20. It is unclear how any of solution parameters could be shared between different solutions, so the only scenario investigated here is that these parameters are unique to each solution. It is worth reiterating that there are only 8 solutions used, as Cases 1 and 8 and Cases 4 and 9 use the same solution.

The average and standard deviation for each of the 10 cases for all 300 realizations is provided in Table 23. The average k_{eff} value changes very little, indicating unbiased sampling, but the standard deviation of the results increases noticeably compared with the prior sets of results. This increase is especially noticeable for the experiments in aluminum tanks, that is Cases 3 through 10. The dimensional uncertainties are smaller for these cases than for the stainless steel tank used in Cases 1 and 2. The aluminum tank cases continue to exhibit significantly lower uncertainties than those reported in the evaluation [15].

The correlation coefficients are provided in Figure 79, and show dramatic differences compared to previous sets of results. The correlations are markedly lower among Cases 5 through 9, and a significant increase is noted in the correlation between Cases 4 and 9. The decreases are caused by the use of different solutions, and, in the same vein, the increase in the correlation between Cases 4 and 9 results from use of the same solution. There is no noticeable increase in the correlation between Cases 1 and 8 because the uncertainties in the tank dimensions in Case 1, using the stainless steel tank, overwhelm the effects of the solution uncertainties. The 95% confidence intervals for the correlations are shown in Figure 80. The convergence of three correlation coefficients is provided in Figure 81, and indicates the selected correlation coefficients are well converged. The representative coefficients were selected from high, medium, and low correlation cases with the intent of providing confidence that all correlation coefficients are likely well converged. The coefficients considering only the first half of the realizations are shown in Figure 82 and considering only the second half of the realizations in Figure 83. These results show good quantitative agreement for all statistically significant correlations, and good qualitative agreement for which correlations are not significant.

These results incorporate perturbations of all uncertain parameters for which information is provided in the evaluation. It is also apparent that the treatment of the tank composition and

Table 23. Average and standard deviation of 300 perturbed k_{eff} values sampling all uncertainties, HST-001

Case	Average k_{eff}	Standard Deviation	Benchmark Uncertainty
1	0.99743	0.00633	0.0060
2	0.99549	0.00647	0.0072
3	1.00142	0.00254	0.0035
4	0.99815	0.00362	0.0053
5	0.99786	0.00248	0.0049
6	1.00106	0.00267	0.0046
7	0.99726	0.00256	0.0040
8	0.99753	0.00232	0.0038
9	0.99395	0.00358	0.0054
10	0.99180	0.00427	0.0054

	1-1	1-2	1-3	1-4	1-5	1-6	1-7	1-8	1-9	1-10
1-1	1	0.98	0.01	-0.04	0.08	-0.01	0.01	0.08	0.00	-0.05
1-2	0.98	1	0.01	-0.04	0.06	-0.02	0.01	0.05	-0.01	-0.05
1-3	0.01	0.01	1	0.37	-0.04	0.03	-0.02	-0.01	-0.03	0.02
1-4	-0.04	-0.04	0.37	1	-0.04	-0.05	0.00	-0.01	0.67	-0.05
1-5	0.08	0.06	-0.04	-0.04	1	0.79	0.77	0.87	0.51	0.07
1-6	-0.01	-0.02	0.03	-0.05	0.79	1	0.76	0.82	0.44	0.08
1-7	0.01	0.01	-0.02	0.00	0.77	0.76	1	0.83	0.53	0.03
1-8	0.08	0.05	-0.01	-0.01	0.87	0.82	0.83	1	0.56	0.06
1-9	0.00	-0.01	-0.03	0.67	0.51	0.44	0.53	0.56	1	-0.04
1-10	-0.05	-0.05	0.02	-0.05	0.07	0.08	0.03	0.06	-0.04	1

Figure 79. Correlation coefficients among HST-001 cases perturbing all variables.

	001-002	001-003	001-004	001-005	001-006	001-007	001-008	001-009	001-010
001-001	(0.970, 0.981)	(-0.104, 0.123)	(-0.155, 0.071)	(-0.038, 0.188)	(-0.121, 0.105)	(-0.102, 0.124)	(-0.034, 0.191)	(-0.116, 0.111)	(-0.160, 0.066)
001-002		(-0.099, 0.127)	(-0.151, 0.075)	(-0.052, 0.173)	(-0.135, 0.091)	(-0.103, 0.124)	(-0.061, 0.164)	(-0.122, 0.105)	(-0.166, 0.060)
001-003			(0.262, 0.459)	(-0.153, 0.073)	(-0.079, 0.147)	(-0.135, 0.091)	(-0.120, 0.106)	(-0.144, 0.082)	(-0.098, 0.128)
001-004				(-0.148, 0.079)	(-0.163, 0.063)	(-0.111, 0.116)	(-0.119, 0.108)	(0.599, 0.725)	(-0.160, 0.066)
001-005					(0.747, 0.831)	(0.722, 0.815)	(0.844, 0.898)	(0.426, 0.593)	(-0.044, 0.181)
001-006						(0.706, 0.803)	(0.784, 0.858)	(0.348, 0.530)	(-0.035, 0.190)
001-007							(0.795, 0.865)	(0.441, 0.605)	(-0.084, 0.142)
001-008								(0.479, 0.634)	(-0.050, 0.176)
001-009		Significant		Not Significant					(-0.149, 0.078)

Figure 80. Confidence intervals for HST-001 correlation coefficients.

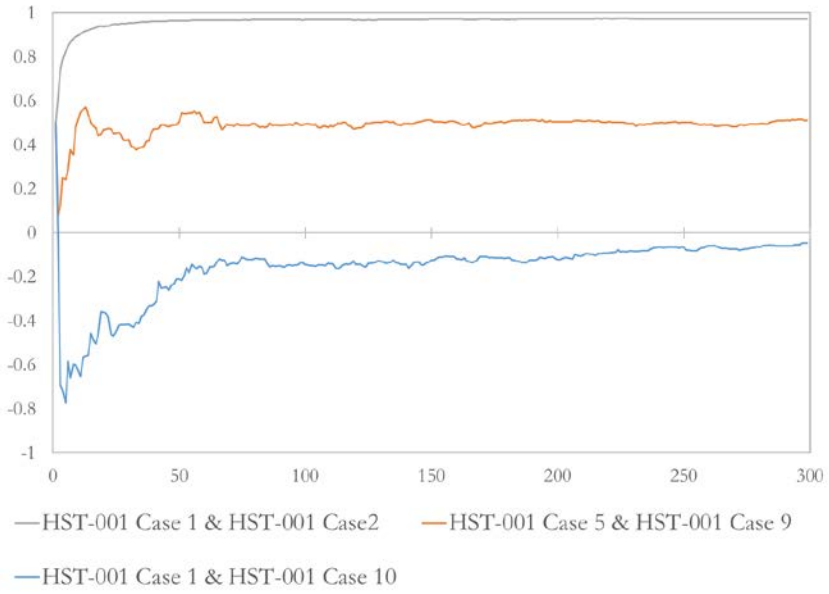

Figure 81. Convergence of three selected correlation coefficients.

	1-1	1-2	1-3	1-4	1-5	1-6	1-7	1-8	1-9	1-10
1-1	1	0.98	-0.01	-0.09	0.00	-0.08	0.01	0.03	-0.04	-0.13
1-2	0.98	1	0.00	-0.08	-0.03	-0.10	0.00	0.00	-0.05	-0.13
1-3	-0.01	0.00	1	0.35	-0.05	0.06	-0.05	-0.02	-0.05	0.01
1-4	-0.09	-0.08	0.35	1	0.01	-0.01	0.04	0.03	0.70	-0.01
1-5	0.00	-0.03	-0.05	0.01	1	0.81	0.75	0.88	0.52	0.08
1-6	-0.08	-0.10	0.06	-0.01	0.81	1	0.74	0.84	0.44	0.05
1-7	0.01	0.00	-0.05	0.04	0.75	0.74	1	0.83	0.52	0.03
1-8	0.03	0.00	-0.02	0.03	0.88	0.84	0.83	1	0.56	0.07
1-9	-0.04	-0.05	-0.05	0.70	0.52	0.44	0.52	0.56	1	0.04
1-10	-0.13	-0.13	0.01	-0.01	0.08	0.05	0.03	0.07	0.04	1

Figure 82. Correlation coefficients among HST-001 cases perturbing all variables, only first half of realizations.

	1-1	1-2	1-3	1-4	1-5	1-6	1-7	1-8	1-9	1-10
1-1	1	0.97	0.02	0.00	0.16	0.07	0.01	0.13	0.05	0.03
1-2	0.97	1	0.03	0.00	0.16	0.07	0.03	0.11	0.04	0.02
1-3	0.02	0.03	1	0.38	-0.02	0.01	0.02	0.01	0.00	0.01
1-4	0.00	0.00	0.38	1	-0.08	-0.10	-0.04	-0.05	0.63	-0.10
1-5	0.16	0.16	-0.02	-0.08	1	0.78	0.79	0.87	0.51	0.06
1-6	0.07	0.07	0.01	-0.10	0.78	1	0.78	0.81	0.44	0.11
1-7	0.01	0.03	0.02	-0.04	0.79	0.78	1	0.84	0.54	0.03
1-8	0.13	0.11	0.01	-0.05	0.87	0.81	0.84	1	0.56	0.05
1-9	0.05	0.04	0.00	0.63	0.51	0.44	0.54	0.56	1	-0.13
1-10	0.03	0.02	0.01	-0.10	0.06	0.11	0.03	0.05	-0.13	1

Figure 83. Correlation coefficients among HST-001 cases perturbing all variables, only last half of realizations.

enrichment uncertainties do not impact the correlation coefficients. The correlation coefficients presented in Figure 79 can therefore be considered as the best estimate correlation coefficients using the Monte Carlo sampling method and information available in the ICSBEP evaluation [15]. The correlation coefficients developed here bear little resemblance to the reference results included in the ICSBEP. Further discussion of possible explanations for these discrepancies is provided in the next section.

Summary of Correlation Coefficients for HST-001

Correlation coefficients have been generated for the 10 cases in the HST-001 evaluation considering the uncertain parameters in related groups. Each group was added together, and two of the four groups were considered separately as both shared and unique uncertainties. The detailed results are reported in the previous sections, and only summarized here. The simplified geometry and shorter run-times for these models allows a more systematic approach to determine the parameters that have the strongest impact on correlation coefficients compared to the LEU pin array systems examined in Chapters V and VI. These results can also be compared with a set of reference results taken from [15] which were originally generated using a deterministic approach as documented in [17].

Comparison With Reference Results

At this point, comparisons can be made between the final correlation coefficients generated in this study (Figure 79) with the reference results included in the ICSBEP [15]. The results from the ICSBEP are taken from [17], which developed a deterministic approach for calculating correlation coefficients. Several uncertainties were arbitrarily partitioned into random and systematic uncertainty components, and the systematic portions were declared to be shared among all cases in an evaluation. These breakdowns were developed based on discussions with experimental personnel at one facility, and apparently assumed to apply to other laboratories as well. The arbitrary decision that half of the solution property uncertainty is shared appears to be responsible for the uniformity of the reference correlation coefficients. This uniformity is at odds with the greater dimensional uncertainties associated with the stainless steel tank in the evaluation. In general, if the uncertainties presented in the evaluation are viewed as credible the reference correlation coefficients are less plausible in their gross characteristics than the ones developed here.

There is another potential source of the differences in the reported correlation coefficients. This alternative explanation is that the correlations being reported are in fact different quantities. The reference correlation coefficients could be an attempt to generate correlation coefficients for the uncertainties in each case, while those developed here are intended as correlation coefficients for the experimental measurements themselves. This is a very fine point, but can have a significant impact on the approach to correlation coefficient generation and use.

Criticality safety validation is primarily concerned with the k_{eff} estimate for each critical experiment, especially in comparison to the expected model. This is the reason that

validation considers calculated-to-expected ratios (C/E) or differences (C-E). In this context, it is the correlation of the measurements themselves that are important. The uncertainties in the measurements are frequently used as a weighting factor such that experiments with lower uncertainties are weighted more heavily in the validation. Thus the important correlation is among measurements, because correlated measurements do not provide as much information as independent measurements. The correlations, if properly treated, will also act to increase the uncertainty in the bias once the amount of unique information provided by each measurement is accounted for more correctly. In the final validation analysis, the correlations will have a modest impact on the bias and a potentially significant impact on the uncertainty of the bias.

Data adjustment analyses must account for correlations in the uncertainties of the measurements. These correlations act as a constraint on the adjustments that can be made to the measurements included in the adjustment process. Thus the correlation of uncertainties is more important for these analyses than the correlations of the measurements themselves. The final result of the adjustment process is affected by the correlations, so both the bias and its uncertainty can be expected to change significantly once the correlations are properly incorporated into the calculations.

The final analysis thus appears to point to the fact that there are two different possible sets of correlation coefficients to be determined for critical experiments. The correlation coefficients do not necessarily agree well, and either set can be generated from a Monte Carlo or a deterministic approach. It is thus essential that correlation coefficients be correctly identified as for measurements or uncertainties and implemented correctly. This will continue to be a very challenging proposition given the dearth of understanding of the correlation impacts within the criticality safety community.

Relative Importance of Parameters on Correlation Coefficients

The uncertain parameters in the HST-001 experiments are grouped into four sets: geometry, tank composition, uranium enrichment, and solution parameters. The geometry variables include the inner diameter of the tank, the tank wall and bottom thicknesses, and the solution height. The tank composition is solely aluminum for the 6061 aluminum tanks used in Cases 3-10, and the constituents of the stainless steel for the tank used in Cases 1 and 2. The enrichment uncertainty relates to the weight fractions of each of the four isotopes of uranium, and the solution parameters include the uranium concentration, the excess acid molarity, and the solution density.

The geometry parameters are perturbed first because the shared and independent geometric parameters appear simple to determine. There are 4 tanks, and it is clear which experiments used each tank. The geometric parameters thus apply identically to all cases in the same tank. The solution height is assumed to be independent for each case. The uncertainty in the inner diameter of each tank is a dominating source of uncertainty. As shown in Figure 72, this results in strong correlations for experiments carried out in the same tank and no correlation among the cases performed in different tanks.

The tank composition variables are added next. It is clear that the stainless steel tank should be treated differently from the aluminum tanks, but it is not necessarily clear that the aluminum used in the remaining three tanks has the same composition. Correlations are determined assuming both shared and unique tank compositions, as shown in Figure 75 and Figure 76. System reactivity is not very sensitive to the tank compositions, so the correlations are largely the same as those resulting from only geometry perturbations. The different assumptions related to shared or unique compositions have no effect on the correlation coefficients.

The third set of parameters introduced is the uranium enrichment. As with the tank compositions, it is not clear if a single feedstock was the source for all solutions or if multiple independent batches were the initial source. The enrichment was therefore sampled both shared across all 8 solutions (10 cases) and unique to each solution. It is also possible that there were a small number of initial feed solutions, and that the enrichment was truly the same for some groups of cases. This possibility was not examined here. The results, shown in Figure 77 and Figure 78, indicate that the enrichment uncertainties were too small to impact the k_{eff} uncertainties to any significant extent and the correlation coefficients were thus also unchanged. As with the tank compositions, the assumptions related to shared or unique enrichment have no effect on the correlation coefficients.

The final uncertain parameters to be included are the solution parameters. There is no known mechanism that can plausibly cause correlations among the different solutions in the state in which they were used in the experiments. Multiple solutions may have been diluted from the same feedstock, but each would have to be diluted by a unique amount to reach its uranium concentration and associated excess acid molarity and density. The solution parameters were thus considered as unique for each solution. Two solutions are used in two cases each; Cases 1 and 8 use the same solution and Cases 4 and 9 also use an identical solution. Incorporation of the solution parameter uncertainties increase the uncertainty in system reactivity for the experiments in aluminum tanks. The geometric uncertainties in the stainless steel tank used in Cases 1 and 2 are the dominant sources of uncertainty in these cases. The resulting correlations shown in Figure 79 show lower correlations among the five cases in the 33.01 cm aluminum tank, and an increased correlation between Cases 4 and 9.

The final results of this study indicate that the important sources of uncertainty in system k_{eff} are also the parameters which dominate the correlation of the experiments. This evaluation included 10 experiments performed in 4 tanks with 8 solutions. In two cases, the geometry uncertainties were dominant. In the other 8 cases, the tank geometry and solution parameter uncertainties combined to influence the correlation coefficients. It is critically important to understand the sources of uncertainty, the sensitivity of the experiments to these sources, and whether the parameters are shared among experiments or unique to each case. There is clearly not a single set of assumptions that can be made about how the uncertain parameters should be combined to determine the correlations between cases.

CHAPTER VIII: RECOMMENDED APPROACH FOR CALCULATION OF CRITICAL EXPERIMENT CORRELATIONS VIA THE MONTE CARLO SAMPLING TECHNIQUE

The primary purpose of determining critical experiment correlations is to enable a more accurate accounting for them in criticality safety validation and data adjustment studies. A robust, reliable approach must be developed whereby these correlations can be determined and applied in these applications. The correlation coefficient determinations presented over the previous three chapters have served to develop and test such a recommended procedure. This chapter provides that procedure in four steps; each step is described generically here and then in more detail in the subsequent subsections. The procedure described here assumes, for the most part, that sufficient detailed information is available describing the uncertain components. This includes the range of the uncertainties as well as which components are shared and which are unique. At this point, much of this detailed information is lost to history and reasonable assumptions must be made. Some discussion is provided to guide the practitioner in the common circumstances in which this information is not available.

The first step is the analysis and study of the evaluation of the critical experiment. In general, this presupposes that the critical experiment or experiments have been included in the ICSBEP handbook [15], but other experiments are available outside the handbook which have been evaluated with similar rigor. These experiments may be held out of the ICSBEP Handbook for commercial or classification reasons. The French HTC experiments [61-64] are an example of a rigorously evaluated set of experiments that have been kept out of the open literature for commercial reasons. Step one includes identification of correlated or potentially correlated experiments, sources of shared and unique uncertainty, and evaluation of these uncertain components.

The second step is the implementation of Monte Carlo sampling for the uncertain parameters. In this work, the implementation has been performed within the Sampler sequence of the SCALE code package [16], but other implementations such as SUnCISTT [37] are equally valid. Portions of the implementation step are largely inseparable from the evaluation of the uncertain components in the first step.

The third step is the execution of the Monte Carlo sampling and subsequent execution of the individual realization calculations. This step is primarily concerned with the mechanics of how many realizations are needed and how low the stochastic uncertainty must be in each realization. Only Monte Carlo transport codes have been used within the Monte Carlo sampling method here or in the literature [34, 36-43], but deterministic transport codes could be used within the Monte Carlo sampling technique with equal validity. The assessment of the third step is inextricably linked to the fourth and final step.

The fourth and final step of procedure for determination of critical experiment correlations is the evaluation of the final correlation coefficients themselves. This mostly consists of

checking that the coefficients are reasonable and can be explained given the input assumptions of shared and unique uncertainties and their magnitudes. It is also important to assess the convergence of the correlation coefficient estimates, as is common to all implementations of Monte Carlo sampling.

Step One: Review the Evaluation

Recommendations for selecting critical experiments to use in validation are included in validation guidance documents available in the literature [23-25]. One of the recommendations is that good documentation is available from which models can be developed; over the last 20 years the best source for such documentation has been the ICSBEP Handbook [15]. Each evaluation in the Handbook contains a description of the experiment, the facility in which it was performed, and often other related experiments in Section 1. Section 2 of the evaluation contains an uncertainty assessment, which is the most important part of the evaluation for this work. The benchmark model itself is described in Section 3. A thorough review of the evaluation is the starting place for any attempt to develop critical experiment correlations. The key aspects of this review are discussed in this section, including the identification of potentially correlated evaluations and experiments, the identification of uncertainty components within each experiment, and most importantly the identification of shared and unique uncertainty components.

Correlated Evaluations and Experiments

The identification of potentially correlated evaluations and experiments is an obvious first step in the development of critical experiment correlations. Sources of correlation are primarily fissile or non-fissile material, experimental facilities, or experimental hardware. In the work documented here, shared fissile material is included in the LCT-007 and LCT-039 evaluations, the LCT-042 evaluation, and in two pairs of experiments in the HST-001 evaluation. Shared non-fissile material includes the steel reflecting wall in the LCT-042 evaluation. Shared facilities are included in the LCT-007 and LCT-039 experiments, both performed on Apparatus B at Valduc, within the LCT-042 experiments performed at PNL, and within the HST-001 experiments performed at Rocky Flats. An example of shared experimental hardware would be support plates for lattice experiments, such as in Case 1 of LCT-007 with the LCT-039 experiments, and within the 7 cases of LCT-042.

The shared materials are usually easy to identify. Exact enrichment matches are indicative of shared fissile material, as are exact matches for solution parameters such as uranium concentration and solution density. These parameters can be identified by searching in the DICE tool. DICE also identifies some evaluations as or containing potentially correlated experiments. In many cases, the evaluation will also identify related experiments at the beginning of Section 1 of the evaluation. The other evaluations can be consulted if there is doubt about shared materials. Non-fissile materials that may be relevant would include reflector walls, such as the steel walls in LCT-042, poison panels such as those used in LCT-042, and tanks such as those used in HST-001. Tanks may also be shared experimental hardware if the same tank is used in multiple cases; HST-001 includes both shared tank

materials used in multiple tanks, 6061 aluminum, and tanks used in multiple experiments. In some cases, the same material may be used in multiple experiments or evaluations but it may be ambiguous if the components were used. The HST-001 tanks are again a good example as it is not clear if the three different aluminum tanks were fabricated from the same lot of material or if they are from different lots and thus have slightly different compositions. More discussion of how to handle these ambiguous situations is provided below.

Each series of experiments is performed in a single facility and is therefore at least potentially subject to correlation among experiments within the series. Some shared uncertainty, for instance related to the same detectors being used in all cases, has very small impact on the systems being measured. Other sources of shared uncertainty, such as contaminants in water, may introduce significant uncertainty. The facility in which each benchmark experiment was performed is well known, so this particular source of shared uncertainty can be identified definitively.

Shared experimental hardware can usually be identified readily for lattice experiments by checking the pitch of the arrays. The pitch by itself is not necessarily irrefutable evidence of shared support plates. Obviously the array shape must be the same as well; for instance, LCT-020 and LCT-050 both contain experiments with a 1.3 cm pitch. The LCT-050 experiments use a square pitch array, but LCT-020 is a triangular pitch array. Clearly the grid plate was not shared between these two experiments. On the other hand, as discussed in Chapter V, the 2.52 cm pitch in LCT-007 Case 4 was achieved by placing fuel rods in one out of every four locations in a 1.26 cm pitch grid plate. This shared component would not have been identified by a simple search on pitch size. Fortunately, other shared components like tanks in solution experiments are identified explicitly as shared components because of the importance of the tank to the experiment.

The identification of evaluations and experiments with shared uncertainty components is the most important step in the determination of critical experiment correlations. Correlation coefficients do not need to be developed for uncorrelated experiments. Also, the identification of correlations among experiments supports the following steps in examining uncertainty components and whether the components are shared or unique. It is somewhat desirable to avoid the use of correlated experiments in validation, but all the experiments can still be used if the correlations among the cases can be quantified and incorporated into the validation methodology or data adjustment technique.

Uncertainty Components

The identification of uncertain components in the evaluation is simple as all material compositions, temperatures, and dimensions are uncertain. The challenges in this area are understanding the uncertainty associated with each component, and whether the components are shared or unique to each case. The uncertainties, as assessed in the evaluation, are discussed in Section 2 of an ICSBEP evaluation [15]. The identification and assessment of uncertainties also involves the implementation of the sampling, which is

discussed in the next section. It is impossible to completely separate these two activities, so there will be some overlap and repetition of the discussion.

Material composition uncertainties can take several forms. One common form is to provide ranges for each constituent element. This is a common approach for alloys; the specification for the alloy will provide acceptable weight percent ranges for each element. In many cases there is no specified nominal value, so it may be impossible to assign a nominal value without an assay of the material used in the experiment. Lacking other information, the mid-range value is typically assumed though this is often not possible for all constituents to sum to 100%. Material specifications can also be provided as nominal values with tolerances. Alternatively, the result of assays of materials can be provided. The assay typically provides a nominal value for constituents in a material, and the uncertainties in the assay are then the uncertainties in the composition. As an example, the fissile material isotopic composition is often measured and reported. With any of these methods of specification, the practitioner still must select a distribution from which to sample. Discussion of this decision is left to the implementation section.

Dimensional uncertainties are most often encountered as nominal values with tolerances. This is particularly true for fabricated parts and their associated dimensions. The application of these uncertainties is generally straightforward. In some cases, a reported uncertainty is or may be composed of more than one underlying uncertain dimension or position. The fuel rod pitch uncertainty is the best example of this situation. The uncertainty in the position of adjacent rods leads to an uncertainty in the pitch of rods. In these situations, it is important to understand uncertainty propagation to maintain the appropriate uncertainty. The equal, independent uncertainty in the location of adjacent rods is combined by the square root of the sum of the squares. The resulting pitch uncertainty is the square root of two times the individual rod placement uncertainty, so it is larger than the individual rod position uncertainty but smaller than twice the uncertainty. This can also lead to complications in implementation, to be discussed below.

Determination of Uncertainty Component Uniqueness

The most important determination to be made regarding uncertainties in this process is the determination of unique and shared uncertainty components. All the uncertainty components must be accounted for so that the total uncertainty is correct. The standard deviation of each case is accounted for in the denominator of the correlation coefficient, as shown in Equation 1. The shared uncertainty components create the covariance, which must also be accurate to calculate the correct correlation coefficient. Other complicating details, such as the uniform pitch or individual rod placement scenarios for fuel array experiments, are discussed in the following section on implementation.

The ideal scenario is a clear delineation in the evaluation of the components that are shared between experiments and those that are not. Typically this is the case for fissile material and some non-fissile materials. Fuel rods drawn from the same population are treated as a shared source of uncertainty, though there may still be some unique effects if different rods or

different numbers of rods are used each experiment. The LCT-007 and many of the LCT-039 cases use different numbers of rods, though some use the same number of rods. It is impossible to establish if the same exact rods were used in each case. The LCT-042 experiments all use the same number of rods, but it is still unknown if some rods were switched between experiments. The steel reflecting walls from LCT-042 are another example of an apparently shared uncertainty component. No information is provided in the evaluation, however, regarding possible disassembly or relocation of the walls between experiments. The ideal scenario of a clear and complete description of shared and unique uncertainty components is extremely rare in any evaluation. Other techniques must therefore be used to assess the impact of different assumptions and/or the most likely shared uncertainties.

One approach is to assess the impact of the assumption of uniqueness on the correlation coefficient. This is demonstrated with the tank composition uncertainties and enrichment uncertainties in the HST-001 results presented above. In both cases, the correlation coefficients were largely invariant to the uniqueness of the uncertainties. This is a best case scenario as the result is the same in both scenarios. For other experiments, the correlation coefficients may be impacted and a choice is needed regarding the most likely scenario.

The best approaches for determining the most likely scenario for uncertainty component uniqueness are consideration of hypothesized mechanisms for sharing and examination of the dates of the various relevant experiments. The dates of the experiments may be documented precisely in the evaluation, or may be available in supporting references. The chances of independence increase as time passes between experiments for most parameters. This does not apply for fixtures and other equipment, but is relevant for components that would be moved, disassembled, and reassembled. The steel reflecting walls in LCT-042 are a prime example of this kind of component that is more likely to change as the time between experiments increases. Another key aspect of the process of determining the most likely case for uniqueness is the consideration of possible mechanisms for sharing materials and fixtures between experiments. The use of the same fissile material, whether rods, solutions, disks, or some other form, is usually readily explained as being used in the same facility in multiple experiments. The solution parameters for HST-001 are an example of a component for which it is difficult to explain shared uncertainty. Shared measurement devices will result in correlations of the uncertainties of the measurements of the parameters, but they cannot, however, create a correlation in unique solutions prepared using different quantities of water, acid, and salt.

In many circumstances, the best plausible assignment of unique and shared uncertainties is all that is possible. Engineering judgment and, when possible, consultation with the experimentalists are needed to make these determinations. It is not feasible, however, for each engineer performing computer code validations to contact the original experimentalists. This information must be captured more completely in evaluations in the future.

Step Two: Implementation

As mentioned several times throughout this document, the implementation of the Monte Carlo sampling method used here is in the SCALE code system [16]. Other Monte Carlo implementations can be used with equal validity. Most of the details discussed here are applicable to any other code because they are generic issues associated with determination of critical experiment correlations. Some details associated specifically with Sampler will be discussed, and identified as uniquely applying to Sampler.

Variables and Cases

The nomenclature of variables and cases is somewhat specific to Sampler, but the concepts are generically applicable. Within Sampler, variable blocks are used for random sampling of variables or for the evaluation of expressions. The cases each variable applies to are also identified in each variable block. The variable blocks represent the overwhelming majority of the Sampler input, and are discussed in this section and the next two sections as well.

The variable parameters are identified as discussed above in step one through careful study of the evaluation. In many cases, these parameters can be sampled directly. An example of this type of variable might be the temperature at which the experiment was performed. Other variable parameters, such as clad thickness, can be sampled but must also be processed for application in the model. The outer radius of the cladding is typically specified in the model and must be calculated from the cladding thickness and its inner radius. The inner radius is probably also sampled, so the clad outer diameter is calculated "on-the-fly" as part of the creation of the realizations.

Sampling on number densities is typically much more complicated, and merits a separate discussion. Composition descriptions provided in the ICSBEP Handbook [15] are specified in terms of isotopes or elements and associated number densities. The uncertainties are never expressed directly in terms of the number densities. In some cases, multiple isotopes or elements are changed at the same time and the largest constituent is calculated for each sample as the remainder of the material. This is common for ^{238}U with the specifications for low enrichment uranium material. In Sampler, it is frequently necessary to set atomic masses in expression variable blocks for subsequent use in other expressions to calculate perturbed number densities. In other cases, perturbed number densities can be calculated based on sampling a ratio or multiplier relative to the nominal number density. Several examples of both these techniques have been described in the discussions of sampling materials in the experiments used in this work.

Significant discussion has been provided in the previous section on determination of uncertainty component uniqueness. The implementation of this in Sampler is provided via the *cases* = … *end* portion of the variable block. Each case specified will share the sampled values for the variable, contributing to the covariance between each pair of specified cases. There is no direct implementation available in Sampler at this time to provide partial correlations or correlated sampling. This would be a desirable feature for modeling correlation between experiments in which the direction of the variation might be shared but

its magnitude would differ. An example of this type of uncertainty could be the volume of diluent added to different samples from a shared stock solution.

Sampling Ranges

The range over which each variable is sampled is an important parameter in the Monte Carlo sampling method. Generally, ranges can be provided directly in the evaluation, indirectly via a material specification, or not at all. The first two cases are easy to implement, but the third is obviously more challenging.

Explicit ranges are often provided directly or indirectly for material specifications. Sometimes these are provided directly in the evaluation, and in other cases they may be provided in the specification for the material in use. Materials with multiple constituents can still pose difficulties because the fractional components must sum to 1. This is a challenge often encountered with alloy specifications. Tolerance values are also provided in some circumstances for thicknesses or other dimensions. These scenarios are typically straightforward to implement.

In other cases, an uncertainty or standard deviation may be provided without absolute bounds on the value of the sampled parameter. In Sampler, it is possible to sample from an unbounded or from a truncated normal distribution. More discussion on considerations of distributions are provided in the next section. Unbounded distributions can be used for sampling some material constituents and some dimensions. In many other cases, restrictions on acceptable or realistic variability are provided by other model components. For example, the inner radius of the cladding must be greater than or equal to the outer radius of the fuel material. At this time, Sampler does not allow variables to be used as limits for sampling other variables. The user must therefore decide on some of these limits as part of implementation and include them in the input prior to execution. Generally, these decisions are based on the sensitivity of the parameters or the ranges allowed to each parameter. One parameter should not generally be limited to a small number of standard deviations if another parameter would be varying by more than two or three. The implementation of variable ranges for parameters with no specified tolerances or limits on variability are more difficult and require some engineering judgment.

Variable Distributions

An essential input for any Monte Carlo sampling process is the distribution from which to sample random variates. Essentially no work has been here investigating the effect of sampling from different distributions. There is some evidence in the literature [41] that the distribution from which the parameters are sampled does not have a significant impact on the critical experiment correlations.

In the work presented here, most variables were sampled uniformly across the specified uncertainty band. This approach was adopted because the resulting uncertainty is larger for the uniform distribution than for the normal distribution [74], assuming both are sampled

over the same range. Larger uncertainties lead to larger correlation coefficients for shared parameters, but lower correlation coefficients when applied to unique uncertainty components. Differences in the ranges of the various parameter uncertainties should have a larger effect on the correlation coefficients than the distribution from which the parameter values are sampled. This is an area that represents a potential for further investigation in the future; the HST-001 evaluation would make a good test bed for these investigations since it has a much lower number of variables than the LEU fuel rod array experiments.

Step Three: Execution

The third step in the process of determining critical experiment correlations is the execution of the sampling to generate the necessary realizations, and the execution of these realizations. This step represents essentially all the computer time needed in the analysis, and the least practitioner time. The two primary concerns in the is phase are how many realizations must be created and run, and how low must the uncertainty be in the individual realization calculations. Each of these issues has been studied here, and the results will be summarized here.

Number of Realizations

The number of realizations is controlled by the convergence behavior of the correlation coefficient. High correlation coefficients resulting from strongly correlated experiments converge much more quickly than low correlation coefficients. This is illustrated in, for example, Figure 81, for three of the HST-001 correlation coefficients. Correlation coefficients converged in fewer than 150 realizations for most LEU fuel rod array cases performed with the uniform pitch assumption. The coefficients took more realizations to converge in the random rod location scenario. As shown in Figure 70, nearly 500 realizations are needed to converge at least one correlation coefficient in the LCT-042 evaluation in this latter scenario. It is therefore difficult to make any categorical recommendation, but 200 – 300 realizations are likely sufficient for high correlation coefficients. More realizations are likely required for lower correlation coefficients, potentially on the order of 300 – 500. As will be discussed later in Step Four, additional realizations can be created and executed to assure convergence as needed for correlation coefficients with questionable convergence.

The visual examination recommended here for assessing convergence is equivalent to most source convergence assessment techniques in Monte Carlo transport calculations. Visual inspection of the convergence of k_{eff} has been recommended for decades. More recent advances, such as Shannon entropy testing [16], are also primarily trying to identify the point at which the entropy has stopped changing. The visual convergence technique, while less than ideal, has a lengthy pedigree in assessing the convergence of Monte Carlo processes in nuclear engineering problems.

Individual Realization Uncertainty

The individual realizations used to calculate correlation coefficients in this work use Monte Carlo transport and therefore have stochastic uncertainty. Other transport techniques could

be used, but deterministic transport codes are rarely used in criticality safety calculations and thus rarely in need of validation for such use. Much of the discussion here on stochastic uncertainty would also be applicable to the convergence criteria in deterministic transport methods if they were used.

The effects of the Monte Carlo, or stochastic, uncertainty on the correlation coefficients have been studied in both LEU fuel rod array evaluations considered in this work. A comparison of Figure 4 and Figure 61 or an examination of Figure 66 illustrates the dramatic effects that the stochastic uncertainty can have on the estimated correlation coefficient. As discussed earlier, the stochastic uncertainty is a source of unique uncertainty which, if not appropriately limited, can reduce the estimated correlation coefficient. The uncertainty in each realization must be significantly less than the variability in k_{eff} resulting from the sampling of the uncertain input parameters. In most cases, stochastic uncertainty on the order of 0.00020 Δk should be acceptable. Some scenarios, such as random fuel rod location scenarios for well characterized fuel array experiments, may require lower uncertainties. Unfortunately, the best method for determining that the individual realization stochastic uncertainties are low enough is to reduce the uncertainty and recalculate the correlation coefficient. This can be a computationally expensive process, but in some cases it may be necessary to provide confidence that the correlation coefficient estimates are not contaminated by excessive stochastic uncertainty.

Step Four: Generate and Review Correlation Coefficients

The final step of the process is to generate and review the correlation coefficients. There are a wide variety of ways to generate the correlation coefficients and then the results must be assessed. Each of these will be covered briefly in this section.

Generation of Correlation Coefficients

The generation of correlation coefficients is straightforward. The k_{eff} values must be collected from all the realizations for each of the cases. Each pair of cases must have the same number of realizations for the calculation of covariance and therefore a correlation coefficient. In all the work performed here, all cases had the same number of realizations. It is possible to generate more realizations for some cases then for others, and to ignore the extra realizations for the case with a greater number. This must be done carefully if there are some shared components of uncertainty to ensure that the covariance is calculated correctly.

Once the k_{eff} values are collected, the correlation coefficient is calculated as shown in Equation 1. In this work, the final correlation coefficients were calculated by Sampler in post-processing mode for some cases, in spreadsheets for others, and using the *correlations_single* FORTRAN program described in Chapter III. The custom written *correlations_single* program includes statistical significance testing and generation of 95% confidence intervals, but these capabilities may be incorporated into Sampler in future releases. These steps can also be performed in a spreadsheet whether the rest of the

correlations are generated in a spreadsheet or not. The statistical testing may be helpful in the assessment of the correlation coefficients, described next.

Assessment of Correlation Coefficients

The first assessment to perform is that the correlation coefficient estimates have converged. This is described in the previous section on executing the calculations, and overlaps both steps. Visual examination of the convergence behavior is the primary technique that has been used and investigated in this work. The correlation coefficient for the first half and the second half of the realizations is calculated in addition to the overall coefficient in *correlations_single* as another crude assessment of convergence, but other techniques and statistical tests would also be applicable. This is an area in which future work could enhance the process of correlation coefficient generation.

A second assessment that should be made is that the stochastic uncertainty of the realizations has been controlled sufficiently. Generally this requires a comparison of the uncertainty in each of the realizations with the variation of the k_{eff} values, typically as measured by their standard deviation. From the results presented in Table 16, it appears that the stochastic uncertainty should be approximately an order of magnitude lower than the standard deviation of the k_{eff} values. As mentioned in the previous section, this is best assessed by reducing the stochastic uncertainty and comparing the resulting correlation coefficients.

The final and perhaps most important check is an assessment of the reasonableness of the correlation coefficients. The results presented for all the evaluations considered in this work ultimately are logical and consistent results of the assumptions made in the implementation of the uncertainty assessment (Step One). Cases with more shared uncertainty should result in higher correlation coefficients. This is demonstrated with Case 1 of LCT-007 having much higher correlation coefficients with the LCT-039 cases than the other LCT-007 cases. In this case, the shared pitch provides the additional shared uncertainty and higher correlation coefficients. The LCT-042 correlations are relatively homogenous, as would be expected since there is no obvious reason for any pair of cases to be more strongly correlated than others. For HST-001, Cases 4 and 9 have a higher correlation coefficient because of the shared solution in tanks with relatively tight geometrical tolerances. Cases 1 and 8 share a solution but do not have a high correlation coefficient because the uncertainty in Case 1 is driven by dimensional uncertainties in the stainless steel tank. Unfortunately, these relative trends do not necessarily provide an indication of the absolute magnitude of the correlation coefficients. More work is needed to develop a predictive capability for the absolute magnitude of the correlation coefficients between critical experiments.

CHAPTER IX: CONCLUSIONS

A range of conclusions can be drawn from the results presented in Chapters V through VII. The most important of these conclusions are presented in the previous chapter describing the methodology for determining critical experiment correlations. Some conclusions have also been developed at the end of each chapter describing correlation coefficients. These will be consolidated here, followed by overarching conclusions and recommendations. Suggestions for future work are presented in Chapter X.

Conclusions Regarding LEU Fuel Rod Arrays

Correlation coefficients have been developed for up to 21 cases from the LCT-007 and LCT-039 evaluations as well for the seven cases in the LCT-042 evaluation. The conclusions presented here focus on the determination of correlation coefficients, and not on the values that were generated. There is insufficient justification for the use of any specific set of assumptions or associated correlation coefficients. All results presented in this work should be regarded as little more than potentially indicative of the real correlation coefficients for the cases studied.

- The computational resources necessary to perform the calculations to determine correlation coefficients among critical experiments can be large. The generation of a matrix of correlation coefficients may require on the order of 4 hours per realization, which will likely be 1200 CPU-hours or more per case. The creation of each realization also requires a few seconds for simple models to 7 minutes or more for random fuel rod location models. This only adds approximately 35 CPU-hours, but this cannot currently be parallelized in Sampler and must be complete before the realizations can be run. The realizations can be executed completely in parallel as they are all separate executions.
- The treatment of the pin pitch uncertainty in LEU fuel rod array experiments is likely the most important factor in the calculated correlation coefficients. The uniform pitch assumption will likely lead to high correlation coefficients, while a random fuel rod placement approach will result in lower correlation coefficients.
- The evidence indicates that the correlations may be largely insensitive to the sampled pitch range in a uniform pitch scenario. A reasonably realistic range, that is at least ± 1 standard deviation, must be used. The resulting correlations are generally higher than 0.9 and represent a significant potential impact on validation and/or data adjustment.
- The number of realizations needed for convergence of calculated correlation coefficients depends largely on the magnitude of the coefficient. High correlation coefficients appear to converge with 150 or fewer realizations, while lower correlation coefficients may require 300 or more realizations.
- The individual realization k_{eff} values need to be determined with the minimum feasible stochastic (Monte Carlo) uncertainty. Significant changes in the correlation coefficients are observed when the uncertainty is reduced from approximately

0.00100 Δk to 0.00020 Δk. Further reductions in uncertainty have smaller effects for the cases examined here, but may be needed for other cases with lower overall uncertainties.

- MG KENO calculations appear to provide sufficient accuracy for the determination of correlation coefficients, even for the random rod placement models. This is a significant finding as it saves a significant amount of runtime for every realization. CE calculations could extend the runtime requirements for executing the realizations by a factor of 2 to 4 [75].

Conclusions Regarding HEU Solution Experiments

Correlation coefficients have been developed for the 10 cases in the HST-001 evaluation. Again, the conclusions here focus on the conclusions that are relevant for the methodology and not on the specific correlation coefficient results. In this case, a more thorough examination of the reasonable assumptions is possible because of the more limited number of variable parameters. The correlation coefficients provided in Figure 79 are plausible correlation coefficients for the evaluation.

- The computational investment will likely be large for solution systems. In this case, the runtime per realizations is on the order of 2. The resulting runtime per case is therefore likely between 600 and 1000 CPU-hours per case. Sampler creates the realizations in seconds because the models are very simple.
- The impact of sharing a solution in two cases can differ dramatically based on the relative effects of other parameters. In this case, the uncertainty due to dimensional uncertainties in the stainless steel tank overwhelmed the correlation due to a shared solution. In the aluminum tanks with smaller dimensional uncertainties, the pair of cases using the same solution had a significantly higher correlation coefficient.

Conclusions for All Systems

Fortunately, several conclusions relevant to both types of systems studied in this work can also be drawn. These conclusions are likely applicable to generating critical experiment correlations for all types of systems.

- A general methodology for generation of critical experiment correlations has been outlined in Chapter VIII. This methodology contains some specific guidance for implementation with the Sampler sequence in the SCALE code system, but is largely applicable to any Monte Carlo sampling system.
- It is possible to determine which variables control the uncertainty in each case, and therefore which variable parameters are most important to the correlation coefficients. Many variables, while important to the overall system behavior, are tightly controlled and thus have little impact on the correlation coefficients. Enrichment is an excellent example of this type of high importance, low uncertainty parameter.

- The correlation coefficients relevant to the critical experiment itself are different from the correlation coefficients of the uncertainties in the experiments. The former are necessary for validation, especially in traditional trending techniques. The correlation coefficients of the uncertainties are necessary for data adjustment techniques. This work has been concerned with the correlations of the experiments, not the correlations of the uncertainties.
- In-depth knowledge of the critical experiment materials, configurations, procedures, and setup are required for correct assessment of shared and unique uncertainty contributions. This level of information is not available in the ICSBEP Handbook [15], which is currently the primary reference for critical experiment descriptions. Without this in-depth knowledge, it is nearly impossible to make defensible determinations regarding the uncertainty sharing among different cases. The lack of this quality information will be a significant impediment to the generation of reliable, defensible critical experiment correlations.

CHAPTER X: FUTURE WORK

Several aspects of the generation of critical experiment correlations could be studied in the future. Several of these areas are outlined here.

- Critical experiment correlations need to be generated for metal systems. Many critical experiments involving metal systems have the potential for high correlation because of shared components. Many experiments have been performed using the same metal system but with different reflectors. In other cases, shells of fissile or reflecting materials have been used in multiple experiments. Thus there is a potential for a large number of correlated experiments within this category of systems.
- More work can be done to investigate the convergence of the correlation coefficient estimates. Many of the same statistical tests used for source convergence in Monte Carlo transport problems can be applied to this Monte Carlo convergence problem. Some of these tests might include comparison of the first and last half of the realizations, the slope of the correlation coefficient estimate as a function of realization number, or other techniques.
- Additional work could be performed on the use of MG KENO for individual realizations. Some critical systems cannot be calculated accurately with MG methods because proper self-shielding models are impossible. These systems would require significantly more computational effort if the correlation coefficients must be established with CE Monte Carlo.
- Some comparisons of correlation coefficients from different code systems have been performed as part of the WPNCS/UACSA benchmark [33]. By the nature of the benchmark, these comparisons only include LEU fuel array systems. Comparisons should be expanded to include more types of critical experiments and more code packages.
- A complete validation technique including critical experiment correlations needs to be developed. This work has begun [50, 51], but further work is needed to complete development and demonstration of the methodology.
- Collaboration with experimentalists is necessary to provide more basis for plausible critical experiment correlations. It may be possible to design a set of experiments to investigate correlations, or repeated measurements of the same configuration may be useful in providing bounding estimates of the correlation coefficients. Some of this information may already exist for repeatability measurements.
- Information about critical experiment correlation determinations should be shared with experimentalists both so that they can look for design features to control correlation and to improve documentation of the uniqueness of uncertainties.
- Additional work can be applied to evaluations such as LEU-COMP-THERM-097. Experiments such as this one, performed at Sandia National Laboratories, are known to have exceptionally well characterized uncertainty components. These experiments also have a unique correspondence of fuel rod to grid plate location, eliminating uncertainty as to which rods are used in each case.

- The brief study on the repeatability of critical experiment correlation determination presented in Chapter V should be expanded to other pairs of cases and other evaluations. The result of that study, if confirmed, would undermine the validity of correlation coefficient estimates from the Monte Carlo sampling method.
- The integration of a deterministic transport code into the Monte Carlo sampling technique may provide useful insights by eliminating stochastic uncertainties. Generally, convergence criteria in these codes can be smaller than Monte Carlo uncertainties.
- A thorough investigation of the impact of the distribution from which random samples are drawn should be performed.

LIST OF REFERENCES

1. R.A. Knief, Nuclear Criticality Safety: Theory and Practice, American Nuclear Society, La Grange Park, IL (1985).
2. ANSI/ANS-8.1-2014, "Nuclear Criticality Safety in Operations with Fissionable Materials Outside Reactors," published by the American Nuclear Society, La Grange Park, IL (2014).
3. Regulations for the Safe Transport of Radioactive Material, Specific Safety Requirements (SSR) Number 6, International Atomic Energy Agency, Vienna, Austria (2012).
4. Title 10 of the Code of Federal Regulations (10 CFR) Part 71, "Packaging and Transportation of Radioactive Material," United States Nuclear Regulatory Commission, Washington, DC (2015).
5. "Standard Review Plan for Transportation Packages for Radioactive Material," NUREG-1609, United States Nuclear Regulatory Commission, Washington, DC (1999).
6. Title 49 of the Code of Federal Regulations (49 CFR) Part 107, "Hazardous Materials Program Procedures," United States Department of Transportation, Washington, DC (2016).
7. Title 49 of the Code of Federal Regulations (49 CFR) Parts 171-180, Volumes 2 and 3, Chapter I, United States Department of Transportation, Washington, DC (2016).
8. Title 49 of the Code of Federal Regulations (49 CFR) Parts 390-397, Volumes 5, Chapter III, United States Department of Transportation, Washington, DC (2016).
9. Title 10 of the Code of Federal Regulations (10 CFR) Part 50.68, "Criticality Accident Requirements," United States Nuclear Regulatory Commission, Washington, DC (2006).
10. Title 10 of the Code of Federal Regulations (10 CFR) Part 72, "Licensing Requirements for the Independent Storage of Spent Nuclear Fuel, High-level Radioactive Waste, and Reactor-related Greater Than Class C Waste," United States Nuclear Regulatory Commission, Washington, DC (2015).
11. "Standard Review Plan for Spent Fuel Dry Storage Facilities," NUREG-1567, United States Nuclear Regulatory Commission, Washington, DC (2000).
12. "Standard Review Plan for Transportation Packages for Spent Nuclear Fuel," NUREG-1617, United States Nuclear Regulatory Commission, Washington, DC (2000).
13. C.V. Parks, M.D. DeHart, and J.C Wagner, "Review and Prioritization of Technical Issues Related to Burnup Credit for LWR Fuel," NUREG/CR-6665 (ORNL/TM-1999/303), prepared for the US Nuclear Regulatory Commission by Oak Ridge National Laboratory, Oak Ridge, TN (2000).
14. ANSI/ANS-8.24-2007:R2012, "Validation of Neutron Transport Methods for Nuclear Criticality Safety Calculations," published by the American Nuclear Society, La Grange Park, IL (2007).
15. "International Handbook of Evaluated Criticality Safety Benchmark Experiments," NEA/NSC/DOC(95)03, Organization for Economic Cooperation and Development/Nuclear Energy Agency, Paris, France (2016).
16. B.T. Rearden and M.A. Jessee, Editors, "SCALE Code System," ORNL/TM-2005/39, Version 6.2, Oak Ridge National Laboratory, Oak Ridge, TN (2016).

17. T. T. Ivanova, M. N. Nikolaev, K. F. Raskach, E. V. Rozhikhin, and A. M. Tsiboula, "Influence of the Correlations of Experimental Uncertainties on Criticality Prediction," *Nucl. Sci. Eng.* **145(1)**, pp. 97–104 (2003).
18. F. Brown, "Fundamentals of Monte Carlo Particle Transport," LA-UR-05-4983, Los Alamos National Laboratory, Los Alamos, NM (2005).
19. "Index of /~rpevey/public/NE582", retrieved July 10, 2016.
20. Iman, Ronald L., A Data-Based Approach to Statistics, Duxbury Press, Belmont, CA (2004).
21. Neter, John, Michael H. Kutner, Christopher J. Nachtsheim, and William Wasserman, Applied Linear Statistical Models, WBC McGraw-Hill, St. Louis, MO (1996).
22. O. Buss, A. Hoefer, J. C. Neuber, and M. Schmid, "Hierarchical Monte-Carlo approach to bias estimation for criticality safety calculations," PHYSOR 2010, Pittsburgh, PA (2010).
23. J.C. Dean and R.W. Tayloe, Jr., "Guide for Validation of Nuclear Criticality Safety Calculational Methodology," NUREG/CR-6698, prepared for the US Nuclear Regulatory Commission by Science Applications International Corporation, Oak Ridge, TN (2001).
24. J.J. Lichtenwalter, S.M. Bowman, M.D. DeHart, and C.M. Hopper, "Criticality Benchmark Guide for Light-Water-Reactor Fuel in Transportation and Storage Packages," NUREG/CR-6361 (ORNL/TM-13211), prepared for the US Nuclear Regulatory Commission by Oak Ridge National Laboratory, Oak Ridge, TN (1997).
25. H.R. Dyer and C.V. Parks, "Recommendations for Preparing the Criticality Safety Evaluation of Transportation Packages," NUREG/CR-5661 (ORNL/TM-11936), prepared for the US Nuclear Regulatory Commission by Oak Ridge National Laboratory, Oak Ridge, TN (1997).
26. E.D. Mennerdahl, "Correlations of Error Sources and Associated Reactivity Influences," *Trans. Am. Nucl. Soc.* **110**, 292-294 (2014).
27. T. Ivanova, E. Ivanov, and G.E. Bianchi, "Establishment of Correlations for Some Critical and Reactor Physics Experiments," *Nucl. Sci. Eng.* **178**, pp. 311-325 (2014).
28. E.D. Mennerdahl, "A Declaration of Independence – What is it Worth," *Trans. Am. Nucl. Soc.* **90,** 109-110 (2004).
29. T. Ivanova, V. Rouyer, Y. Rozhikhin, and A. Tsiboulia, "Towards Validation of Criticality Calculations for Systems with MOX Powders," *Annals of Nucl. Energy* **36**, pp. 305-309 (2009).
30. M. Salvatores and G. Palmiotti, "Methods and Issues for the Combined Use of Integral Experiments and Covariance Data," NEA/NSC/WPEC/DOC(2013)445, Organisation for Economic Co-operation and Development/Nuclear Energy Agency (2013).
31. G. Palmiotti et al., "Combined Use of Integral Experiments and Covariance Data," *Nuclear Data Sheets* **118**, pp. 596-636 (2014).
32. M. Salvatores et al., "Methods and Issues for the Combined Use of Integral Experiments and Covariance Data: Results of a NEA International Collaborative Study," *Nucl. Data Sheets* **118**, pp. 38-71 (2014).
33. Axel Hoefer et al., "Proposal for Benchmark Phase IV Role of Integral Experiment Covariance Data for Criticality Safety," Benchmark Proposal, OECD/NEA (2015).

34. M. Bock and M. Stuke, "Determination of Correlations Among Benchmark Experiments by Monte Carlo Sampling Techniques," ANS Nuclear Criticality Safety Division Topical Meetings (NCSD2013), Wilmington, NC (2013).
35. I. Hill, "Generation of Low Fidelity Experimental Covariance Matrices for ICSBEP Cases," *Trans. Am. Nucl. Soc.* **115**, pp. 692-695 (2016).
36. B. T. Rearden, K. J. Duggan and F. Havluj, "Quantification of Uncertainties and Correlations in Criticality Experiments with SCALE," ANS Nuclear Criticality Safety Division Topical Meetings (NCSD2013), Wilmington, NC (2013).
37. M. Stuke, M. Behler, M. Bock, and F. Rowold, "SUnCISTT: A Generic Code Interface for Uncertainty and Sensitivity Analysis," Probabilistic Safety Assessment and Management 12 (PSAM12), Honolulu, HI (2014).
38. J.C. Neuber and A. Hoeffer, "Frequentist and Bayesian Approach in Criticality Safety Uncertainty Evaluations," ANS Nuclear Criticality Safety Division Topical Meeting (NCSD2009), Richland, WA (2009).
39. W.J. Marshall and B.T. Rearden, "Determination of Experimental Correlations Using the Sampler Sequence Within SCALE 6.2," *Trans. Am. Nucl. Soc.* **111**, pp. 867-870 (2014).
40. W.J. Marshall and B.T. Rearden, "Determination of Critical Experiment Correlations Using the Sampler Sequence Within SCALE 6.2," *Proceedings of International Conference on Nuclear Criticality Safety*, Charlotte, NC (2015).
41. E. Peters, F. Sommer, and M. Stuke, "Sensitivities and Correlations of Critical Experiments Due to Uncertainties of System Parameters and Nuclear Data," *Proceedings of International Conference on Nuclear Criticality Safety*, Charlotte, NC (2015).
42. W.J. Marshall and B.T. Rearden, "ORNL Results for Critical Experiment Correlations Benchmark," presentation to WPNCS UACSA meeting, Paris, France (2015).
43. W.J. Marshall, "Recent developments for the UACSA benchmark on LCT-007 and LCT-039," Proceedings of the Workshop on Integral Experiment Covariance Data, GRS-414, Garching, Germany (2016).
44. B.T. Rearden, M.L. Williams, M.A. Jessee, D.E. Mueller, and D.A. Wiarda, "Sensitivity and Uncertainty Analysis Capabilities and Data in SCALE," Nucl. Technol. **174**, pp. 236-288 (2011).
45. B.C. Kiedrowski, et al., "Whisper: Sensitivity/Uncertainty-Based Computational Methods and Software for Determining Baseline Upper Subcritical Limits," LA-UR-14-26558, Los Alamos National Laboratory, Los Alamos, NM (2014).
46. "ROOT a Data analysis Framework," https://root.cern.ch, retrieved May 7, 2016.
47. Thomas Müller, "RooFiLab: Root Fit for Laboratory courses," http://physik.leech.it/pub/Rechnernutzung/Vorlesungsfolien/WS_11-12/V14Anleitung_RooFiLab.pdf, retrieved May 7, 2016 (in German).
48. M. Bock and M. Behler, "Impact of Correlated Benchmark Experiments on the Computational Bias in Criticality Safety Assessment," ANS Nuclear Criticality Safety Division Topical Meetings (NCSD2013), Wilmington, NC (2013).
49. E. Peters, F. Sommer, and M. Stuke, "Impact of Correlated Data in Validation Procedures," *Proceedings of International Conference on Nuclear Criticality Safety*, Charlotte, NC (2015).

50. V. Sobes, B. T. Rearden, D. E. Mueller, W. J. Marshall, J. M. Scaglione, and M. E. Dunn, "Upper Subcritical Limit Calculations with Correlated Integral Experiments," *Trans. Am. Nucl. Soc.* **112**, 467-470 (2015).
51. V. Sobes, B. T. Rearden, D. E. Mueller, W. J. Marshall, J. M. Scaglione, and M. E. Dunn, "Upper Subcritical Limit Calculations Based on Correlated Experimental Data," International Conference on Nuclear Criticality Safety (ICNC 2015), Charlotte, NC (2015).
52. B.C. Kiedrowski, et al., "Validation of MCNP6.1 for Criticality Safety of Pu-Metal, -Solution, and -Oxide Systems," LA-UR-14-23352, Los Alamos National Laboratory, Los Alamos, NM (2014).
53. Gumbel, E.J., Statistics of Extremes, Dover Publications Inc., Mineola, MN (2004).
54. J.A. Roberts, B.T. Rearden, P.H. Wilson, "Determination and Application of Partial Biases in Criticality Safety Validation," *Nucl. Sci. Eng.*, **173**, pp. 43-57 (2013).
55. J.M Scaglione, D.E. Mueller, J.C Wagner, and W.J. Marshall, "An Approach for Validating Actinide and Fission Product Burnup Credit Criticality Safety Analyses – Criticality (k_{eff}) Predictions," NUREG/CR-7109 (ORNL/TM-2011/514), prepared for the US Nuclear Regulatory Commission by Oak Ridge National Laboratory, Oak Ridge, TN (2012).
56. S. Goluoglu, L.M. Petrie, M.E. Dunn, D.F. Hollenbach, and B.T. Rearden, "Monte Carlo Criticality Methods and Analysis Capabilities in SCALE," Nucl. Technol. **174**, pp. 214-235 (2011).
57. M.B. Chadwick, et al., "ENDF/B-VII.1 Nuclear Data for Science and Technology: Cross Sections, Covariances, Fission Product Yields and Decay Data," Nucl. Data Sheets, **112**, pp. 2887-2996 (2011).
58. "Gamma Function - - from Wolfram MathWorld," http://mathworld.wolfram.com/GammaFunction.html, retrieved February 18, 2017.
59. N. Leclair, "Propagation of rod position uncertainty in lattices: an issue to correctly assess uncertainties of associated benchmarks and their correlations," Proceedings of the Workshop on Integral Experiment Covariance Data, GRS-414, Garching, Germany (2016).
60. W. J. Marshall and B. T. Rearden, "The SCALE Verified, Archived Library of Inputs and Data – VALID," *Proceedings of ANS NCSD 2013 - Criticality Safety in the Modern Era: Raising the Bar,* Wilmington, NC, on CD-ROM, American Nuclear Society, LaGrange Park, IL (2013).
61. F. Fernex, "Programme HTC – Phase 1: Réseaux de crayons dans l'eau pure (Water-moderated and reflected simple arrays) - Réévaluation des expériences," DSU/SEC/T/2005-33/D.R., Institut de Radioprotection et de Sûreté Nucléaire (2008). (Proprietary)
62. F. Fernex, "Programme HTC – Phase 2: Réseaux simples en eau empoisonnee (bore et gadolinium) (Reflected simple arrays moderated by poisoned water with gadolinium or boron) - Réévaluation des expériences," DSU/SEC/T/2005-38/D.R., Institut de Radioprotection et de Sûreté Nucléaire (2008). (Proprietary)
63. F. Fernex, "Programme HTC – Phase 3: Configurations 'stockage en piscine' (Pool storage) - Réévaluation des expériences," DSU/SEC/T/2005-36/D.R., Institut de Radioprotection et de Sûreté Nucléaire (2008). (Proprietary)

64. F. Fernex, "Programme HTC – Phase 4: Configurations 'châteaux de transport' (Shipping cask) - Réévaluation des expériences," DSU/SEC/T/2005-37/D.R., Institut de Radioprotection et de Sûreté Nucléaire (2008). (Proprietary)
65. E. Letang, "Measurements of Grid Plates used for HTC experiments," DEU/SEC/A/2009-294 (2009).
66. W.J. Marshall and B.T. Rearden, "Criticality Safety Validation of Scale 6.1," ORNL/TM-2011/450 (revised), Oak Ridge National Laboratory, Oak Ridge, TN (2013).
67. W.J. Marshall, B.T. Rearden, and E.L. Jones, "Validation of SCALE 6.2 Criticality Calculations Using KENO V.a and KENO-VI," *Proceedings of International Conference on Nuclear Criticality Safety*, Charlotte, NC (2015).
68. E.M. Baum, H.D. Knox, and T.R. Miller, "Nuclides and Isotopes: Chart of the Nuclides, 16th Edition," Knolls Atomic Power Laboratory, Niskayuna, NY (2002).
69. S.R. Bierman, E.S. Murphy, E.D. Clayton, and R.T. Keay, "Criticality Experiments with Low Enriched UO_2 Fuel Rods in Water Containing Dissolved Gadolinium," PNL-4976, Battelle Pacific Northwest Laboratories, Richland, Washington (1984).
70. B.M. Durst, S.R. Bierman, and E.D. Clayton, "Critical Experiments with 4.31 wt% ^{235}U Enriched UO_2 Rods in Highly Borated Water Lattices," NUREG/CR-2709 (PNL-4267), Battelle Pacific Northwest Laboratories, Richland, Washington (1982).
71. S.R. Bierman, "Criticality Experiments to Provide Benchmark Data on Neutron Flux Traps," PNL-6205, UC-714, Battelle Pacific Northwest Laboratories, Richland, Washington (1988).
72. S.R. Bierman, "Criticality Experiments with Neutron Flux Traps Containing Voids," PNL-7167, TTC-0969, UC-722, Battelle Pacific Northwest Laboratories, Richland, Washington (1990).
73. "beta distribution – Wolfram|Alpha Results," http://m.wolframalpha.com/input/?i=beta+distribution, retrieved April 9, 2017.
74. "2.5.4.1 Standard deviations from assumed distributions," http://www.itl.nist.gov/div898/handbook/mpc/section5/mpc541.htm, retrieved June 1, 2017.
75. W.J. Marshall, D. Wiarda, C. Celik, B.T. Rearden, and D.R. Wentz, "Validation of Criticality Safety Calculations with SCALE 6.2," *Proceedings of ANS NCSD 2013 - Criticality Safety in the Modern Era: Raising the Bar,* Wilmington, NC, on CD-ROM, American Nuclear Society, LaGrange Park, IL (2013).

APPENDICES

Appendix A: Source code for correlations_single.f90

```
program correlations_single
!
! correlations - This program reads dat files that contain keff results
!                from Sampler-generated KENO inputs and calculates the
!                average and standard deviation for each Case, as well
!                as the correlation coefficients for each pair of
Cases.
!                This is being modified in December of 2016 to
!                support work on the LCT-042 correlations as part of my
!                dissertation.  The primary modification here is that
!                each case has a unique number of variables so two sets
!                of calculations aren't needed.  This version may see
!                more use later.
!
! variables
!
!  numcases is the number of separate cases
!  numreal  is the number of realizations for each case
!  datfile  is the name of the file containing the names of the dat
files
!  datnames is the array variable with the dat file names in it
!  casenamefile is a file with Case designators, like 007-001
!  casename(i) is the Case designator for each case, 10 characters for
now
!  avg(i) is the average keff value for case(i)
!  delta(i,j) is (x-xbar) for each realization(j) for each case(i)
!  sumdelsq is a running sum of the delta(i,j) values squared
!  var(i) is the variance for each case(i)
!  stdev(i) is the standard deviation for each case(i)
!  top is the product of delta(i,j) values for a realization for two
cases
!  sumtop is the running sum of the numerator for one covariance
calculation
!  covar(ifirst,isecond) is the covariance between two cases
!  corr(ifirst,isecond) is the correlation coefficient between the two
cases
!  fhavg, fhvar, fhstdev, fhdelta are for the first half of
realizations
!  shavg, shvar, shstdev, shdelta are for the second half of
realizations
!
      character*120 datfile, casenamefile
      character*10, dimension(:), allocatable :: casename
      character*120, dimension(:), allocatable :: datnames
      real*8, dimension(:, :), allocatable :: kcase, delta
      real*8, dimension(:, :), allocatable :: fhdelta, shdelta
      real*8, dimension(:, :), allocatable :: covar, corr, squiggle
      real*8, dimension(:, :), allocatable :: cihigh, cilow
      real*8, dimension(:, :), allocatable :: rhocihigh, rhocilow
      real*8, dimension(:), allocatable :: avg, var, stdev
      real*8, dimension(:), allocatable :: fhavg, fhvar, fhstdev
      real*8, dimension(:), allocatable :: shavg, shvar, shstdev
      real*8 casesum, sumdelsq, sumtop, denom
```

```
!
! print some general info about the program to the user
!
      print *, '=====================================================&
       ========================= '
      print *, 'This program will read a file dat files from KENO &
       calculations and determine '
      print *, 'the correlation coefficient between pairs of cases.'
      print *
      print *, '=====================================================&
       ========================= '
!
! get info from user about the paths to the templates and profile file
!
      print *, 'What is the path to the file listing dat files?'
      read '(a)', datfile
      print *, 'What is the path to the file listing Case names?'
      read '(a)', casenamefile
      print *, 'How many cases are in the matrix?'
      read *, numcases
      print *, 'How many realizations are there for each case?'
      print *, 'At this point, all cases have equal realizations.'
      read *, numreal
      print *, 'Note that all statistical testing performed by this'
      print *, 'program assumes 300 samples at 95% confidence!'
!
! allocate size of arrays
!
      allocate (kcase(numcases,numreal))
      allocate (delta(numcases,numreal))
      allocate (fhdelta(numcases,numreal))
      allocate (shdelta(numcases,numreal))
      allocate (covar(numcases, numcases))
      allocate (corr(numcases, numcases))
      allocate (squiggle(numcases, numcases))
      allocate (cilow(numcases, numcases))
      allocate (cihigh(numcases, numcases))
      allocate (rhocilow(numcases, numcases))
      allocate (rhocihigh(numcases, numcases))
      allocate (datnames(numreal))
      allocate (avg(numcases))
      allocate (var(numcases))
      allocate (stdev(numcases))
      allocate (fhavg(numcases))
      allocate (fhvar(numcases))
      allocate (fhstdev(numcases))
      allocate (shavg(numcases))
      allocate (shvar(numcases))
      allocate (shstdev(numcases))
      allocate (casename(numcases))
!
! Set zscore and tscore variables
!  tscore is taken from Excel 2016 t.inv(0.975,297) after comparisons
with
```

```
!    references - Neter, Kutner, Nachtsheim, & Wasserman, and the NIST
table
!  zscore is taken from Excel 2016 norm.s.inv(0.975,sqrt(297)) which is
in good
!    agreement with the known value of 1.96.
!
! NOTE THAT THESE VALUES ARE ONLY GOOD for:
!    95% confidence
!    300 samples (t score is selected with 297 degrees of freedom)
!
      tscore=1.967957
      zscore=1.959964
! civar is variance for confidence interval = 1/n-3
! cistdev is standard deviation for confidence interval
! zsig is product of zscore multiplier and cistdev
      civar=1.0/(numreal-3.0)
      cistdev=sqrt(civar)
      zsig = zscore * cistdev
!      print *, 'zsig= ',zsig
!      print *, 'zscore= ',zscore
!      print *, 'civar= ',civar

!
! test all data are read correctly
!
!      print *, datfile
!      print *, casenamefile
!      print *, numcases
!      print *, numreal
!
! open file with casenames and read it to casename array
!
      open(unit=10,file=casenamefile)
      do i = 1,numcases
         read (10,'(a10)') casename(i)
      enddo
      close (10)
! test reading
!      do itest = 1,numcases
!         print '(a)', casename(itest)
!      enddo
!
! open file with datfile names and read names to datnames array
!
      open(unit=11,file=datfile)
      do ifiles = 1,numcases
         read (11,'(a120)') datnames(ifiles)
      enddo
      close(11)
! test reading
!      do itest = 1,numreal
!         print '(a)', datnames(itest)
!      enddo
!
```

```
      nfirsthalf = numreal / 2.0
      nsecondhalf = nfirsthalf + 1.0
!
! define kcasecount to keep track of dat file name
!
!      kcasecount = 1
!
! read keff for first case.  There is only one set for this case
!
!      open(unit=10,file=datnames(kcasecount))
!      kcasecount = kcasecount + 1
!      do i=1,numreal
!         read (10,'(f7.5)') kcase(1,i,1)
!      enddo
!      close(10)
! test reading
!      open(unit=12,file="tmp.txt")
!      do itest=1,numreal
!         write(12,'(f7.5)') kcase(1,itest,1)
!      enddo
!      close(12)
!
! read keff for cases with two sets.  This is now all of them.
!
      do icase=1,numcases
         open(unit=10,file=datnames(icase))
         do i=1,numreal
            read (10, '(f8.6)') kcase(icase,i)
         enddo  ! on number of realizations
         close(10)
      enddo  ! on cases
!
!      print *, 'Past reading k effectives'
!
! test read
!      open(unit=12,file="tmp.txt")
!      do itest=1,numreal
!         write(12,'(f8.6,1x,f8.6)') (kcase(j,itest), j=1,numcases)
!      enddo
!      close(12)
!      stop
!
! now calculate averages for each case
!
      do icases=1,numcases
         casesum=0
         do i=1,numreal
            casesum = casesum + kcase(icases,i)
         enddo
         avg(icases) = casesum / numreal
!         print *, 'casesum(',icases,') = ',casesum
!         print *, 'Avg(',icases,') = ',avg(icases)
      enddo
!
```

```
! first half average
      do icases=1,numcases
         casesum=0
         do i=1,nfirsthalf
            casesum = casesum + kcase(icases,i)
         enddo
         fhavg(icases) = casesum / nfirsthalf
      enddo
!
! second half average
      do icases=1,numcases
         casesum=0
         do i=nsecondhalf,numreal
            casesum = casesum + kcase(icases,i)
         enddo
         ndivisor = numreal - nfirsthalf
         shavg(icases) = casesum / ndivisor
      enddo
!
! calculate delta values for each realization in each case for both
sets
! also calculate standard deviation for each case and set
!
      do icases=1,numcases
         sumdelsq=0
         do jreal=1,numreal
            delta(icases,jreal)=kcase(icases,jreal)-avg(icases)
            sumdelsq = sumdelsq + delta(icases,jreal)**2
         enddo ! on realizations for middle cases
         var(icases) = sumdelsq / (numreal - 1.0)
!         print *, 'Variance of case: ', icases, 'is: ',var(icases)
         stdev(icases) = sqrt(var(icases))
!         endif
      enddo ! on cases
! test delta calculation
!      open(unit=12,file="tmp.txt")
!      do itest=1,numreal
!         write(12,'(f8.6,1x,f8.6)') (delta(i,itest), i=1,numcases)
!      enddo
!      close(12)
!
! write stdev and stdev for each case to file
      open(unit=12,file="mean_stdev.dat")
      do iprt=1,numcases
         write(12,100) casename(iprt), avg(iprt),stdev(iprt)
      enddo
      close(12)
!      stop
!
! Calculate standard deviations for the first half and second half
!  of the realizations
!
! first half
      do icases=1,numcases
```

```
         sumdelsq=0
         do jreal=1,nfirsthalf
            fhdelta(icases,jreal)=kcase(icases,jreal)-fhavg(icases)
            sumdelsq = sumdelsq + fhdelta(icases,jreal)**2
         enddo ! on realizations for middle cases
         fhvar(icases) = sumdelsq / (nfirsthalf - 1.0)
!         print *, 'Variance of case: ', icases, 'is: ',var(icases)
         fhstdev(icases) = sqrt(fhvar(icases))
!         endif
      enddo ! on cases
!
! second half
      do icases=1,numcases
         sumdelsq=0
         do jreal=nsecondhalf,numreal
            jnum = jreal - nfirsthalf
            shdelta(icases,jnum)=kcase(icases,jreal)-shavg(icases)
            sumdelsq = sumdelsq + shdelta(icases,jnum)**2
         enddo ! on realizations for middle cases
         shvar(icases) = sumdelsq / (ndivisor - 1.0)
!         print *, 'Variance of case: ', icases, 'is: ',var(icases)
         shstdev(icases) = sqrt(shvar(icases))
!         endif
      enddo ! on cases

! test math
!      do i=1,numcases
!         print *, 'Case #', i
!         print *, 'Avg and stdev are:', avg(i), stdev(i)
!         print *,'First half avg and stdev are:',fhavg(i),fhstdev(i)
!         print *,'Scnd half avg and stdev are:',shavg(i),shstdev(i)
!      enddo
!      stop
!=======================================================================
=
!
! Here we calculate correlation coefficients.
!
!-----------------------------------------------------------------------
-
!
! Loop through cases from 1 to n-1
!   calculate covariance for each pair (first,second)
!   calculate correlation coefficient for each pair
!
! Open unit 15 (signficant.dat) to contain results of t testing
      open(unit=15,file="significant.dat")
!
!      open(unit=12,file="tmp.txt")  ! for checking sumtop
      do ifirst=1,numcases-1
         do isecond=ifirst+1,numcases
            sumtop=0
            do j=1,numreal
               sumtop = sumtop+delta(ifirst,j)*delta(isecond,j)
```

```
! test sumtop calculation
!               write(12,'(e12.5,1x,e12.5)') sumtop
            enddo ! realizations
            covar(ifirst,isecond) = sumtop/(numreal-1)
            denom=stdev(ifirst)*stdev(isecond)
! calculate correlation coefficient
            corr(ifirst,isecond) = covar(ifirst,isecond) / denom
! fisher transformed to z' aka squigle
            squiggle(ifirst,isecond) =
0.5*log((1+corr(ifirst,isecond))&
             / (1-corr(ifirst,isecond)))
!            if (ifirst .eq. 1) then
!               print *, ifirst, isecond, corr(ifirst,isecond),
squiggle(ifirst,isecond)
!            endif
! confidence interval top and ottom values
            cihigh(ifirst,isecond) = squiggle(ifirst,isecond) + zsig
            cilow(ifirst,isecond) = squiggle(ifirst,isecond) - zsig
!            if (ifirst .eq. 1) then
!               print *, ifirst, isecond, cihigh(ifirst,isecond),
cilow(ifirst,isecond)
!            endif
! untransform cihigh and cilow to correlation coefficient space
(rhocihigh and
! rhocilow)
            rhocihigh(ifirst,isecond)=(exp(2*cihigh(ifirst,isecond))-
1)&
                                     /(exp(2*cihigh(ifirst,isecond))+1)
            rhocilow(ifirst,isecond)=(exp(2*cilow(ifirst,isecond))-1) &
                                    /(exp(2*cilow(ifirst,isecond))+1)
!            if (ifirst .eq. 1) then
!               print *, ifirst, isecond, rhocihigh(ifirst,isecond), &
!                                         rhocilow(ifirst,isecond)
!            endif
! calculate tstar test sttistic for testing non-zero null hypothesis
            radicand=numcases - 2
            tstar=corr(ifirst,isecond)*sqrt(radicand)/sqrt(1- &
                      corr(ifirst,isecond)**2)
!     do test on tstar and write result to significant.dat
            if (tstar .gt. tscore) then
               write(15,1100) casename(ifirst), casename(isecond), &
                              "nonzero"
            else
               write(15,1100) casename(ifirst), casename(isecond),&
                             "insignificant"
            endif
!            print *, ifirst, isecond, corr
!            print *, 'covariance:
',ifirst,isecond,covar(ifirst,isecond)
!            print '(a,2i3,f6.3)', 'correlation:
',ifirst,isecond,corr(ifirst,isecond)
         enddo ! second cases
       enddo ! first cases
       close(15)
```

```
!       close(12)  ! for checking sumtop
!
! write data to file
!
      open(unit=12,file="correlations.dat")
      open(unit=13,file="confidence_intervals.dat")
      write(12,1000) (casename(i),i=1,numcases)
      write(13,2000) (casename(i),i=1,numcases)
      if (numcases .eq. 10) then
         write(12,1001) casename(1), (corr(1,j),j=2,numcases)
         write(12,1002) casename(2), (corr(2,j),j=3,numcases)
         write(12,1003) casename(3), (corr(3,j),j=4,numcases)
         write(12,1004) casename(4), (corr(4,j),j=5,numcases)
         write(12,1005) casename(5), (corr(5,j),j=6,numcases)
         write(12,1006) casename(6), (corr(6,j),j=7,numcases)
         write(12,1007) casename(7), (corr(7,j),j=8,numcases)
         write(12,1008) casename(8), (corr(8,j),j=9,numcases)
         write(12,1009) casename(9), (corr(9,j),j=10,numcases)
!
! write CIs
!
         write(13,2001) casename(1),('(',rhocilow(1,j),',', &
                                    rhocihigh(1,j),')',j=2,numcases)
         write(13,2002) casename(2),('(',rhocilow(2,j),',', &
                                    rhocihigh(2,j),')',j=3,numcases)
         write(13,2003) casename(3),('(',rhocilow(3,j),',', &
                                    rhocihigh(3,j),')',j=4,numcases)
         write(13,2004) casename(4),('(',rhocilow(4,j),',', &
                                    rhocihigh(4,j),')',j=5,numcases)
         write(13,2005) casename(5),('(',rhocilow(5,j),',', &
                                    rhocihigh(5,j),')',j=6,numcases)
         write(13,2006) casename(6),('(',rhocilow(6,j),',', &
                                    rhocihigh(6,j),')',j=7,numcases)
         write(13,2007) casename(7),('(',rhocilow(7,j),',', &
                                    rhocihigh(7,j),')',j=8,numcases)
         write(13,2008) casename(8),('(',rhocilow(8,j),',', &
                                    rhocihigh(8,j),')',j=9,numcases)
         write(13,2009) casename(9),('(',rhocilow(9,j),',', &
                                    rhocihigh(9,j),')',j=10,numcases)
      else
         write(12,1001) casename(1), (corr(1,j),j=2,numcases)
         write(12,1002) casename(2), (corr(2,j),j=3,numcases)
         write(12,1003) casename(3), (corr(3,j),j=4,numcases)
         write(12,1004) casename(4), (corr(4,j),j=5,numcases)
         write(12,1005) casename(5), (corr(5,j),j=6,numcases)
         write(12,1006) casename(6), (corr(6,j),j=7,numcases)
!
! write CIs
!
         write(13,2001) casename(1),('(',rhocilow(1,j),',', &
                                    rhocihigh(1,j),')',j=2,numcases)
         write(13,2002) casename(2),('(',rhocilow(2,j),',', &
                                    rhocihigh(2,j),')',j=3,numcases)
         write(13,2003) casename(3),('(',rhocilow(3,j),',', &
```

```
                                    rhocihigh(3,j),')',j=4,numcases)
         write(13,2004) casename(4),('(',rhocilow(4,j),',', &
                                    rhocihigh(4,j),')',j=5,numcases)
         write(13,2005) casename(5),('(',rhocilow(5,j),',', &
                                    rhocihigh(5,j),')',j=6,numcases)
         write(13,2006) casename(6),('(',rhocilow(6,j),',', &
                                    rhocihigh(6,j),')',j=7,numcases)
      endif
      close(12)
      close(13)
      covar=0
      corr=0
!
! Calculate correlations for first half of realizations
!
      do ifirst=1,numcases-1
         do isecond=ifirst+1,numcases
            sumtop=0
            do j=1,nfirsthalf
               sumtop = sumtop+fhdelta(ifirst,j)*fhdelta(isecond,j)
            enddo ! realizations
            covar(ifirst,isecond) = sumtop/(nfirsthalf-1)
            denom=fhstdev(ifirst)*fhstdev(isecond)
            corr(ifirst,isecond) = covar(ifirst,isecond)/denom
!            print *, 'covariance:
',ifirst,isecond,covar(ifirst,isecond)
!            print '(a,2i3,f6.3)', 'correlation:
!            ',ifirst,isecond,corr(ifirst,isecond)
         enddo ! second cases
       enddo ! first cases
!
! write data to file
!
      open(unit=12,file="correlations_firsthalf.dat")
      write(12,1000) (casename(i),i=1,numcases)
      if (numcases .eq. 10) then
         write(12,1001) casename(1), (corr(1,j),j=2,numcases)
         write(12,1002) casename(2), (corr(2,j),j=3,numcases)
         write(12,1003) casename(3), (corr(3,j),j=4,numcases)
         write(12,1004) casename(4), (corr(4,j),j=5,numcases)
         write(12,1005) casename(5), (corr(5,j),j=6,numcases)
         write(12,1006) casename(6), (corr(6,j),j=7,numcases)
         write(12,1007) casename(7), (corr(7,j),j=8,numcases)
         write(12,1008) casename(8), (corr(8,j),j=9,numcases)
         write(12,1009) casename(9), (corr(9,j),j=10,numcases)
      else
         write(12,1001) casename(1), (corr(1,j),j=2,numcases)
         write(12,1002) casename(2), (corr(2,j),j=3,numcases)
         write(12,1003) casename(3), (corr(3,j),j=4,numcases)
         write(12,1004) casename(4), (corr(4,j),j=5,numcases)
         write(12,1005) casename(5), (corr(5,j),j=6,numcases)
         write(12,1006) casename(6), (corr(6,j),j=7,numcases)
      endif
      close(12)
```

```
      covar=0
      corr=0
!
! Calculate correlations for second half of realizations
!
!
      do ifirst=1,numcases-1
         do isecond=ifirst+1,numcases
            sumtop=0
            do j=nsecondhalf,numreal
               jnum = j - nfirsthalf
               sumtop=sumtop+shdelta(ifirst,jnum)*shdelta(isecond,jnum)
            enddo ! realizations
            covar(ifirst,isecond) = sumtop/(nfirsthalf-1)
            denom=shstdev(ifirst)*shstdev(isecond)
            corr(ifirst,isecond) = covar(ifirst,isecond)/denom
!            print *, 'covariance:
',ifirst,isecond,covar(ifirst,isecond)
!            print '(a,2i3,f6.3)', 'correlation:
!            ',ifirst,isecond,corr(ifirst,isecond)
         enddo ! second cases
       enddo ! first cases
!
! write data to file
!
      open(unit=12,file="correlations_secondhalf.dat")
      write(12,1000) (casename(i),i=1,numcases)
      if (numcases .eq. 10) then
         write(12,1001) casename(1), (corr(1,j),j=2,numcases)
         write(12,1002) casename(2), (corr(2,j),j=3,numcases)
         write(12,1003) casename(3), (corr(3,j),j=4,numcases)
         write(12,1004) casename(4), (corr(4,j),j=5,numcases)
         write(12,1005) casename(5), (corr(5,j),j=6,numcases)
         write(12,1006) casename(6), (corr(6,j),j=7,numcases)
         write(12,1007) casename(7), (corr(7,j),j=8,numcases)
         write(12,1008) casename(8), (corr(8,j),j=9,numcases)
         write(12,1009) casename(9), (corr(9,j),j=10,numcases)
      else
         write(12,1001) casename(1), (corr(1,j),j=2,numcases)
         write(12,1002) casename(2), (corr(2,j),j=3,numcases)
         write(12,1003) casename(3), (corr(3,j),j=4,numcases)
         write(12,1004) casename(4), (corr(4,j),j=5,numcases)
         write(12,1005) casename(5), (corr(5,j),j=6,numcases)
         write(12,1006) casename(6), (corr(6,j),j=7,numcases)
      endif
      close(12)
!
! deallocate arrays
!
      deallocate (kcase)
      deallocate (delta)
      deallocate (fhdelta)
      deallocate (shdelta)
      deallocate (covar)
```

```
      deallocate (corr)
      deallocate (datnames)
      deallocate (avg)
      deallocate (var)
      deallocate (stdev)
      deallocate (fhavg)
      deallocate (fhvar)
      deallocate (fhstdev)
      deallocate (shavg)
      deallocate (shvar)
      deallocate (shstdev)
      deallocate (casename)
!
!-----------------------------------------------------------------------
-
! format statements
100   format(a9,4f9.6)
1000  format(12x,21a11)
1001  format(a9,11x,9f11.3)
1002  format(a9,22x,8f11.3)
1003  format(a9,33x,7f11.3)
1004  format(a9,44x,6f11.3)
1005  format(a9,55x,5f11.3)
1006  format(a9,66x,4f11.3)
1007  format(a9,77x,3f11.3)
1008  format(a9,88x,2f11.3)
1009  format(a9,99x,1f11.3)
1100  format(1x,2a11,a13)
2000  format(10x,10(3x,a9,4x))
2001  format(a9,15x,9(a,f6.3,a,f6.3,a,1x))
2002  format(a9,31x,8(a,f6.3,a,f6.3,a,1x))
2003  format(a9,47x,7(a,f6.3,a,f6.3,a,1x))
2004  format(a9,63x,6(a,f6.3,a,f6.3,a,1x))
2005  format(a9,79x,5(a,f6.3,a,f6.3,a,1x))
2006  format(a9,95x,4(a,f6.3,a,f6.3,a,1x))
2007  format(a9,111x,3(a,f6.3,a,f6.3,a,1x))
2008  format(a9,127x,2(a,f6.3,a,f6.3,a,1x))
2009  format(a9,143x,1(a,f6.3,a,f6.3,a,1x))
!
      stop
      end
```

Appendix B: Input for LEU-COMP-THERM-007-001, Uniform Pitch Assumption

The model supporting calculations with the uniform pitch assumption is provided here for the sake of brevity. This input is just under 500 lines, while the model with each fuel rod in its own unit for random placement is in excess of 17,500 lines.

```
=csas25
LEU-COMP-THERM-007-001
v7.1-252n
read comp
'
'uo2 fuel - in water
'
u-234  1 0 7.1087e-6 295.15 end
u-235  1 0 1.1104e-3 295.15 end
u-236  1 0 3.1792e-5 295.15 end
u-238  1 0 2.2006e-2 295.15 end
o      1 0 4.1202e-2 295.15 end
al     1 0 4.1701e-6 295.15 end
fe     1 0 9.5140e-6 295.15 end
si     1 0 2.2479e-5 295.15 end
b-10   1 0 6.9037e-8 295.15 end
b-11   1 0 2.7788e-7 295.15 end
'
'uo2 fuel - in air
'
u-234  10 0 7.1087e-6 295.15 end
u-235  10 0 1.1104e-3 295.15 end
u-236  10 0 3.1792e-5 295.15 end
u-238  10 0 2.2006e-2 295.15 end
o      10 0 4.1202e-2 295.15 end
al     10 0 4.1701e-6 295.15 end
fe     10 0 9.5140e-6 295.15 end
si     10 0 2.2479e-5 295.15 end
b-10   10 0 6.9037e-8 295.15 end
b-11   10 0 2.7788e-7 295.15 end
'
'
'AGS - used for gapd=0.82 3 cladding and end plugs - in water
'
al  2 0 5.9569e-2 295.15 end
mg  2 0 3.1442e-4 295.15 end
si  2 0 2.4894e-4 295.15 end
zn  2 0 7.4597e-6 295.15 end
fe  2 0 6.4052e-5 295.15 end
'
'AGS - used for gapd=0.82 3 cladding and end plugs - in water
'
al  20 0 5.9569e-2 295.15 end
mg  20 0 3.1442e-4 295.15 end
si  20 0 2.4894e-4 295.15 end
zn  20 0 7.4597e-6 295.15 end
fe  20 0 6.4052e-5 295.15 end
```

```
'
'air
'
n   3 0 4.1985e-5 295.15 end
o   3 0 1.1263e-5 295.15 end
'
'air
'
n   30 0 4.1985e-5 295.15 end
o   30 0 1.1263e-5 295.15 end
'
'water - in lattice
'
o   4 0 3.3353e-2 295.15 end
h   4 0 6.6706e-2 295.15 end
'
'
'water - first 5 cm outside of the lattice
'
o   40 0 3.3353e-2 295.15 end
h   40 0 6.6706e-2 295.15 end
'
'
'water - outside of first 5 cm outside of lattice
'
o   400 0 3.3353e-2 295.15 end
h   400 0 6.6706e-2 295.15 end
'
'stainless steel - used for grid and pedistal
'
c    1000 0 5.9414e-5 295.15 end
cr   1000 0 1.6469e-2 295.15 end
fe   1000 0 6.0014e-2 295.15 end
mn   1000 0 8.6597e-4 295.15 end
ni   1000 0 8.1061e-3 295.15 end
si   1000 0 8.4696e-4 295.15 end
s    1000 0 2.2256e-5 295.15 end
p-31 1000 0 3.0719e-5 295.15 end
'
end comp
'
read cell
 latticecell squarepitch pitch=1.26 4 fueld=0.7892 1 gapd=0.82 3
cladd=0.940 2 end
end cell
'
read parm
  tme=10000 tba=60
  npg=10000 nsk=100 sig=0.00100 htm=no gen=10100
end parm
'
read geometry
'
unit 1
```

```
' bottom end plug - below lower grid plate
 cylinder 2 1  0.47                    1.50 0.53 origin 0.63 0.63
 cuboid   4 1  1.26 0.0  1.26  0.0  1.50 0.53
'
unit 11
'array of bottom end plugs -  below lower grid plate
 array 11 -13.86 -13.86 0.53
 cuboid 40   1  18.86 -18.86 18.86 -18.86 1.50 0.53
 cuboid 400  1  60.00 -60.00 60.00 -60.00 1.50 0.53
 cuboid 1000 1  60.30 -60.30 60.30 -60.30 1.50 0.53
'
 unit 2
' bottom end plug - in lower grid plate
 cylinder 2 1     0.47                   1.75 1.50 origin 0.63 0.63
 cylinder 4 1     0.5                    1.75 1.50 origin 0.63 0.63
 cuboid   1000 1  1.26 0.0  1.26  0.0    1.75 1.50
'
unit 22
'array of bottom end plugs - in the bottom grid plate
 array 22 -13.86 -13.86 1.50
 cuboid 1000 1  30.00 -30.00 30.00 -30.00 1.75 1.50
 cuboid 400  1  60.00 -60.00 60.00 -60.00 1.75 1.50
 cuboid 1000 1  60.30 -60.30 60.30 -60.30 1.75 1.50
'
 unit 3
' bottom end plug - above lower grid plate
 cylinder 2 1  0.47                   1.80 1.75 origin 0.63 0.63
 cuboid   4 1  1.26 0.0  1.26  0.0 1.80 1.75
'
unit 33
' array for bottom end plugs above the bottom grid plate
 array 33 -13.86 -13.86 1.75
 cuboid 40   1  18.86 -18.86 18.86 -18.86 1.80 1.75
 cuboid 400  1  60.00 -60.00 60.00 -60.00 1.80 1.75
 cuboid 1000 1  60.30 -60.30 60.30 -60.30 1.80 1.75
'
unit 4
' submerged portion of fuel stack
 cylinder 1 1 0.3946                  89.70  0.0  origin 0.63 0.63
 cylinder 30 1 0.41                    89.70  0.0  origin 0.63 0.63
 cylinder 2 1 0.47                    89.70  0.0  origin 0.63 0.63
 cuboid   4 1 1.26 0.0  1.26 0.0      89.70  0.0
'
unit 44
' array for submerged fuel
 array 44 -13.86 -13.86 0.0
 cuboid 40   1  18.86 -18.86 18.86 -18.86 89.70  0.0
 cuboid 400  1  60.00 -60.00 60.00 -60.00 89.70  0.0
 cuboid 1000 1  60.30 -60.30 60.30 -60.30 89.70  0.0
'
unit 5
'water above fuel level
 cylinder 30  1 0.41                   90.69  89.70  origin 0.63 0.63
 cylinder 2  1 0.47                   90.69  89.70  origin 0.63 0.63
```

```
 cuboid   4  1 1.26 0.0  1.26 0.0     90.69  89.70
'
unit 55
'water above fuel level
 array 55  -13.86 -13.86 89.70
 cuboid 40   1  18.86 -18.86 18.86 -18.86 90.69  89.70
 cuboid 400  1  60.00 -60.00 60.00 -60.00 90.69  89.70
 cuboid 1000 1  60.30 -60.30 60.30 -60.30 90.69  89.70
'
unit 6
'spring region of fuel rod - below grid plate
 cylinder 30  1 0.41                  96.45  90.69   origin 0.63 0.63
 cylinder 2  1 0.47                  96.45  90.69   origin 0.63 0.63
 cuboid   3  1 1.26 0.0  1.26 0.0     96.45  90.69
'
unit 66
'array of springs in fuel rods - below grid plate
 array 66  -13.86 -13.86 90.69
 cuboid   3  1  60.00 -60.00 60.00 -60.00 96.45  90.69
 cuboid 1000 1  60.30 -60.30 60.30 -60.30 96.45  90.69
'
unit 7
'spring region of fuel rod - in grid plate
 cylinder 30  1 0.41                 96.70   96.45  origin 0.63 0.63
 cylinder 2  1 0.47                 96.70   96.45  origin 0.63 0.63
 cylinder 3  1 0.50                 96.70   96.45  origin 0.63 0.63
 cuboid  1000  1 1.26 0.0  1.26 0.0 96.70   96.45
'
unit 77
'array of springs in fuel rods - in grid plate
 array 77   -13.86 -13.86 96.45
 cuboid 1000 1  30.00 -30.00 30.00 -30.00   96.70   96.45
 cuboid   3  1  60.00 -60.00 60.00 -60.00   96.70   96.45
 cuboid 1000 1  60.30 -60.30 60.30 -60.30   96.70   96.45
'
unit 8
'spring region of fuel rod - above grid plate
 cylinder 30  1 0.41                  96.90 96.70    origin 0.63 0.63
 cylinder 2  1 0.47                  96.90 96.70    origin 0.63 0.63
 cuboid   3  1 1.26 0.0  1.26 0.0     96.90 96.70
'
unit 88
'array of spring region of fuel rod - above grid plate
 array 88  -13.86 -13.86 96.70
 cuboid   3   1  60.00 -60.00 60.00 -60.00  96.90 96.70
 cuboid 1000  1  60.30 -60.30 60.30 -60.30  96.90 96.70
'
unit 9
'top end plug
 cylinder 2  1 0.47                98.20  96.90    origin 0.63 0.63
 cuboid   3  1 1.26 0.0  1.26 0.0  98.20  96.90
'
unit 99
'array of top end plugs
```

```
 array 99  -13.86 -13.86 96.90
 cuboid   3   1  60.00 -60.00 60.00 -60.00   98.20  96.90
 cuboid 1000  1  60.30 -60.30 60.30 -60.30   98.20  96.90
'
unit 100
'pedestal
 cuboid 1000 1 47.5 -47.5  47.5 -47.5 0.0 -0.8
'
unit 101
'lower portion of the tank
cuboid 400  1  60.00 -60.00 60.00 -60.00   0.53 -20.0
hole 100 0.0 0.0 0.0
cuboid 1000  1  60.30 -60.30 60.30 -60.30   0.53  -20.30
'
global unit 102
'final assembly of axial slices
array 102 0.0 0.0 0.0
'
end geom
'
read array
'
'
ara=11  nux=22 nuy=22 nuz=1
'array of bottom end plugs -  below support grid
 fill
   1 1 1 1 1 1 1 1 1 1 1 1 1 1 1 1 1 1 1 1 1 1
   1 1 1 1 1 1 1 1 1 1 1 1 1 1 1 1 1 1 1 1 1 1
   1 1 1 1 1 1 1 1 1 1 1 1 1 1 1 1 1 1 1 1 1 1
   1 1 1 1 1 1 1 1 1 1 1 1 1 1 1 1 1 1 1 1 1 1
   1 1 1 1 1 1 1 1 1 1 1 1 1 1 1 1 1 1 1 1 1 1
   1 1 1 1 1 1 1 1 1 1 1 1 1 1 1 1 1 1 1 1 1 1
   1 1 1 1 1 1 1 1 1 1 1 1 1 1 1 1 1 1 1 1 1 1
   1 1 1 1 1 1 1 1 1 1 1 1 1 1 1 1 1 1 1 1 1 1
   1 1 1 1 1 1 1 1 1 1 1 1 1 1 1 1 1 1 1 1 1 1
   1 1 1 1 1 1 1 1 1 1 1 1 1 1 1 1 1 1 1 1 1 1
   1 1 1 1 1 1 1 1 1 1 1 1 1 1 1 1 1 1 1 1 1 1
   1 1 1 1 1 1 1 1 1 1 1 1 1 1 1 1 1 1 1 1 1 1
   1 1 1 1 1 1 1 1 1 1 1 1 1 1 1 1 1 1 1 1 1 1
   1 1 1 1 1 1 1 1 1 1 1 1 1 1 1 1 1 1 1 1 1 1
   1 1 1 1 1 1 1 1 1 1 1 1 1 1 1 1 1 1 1 1 1 1
   1 1 1 1 1 1 1 1 1 1 1 1 1 1 1 1 1 1 1 1 1 1
   1 1 1 1 1 1 1 1 1 1 1 1 1 1 1 1 1 1 1 1 1 1
   1 1 1 1 1 1 1 1 1 1 1 1 1 1 1 1 1 1 1 1 1 1
   1 1 1 1 1 1 1 1 1 1 1 1 1 1 1 1 1 1 1 1 1 1
   1 1 1 1 1 1 1 1 1 1 1 1 1 1 1 1 1 1 1 1 1 1
   1 1 1 1 1 1 1 1 1 1 1 1 1 1 1 1 1 1 1 1 1 1
   1 1 1 1 1 1 1 1 1 1 1 1 1 1 1 1 1 1 1 1 1 1
 end fill
'
ara=22  nux=22 nuy=22 nuz=1
'array of bottom end plugs - in support grid
 fill
   2 2 2 2 2 2 2 2 2 2 2 2 2 2 2 2 2 2 2 2 2 2
```

```
   2 2 2 2 2 2 2 2 2 2 2 2 2 2 2 2 2 2 2 2 2 2
   2 2 2 2 2 2 2 2 2 2 2 2 2 2 2 2 2 2 2 2 2 2
   2 2 2 2 2 2 2 2 2 2 2 2 2 2 2 2 2 2 2 2 2 2
   2 2 2 2 2 2 2 2 2 2 2 2 2 2 2 2 2 2 2 2 2 2
   2 2 2 2 2 2 2 2 2 2 2 2 2 2 2 2 2 2 2 2 2 2
   2 2 2 2 2 2 2 2 2 2 2 2 2 2 2 2 2 2 2 2 2 2
   2 2 2 2 2 2 2 2 2 2 2 2 2 2 2 2 2 2 2 2 2 2
   2 2 2 2 2 2 2 2 2 2 2 2 2 2 2 2 2 2 2 2 2 2
   2 2 2 2 2 2 2 2 2 2 2 2 2 2 2 2 2 2 2 2 2 2
   2 2 2 2 2 2 2 2 2 2 2 2 2 2 2 2 2 2 2 2 2 2
   2 2 2 2 2 2 2 2 2 2 2 2 2 2 2 2 2 2 2 2 2 2
   2 2 2 2 2 2 2 2 2 2 2 2 2 2 2 2 2 2 2 2 2 2
   2 2 2 2 2 2 2 2 2 2 2 2 2 2 2 2 2 2 2 2 2 2
   2 2 2 2 2 2 2 2 2 2 2 2 2 2 2 2 2 2 2 2 2 2
   2 2 2 2 2 2 2 2 2 2 2 2 2 2 2 2 2 2 2 2 2 2
   2 2 2 2 2 2 2 2 2 2 2 2 2 2 2 2 2 2 2 2 2 2
   2 2 2 2 2 2 2 2 2 2 2 2 2 2 2 2 2 2 2 2 2 2
   2 2 2 2 2 2 2 2 2 2 2 2 2 2 2 2 2 2 2 2 2 2
   2 2 2 2 2 2 2 2 2 2 2 2 2 2 2 2 2 2 2 2 2 2
   2 2 2 2 2 2 2 2 2 2 2 2 2 2 2 2 2 2 2 2 2 2
   2 2 2 2 2 2 2 2 2 2 2 2 2 2 2 2 2 2 2 2 2 2
 end fill
'
ara=33  nux=22 nuy=22 nuz=1
'array of bottom end plugs - above support grid
 fill
   3 3 3 3 3 3 3 3 3 3 3 3 3 3 3 3 3 3 3 3 3 3
   3 3 3 3 3 3 3 3 3 3 3 3 3 3 3 3 3 3 3 3 3 3
   3 3 3 3 3 3 3 3 3 3 3 3 3 3 3 3 3 3 3 3 3 3
   3 3 3 3 3 3 3 3 3 3 3 3 3 3 3 3 3 3 3 3 3 3
   3 3 3 3 3 3 3 3 3 3 3 3 3 3 3 3 3 3 3 3 3 3
   3 3 3 3 3 3 3 3 3 3 3 3 3 3 3 3 3 3 3 3 3 3
   3 3 3 3 3 3 3 3 3 3 3 3 3 3 3 3 3 3 3 3 3 3
   3 3 3 3 3 3 3 3 3 3 3 3 3 3 3 3 3 3 3 3 3 3
   3 3 3 3 3 3 3 3 3 3 3 3 3 3 3 3 3 3 3 3 3 3
   3 3 3 3 3 3 3 3 3 3 3 3 3 3 3 3 3 3 3 3 3 3
   3 3 3 3 3 3 3 3 3 3 3 3 3 3 3 3 3 3 3 3 3 3
   3 3 3 3 3 3 3 3 3 3 3 3 3 3 3 3 3 3 3 3 3 3
   3 3 3 3 3 3 3 3 3 3 3 3 3 3 3 3 3 3 3 3 3 3
   3 3 3 3 3 3 3 3 3 3 3 3 3 3 3 3 3 3 3 3 3 3
   3 3 3 3 3 3 3 3 3 3 3 3 3 3 3 3 3 3 3 3 3 3
   3 3 3 3 3 3 3 3 3 3 3 3 3 3 3 3 3 3 3 3 3 3
   3 3 3 3 3 3 3 3 3 3 3 3 3 3 3 3 3 3 3 3 3 3
   3 3 3 3 3 3 3 3 3 3 3 3 3 3 3 3 3 3 3 3 3 3
   3 3 3 3 3 3 3 3 3 3 3 3 3 3 3 3 3 3 3 3 3 3
   3 3 3 3 3 3 3 3 3 3 3 3 3 3 3 3 3 3 3 3 3 3
   3 3 3 3 3 3 3 3 3 3 3 3 3 3 3 3 3 3 3 3 3 3
   3 3 3 3 3 3 3 3 3 3 3 3 3 3 3 3 3 3 3 3 3 3
 end fill
'
ara=44  nux=22 nuy=22 nuz=1
 fill
' array for submerged fuel
   4 4 4 4 4 4 4 4 4 4 4 4 4 4 4 4 4 4 4 4 4 4
```

```
    4 4 4 4 4 4 4 4 4 4 4 4 4 4 4 4 4 4 4 4 4 4
    4 4 4 4 4 4 4 4 4 4 4 4 4 4 4 4 4 4 4 4 4 4
    4 4 4 4 4 4 4 4 4 4 4 4 4 4 4 4 4 4 4 4 4 4
    4 4 4 4 4 4 4 4 4 4 4 4 4 4 4 4 4 4 4 4 4 4
    4 4 4 4 4 4 4 4 4 4 4 4 4 4 4 4 4 4 4 4 4 4
    4 4 4 4 4 4 4 4 4 4 4 4 4 4 4 4 4 4 4 4 4 4
    4 4 4 4 4 4 4 4 4 4 4 4 4 4 4 4 4 4 4 4 4 4
    4 4 4 4 4 4 4 4 4 4 4 4 4 4 4 4 4 4 4 4 4 4
    4 4 4 4 4 4 4 4 4 4 4 4 4 4 4 4 4 4 4 4 4 4
    4 4 4 4 4 4 4 4 4 4 4 4 4 4 4 4 4 4 4 4 4 4
    4 4 4 4 4 4 4 4 4 4 4 4 4 4 4 4 4 4 4 4 4 4
    4 4 4 4 4 4 4 4 4 4 4 4 4 4 4 4 4 4 4 4 4 4
    4 4 4 4 4 4 4 4 4 4 4 4 4 4 4 4 4 4 4 4 4 4
    4 4 4 4 4 4 4 4 4 4 4 4 4 4 4 4 4 4 4 4 4 4
    4 4 4 4 4 4 4 4 4 4 4 4 4 4 4 4 4 4 4 4 4 4
    4 4 4 4 4 4 4 4 4 4 4 4 4 4 4 4 4 4 4 4 4 4
    4 4 4 4 4 4 4 4 4 4 4 4 4 4 4 4 4 4 4 4 4 4
    4 4 4 4 4 4 4 4 4 4 4 4 4 4 4 4 4 4 4 4 4 4
    4 4 4 4 4 4 4 4 4 4 4 4 4 4 4 4 4 4 4 4 4 4
    4 4 4 4 4 4 4 4 4 4 4 4 4 4 4 4 4 4 4 4 4 4
    4 4 4 4 4 4 4 4 4 4 4 4 4 4 4 4 4 4 4 4 4 4
  end fill
'
ara=55  nux=22 nuy=22 nuz=1
'array for water above fuel level
  fill
    5 5 5 5 5 5 5 5 5 5 5 5 5 5 5 5 5 5 5 5 5 5
    5 5 5 5 5 5 5 5 5 5 5 5 5 5 5 5 5 5 5 5 5 5
    5 5 5 5 5 5 5 5 5 5 5 5 5 5 5 5 5 5 5 5 5 5
    5 5 5 5 5 5 5 5 5 5 5 5 5 5 5 5 5 5 5 5 5 5
    5 5 5 5 5 5 5 5 5 5 5 5 5 5 5 5 5 5 5 5 5 5
    5 5 5 5 5 5 5 5 5 5 5 5 5 5 5 5 5 5 5 5 5 5
    5 5 5 5 5 5 5 5 5 5 5 5 5 5 5 5 5 5 5 5 5 5
    5 5 5 5 5 5 5 5 5 5 5 5 5 5 5 5 5 5 5 5 5 5
    5 5 5 5 5 5 5 5 5 5 5 5 5 5 5 5 5 5 5 5 5 5
    5 5 5 5 5 5 5 5 5 5 5 5 5 5 5 5 5 5 5 5 5 5
    5 5 5 5 5 5 5 5 5 5 5 5 5 5 5 5 5 5 5 5 5 5
    5 5 5 5 5 5 5 5 5 5 5 5 5 5 5 5 5 5 5 5 5 5
    5 5 5 5 5 5 5 5 5 5 5 5 5 5 5 5 5 5 5 5 5 5
    5 5 5 5 5 5 5 5 5 5 5 5 5 5 5 5 5 5 5 5 5 5
    5 5 5 5 5 5 5 5 5 5 5 5 5 5 5 5 5 5 5 5 5 5
    5 5 5 5 5 5 5 5 5 5 5 5 5 5 5 5 5 5 5 5 5 5
    5 5 5 5 5 5 5 5 5 5 5 5 5 5 5 5 5 5 5 5 5 5
    5 5 5 5 5 5 5 5 5 5 5 5 5 5 5 5 5 5 5 5 5 5
    5 5 5 5 5 5 5 5 5 5 5 5 5 5 5 5 5 5 5 5 5 5
    5 5 5 5 5 5 5 5 5 5 5 5 5 5 5 5 5 5 5 5 5 5
    5 5 5 5 5 5 5 5 5 5 5 5 5 5 5 5 5 5 5 5 5 5
    5 5 5 5 5 5 5 5 5 5 5 5 5 5 5 5 5 5 5 5 5 5
  end fill
'
ara=66  nux=22 nuy=22 nuz=1
'array of springs in fuel rods - below grid plate
  fill
    6 6 6 6 6 6 6 6 6 6 6 6 6 6 6 6 6 6 6 6 6 6
```

```
    6 6 6 6 6 6 6 6 6 6 6 6 6 6 6 6 6 6 6 6 6 6
    6 6 6 6 6 6 6 6 6 6 6 6 6 6 6 6 6 6 6 6 6 6
    6 6 6 6 6 6 6 6 6 6 6 6 6 6 6 6 6 6 6 6 6 6
    6 6 6 6 6 6 6 6 6 6 6 6 6 6 6 6 6 6 6 6 6 6
    6 6 6 6 6 6 6 6 6 6 6 6 6 6 6 6 6 6 6 6 6 6
    6 6 6 6 6 6 6 6 6 6 6 6 6 6 6 6 6 6 6 6 6 6
    6 6 6 6 6 6 6 6 6 6 6 6 6 6 6 6 6 6 6 6 6 6
    6 6 6 6 6 6 6 6 6 6 6 6 6 6 6 6 6 6 6 6 6 6
    6 6 6 6 6 6 6 6 6 6 6 6 6 6 6 6 6 6 6 6 6 6
    6 6 6 6 6 6 6 6 6 6 6 6 6 6 6 6 6 6 6 6 6 6
    6 6 6 6 6 6 6 6 6 6 6 6 6 6 6 6 6 6 6 6 6 6
    6 6 6 6 6 6 6 6 6 6 6 6 6 6 6 6 6 6 6 6 6 6
    6 6 6 6 6 6 6 6 6 6 6 6 6 6 6 6 6 6 6 6 6 6
    6 6 6 6 6 6 6 6 6 6 6 6 6 6 6 6 6 6 6 6 6 6
    6 6 6 6 6 6 6 6 6 6 6 6 6 6 6 6 6 6 6 6 6 6
    6 6 6 6 6 6 6 6 6 6 6 6 6 6 6 6 6 6 6 6 6 6
    6 6 6 6 6 6 6 6 6 6 6 6 6 6 6 6 6 6 6 6 6 6
    6 6 6 6 6 6 6 6 6 6 6 6 6 6 6 6 6 6 6 6 6 6
    6 6 6 6 6 6 6 6 6 6 6 6 6 6 6 6 6 6 6 6 6 6
    6 6 6 6 6 6 6 6 6 6 6 6 6 6 6 6 6 6 6 6 6 6
    6 6 6 6 6 6 6 6 6 6 6 6 6 6 6 6 6 6 6 6 6 6
 end fill
'
ara=77  nux=22 nuy=22 nuz=1
'array of springs in fuel rods - in grid plate
 fill
    7 7 7 7 7 7 7 7 7 7 7 7 7 7 7 7 7 7 7 7 7 7
    7 7 7 7 7 7 7 7 7 7 7 7 7 7 7 7 7 7 7 7 7 7
    7 7 7 7 7 7 7 7 7 7 7 7 7 7 7 7 7 7 7 7 7 7
    7 7 7 7 7 7 7 7 7 7 7 7 7 7 7 7 7 7 7 7 7 7
    7 7 7 7 7 7 7 7 7 7 7 7 7 7 7 7 7 7 7 7 7 7
    7 7 7 7 7 7 7 7 7 7 7 7 7 7 7 7 7 7 7 7 7 7
    7 7 7 7 7 7 7 7 7 7 7 7 7 7 7 7 7 7 7 7 7 7
    7 7 7 7 7 7 7 7 7 7 7 7 7 7 7 7 7 7 7 7 7 7
    7 7 7 7 7 7 7 7 7 7 7 7 7 7 7 7 7 7 7 7 7 7
    7 7 7 7 7 7 7 7 7 7 7 7 7 7 7 7 7 7 7 7 7 7
    7 7 7 7 7 7 7 7 7 7 7 7 7 7 7 7 7 7 7 7 7 7
    7 7 7 7 7 7 7 7 7 7 7 7 7 7 7 7 7 7 7 7 7 7
    7 7 7 7 7 7 7 7 7 7 7 7 7 7 7 7 7 7 7 7 7 7
    7 7 7 7 7 7 7 7 7 7 7 7 7 7 7 7 7 7 7 7 7 7
    7 7 7 7 7 7 7 7 7 7 7 7 7 7 7 7 7 7 7 7 7 7
    7 7 7 7 7 7 7 7 7 7 7 7 7 7 7 7 7 7 7 7 7 7
    7 7 7 7 7 7 7 7 7 7 7 7 7 7 7 7 7 7 7 7 7 7
    7 7 7 7 7 7 7 7 7 7 7 7 7 7 7 7 7 7 7 7 7 7
    7 7 7 7 7 7 7 7 7 7 7 7 7 7 7 7 7 7 7 7 7 7
    7 7 7 7 7 7 7 7 7 7 7 7 7 7 7 7 7 7 7 7 7 7
    7 7 7 7 7 7 7 7 7 7 7 7 7 7 7 7 7 7 7 7 7 7
    7 7 7 7 7 7 7 7 7 7 7 7 7 7 7 7 7 7 7 7 7 7
 end fill
'
ara=88  nux=22 nuy=22 nuz=1
'array of springs in fuel rods - above grid plate
 fill
    8 8 8 8 8 8 8 8 8 8 8 8 8 8 8 8 8 8 8 8 8 8
```

```
    8 8 8 8 8 8 8 8 8 8 8 8 8 8 8 8 8 8 8 8 8 8
    8 8 8 8 8 8 8 8 8 8 8 8 8 8 8 8 8 8 8 8 8 8
    8 8 8 8 8 8 8 8 8 8 8 8 8 8 8 8 8 8 8 8 8 8
    8 8 8 8 8 8 8 8 8 8 8 8 8 8 8 8 8 8 8 8 8 8
    8 8 8 8 8 8 8 8 8 8 8 8 8 8 8 8 8 8 8 8 8 8
    8 8 8 8 8 8 8 8 8 8 8 8 8 8 8 8 8 8 8 8 8 8
    8 8 8 8 8 8 8 8 8 8 8 8 8 8 8 8 8 8 8 8 8 8
    8 8 8 8 8 8 8 8 8 8 8 8 8 8 8 8 8 8 8 8 8 8
    8 8 8 8 8 8 8 8 8 8 8 8 8 8 8 8 8 8 8 8 8 8
    8 8 8 8 8 8 8 8 8 8 8 8 8 8 8 8 8 8 8 8 8 8
    8 8 8 8 8 8 8 8 8 8 8 8 8 8 8 8 8 8 8 8 8 8
    8 8 8 8 8 8 8 8 8 8 8 8 8 8 8 8 8 8 8 8 8 8
    8 8 8 8 8 8 8 8 8 8 8 8 8 8 8 8 8 8 8 8 8 8
    8 8 8 8 8 8 8 8 8 8 8 8 8 8 8 8 8 8 8 8 8 8
    8 8 8 8 8 8 8 8 8 8 8 8 8 8 8 8 8 8 8 8 8 8
    8 8 8 8 8 8 8 8 8 8 8 8 8 8 8 8 8 8 8 8 8 8
    8 8 8 8 8 8 8 8 8 8 8 8 8 8 8 8 8 8 8 8 8 8
    8 8 8 8 8 8 8 8 8 8 8 8 8 8 8 8 8 8 8 8 8 8
    8 8 8 8 8 8 8 8 8 8 8 8 8 8 8 8 8 8 8 8 8 8
    8 8 8 8 8 8 8 8 8 8 8 8 8 8 8 8 8 8 8 8 8 8
    8 8 8 8 8 8 8 8 8 8 8 8 8 8 8 8 8 8 8 8 8 8
  end fill
'
ara=99  nux=22 nuy=22 nuz=1
'top end plugs
  fill
    9 9 9 9 9 9 9 9 9 9 9 9 9 9 9 9 9 9 9 9 9 9
    9 9 9 9 9 9 9 9 9 9 9 9 9 9 9 9 9 9 9 9 9 9
    9 9 9 9 9 9 9 9 9 9 9 9 9 9 9 9 9 9 9 9 9 9
    9 9 9 9 9 9 9 9 9 9 9 9 9 9 9 9 9 9 9 9 9 9
    9 9 9 9 9 9 9 9 9 9 9 9 9 9 9 9 9 9 9 9 9 9
    9 9 9 9 9 9 9 9 9 9 9 9 9 9 9 9 9 9 9 9 9 9
    9 9 9 9 9 9 9 9 9 9 9 9 9 9 9 9 9 9 9 9 9 9
    9 9 9 9 9 9 9 9 9 9 9 9 9 9 9 9 9 9 9 9 9 9
    9 9 9 9 9 9 9 9 9 9 9 9 9 9 9 9 9 9 9 9 9 9
    9 9 9 9 9 9 9 9 9 9 9 9 9 9 9 9 9 9 9 9 9 9
    9 9 9 9 9 9 9 9 9 9 9 9 9 9 9 9 9 9 9 9 9 9
    9 9 9 9 9 9 9 9 9 9 9 9 9 9 9 9 9 9 9 9 9 9
    9 9 9 9 9 9 9 9 9 9 9 9 9 9 9 9 9 9 9 9 9 9
    9 9 9 9 9 9 9 9 9 9 9 9 9 9 9 9 9 9 9 9 9 9
    9 9 9 9 9 9 9 9 9 9 9 9 9 9 9 9 9 9 9 9 9 9
    9 9 9 9 9 9 9 9 9 9 9 9 9 9 9 9 9 9 9 9 9 9
    9 9 9 9 9 9 9 9 9 9 9 9 9 9 9 9 9 9 9 9 9 9
    9 9 9 9 9 9 9 9 9 9 9 9 9 9 9 9 9 9 9 9 9 9
    9 9 9 9 9 9 9 9 9 9 9 9 9 9 9 9 9 9 9 9 9 9
    9 9 9 9 9 9 9 9 9 9 9 9 9 9 9 9 9 9 9 9 9 9
    9 9 9 9 9 9 9 9 9 9 9 9 9 9 9 9 9 9 9 9 9 9
    9 9 9 9 9 9 9 9 9 9 9 9 9 9 9 9 9 9 9 9 9 9
  end fill
'
ara=102 nux=1 nuy=1 nuz=10
'final assembly of axial slices
  fill
  101
```

```
 11
 22
 33
 44
 55
 66
 77
 88
 99
 end fill
end array
'
read bounds
 all=void
end bounds
'
end data
end
```

Appendix C: Input for LEU-COMP-THERM-042-001, Uniform Pitch Assumption

As with the LCT-007-001 model, the uniform pitch assumption model is included here to save space. Tis input is 184 lines, compared to almost 39,000 lines for the expanded model supporting independent fuel pin location perturbations.

```
=csas25     parm=centrm
LEU-COMP-THERM-042-001
v7.1-252n
read comp
'uo2 fuel
u-234  1 0 2.8563e-6 295.15 end
u-235  1 0 4.8785e-4 295.15 end
u-236  1 0 3.5348e-6 295.15 end
u-238  1 0 2.0009e-2 295.15 end
o      1 0 4.1202e-2 295.15 end
' Al 1100 - top end plug alloy
al  2 0 5.9660e-2 295.15 end
cu  2 0 3.0705e-5 295.15 end
mn  2 0 7.3991e-6 295.15 end
zn  2 0 1.2433e-5 295.15 end
si  2 0 2.3302e-4 295.15 end
fe  2 0 1.1719e-4 295.15 end
' Al 5052 - bottom end plug alloy
al  3 0 5.8028e-2 295.15 end
cr  3 0 7.7888e-5 295.15 end
cu  3 0 1.2746e-5 295.15 end
mg  3 0 1.6663e-3 295.15 end
mn  3 0 1.4743e-5 295.15 end
zn  3 0 1.2387e-5 295.15 end
si  3 0 1.2978e-4 295.15 end
fe  3 0 6.5265e-5 295.15 end
' Al 6061 - clad alloy - top end plug
al  4 0 5.8433e-2 295.15 end
cr  4 0 6.2310e-5 295.15 end
cu  4 0 6.3731e-5 295.15 end
mg  4 0 6.6651e-4 295.15 end
mn  4 0 2.2115e-5 295.15 end
ti  4 0 2.5375e-5 295.15 end
zn  4 0 3.0967e-5 295.15 end
si  4 0 3.4607e-4 295.15 end
fe  4 0 1.0152e-4 295.15 end
' Al 6061 - clad alloy - bottom end plug
al  5 0 5.8433e-2 295.15 end
cr  5 0 6.2310e-5 295.15 end
cu  5 0 6.3731e-5 295.15 end
mg  5 0 6.6651e-4 295.15 end
mn  5 0 2.2115e-5 295.15 end
ti  5 0 2.5375e-5 295.15 end
zn  5 0 3.0967e-5 295.15 end
si  5 0 3.4607e-4 295.15 end
fe  5 0 1.0152e-4 295.15 end
' Al 6061 - clad alloy - fuel
```

```
al  6 0 5.8433e-2 295.15 end
cr  6 0 6.2310e-5 295.15 end
cu  6 0 6.3731e-5 295.15 end
mg  6 0 6.6651e-4 295.15 end
mn  6 0 2.2115e-5 295.15 end
ti  6 0 2.5375e-5 295.15 end
zn  6 0 3.0967e-5 295.15 end
si  6 0 3.4607e-4 295.15 end
fe  6 0 1.0152e-4 295.15 end
' steel reflector wall
fe  7 0 8.1810e-2 295.15 end
c   7 0 7.4686e-4 295.15 end
mn  7 0 1.1000e-3 295.15 end
p   7 0 6.0971e-6 295.15 end
s   7 0 8.8332e-6 295.15 end
si  7 0 3.6983e-4 295.15 end
ni  7 0 6.3552e-4 295.15 end
mo  7 0 2.4114e-4 295.15 end
cr  7 0 1.0896e-4 295.15 end
cu  7 0 9.6587e-5 295.15 end
' steel absorber panels
cr  8 0 1.7046e-2 295.15 end
cu  8 0 2.0291e-4 295.15 end
fe  8 0 5.8353e-2 295.15 end
mn  8 0 1.3734e-3 295.15 end
mo  8 0 1.2942e-4 295.15 end
ni  8 0 9.0238e-3 295.15 end
' water moderator
h  9 0 6.6706e-2 295.15 end
o  9 0 3.3353e-2 295.15 end
' water reflector
h  10 0 6.6706e-2 295.15 end
o  10 0 3.3353e-2 295.15 end
' acrylic bottom support plate
h-poly 11 0 5.6642e-2 295.15 end
c      11 0 3.5648e-2 295.15 end
o      11 0 1.4273e-2 295.15 end
end comp
'
read cell
 latticecell squarepitch pitch=1.684 9 fueld=1.1176 1 cladd=1.270 6 end
end cell
'
read parm
  tme=10000 tba=60
  gen=10010 npg=10000 nsk=10 htm=no sig=0.00010
end parm
'
read geometry
'
 unit 1
' bottom end plug
 cylinder 3 1  0.5588 1.27 0
 cylinder 5 1  0.6350 1.27 0
```

```
 cuboid  10 1  0.842 -0.842  0.842 -0.842  1.27 0
'
 unit 2
' fueled section
 cylinder 1 1  0.5588 91.44 0
 cylinder 6 1  0.6350 91.44 0
 cuboid   9 1  0.842 -0.842  0.842 -0.842  91.44 0
'
 unit 3
' clad top end plug
 cylinder 2 1  0.5588 0.48 0
 cylinder 4 1  0.6350 0.48 0
 cuboid  10 1  0.842 -0.842  0.842 -0.842  0.48 0
'
 unit 4
' top end plug
 cylinder 2 1  0.6350 4.6 0
 cuboid  10 1  0.842 -0.842  0.842 -0.842  4.6 0
'
 unit 5
' axial stack of fuel rod
 array 1 0.0 0.0 0.0
'
 unit 6
' absorber panel
 cuboid  8 1 0.302 0.0  15.1 -15.1  92.77 1.27
'
 unit 7
' middle array of fuel rods
 array 10 -21.05 -15.156 0.0
'
 unit 8
' flanking array of fuel rods
 array 11 -16.840 -15.156 0.0
'
 unit 9
' acrylic support plate
 cuboid 11 1 62.596 -62.596  15.156 -15.156  2.54 0
'
 unit 11
' steel reflector walls
 cuboid 7 1  73.65 -73.65  17.85 0  104.06 -17.84
'
 global unit 12
' insert components as holes into large cuboid of water
 cuboid 10 1  104.15 -104.15  45.656 -45.656  107.71 -17.84
' first is central array of fuel rods
 hole 7 0 0 0
' next is poison to the left and to the right
 hole 6  -21.352  0 0
 hole 6   21.050  0 0
' then side arrays
 hole 8  -45.756 0 0
 hole 8   45.756 0 0
```

```
' then acrylic support plate
 hole 9  0 0 -2.54
' finally reflecting walls
 hole 11  0  16.477 0
 hole 11  0 -34.327 0
end geom
'
read array
'
' axial stack of fuel rod
ara=1  nux=1 nuy=1 nuz=4
 fill 1 2 3 4 end fill
'
' middle fuel rod array
ara=10  nux=25 nuy=18 nuz=1
 fill 450r5 end fill
'
' flanker fuel rod array
ara=11  nux=20 nuy=18 nuz=1
 fill 360r5 end fill
'
end array
'
read bounds
 all=void
end bounds
'
end data
end
```

Appendix D: Input for HEU-SOL-THERM-001-001

Only one set of inputs is needed for the HST-001 evaluation. The input for Case 1 is provided here.

```
=csas25
HEU-SOL-THERM-001-001
v7-238
read composition
 u-235       1 0 0.00034777 300   end
 u-234       1 0 3.831e-06 300   end
 u-236       1 0 1.613e-06 300   end
 u-238       1 0 1.9798e-05 300   end
 o           1 0 0.035037 300   end
 n           1 0 0.00092307 300   end
 h           1 0 0.06322 300   end
 c           2 0 0.00026231 300   end
 si          2 0 0.0013768 300   end
 p           2 0 3.853e-05 300   end
 s           2 0 2.8282e-05 300   end
 cr          2 0 0.016985 300   end
 mn          2 0 0.0011209 300   end
 fe          2 0 0.059852 300   end
 ni          2 0 0.00754 300   end
 mo          2 0 8.9563e-06 300   end
end composition
read celldata
 multiregion cylindrical left_bdy=reflected right_bdy=vacuum end
 1 13.96
 2 14.28
 end zone
end celldata
read parameter
 gen=100000
 npg=10000
 nsk=20
 htm=no
 sig=0.0001
end parameter
read geometry
global unit 1
com='he uranyl nitrate in tank suspended in large room'
 zcylinder 1 1   13.96     31.2        0
 zcylinder 0 1   13.96     41.6        0
 zcylinder 2 1   14.28     41.6    -0.64
 cuboid 0 1    14.28   -14.28    14.28   -14.28     41.6    -0.64
end geometry
end data
end
```

Appendix E: HTC Grid Plate Measurements

IRSN
INSTITUT
DE RADIOPROTECTION
ET DE SÛRETÉ NUCLÉAIRE

Fontenay-aux-Roses, July 17, 2009

Dr. Cecil V. Parks
Manager - Nuclear Systems Analysis, Design, and Safety
Oak Ridge National Laboratory
P.O. Box 2008
Oak Ridge, TN 37831-6170

N° Chrono DSU/SEC/A/2009-294

Object : Measurements of Grid Plates used for HTC experiments

Reference : [1] Email from D. Mueller to E. Létang from April 14, 2008

Direction de la sûreté
des usines, des laboratoires,
des transports et des déchets

Service d'expertise, d'études
et de recherches en criticité

Dear Cecil,

Following the request of Don Mueller [1], measurements were made on each of ten grid plates used for the HTC experiments. Distances between centres of extreme holes were measured in six directions. Details of the measurements please find in Appendix 1. The schemes of the requested and performed measurements are shown in Figures 1 and 2, respectively. The results of the measurements are given in Tables 1-5 for pairs of the grid plates of 1.3-, 1.5-, 1.7-, 1.9-, and 2.3-cm pitches.

The measurements were made by "CLM Industry Company". The first invoice given in Appendix 2 provides a cost of the requested measurements performed on a single plate. In total the IRSN paid 6150 € (615 € x 10) for the measurements requested by the ORNL.

The correspondent on technical issues of the HTC experiments is Tatiana Ivanova (tatiana.ivanova@irsn.fr). Please do not hesitate to contact her if you have any questions on this subject.

Adresse Courrier
BP 17
92262 Fontenay-aux-Roses
Cedex France

Tél. +33 (0)1 58 35 91 65
Fax +33 (0)1 46 57 29 98
eric.letang@irsn.fr

Best Regards,

Eric LETANG
Head of Criticality Safety Study and Research Department

Siège social
31, av. de la Division Leclerc
92260 Fontenay-aux-Roses
Standard +33 (0)1 58 35 88 88
RCS Nanterre B 440 546 018

IRSN
INSTITUT
DE RADIOPROTECTION
ET DE SÛRETÉ NUCLÉAIRE

Copy:

DSU/DIR
DSU/SEC/LERD

APPENDIX 1: Measurements Performed on Grid Plates Used for HTC Experiments

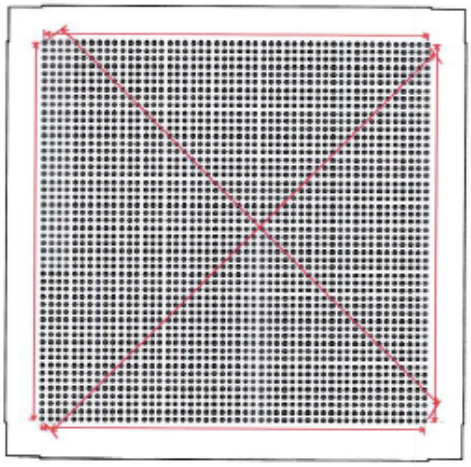

Fig. 1. Scheme of requested measurements (shown with red)

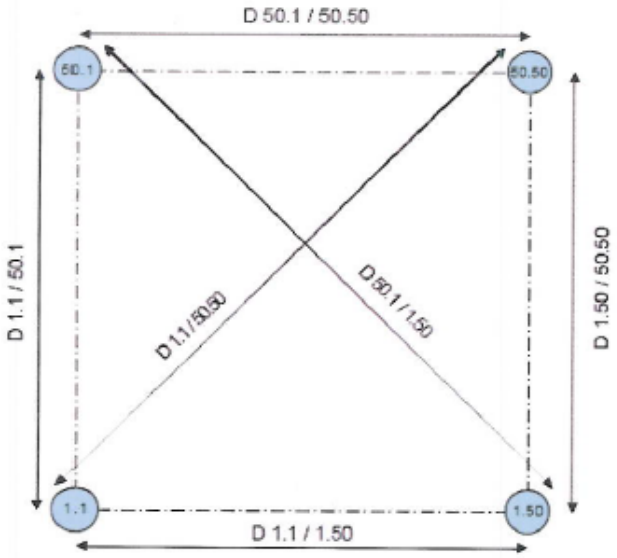

Fig. 2. Scheme of performed measurements

Table 1. Results of Measurements for Grid Plates of 1.3-cm Pitch

Direction (see Fig. 2)	Distance, mm		Uncertainty (2σ), μm
	Grid Plate 1	Grid Plate 2	Grid Plate 1&2
D1.1/1.50	636.981	636.981	3.6
D1.1/50.50	900.830	900.837	4.3
D1.1/50.1	636.970	637.032	3.6
D50.1/50.50	637.053	636.962	3.6
D50.1/1.50	900.869	900.855	4.3
D1.50/50.50	636.982	637.002	3.6

Table 2. Results of Measurements for Grid Plates of 1.5-cm Pitch

Direction (see Fig. 2)	Distance, mm		Uncertainty (2σ), μm
	Grid Plate 1	Grid Plate 2	Grid Plate 1&2
D1.1/1.50	735.007	735.031	3.9
D1.1/50.50	1039.476	1039.469	4.7
D1.1/50.1	735.035	735.022	3.9
D50.1/50.50	735.003	735.001	3.9
D50.1/1.50	1039.468	1039.469	4.7
D1.50/50.50	735.026	735.009	3.9

Table 3. Results of Measurements for Grid Plates of 1.7-cm Pitch

Direction (see Fig. 2)	Distance, mm		Uncertainty (2σ), μm
	Grid Plate 1	Grid Plate 2	Grid Plate 1&2
D1.1/1.50	833.006	832.988	4.1
D1.1/50.50	1178.034	1178.027	5.0
D1.1/50.1	832.998	832.948	4.1
D50.1/50.50	833.094	833.087	4.1
D50.1/1.50	1178.066	1177.952	5.0
D1.50/50.50	832.930	832.835	4.1

Table 4. Results of Measurements for Grid Plates of 1.9-cm Pitch

Direction (see Fig. 2)	Distance, mm		Uncertainty (2σ), μm
	Grid Plate 1	Grid Plate 2	Grid Plate 1&2
D1.1/1.50	930.892	930.981	4.4
D1.1/50.50	1316.505	1316.575	5.4
D1.1/50.1	930.939	930.939	4.4
D50.1/50.50	930.890	930.945	4.4
D50.1/1.50	1316.463	1316.654	5.4
D1.50/50.50	930.859	931.084	4.4

Table 5. Results of Measurements for Grid Plates of 2.3-cm Pitch

Direction (see Fig. 2)	Distance, mm		Uncertainty (2σ), μm
	Grid Plate 1	Grid Plate 2	Grid Plate 1&2
D1.1/1.50	1126.996	1126.930	11.1
D1.1/50.50	1594.140	1594.058	13.5
D1.1/50.1	1127.067	1127.027	11.1
D50.1/50.50	1126.978	1127.171	11.1
D50.1/1.50	1593.702	1593.595	13.5
D1.50/50.50	1126.896	1126.896	11.1

IRSN
INSTITUT
DE RADIOPROTECTION
ET DE SÛRETÉ NUCLÉAIRE

APPENDIX 2: Duplicate Invoice for the Measurements on one of the HTC Grid Plates

CLM industrie

Galilé groupe

CONCEVOIR, REALISER, ASSEMBLER

3 Impasse du Champ Chardon Parc Excellence 2000
21 600 Chevigny Saint Sauveur

Tél. : 03 80 74 40 10 – Fax : 03 80 74 47 22
E-mail : clm@galile.fr – www.clm-industrie.com

SA au capital de 249 848 – RC 91B771 Dijon
Siret 399 772 730 000 46 – Code APE 2852B
N° TVA intracom FR13399772730

CEA VALDUC
A l'attention de M. GIRAULT

BATIMENT 010
SITE DE VALDUC
21120 IS SUR TILLE

Nos Réf : 08050030AD

Chevigny, le jeudi 15 mai 2008

Monsieur,

Suite à votre demande de prix du 30/04/2008, nous avons le plaisir de vous communiquer nos meilleures conditions de prix pour la fourniture éventuelle de :

CONTROLE TRI DIM DE:

- 1 GRILLE N°1 SOIT :

LONGUEUR
LARGEUR
2 DIAGONALES

PRIX H.T. DE L'ENSEMBLE : 615.00 €

SOIT : MAIN D'ŒUVRE 1H X 32.64 € = 32.64 €
MATIERE ET FOURNITURE = 582.36 €

- 1 GRILLE N°2 SOIT :

LONGUEUR
LARGEUR
2 DIAGONALES
5 SERIES DE 100 TROUS DIAMETRE ET ENTRE AXES X ET Y

PRIX H.T. DE L'ENSEMBLE : 1 680.00 €

SOIT : MAIN D'ŒUVRE 1H X 32.64 € = 32.64 €
MATIERE ET FOURNITURE = 1 647.36 €

DELAI : 4 Semaines à réception de commande.

Compte tenu de la fluctuation du prix de la matière, nous garantissons nos prix pour une durée de 30 jours, passé ce délai ils seront révisables en fonction de l'évolution des cours.

La marchandise sera acheminée au lieu de livraison par nos soins **à titre gracieux.**

Espérant recevoir la faveur de vos ordres, nous vous prions d'agréer, Monsieur, l'expression de nos salutations distinguées.

LE CHARGE D'AFFAIRES
Alain DEJEUX

5 /5

VITA

William Marshall was born and raised in northwest suburban Chicago. He attended public schools for his entire education, graduating from Prospect High School on June 2, 1996. That fall he enrolled at the University of Missouri-Rolla (now the Missouri University of Science and Technology), graduating Cum Laude with a Bachelor of Science Degree in Nuclear Engineering on December 18, 1999. In January of 2000, William began his graduate studies at the University of Tennessee-Knoxville. He received a Master of Science Degree in Nuclear Engineering in August, 2001. William worked at Knolls Atomic Power Laboratory (KAPL) from November 5, 2001, until July 14, 2006. He then worked at the Westinghouse Electric Company from July 24, 2006, to May 28, 2010. William has been working in the Reactor and Nuclear Systems Division at Oak Ridge National Laboratory since June 1, 2010. He resumed his graduate education at the University of Tennessee-Knoxville in August, 2012, and will complete a Doctor of Philosophy degree in Nuclear Engineering in 2017.